12

AD

USAAVLABS TECHNICAL REPORT 67-66

INVESTIGATION OF MICROMECHANICAL BEHAVIOR OF FIBER REINFORCED PLASTICS

By

Juan Haener
Noel Ashbaugh
Chuen-Yuan Chia
Ming-Yuan Feng

February 1968

U. S. ARMY AVIATION MATERIEL LABORATORIES
FORT EUSTIS, VIRGINIA

CONTRACT DA 44-177-AMC-441(T)

WHITTAKER CORPORATION
NARMCO RESEARCH & DEVELOPMENT DIVISION
SAN DIEGO, CALIFORNIA

233

DISCLAIMERS

The findings in this report are not to be construed as an official Department of the Army position unless so designated by other authorized documents.

When Government drawings, specifications, or other data are used for any purpose other than in connection with a definitely related Government procurement operation, the United States Government thereby incurs no responsibility nor any obligation whatsoever; and the fact that the Government may have formulated, furnished, or in any way supplied the said drawings, specifications, or other data is not to be regarded by implication or otherwise as in any manner licensing the holder or any other person or corporation, or conveying any rights or permission, to manufacture, use, or sell any patented invention that may in any way be related thereto.

Trade names cited in this report do not constitute an official endorsement or approval of the use of such commercial hardware or software.

DISPOSITION INSTRUCTIONS

Destroy this report when no longer needed. Do not return it to the originator.

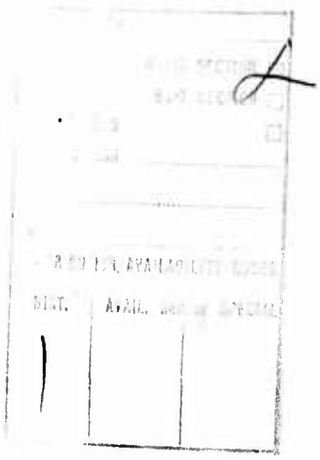

INVESTIGATION OF MICROMECHANICAL BEHAVIOR OF FIBER REINFORCED PLASTICS

Juan Haener, et al

Whittaker Corporation
San Diego, California

February 1968

DEPARTMENT OF THE ARMY
U. S. ARMY AVIATION MATERIEL LABORATORIES
FORT EUSTIS, VIRGINIA 23604

This program was performed under Contract DA 44-177-AMC-441(T) with the Whittaker Corporation, Narmco Research and Development Division.

The data contained in this report are the result of research conducted to determine (1) the load transmission in the matrix of a composite material, (2) the instability of fibers in a composite under compressive loads, and (3) the feasibility of theoretically obtaining elastic moduli of short-fiber composites.

The report has been reviewed by the U. S. Army Aviation Materiel Laboratories and is considered to be technically sound. It is published for the exchange of information and the stimulation of future research.

Task 1F125901A17002
Contract DA 44-177-AMC-441(T)
USAAVLABS Technical Report 67-66
February 1968

INVESTIGATION OF MICROMECHANICAL BEHAVIOR OF FIBER REINFORCED PLASTICS

Final Report

by

Juan Haener
Noel Ashbaugh
Chuen-Yuan Chia
Ming-Yuan Feng

Prepared by

WHITTAKER CORPORATION
Narmco Research & Development Division
San Diego, California

for

U. S. ARMY AVIATION MATERIEL LABORATORIES
FORT EUSTIS, VIRGINIA

ABSTRACT

The stress fields in the components of a unidirectional composite due to shrinkage and external loads are computed for 20 matrix/reinforcement combinations having various volumetric contents. Further, the load transmissions between loaded and unloaded fibers are formulated as three-dimensional elasticity solutions. The instability problem of a composite is treated by both the static and the energy method, resulting in critical loads and buckling wavelengths which depend on material constants and geometries. The theoretical results are in good agreement with experiments. The work reported herein encompasses the following principal areas:

1. Parametric studies (internal stresses and displacements computed for unidirectional composites composited of different combinations of matrices and reinforcements and different volumetric contents)
2. Three-dimensional load transfer among loaded and unloaded fibers in a matrix
3. Buckling of fibers in a matrix under axial load as an elasticity solution
4. Buckling of fibers in a matrix under axial load, solved with the Ritz-Galerkin method
5. Buckling of fibers in a matrix due to matrix shrinkage

FOREWORD

This report was prepared by Whittaker Corporation, Narmco Research & Development Division, San Diego, California, under USAAVLABS Contract DA 44-177-AMC-441(T), entitled "Investigation of Micromechanical Behavior of Fiber Reinforced Plastics," for the U. S. Army Aviation Materiel Laboratories, Fort Eustis, Virginia. The work was administered by Mr. R. P. McKinnon, Contracting Officer.

This report covers the period from 14 June 1966 through 14 March 1967.

Work on this project was carried out at Narmco under the overall direction of Dr. Juan Haener. Principal investigators also include Messrs. Noel Ashbaugh, Chuen-Yuan Chia, and Ming-Yuan Feng. The program was administered by Mr. Boris Levenetz, Assistant Manager of Narmco's Engineering Department.

TABLE OF CONTENTS

TABLE OF CONTENTS (Continued)

LIST OF ILLUSTRATIONS

LIST OF ILLUSTRATIONS (Continued)

LIST OF ILLUSTRATIONS (Continued)

LIST OF ILLUSTRATIONS (Continued)

LIST OF ILLUSTRATIONS (Continued)

LIST OF TABLES

LIST OF SYMBOLS

a	fiber radius
$\bar{a}$	defined in equation (280)
$A,B,C,D,F,$ $\bar{A},\bar{B},\bar{C},\bar{D}$	arbitrary or integration constants (when subscript); also defined in (329) through (331)
A	area (when superscript)
b	half distance between two neighboring fiber axes
$\bar{b}$	defined in equation (281)
c	parameter defined by $c = -\dfrac{1}{\alpha_n\left(1 - 2\nu^{II}\right)}$
c_i	arbitrary constants ($i = 1,2$)
d	$= b - a$
d_n	$= \alpha_n d$
e	dilatation defined by $\varepsilon_{11} + \varepsilon_{22} + \varepsilon_{33}$
$\underset{\sim}{e}$	unit vectors associated with coordinate directions, as indicated by subscripts
E	Young's modulus (when superscript) or constant
f	function of z
f_o	function of r
f_i	functions of ρ ($i = 1,2,3,4,5,6,7,8$)
$\underset{\sim}{F}$	body force vector
g	function of z
g_o	function of ρ
G	shear modulus (when superscript)
G_o	function of ρ and z
h	distance between fiber axis and hexagonal boundary for load transfer problem
I	area moment of inertia about centroid (when superscript)

LIST OF SYMBOLS (Continued)

I_n	modified Bessel function of the first kind of order n
J_1, J_2, J_3, J_4	defined in equations (305) through (309)
$J_I, J_{II}, J_{III}, J_{IV}$	defined in equations (315) through (319)
k	unit interfacial force per unit lateral deflection
$\bar{k}$	defined in equation (292)
K_n	modified Bessel function of the second kind of order n
ℓ	half the length of the composite
ℓ_{cr}	critical buckling wavelength
$L\ (= 2\ell)$	length of composite cylinder
L_i	function of r, φ, and z
M	internal moment acting on fiber cross section
M_s	moment per unit length produced by axial shear at fiber surface
n	number of half wavelength
$\bar{n}$	defined in equation (324)
N	internal axial force acting on fiber cross section
p	defined in equation (284)
p_1	interfacial force per unit length
p_{1n}	amplitudes of assumed interfacial force curve
$\underset{\sim}{P}$	Papkovitch vector
$\bar{P}, \bar{Q}, \bar{R}$	defined in equations (271) through (273)
P*	compressive load applied at the ends of composite cylinder corresponding to P^I_{cr}
$\tilde{P}$	internal compressive load on fiber element
$\left(P^I_{cr}\right)_{min}$	smallest critical buckling load of fiber

LIST OF SYMBOLS (Continued)

P_i	components of Papkovitch vector (i = 1,2,3)
P_o	scalar Papkovitch function
P^I	compressive force applied at fiber ends before buckling
P^I_{cr}	critical compressive load of the fiber
P^{II}	compressive force applied at matrix ends corresponding to P^I_{cr}
q	defined in equation (285)
Q	transverse shearing force acting on fiber cross section
r,φ,z	cylindrical coordinates
r_i,φ_i	polar radius and polar angle (i = 1,2) in the interior of unloaded fiber, defined by equation (4) respectively
r_m	radius of a cylindrical surface, defined by equation (23)
r_3,φ_3	plane polar coordinates at the interface between matrix and unloaded fiber
R	radius of curvature of a fiber element during bending
$\underset{\sim}{R}$	position vector
s	deformed length of fiber axis
S	lateral normal force per unit length acting on the fiber surface
t	$sn\zeta$
T	axial shearing force per unit length acting on the fiber surface
T_e	total potential energy of fiber during loading
U_b	strain energy due to bending of the fiber
U_e	strain energy due to shortening of the fiber
U_p	strain energy due to interfacial pressure applied by matrix on the fiber
U_s	strain energy due to longitudinal shear applied by matrix on fiber at interface

LIST OF SYMBOLS (Continued)

v	deflection of fiber
v_o	amplitude of deflection wave
V^I	volume percentage content of fiber
w	change of length of fiber axis
W	work done by external load
x,y,z	Cartesian coordinates
X	defined in equation (215)
$\overline{y}$	defined in equation (90)
Y	defined in equation (198)
z_w	buckling wavelength under shrinkage loads
α_n	parameter defined by $\alpha_n = \frac{n\pi}{L}$
$\alpha,\beta,\gamma,\delta,$ ϵ,ζ,η,μ	arbitrary constants or parameters (when subscript two or more times)
β	coefficient of shrinkage
δ	displacement normal to hexagonal boundary in load transfer problem
δ_{ij}	Kronecker delta
Δ	defined in equation (427)
$\underset{\sim}{\nabla}$	gradient operator
∇^2	Laplacian operator in cylindrical coordinates
ϵ	strain at the fiber axis
ϵ_o	half the displacement between two adjacent fibers after stress develops
ϵ_{ij}	strain components (i,j = 1,2,3) in cylindrical coordinate system
ζ	defined in equation (288)
$\overline{\theta}$	bending angle of fiber axis

LIST OF SYMBOLS (Continued)

$\varkappa$	defined in equation (296)
λ	Lagrange multiplier
μ_{mn}	eigenvalues
ν	Poisson's ratio
$\underset{\sim}{\xi}$	displacement vector
ξ_i	displacement components (i = 1,2,3) in the r, φ, and z directions, respectively
ξ_{in}	amplitudes of deflection curve
ρ	parameter defined by $\rho = \alpha_n r$
$\bar{\rho},\theta$	plane polar coordinates with origin at unloaded fiber axis
ρ_1	parameter defined by $\rho_1 = 2\alpha_n b$
ρ_2	parameter defined by $\rho_2 = \alpha_n a$
σ_ℓ	external axial stress applied at composite ends
$\bar{\sigma}_\ell$	average external composite axial stress
σ_{ij}	components of stress tensor associated with coordinate directions as indicated by subscripts
σ^o_{1i}	constants (i = 1,2,3)
τ_{ij}	functions of ρ (i,j = 1,2,3)
Φ	Airy's stress function
ψ	defined by $\psi = \frac{\pi}{6} - \varphi$
ψ_i	functions of ρ (i = 1,2,3)

Superscripts:

I,II	fiber and matrix, respectively
III	unloaded fiber in load transfer problem
( )'	differentiation with respect to ρ

Subscripts:

i,j = 1,2,3	cylindrical coordinates r, φ, and z respectively
x,y,z	rectangular Cartesian coordinates

BLANK PAGE

CHAPTER 1

INTRODUCTION

The strength-to-weight efficiency of composite materials such as glass reinforced plastics has been demonstrated, through both theoretical and experimental investigations, to be superior to that of present-day metallic materials. While the application of these materials to airframe structures obviously would be beneficial, their practical utilization has been limited because reliable structural data have not yet been developed, and because the micromechanical influence of the composite constituents, along with their failure initiation and crack propagation, has not been fully understood.

During the performance of Contract DA 44-177-AMC-208(T),* mathematical relationships were derived for a single fiber embedded in a resin cylinder for the case of static loading with general (mathematical) boundary conditions. These relationships were later extended** to encompass the unidirectional multifiber composite subjected to forces of thermal contraction during the cure cycle, as well as to external loads.

This report describes a continuation of these efforts to define the mechanical behavior of fiber reinforced plastic composites in order that optimized materials and structural concepts can be developed for airframe components of US Army aircraft. Work was devoted to the following areas:

1. Internal stresses and displacements for unidirectional composites composed of different matrix/reinforcement combinations having different volumetric contents

2. Three-dimensional load transfer among loaded and unloaded fibers in a matrix

3. Buckling of fibers in a matrix under axial load as an elasticity solution

4. Buckling of fibers in a matrix under axial load, solved with the Ritz-Galerkin method

5. Buckling of fibers in a matrix due to matrix shrinkage

---

* See USAAVLABS Technical Report 65-58.

** Contract DA 44-177-AMC-320(T); USAAVLABS Technical Report 66-62.

CHAPTER 2

SUMMARY OF RESULTS

The three-dimensional analysis of a multifiber composite, such as that depicted in Figure 1,

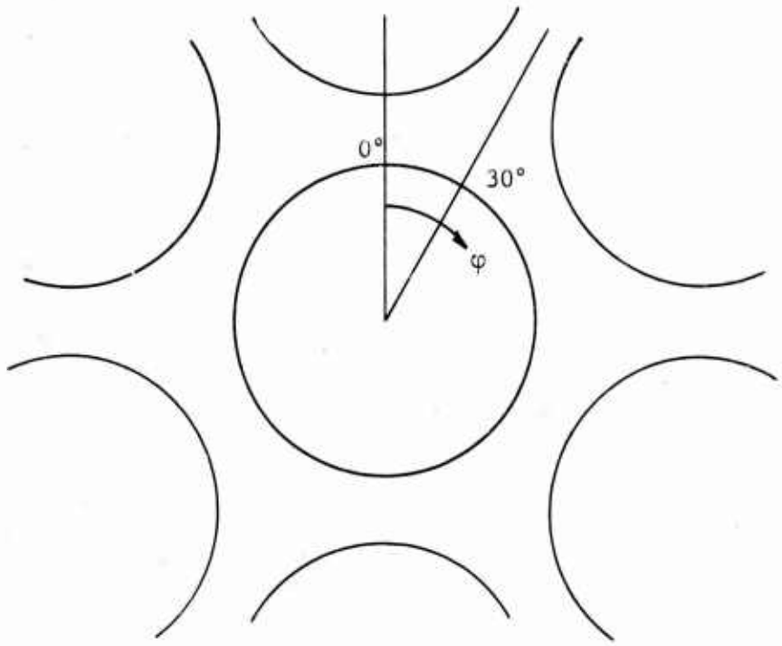

Figure 1. General Arrangement of a Multifiber Composite

reveals stresses which may not be easily anticipated by simple reasoning. For instance, under an external compression load in the direction of the fibers, a tensile stress is generated perpendicular to the fiber at $\varphi = 0°$ and becomes compressive at $\varphi = 30°$. For the tension case, these stresses are reversed. Therefore, radial tension will exist in the bond regardless of the direction of the axial load. For a 200,000-psi axial load, for example, these stresses are between 2000 and 4000* psi and, therefore, a weakening of the bond between fiber and resin occurs.

One would expect the shrinkage stresses in the resin to be universally tensile; in the radial direction of the interface, however, these stresses are compressive where the fibers are closer together ($\varphi = 0°$), and are tensile where the fibers are further apart.

One would expect the stress in the fiber direction due to resin shrinkage to be compressive. However, in high-density fiber composites, part of

* In a 64% glass reinforced epoxy composite.

this stress in the fiber is tensile due to Poisson's effect and the high radial compressive stress where the fibers were closer together. This stress seems to increase stability in closely packed composites. In an irregularly packed composite, it would tend to prebuckle the reinforcement.

The instability solution indicates that the force required to buckle a fiber in a multifiber composite is much higher than expected based on simpler analyses. One would be tempted to conclude that a densely packed composite fails under loads other than buckling.

The buckling wavelength was also an outcome of this investigation. It is remarkable that the wavelength obtained from an analysis with interfacial shear taken into account and an analysis where no interfacial shear was considered yield very similar results. From this, one might conclude that the buckling wavelength in a composite is independent of the interfacial shear. By comparing the two instability analyses, however, the buckling force was found to be very dependent on the interfacial shear.

In general, the results of the parametric studies and the instability analysis complement each other, leading to the same conclusions.

On the basis of the stresses computed during this program, it has been determined that a composite loaded in compression can have a higher fiber density than one loaded in tension.

CHAPTER 3

ANALYTICAL WORK

PART I — PARAMETRIC STUDIES

This study was made in order to investigate the stress, strain, and displacement fields in the fiber and matrix for composites under external and residual shrinkage loads. The following parameters were varied: fiber and matrix modulus, fiber radius, fiber length, and fiber volumetric content. Combinations of the above parameters were picked in order to provide data on some presently used fiber and resin materials in composites. From the analytical work, a computer program was written in order to obtain stress, strain, and displacement values in the composite. A discussion of the analytical work and the computer program is given in Appendix I.

In general, the objectives were to predict the weaknesses in a composite which would be created by residual shrinkage loads and external loading, and, if possible, to deduce simplified equations for the pertinent stress, strain, or displacement fields. Figures 2 through 28 demonstrate that these curves could be fitted by fairly simple equations which are functions of, say, φ or z , but to include the stress level in such simplified equations and determine how it varies as a function of fiber and resin modulus and of Poisson's ratio and fiber volumetric content proved to be very difficult.

Table I shows the various parametric combinations which were chosen in the study. The cases in Table I are comparable to boron/epoxy and E-glass/epoxy composites under residual shrinkage and external loading. The elastic moduli of boron and E-glass were taken as 60×10^6 psi and 10×10^6 psi, respectively. The epoxy modulus was varied for the E-glass case to obtain more pronounced effects on the field values than would be obtained for the boron epoxy cases.

The length of the boron fibers were varied to see what effects would result from the long and short boron fibers. The values for the fiber volumetric content were picked to include typical composite values (V^I = 64% and 70%) and high fiber density packing (V^I = 80%). The radius of the E-glass fiber was varied because the E-glass fiber is made with various radii, while boron fiber has a typical radius of 2 mils. Poisson's ratios for all cases were 0.2 for the fiber and 0.35 for the epoxy.

Stress, strain, and displacement fields were obtained for each case. The most revealing effects, however, occurred in the stress fields. Since it is also experimentally possible to measure the stresses, the study concentrated on the changes in the stress field due to variation of the parameters. From the computer results, the maximum and minimum values of the six stresses occurred at the fiber-resin interface. The stresses shown in the figures are therefore the stress at the interface, $r = a$. Thus, these stresses provide an indication of possible weaknesses and areas of failure in a composite.

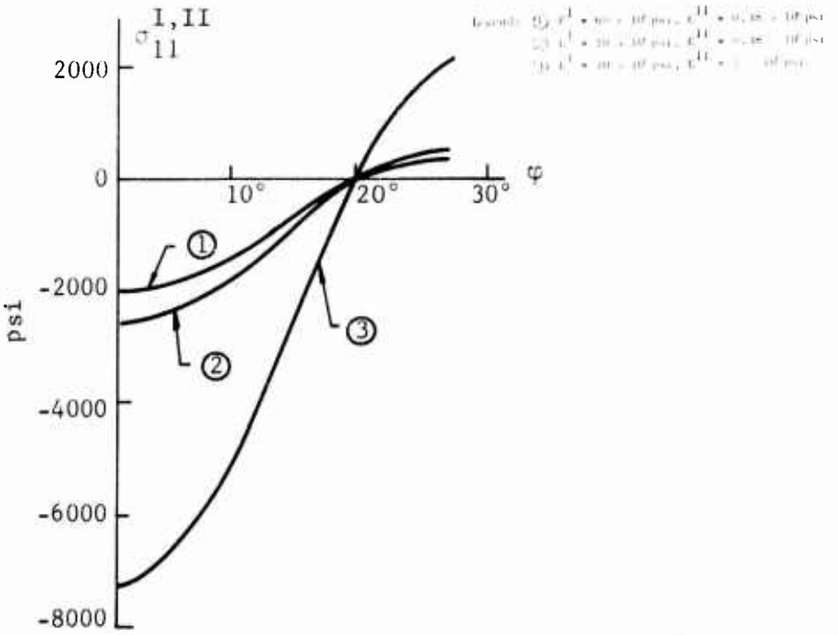

Figure 2. Residual Shrinkage Stresses at Interface for Combinations of Fiber and Resin Moduli at $V^I = 0.64$. Radial Stress versus φ

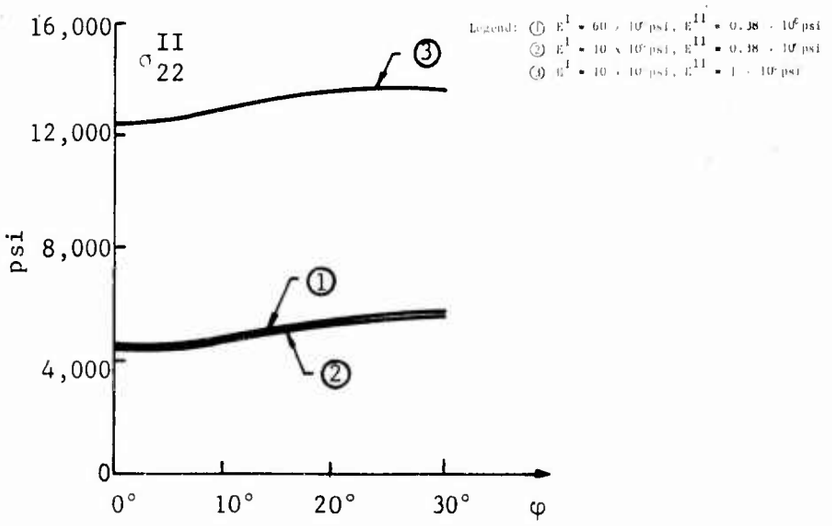

Figure 3. Residual Shrinkage Stresses at Interface for Combinations of Fiber and Resin Moduli at $V^I = 0.64$. Resin Hoop Stress versus φ

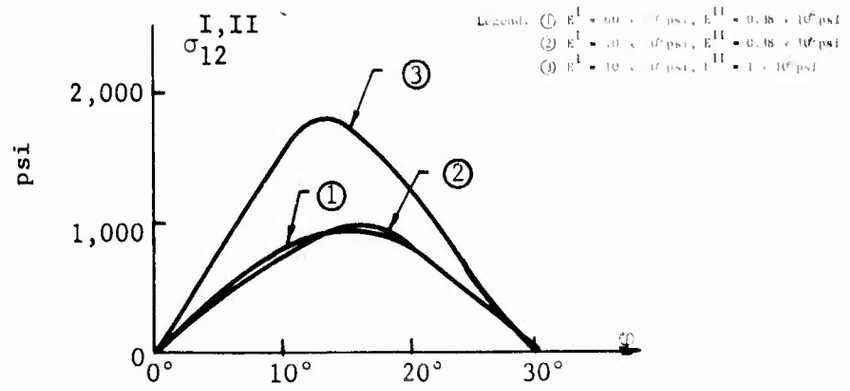

Figure 4. Residual Shrinkage Stresses at Interface for Combinations of Fiber and Resin Moduli at $V^I = 0.64$. Shear Stress versus φ

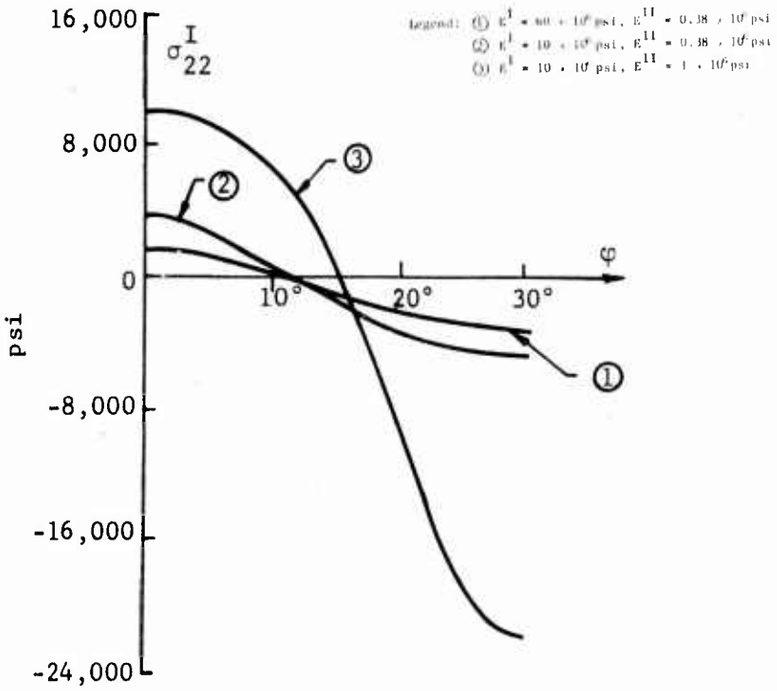

Figure 5. Residual Shrinkage Stresses at Interface for Combinations of Fiber and Resin Moduli at $V^I = 0.64$. Fiber Hoop Stress versus φ

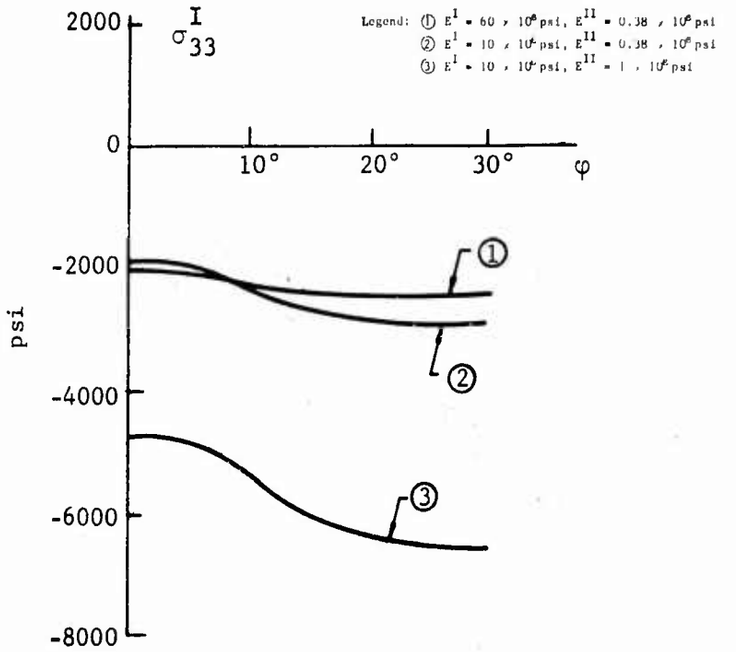

Figure 6. Residual Shrinkage Stresses at Interface for Combinations of Fiber and Resin Moduli at V^{I} = 0.64. Fiber Axial Stress versus φ

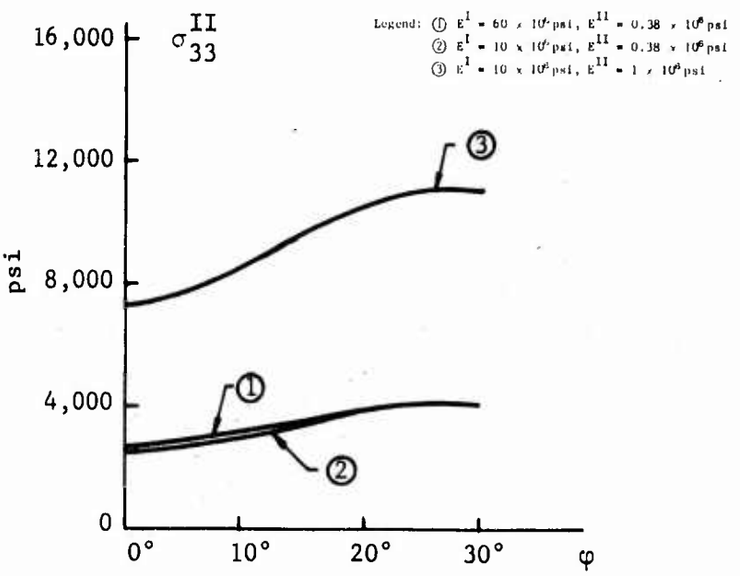

Figure 7. Residual Shrinkage Stresses at Interface for Combinations of Fiber and Resin Moduli at V^{I} = 0.64. Resin Axial Stress versus φ

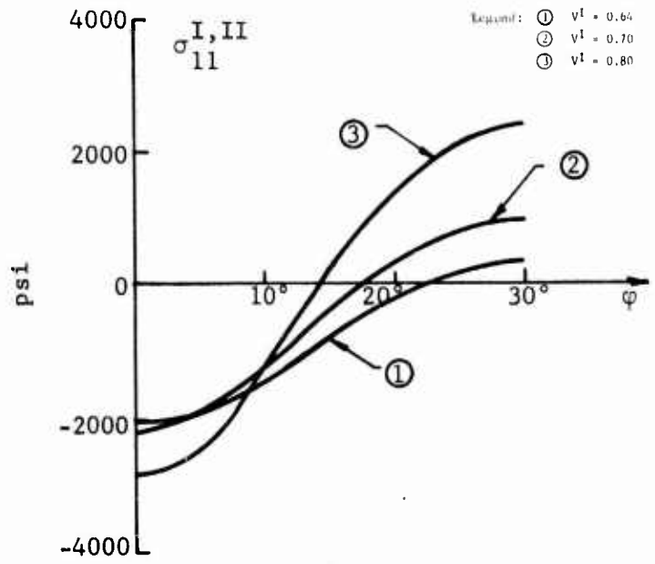

Figure 8. Residual Shrinkage Stresses at Interface When $E^I = 60 \times 10^6$ psi and $E^{II} = 0.38 \times 10^6$ psi for Different Fiber Volumetric Content. Radial Stress versus φ

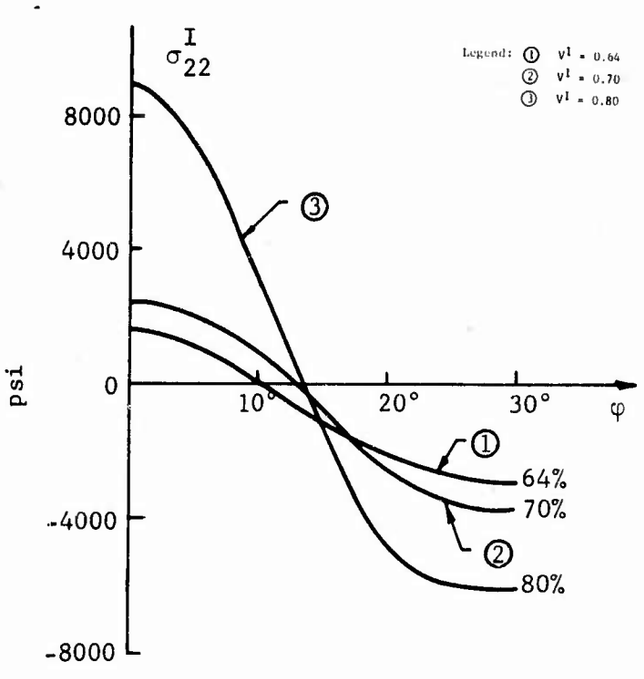

Figure 9. Residual Shrinkage Stresses at Interface When $E^I = 60 \times 10^6$ psi and $E^{II} = 0.38 \times 10^6$ psi for Different Fiber Volumetric Content. Fiber Hoop Stress versus φ

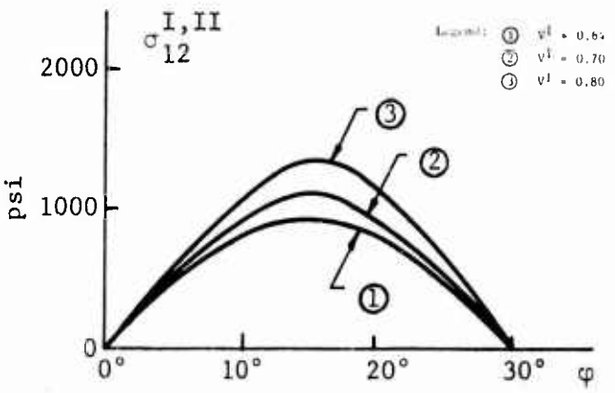

Figure 10. Residual Shrinkage Stresses at Interface When $E^{I} = 60 \times 10^{6}$ psi and $E^{II} = 0.38 \times 10^{6}$ psi for Different Fiber Volumetric Content. Shear Stress versus φ

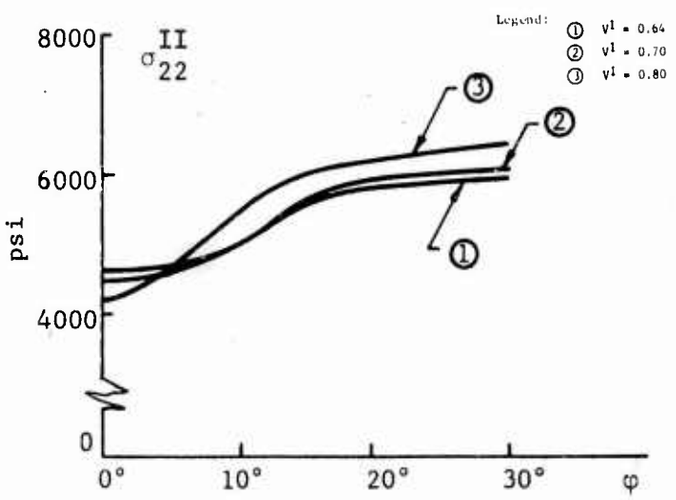

Figure 11. Residual Shrinkage Stresses at Interface When $E^{I} = 60 \times 10^{6}$ psi and $E^{II} = 0.38 \times 10^{6}$ psi for Different Fiber Volumetric Content. Resin Hoop Stress versus φ

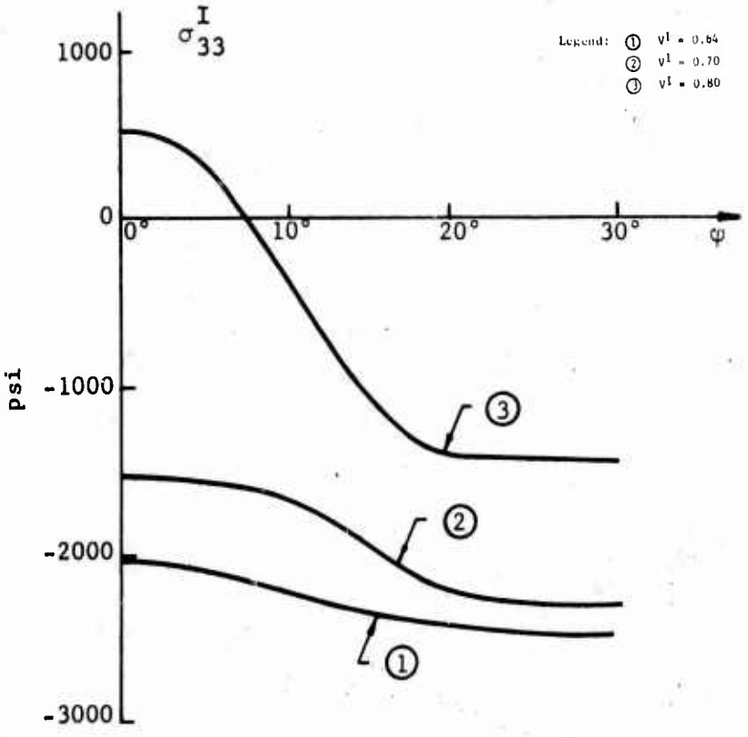

Figure 12. Residual Shrinkage Stresses at Interface When $E^I = 60 \times 10^6$ psi and $E^{II} = 0.38 \times 10^6$ psi for Different Fiber Volumetric Content. Fiber Axial Stress

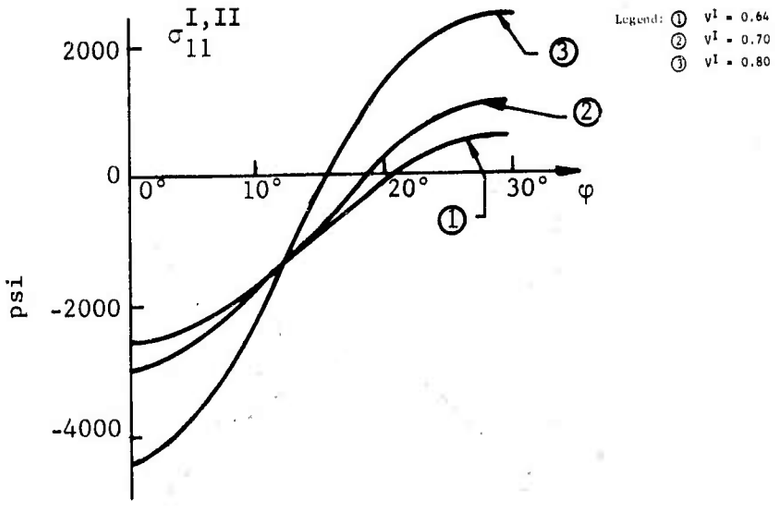

Figure 13. Residual Shrinkage Stresses at Interface When $E^I = 10 \times 10^6$ psi and $E^{II} = 0.38 \times 10^6$ psi for Different Fiber Volumetric Content. Radial Stress versus φ

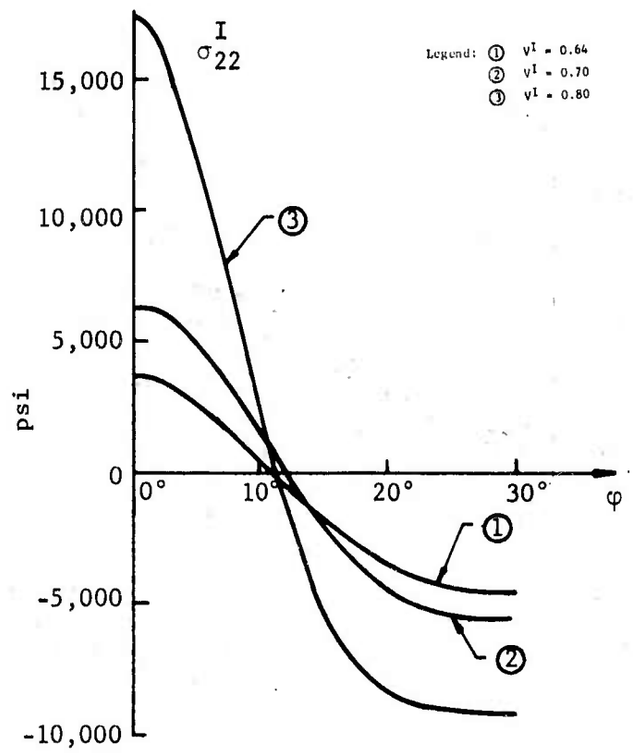

Figure 14. Residual Shrinkage Stresses at Interface When $E^I = 10 \times 10^6$ psi and $E^{II} = 0.38 \times 10^6$ psi for Different Fiber Volumetric Content. Fiber Hoop Stress versus φ

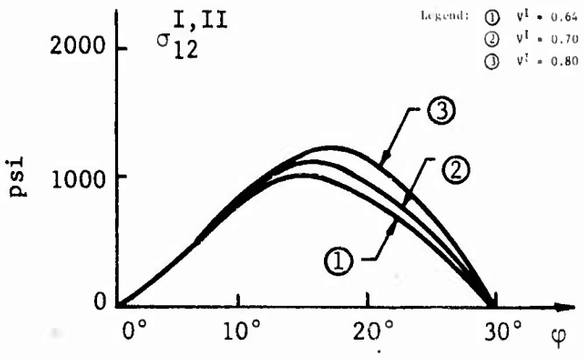

Figure 15. Residual Shrinkage Stresses at Interface When $E^I = 10 \times 10^6$ psi and $E^{II} = 0.38 \times 10^6$ psi for Different Fiber Volumetric Content. Shear Stresses versus φ

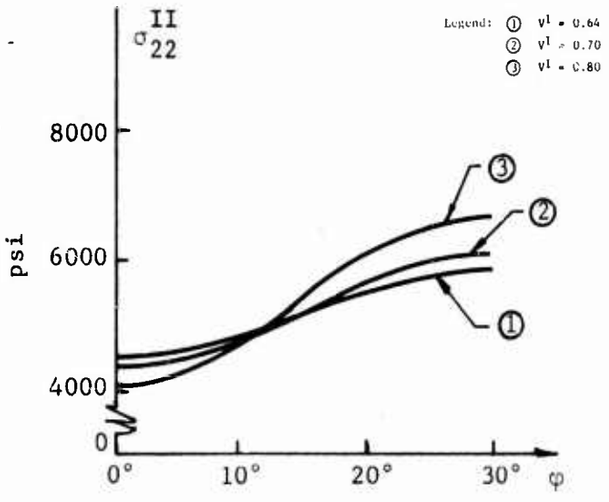

Figure 16. Residual Shrinkage Stresses at Interface When $E^I = 10 \times 10^6$ psi and $E^{II} = 0.38 \times 10^6$ psi for Different Fiber Volumetric Content. Resin Hoop Stress versus φ

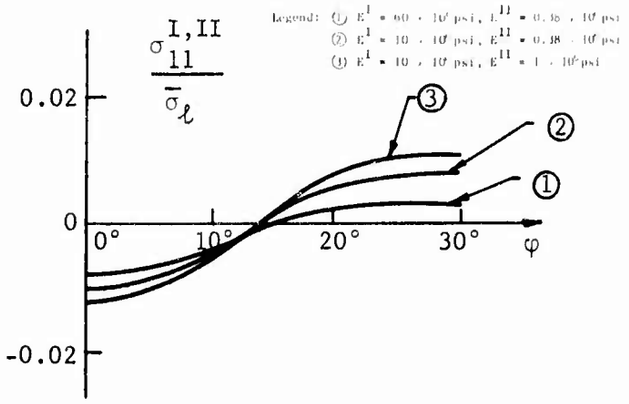

Figure 17. Stresses at Interface Due to External Load for Combinations of Fiber and Resin Moduli at V^I = 0.64. Radial Stress versus φ

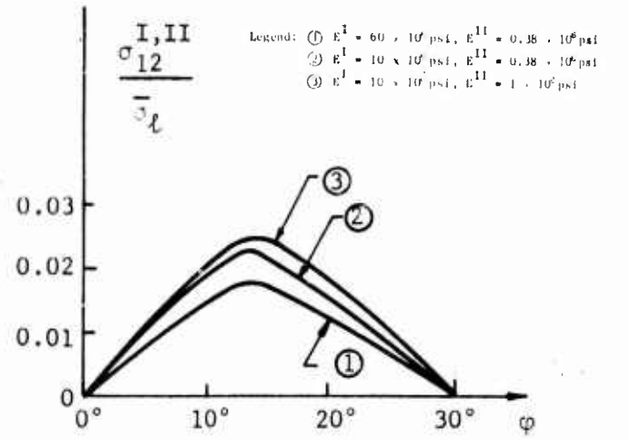

Figure 18. Stresses at Interface Due to External Load for Combinations of Fiber and Resin Moduli at V^I = 0.64. Shear Stress versus φ

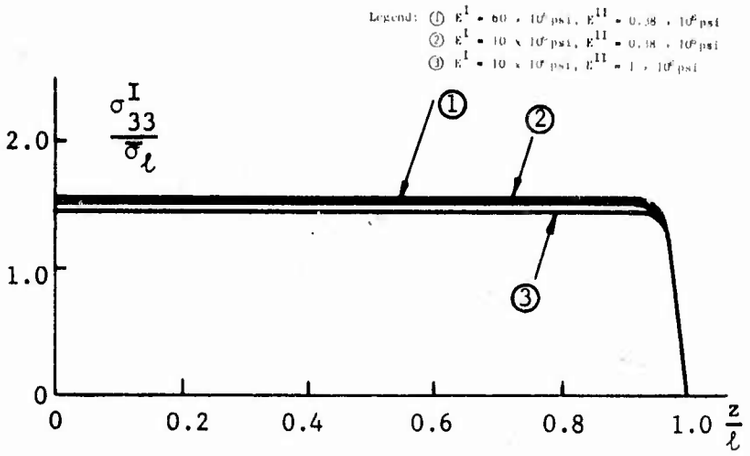

Figure 19. Stresses at Interface Due to External Load for Combinations of Fiber and Resin Moduli at $V^I = 0.64$. Fiber Axial Stress versus z/ℓ

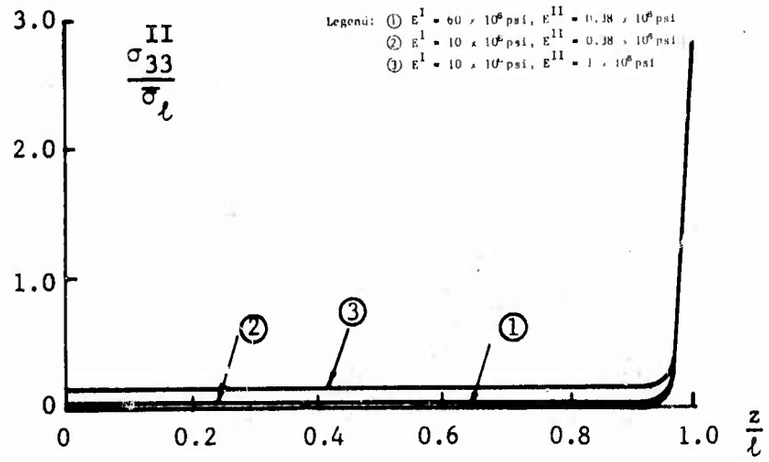

Figure 20. Stresses at Interface Due to External Load for Combinations of Fiber and Resin Moduli at $V^I = 0.64$. Resin Axial Stress versus z/ℓ

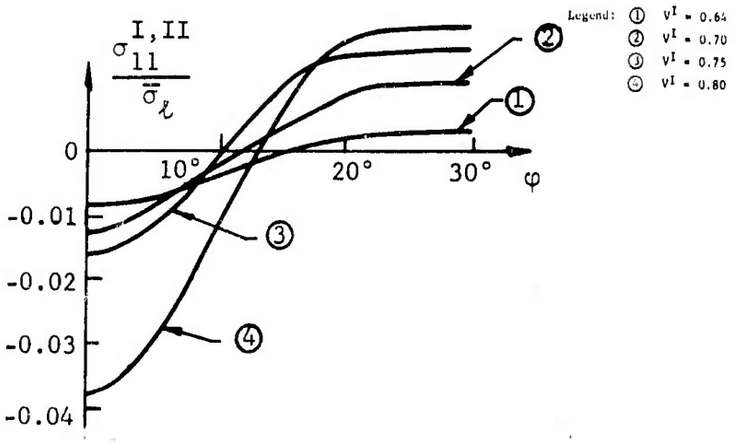

Figure 21. Stresses at Interface Due to External Load When $E^I = 60 \times 10^6$ psi and $E^{II} = 0.38 \times 10^6$ psi for Different Fiber Volumetric Content. Radial Stress versus φ

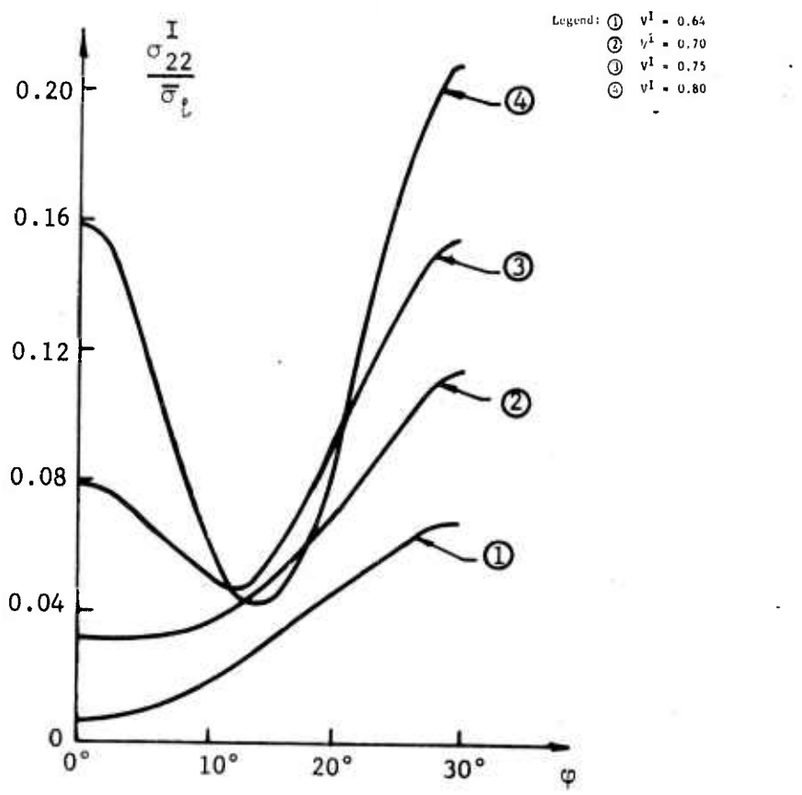

Figure 22. Stresses at Interface Due to External Load When $E^I = 60 \times 10^6$ psi and $E^{II} = 0.38 \times 10^6$ psi for Different Fiber Volumetric Content. Fiber Hoop Stress versus φ

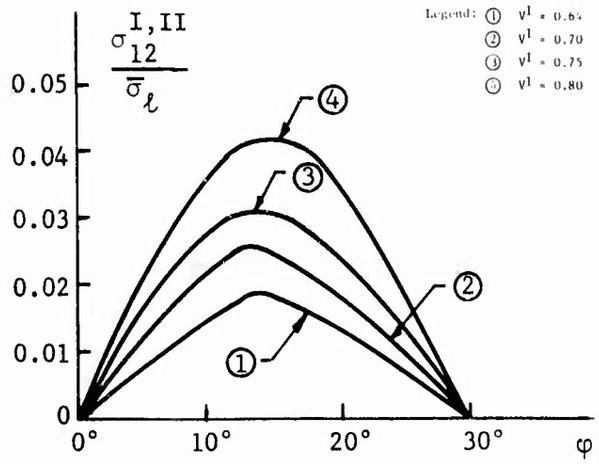

Figure 23. Stresses at Interface Due to External Load When $E^I = 60 \times 10^6$ psi and $E^{II} = 0.38 \times 10^6$ psi for Different Fiber Volumetric Content. Shear Stress versus φ

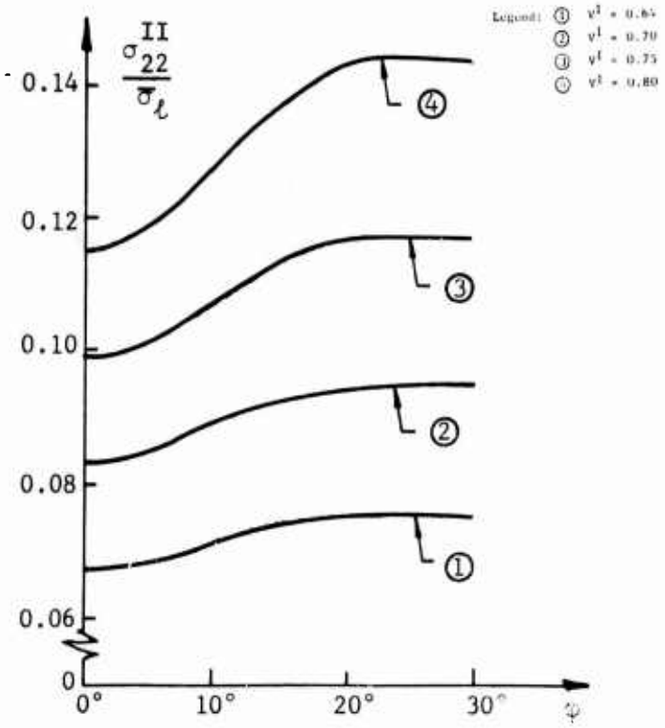

Figure 24. Stresses at Interface Due to External Load When $E^I = 60 \times 10^6$ psi and $E^{II} = 0.38 \times 10^6$ psi for Different Fiber Volumetric Content. Resin Hoop Stress versus φ

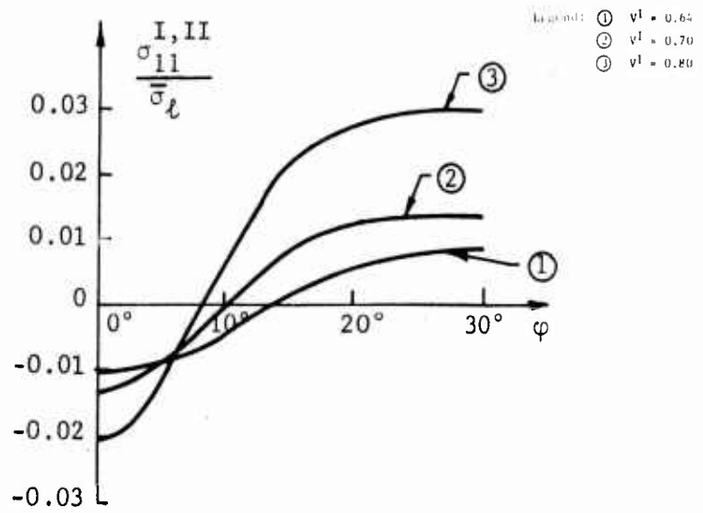

Figure 25. Stresses at Interface Duc to External Load When $E^I = 10 \times 10^6$ psi and $E^{II} = 0.38 \times 10^6$ psi for Different Fiber Volumetric Content. Radial Stress versus φ

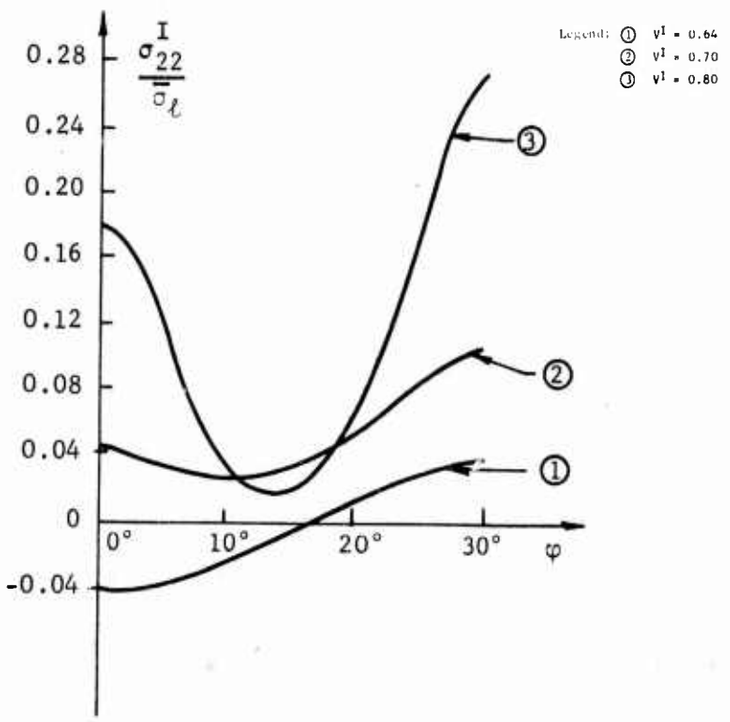

Figure 26. Stresses at Interface Due to External Load When $E^I = 10 \times 10^6$ psi and $E^{II} = 0.38 \times 10^6$ psi for Different Fiber Volumetric Content. Hoop Stress versus φ

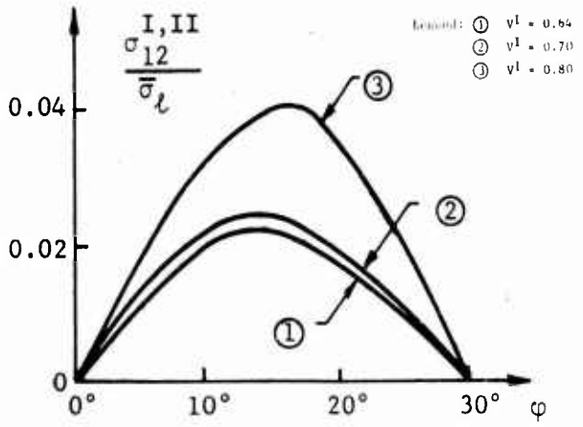

Figure 27. Stresses at Interface Due to External Load When $E^I = 10 \times 10^6$ psi and $E^{II} = 0.38 \times 10^6$ psi for Different Fiber Volumetric Content. Fiber Shear Stress versus φ

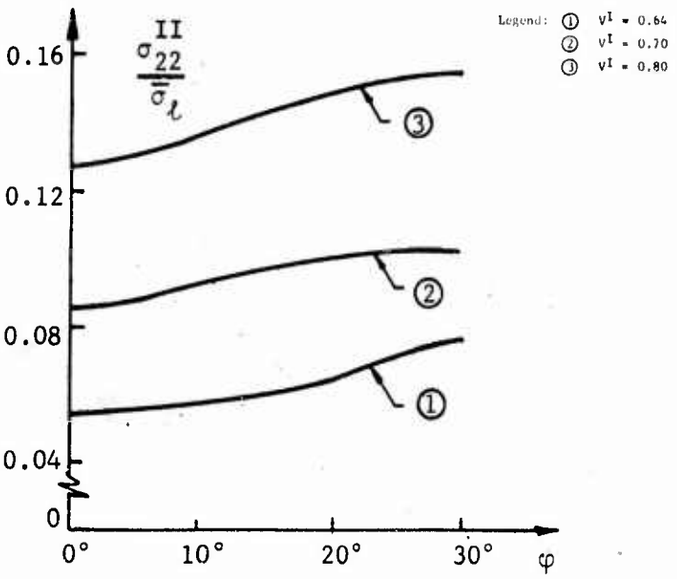

Figure 28. Stresses at Interface Due to External Load When $E^I = 10 \times 10^6$ psi and $E^{II} = 0.38 \times 10^6$ psi for Different Fiber Volumetric Content. Resin Hoop Stress versus φ

TABLE I

CASES USED FOR THE PARAMETRIC STUDY

Parameters					
Fiber Modulus, 10^6 psi	General State of Stress*	Fiber Radius, 10^{-3} in.	Fiber Length, in.	Epoxy Modulus, 10^6 psi	Fiber Vol. Content, %
60	S	2	3	0.38	64
↓	↓	↓	↓	↓	70
					80
			0.5		64
			10.0		↓
	L		3		
	↓		↓		70
					75
↓	↓	↓			80
10	S	2.5			64
↓	↓	↓			70
					80
				1.0	64
		5.0		0.38	↓
	L	2.5		↓	
	↓	↓			70
					80
↓		↓		1.0	64
		5.0		1.0	64

* S = resin shrinkage which includes both cure shrinkage and differential thermal contraction.

L = constant load applied at the ends on the resin.

Also, the computer results indicate that the stress field away from the ends of the fiber has little dependence on the z coordinate. In Figures 2 through 7, then, the stresses which are not plotted as functions of z/ℓ can be considered as constant away from the fiber ends with respect to the z coordinate.

Residual Shrinkage Load

From the cases shown in Table I, the effects of changing the following parameters can be investigated for the residual shrinkage load. In all these cases, the fiber shrinkage was zero and the resin shrinkage was 1%.

1. Changes in the Combinations of Fibers and Resin Modulus at $V_f = 0.64$

The three combinations of fiber and resin moduli are shown in Table II.

TABLE II

COMBINATIONS OF FIBER AND RESIN MODULI

$E^I(10^6 \text{ psi})$	60	10	10
$E^{II}(10^6 \text{ psi})$	0.38	0.38	1.0

The change from a fiber modulus of 60×10^6 psi to 10×10^6 psi did not have much effect on the shrinkage stresses. However, changing the resin modulus from 0.38×10^6 psi to 1×10^6 psi increased the stresses, σ_{11}^I, σ_{11}^{II}, and σ_{22}^{II}, by a factor of 1 divided by 0.38. In other words, when the ratio of resin to fiber moduli is small, the change of residual stresses, σ_{11}^I, σ_{11}^{II}, and σ_{22}^{II}, is proportional to the change in resin modulus. See Figures 2 and 3. Three other stresses, σ_{12}^I, σ_{12}^{II}, and σ_{22}^I, are shown in Figures 4 and 5.

Figures 6 and 7 indicate a possible ±20% variation in the axial residual stress in both the resin and the fiber.

2. Changes in the Fiber Volumetric Content

Figures 8 through 16 show the effects on the stresses due to fiber volumetric content. Figures 8 and 13 reveal a possible weakness in the composite. The radial stress along the interface has positive values. If

this stress were large enough, the fiber-resin interface could fail and the composite effectiveness would be lowered. Also the shear stress at the interface (Figures 10 and 15) would additionally stress the interface bond. It is also noted that increasing the fiber volumetric content in general increases the maximum stresses at the interface.

The fiber axial stress, shown in Figure 12, indicates another composite weakness. Since the residual stress in part of the fiber is positive for $V^I = 0.80$, the fiber will fail at a lower stress level when a tensile load is applied to it. From Figure 12, the residual positive stress will become even higher for higher volumetric content.

3. Changes in Fiber Radius at $V^I = 0.64$

The fiber radius was doubled, from 0.0025 to 0.005; no effects within the accuracy of the calculations could be seen in the stress fields.

4. Changes in the Fiber Length at $V^I = 0.64$

The fiber length was taken at 10 inches, 3 inches, and 0.5 inch. There were no effects within the accuracy of the calculations on the stress field.

Externally Applied Load

From the cases shown in Table I, the effects of changing the following parameters can be investigated for an externally applied load. In Figures 17 through 28, the stress is divided by the average external load.

1. Changes in the Combination of Fiber and Resin Moduli

The three combinations of fiber and resin moduli for fixed fiber volumetric content, $V^I = 0.64$, are shown in Table II. In general, the stresses in the plane perpendicular to the fiber axis were not affected much (see Figures 17 through 20). However, the radial stresses at the interface would indicate weaknesses in the bond. Since the radial stress goes from minus to plus for $\varphi = 0°$ to $\varphi = 30°$, there will be tension in the bond regardless of whether the axial load is tension or compression. For a compression load, $\bar{\sigma}_\ell < 0$, the results in Figure 17 would tend to cancel the residual stresses in Figure 2, but the radial stresses for a tensile load will add to the residual stresses and weaken the bond even further.

The axial stresses, σ_{33}^{I} and σ_{33}^{II} , for the three combinations were independent of φ and within ±5% of the stresses calculated by the following simple equations.

$$\sigma_{33}^{I} = \frac{E^{I}\,\bar{\sigma}_{\ell}}{E^{I}\,V^{I} + E^{II}\left(1 - V^{I}\right)}$$

$$\sigma_{33}^{II} = \frac{E^{II}\,\bar{\sigma}_{\ell}}{E^{I}\,V^{I} + E^{II}\left(1 - V^{I}\right)}$$

These equations for the axial stress due to external load are valid for higher fiber volumetric content, as will be described in the next section.

In addition to the radial stress, the shear stress at the interface (see Figure 18), when superimposing the residual shrinkage and external load, will also increase the total shear for tensile load and reduce the shear for compressive load.

The axial stress for fiber and resin is shown in Figures 19 and 20 respectively.

2. Changes in Fiber Volumetric Content

The values for the fiber volumetric content were normally 0.64, 0.70, and 0.80. However, an unusual change in the fiber hoop stress occurred when fiber content was changed from 0.70 to 0.80 (see Figures 22 and 27). As a result, an additional value of fiber content, 0.75, was taken to determine whether the fiber hoop stress change was abrupt or gradual. From Figure 22, this stress distribution occurred between a fiber content of 0.70 and 0.80, and can be expected to be more pronounced beyond 0.80 fiber content.

The radial stresses from external load were similar to the previous results. The maximum stress is positive and the minimum is negative, and they both increase in magnitude as the fiber volumetric content increases.

The axial stresses were of the same magnitude as calculated from the equations in the previous section.

3. Changes in the Fiber Radius at $V^{I} = 0.64$

There was no effect on the stress fields due to a change in the fiber radius from 0.0025 inch to 0.005 inch for externally applied load at constant volumetric content.

PART II — THREE-DIMENSIONAL LOAD TRANSFER AMONG THE FIBERS IN A MATRIX

The fact that uneven loading occurs in a composite material, especially near the boundaries and near microfractures, makes it necessary to understand the load transfer among the filaments. Since an arbitrary arrangement would create insurmountable mathematical difficulties, the mathematical model chosen was one of periodically repeating characteristics. The unidirectional fibers were assumed to be in a hexagonal array, with every third fiber axially stressed by an external load. The rest of the fibers were assumed to be stressed by load transmission through the matrix, which was the main subject of this portion of the investigation.

A. General Arrangements and Assumptions

The composite is considered to be free from residual stresses, and axially finite but laterally infinite. Figure 29 depicts part of the cross section of the composite, with the shadowed circles representing the externally stressed fibers.

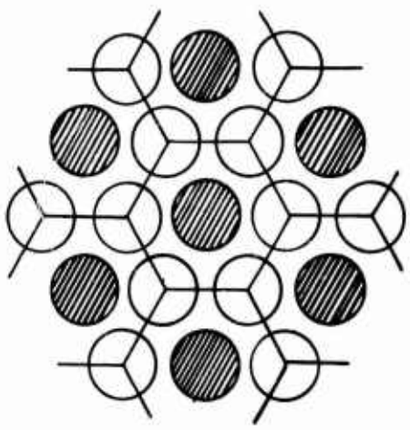

Figure 29. Geometric Arrangement of Fibers in a Unidirectional Multifiber Composite

Displacements and stresses of a typical hexagonal segment in the composite will be determined by assuming that the segment before deformation changes size yet remains hexagonal after deformation. However, an undeformed cross-sectional plane of the segment may not remain plane during deformation. Therefore, the segment is treated by the classical theory of elasticity as a three-dimensional body.

Since displacements and stresses in fibers and matrix are hexagonally symmetric, a triangular prism of the hexagonal segment with its cross section Δ O C D and coordinate systems as shown in Figure 30 will be studied.

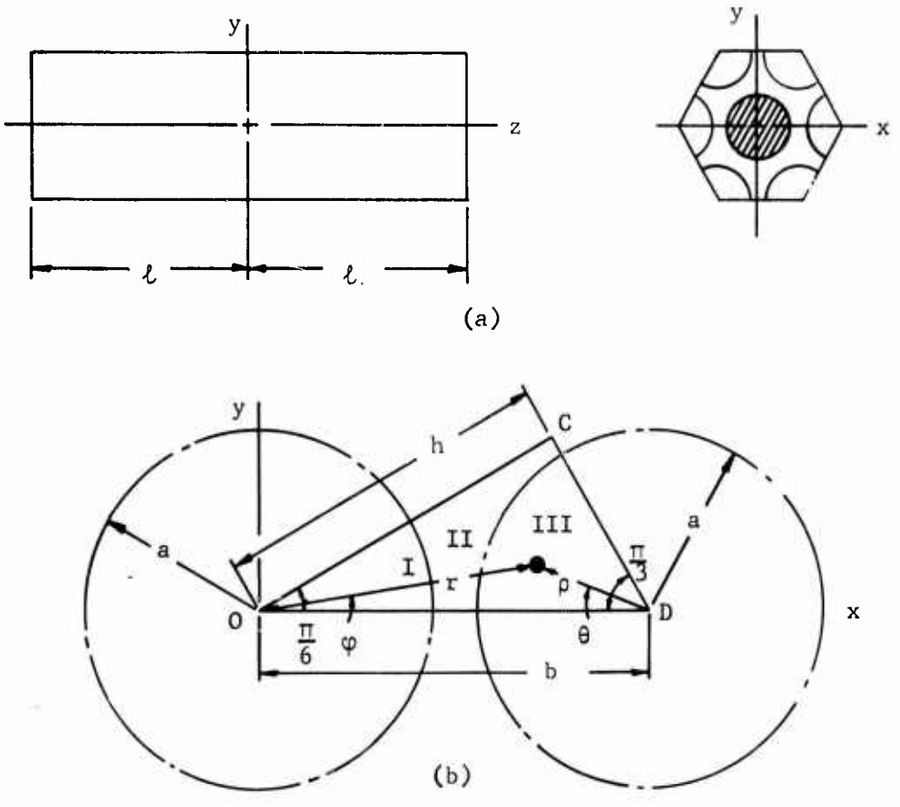

Figure 30. Geometry of a Typical Segment in the Composite

The natural way to attack the problem is to divide the prism into loaded fiber (domain I), matrix (domain II), and unloaded fiber (domain III), at their interfaces. The elasticity solution derived from Papkovitch functions is then applied to each of these domains by determining arbitrary constants with appropriate physical conditions. The present domains are now defined as

Domain I (Loaded Fiber):

$$0 \le r \le a \quad , \quad 0 \le \varphi \le \frac{\pi}{6} \quad , \quad -\ell \le z \le \ell$$

Domain II (Matrix):

$$a \le r \le \left[a^2 \sin\theta + (b - a\cos\theta)^2\right]^{1/2}$$

for $0 \le \varphi \le \frac{\pi}{6} - \tan^{-1}\left(\frac{b-2a}{2h}\right)$

$$a \le r \le h \sec\left(\frac{\pi}{6} - \varphi\right)$$

for $\frac{\pi}{6} - \tan^{-1}\left(\frac{b-2a}{2h}\right) \le \varphi \le \frac{\pi}{6}$

$$-\ell \le z \le \ell$$

Domain III (Unloaded Fiber):

$$\left[a^2 \sin^2\theta + (b - a\cos\theta)^2\right]^{1/2} \le r \le h \sec\left(\frac{\pi}{6} - \varphi\right)$$

$$0 \le \varphi \le \frac{\pi}{6} - \tan^{-1}\left(\frac{b-2a}{2h}\right)$$

$$-\ell \le z \le \ell$$

The quantities a, b, h, ℓ, and θ are defined in Figure 30.

B. Formulation of Physical Conditions

The symmetry of radial, circumferential, and axial displacements ξ_i $(i = 1,2,3)$ with respect to zx- and xy-planes dictates that in loaded fiber, matrix, and unloaded fiber,

$$\xi_1^k(r,\varphi,z) = \xi_1^k(r,-\varphi,z) = \xi_1^k(r,\varphi,-z)$$

$$\xi_2^k(r,\varphi,z) = \xi_2^k(r,-\varphi,z) = \xi_2^k(r,\varphi,-z)$$

$$\xi_3^k(r,\varphi,z) = \xi_3^k(r,-\varphi,z) = \xi_3^k(r,\varphi,-z) \qquad (1)$$

where the superscript k refers to the corresponding domains I, II, or III.

The periodic characteristic of displacements in loaded fiber, matrix, and unloaded fiber leads to

$$\xi_i^k(r,\varphi,z) = \xi_i^k\left(r,\varphi + \frac{\pi}{3},z\right) \tag{2}$$

where $k = I,II$, and $i = 1,2,3$.

$$\xi_2^{III}\left(r_1,\varphi_1,z\right) \sin\left(\varphi_1 + \theta\right) - \xi_1^{III}\left(r_1,\varphi_1,z\right) \cos\left(\varphi_1 + \theta\right)$$

$$= \xi_1^{III}\left(r_2,\varphi_2,z\right) \cos\left(\frac{\pi}{3} - \theta - \varphi_2\right) + \xi_2^{III}\left(r_2,\varphi_2,z\right) \sin\left(\frac{\pi}{3} - \theta - \varphi_2\right)$$

$$\xi_2^{III}\left(r_1,\varphi_1,z\right) \cos\left(\varphi_1 + \theta\right) + \xi_1^{III}\left(r_1,\varphi_1,z\right) \sin\left(\varphi_1 + \theta\right)$$

$$= \xi_1^{III}\left(r_2,\varphi_2,z\right) \sin\left(\frac{\pi}{3} - \theta - \varphi_2\right) - \xi_2^{III}\left(r_2,\varphi_2,z\right) \cos\left(\frac{\pi}{3} - \theta - \varphi_2\right)$$

$$\xi_3^{III}\left(r_1,\varphi_1,z\right) = \xi_3^{III}\left(r_2,\varphi_2,z\right) \tag{3}$$

The values of r_1 , φ_1 , r_2 , φ_2 in equation (3) are expressed in terms of another set of polar coordinates $\rho(0 \le \rho \le a)$ and $\left(\Theta\ 0 \le \Theta \le \frac{\pi}{6}\right)$ with its origin at D (see Figure 31).

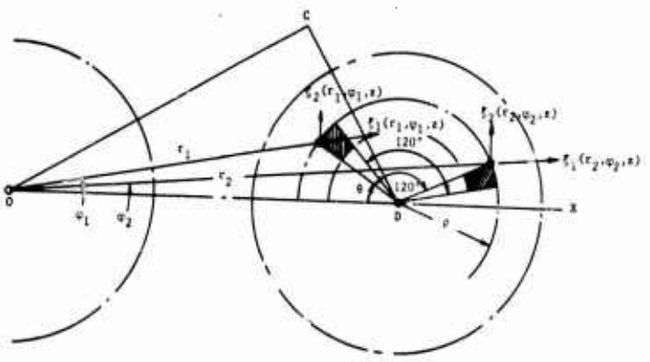

Figure 31. Periodic Characteristic of the Unloaded Fiber

These values are given by

$$r_1 = \sqrt{\rho^2 \sin^2\theta + (b - \rho\cos\theta)^2}$$

$$\varphi_1 = \tan^{-1}\frac{\rho\sin\theta}{b - \rho\cos\theta}$$

$$r_2 = \sqrt{\rho^2 \sin^2\left(\theta + \frac{2\pi}{3}\right) + \left[b - \rho\cos\left(\theta + \frac{2\pi}{3}\right)\right]^2}$$

$$\varphi_2 = \tan^{-1}\frac{\rho\sin\left(\theta + \frac{2\pi}{3}\right)}{b - \rho\cos\left(\theta + \frac{2\pi}{3}\right)} \qquad (4)$$

Equation (2) states that the displacement vectors of matrix and externally stressed fiber possess sixfold symmetry. Equations (3) are the condition that radial, tangential, and axial displacements of the unloaded fiber with respect to its axis are identical for every multiple of $2\pi/3$ of the polar angle θ .

If continuity in displacements ξ_i and appropriate stresses σ_{1i} at the interface exist, then

$$\xi_i^{I}(a,\varphi,z) = \xi_i^{II}(a,\varphi,z)$$

$$\sigma_{1i}^{I}(a,\varphi,z) = \sigma_{1i}^{II}(a,\varphi,z)$$

$$\xi_i^{II}\left(r_3,\varphi_3,z\right) = \xi_i^{III}\left(r_3,\varphi_3,z\right) \qquad (5)$$

where $i = 1,2,3$.

$$\left[\sigma_{11}^{II}\left(r_3,\varphi_3,z\right) - \sigma_{11}^{III}\left(r_3,\varphi_3,z\right)\right] \cos^2\left(\varphi_3 + \theta\right) +$$

$$\left[\sigma_{22}^{II}\left(r_3,\varphi_3,z\right) - \sigma_{22}^{III}\left(r_3,\varphi_3,z\right)\right] \sin^2\left(\varphi_3 + \theta\right) -$$

$$\left[\sigma_{12}^{II}\left(r_3,\varphi_3,z\right) - \sigma_{12}^{III}\left(r_3,\varphi_3,z\right)\right] \sin 2\left(\varphi_3 + \theta\right) = 0$$

$$\sigma_{11}^{II}\left(r_3,\varphi_3,z\right) - \sigma_{11}^{III}\left(r_3,\varphi_3,z\right) - \sigma_{22}^{II}\left(r_3,\varphi_3,z\right) + \sigma_{22}\left(r_3,\varphi_3,z\right) +$$

$$2\left[\sigma_{12}^{II}\left(r_3,\varphi_3,z\right) - \sigma_{12}^{III}\left(r_3,\varphi_3,z\right)\right] \cot 2\left(\varphi_3 + \theta\right) = 0$$

$$\left[\sigma_{13}^{II}\left(r_3,\varphi_3,z\right) - \sigma_{13}^{III}\left(r_3,\varphi_3,z\right)\right] \cos\left(\varphi_3 + \theta\right) -$$

$$\left[\sigma_{23}^{II}\left(r_3,\varphi_3,z\right) - \sigma_{23}^{III}\left(r_3,\varphi_3,z\right)\right] \sin\left(\varphi_3 + \theta\right) = 0 \qquad (6)$$

where

$$r_3 = \left[a^2 \sin^2\theta + (b - a\cos\theta)^2\right]^{1/2}, \quad \varphi_3 = \tan^{-1}\left(\frac{a \sin\theta}{b - a\cos\theta}\right) \qquad (7)$$

For a given value of Θ in the range $0 \le \Theta \le \frac{\pi}{3}$, the values of r_3 and φ_3 calculated by equation (7) are the coordinates of a point at the interface between domains II and III. Equations (6) are the continuity condition on normal stress in the ρ direction and circumferential and axial shearing stresses at the interface between domains II and III.

In order that the fibers remain in the regular hexagonal arrangement during deformation, the displacement normal to the hexagonal boundary must be a constant, denoted by

$$\xi_1^k(h \sec\psi,\varphi,z) \cos\psi + \xi_2^k(h \sec\psi,\varphi,z) \sin\psi = \delta \qquad (8)$$

$$k = II, III$$

where

$$\psi = \frac{\pi}{6} - \varphi \tag{9}$$

Note that the vanishing of the circumferential displacements ξ_2 at the lines OC and OD (Figure 30) will be automatically satisfied once the symmetry condition (1) is fulfilled.

Now that the hexagonal boundary is a symmetrical plane, shearing stresses vanish at the boundary. Thus, in the directions of the boundary line CD and the z axis,

$$\sigma^k_{11}(h\ \sec\psi,\varphi,z) - \sigma^k_{22}(h\ \sec\psi,\varphi,z)$$

$$- 2\ \sigma^k_{12}(h\ \sec\psi,\varphi,z)\ \cot 2\psi = 0$$

$$\sigma^k_{13}(h\ \sec\psi,\varphi,z) + \sigma^k_{23}(h\ \sec\psi,\varphi,z)\ \tan\psi = 0 \tag{10}$$

$$k = II, III$$

If the axial stress applied at the ends of the central fiber as shown in Figure 30(a) is denoted by σ_o, the appropriate condition is

$$\sigma^I_{33}(r,\varphi,\pm\ell) = \sigma_o \tag{11}$$

and if the ends of other fibers and matrix are free from axial stresses, then

$$\sigma^k_{33}(r,\varphi,\pm\ell) = 0 \tag{12}$$

$$k = II, III$$

It can be seen from the hexagonal symmetry that shearing forces acting at the ends of a hexagonal segment automatically vanish as soon as the condition (2) is fulfilled. If the ends are required to be free from shearing stresses, then

$$\sigma_{3i}^{k}(r,\varphi,\pm\ell) = 0 \qquad (13)$$

$$k = I,II,III \quad i = 1,2$$

The formulation of physical conditions is now complete. In total, we have 54 conditions to be satisfied in this analysis. The solution derived from Papkovitch-Neuber functions for the deformation of each domain must satisfy appropriate conditions as described above.

C. General Displacements and Stresses

An elasticity solution derived from Papkovitch functions was given in a previous report (Reference 1). If nonperiodic terms are taken into account, the solution to Laplace's equation $\nabla^2 P_j = 0$ can be written as

$$\begin{aligned} P_j = {} & \sum_{n>0} \sum_{k>0} \left[\alpha_{jnk} I_n(\mu r) + \beta_{jnk} K_n(\mu r)\right] \cdot \left[\gamma_{jnk} \sin(\mu z) + \right. \\ & \left. \delta_{jnk} \cos(\mu z)\right] \cdot \epsilon_{jn} \sin(n\varphi) + \zeta_{jn} \cos(n\varphi)\Big] + \\ & \sum_{n>0} \left(\alpha_{jno} r^{n} + \beta_{jno} r^{-n}\right)\left(\gamma_{jno} + \delta_{jno} z\right)\left[\epsilon_{jn} \sin(n\varphi) + \right. \\ & \left. \zeta_{jn} \cos(n\varphi)\right] + \sum_{k>0} \left[\alpha_{jok} I_o(\mu r) + \beta_{jok} K_o(\mu r)\right] \cdot \left[\gamma_{jok} \sin(\mu z) + \right. \\ & \left. \delta_{jok} \cos(\mu z)\right] \cdot \left(\epsilon_{jo} + \zeta_{jo} z\right) + \left(\alpha_{joo} + \beta_{joo} \log r\right)\left(\gamma_{joo} + \right. \\ & \left. \delta_{joo} z\right)\left(\epsilon_{jo} + \zeta_{jo} \varphi\right) \end{aligned} \qquad (14)$$

$$j = 0,3$$

where P_o is a scalar Papkovitch function and P_3 the component of the Papkovitch vector in the axial direction, and where α , β , γ , δ , ϵ , ζ , η , and μ are arbitrary constants. The solution P_j can be expressed in terms of Bessel functions of first and second kinds of r , hyperbolic functions of z , and trigonometric functions of φ . However, solution (14) has the advantage that the argument of modified Bessel functions $I_n(\mu r)$ and $K_n(\mu r)$ is real in this work.

The solution to the following equations,

$$\nabla^2 \left(P_1 \cos\varphi - P_2 \sin\varphi \right) = 0$$

$$\nabla^2 \left(P_1 \sin\varphi + P_2 \cos\varphi \right) = 0 \qquad (15)$$

can be written in a similar form, and the Papkovitch functions P_i and P_z in radial and circumferential directions can be determined from these two solutions.

Displacement components are related to Papkovitch functions by

$$\xi_1 = P_1 - \frac{1}{4(1-\nu)} \frac{\partial}{\partial r} \left[rP_1 + zP_3 + P_o \right]$$

$$\xi_2 = P_2 - \frac{1}{4(1-\nu)} \frac{\partial}{r\partial\varphi} \left[rP_1 + zP_3 + P_o \right]$$

$$\xi_3 = P_3 - \frac{1}{4(1-\nu)} \frac{\partial}{\partial z} \left[rP_1 + zP_3 + P_o \right] \qquad (16)$$

Thus, the general displacement function, expressed in terms of cylindrical polar coordinates, can be found and simplified, as shown in Appendix II.*

Stresses of an elastic body are related to strains ϵ_{ij} by generalized Hooke's law as follows:

$$\sigma_{ij} = \frac{E}{2(1+\nu)} \left[\left(1 + \delta_{ij} \right) \epsilon_{ij} + \delta_{ij} \frac{2\nu\, \epsilon_{kk}}{1-2\nu} \right] \qquad (17)$$

---

* Equations (146) through (148).

where δ_{ij} is the Kronecker delta and where strains ϵ_{ij} are related to displacements by

$$\left.\begin{aligned} \epsilon_{11} &= \frac{\partial \xi_1}{\partial r}, \qquad \epsilon_{22} = \frac{\xi_1}{r} + \frac{1}{r}\frac{\partial \xi_z}{\partial \varphi} \\ \epsilon_{33} &= \frac{\partial \xi_3}{\partial z}, \qquad \epsilon_{12} = \frac{1}{r}\frac{\partial \xi_1}{\partial \varphi} + \frac{\partial \xi_2}{\partial r} - \frac{\xi_z}{r} \\ \epsilon_{13} &= \frac{\partial \xi_1}{\partial z} + \frac{\partial \xi_3}{\partial r}, \quad \epsilon_{23} = \frac{\partial \xi_z}{\partial z} + \frac{\partial \xi_3}{r\partial \varphi} \end{aligned}\right\} \qquad (18)$$

The stresses corresponding to the above displacement function are computed from equations (16), (17), and (18). The equations for stresses are given in detail in Appendix II.*

D. Determination of the Arbitrary Constants

Arbitrary constants, which enter through equation (14) into solutions (16) and (17), are to be determined by appropriate conditions of each domain. Solutions (16) and (17) have been expressed by the solutions in Appendix II.** To satisfy the periodic condition (2) of matrix and loaded fiber, we specify, after substituting solutions (14) and (15) into (16),

$$n = 6, 12, 18, 24, \ldots \qquad (19)$$

Displacements (16) specified by (19) have been applied by Haener and Ashbaugh (Reference 2) to a unidirectional multifiber composite under residual shrinkage and axial load. The choice of (19) results in eight of the integration constants in the displacements becoming zero for the domains I and II respectively.*** In order that the displacements and stresses remain bounded at the center of the fiber, the coefficients β_{jnk} in equation (14) must be zero for the solutions pertaining to the fiber. Satisfying

---

* Equations (149) through (154).

** Equations (146) through (154).

*** Equation (156).

the loading condition (1), we choose in the expression for σ_{33} (see Appendix II*) the μ so that $\cos\mu\ell = 0$; therefore,

$$\mu^{I} = \frac{k\pi}{2\ell} \qquad (20)$$

$$k = 1,3,5 \ldots$$

In the stress expression σ_{33}^{I} for the fiber, all the terms involving cosz will automatically be zero by reason of the above choice (20). However, the terms involving sin z will not be zero and will contribute a loading at the end which is a function of r . Since this is compatible with the boundary condition (11), the coefficients of sinz in the stresses must be zero.** Therefore, additional relationship between these coefficients can be obtained.***

Additionally, the unloaded condition (12) of domain II leads to

$$\mu^{II} = \frac{k\pi}{2\ell} \qquad (21)$$

$$k = 1,3,5 \ldots$$

and to the discarding of six further integration constants and a relation between four additional integration constants.†

The periodic condition that displacements of the unloaded fiber are identical for every multiple of $2\pi/3$ with respect to θ has been described by equation (3). The displacements in domain III do not have any periodic property†† in the polar angle φ , the fourteen terms contained in the P functions in (16) and (17) being characterized by the factor $\sin n\varphi$ or $\cos n\varphi$ for domain III.

---

* Equation (154).

** Equation (154).

*** Equation (155).

† Equation (157).

†† As far as a hexagonal element as shown in Figure 30(a) is concerned, displacements of the six unloaded fibers possess sixfold symmetry. However, an elasticity solution is not valid for a discontinuous medium.

The resulting solution is the special case corresponding to the vanishing of n in the expressions P and $_{ij}$ in the solutions (16) and (17). The vanishing of the axial stress at $z = \pm\ell$ in equation (12) requires at the end of domain III

$$\mu^{III} = \frac{k\pi}{2\ell} \qquad (22)$$

$$k = 1,3,5 \ldots$$

On the basis of equations (22) and (12), conclusions similar to that made for the loaded part can be made in this case.*

It can be seen that displacements and stresses are composed of products of functions of r and orthogonal functions of φ and z. The functions of φ will no longer be orthogonal, however, as displacements (16) are introduced into conditions (3) and (8) and stresses (17) into conditions (6) and (10). This arises from the following parameters:

1. The polar radius r is related to the polar angle φ at the hexagonal boundary.

2. The polar coordinates r and φ at the interface between domains II and III are related to each other by condition (7).

3. Coordinates r and φ in domain III are related by conditions (4).

Because of the existence of certain relations between r and φ, it is impossible to determine the arbitrary constants in solutions (16) and (17) by conditions (3), (6), (8), and (10) as they stand. Therefore, the following approximation is developed such that these conditions will be satisfied with any desired or sufficient accuracy.

In the design of a fiber reinforced composite structure, a high ratio of fiber to matrix is desired, and, hence, the angle subtended by the hexagonal boundary of the matrix toward the z-axis is small in a cross-sectional plane. For example, this angle is about 5° for the volume of fibers in a composite being 65%. Therefore, the hexagonal boundary of the matrix (not fibers) can be replaced by a circular cylindrical surface with its axis coinciding with the z-axis and with its radius being

$$r_m = \frac{1}{4}\left[2h + \sqrt{4h^2 + (b - 2a)^2}\right] \qquad (23)$$

---

* Refer to equation (160).

With such a substitution, conditions (10a) and (10b) become

$$\sigma_{12}^{II}\left(r_m,\varphi,z\right) = 0$$

$$\sigma_{13}^{II}\left(r_m,\varphi,z\right) = 0 \qquad (24)$$

The approximation to conditions (3), (6), (8), and (10) will now be developed.

Based on the periodic condition (3) of the unloaded fiber, average displacement components of a volume element in the directions at $\theta = 0$ and $\theta = \pi/2$ and in the axial direction are respectively equal to those of a corresponding element in the directions at $\theta = 2\pi/3$ and $\theta = 7\pi/6$ and in the axial direction.

$$\iiint_{V_i}\left[\xi_2^{III}\left(r_1,\varphi_1,z\right)\sin\varphi_1 - \xi_1^{III}\left(r_1,\varphi_1,z\right)\cos\varphi_1\right]\rho\,d\theta\,d\rho\,dz$$

$$= \iiint_{V_i'}\left[\xi_2^{III}\left(r_2,\varphi_2,z\right)\sin\left(\frac{\pi}{3}-\varphi_2\right) + \xi_1^{III}\left(r_2,\varphi_2,z\right)\cos\left(\frac{\pi}{3}-\varphi_2\right)\right]\rho\,d\theta\,d\rho\,dz$$

$$\iiint_{V_i}\left[\xi_1^{III}\left(r_1,\varphi_1,z\right)\sin\varphi_1 + \xi_2^{III}\left(r_1,\varphi_1,z\right)\cos\varphi_1\right]\rho\,d\theta\,d\rho\,dz$$

$$= \iiint_{V_i'}\left[\xi_1^{III}\left(r_2,\varphi_2,z\right)\sin\left(\frac{\pi}{3}-\varphi_2\right) - \xi_2^{III}\left(r_2,\varphi_2,z\right)\cos\left(\frac{\pi}{3}-\varphi_2\right)\right]\rho\,d\theta\,d\rho\,dz$$

$$\iiint_{V_i}\xi_3^{III}\left(r_1,\varphi_1,z\right)\rho\,d\theta\,d\rho\,dz = \iiint_{V_i'}\xi_3^{III}\left(r_2,\varphi_2,z\right)\rho\,d\theta\,d\rho\,dz \qquad (25)$$

$$i = 1,2,3,\ldots m_1$$

where m_1 is the number of volume elements of domain III, and V_i and V_i' are two corresponding equal elements as shown in Figure 31 (shadowed areas with the same axial length).

According to conditions (6a) through (6c), the average displacement of the matrix at an element of the interfacial surface between domains II and III is equal to the corresponding average displacement of the unloaded fiber.

$$\iint_{A_i}\left[\xi_1^{II}\left(r_3,\varphi_3,z\right)\cos\varphi_3 - \xi_2^{II}\left(r_3,\varphi_3,z\right)\sin\varphi_3\right] a\,d\theta\,dz$$

$$= \iint_{A_i}\left[\xi_1^{III}\left(r_3,\varphi_3,z\right)\cos\varphi_3 - \xi_2^{III}\left(r_3,\varphi_3,z\right)\sin\varphi_3\right] a\,d\theta\,dz$$

$$\iint_{A_i}\left[\xi_1^{II}\left(r_3,\varphi_3,z\right)\sin\varphi_3 + \xi_2^{II}\left(r_3,\varphi_3,z\right)\cos\varphi_3\right] a\,d\theta\,dz$$

$$= \iint_{A_i}\left[\xi_1^{III}\left(r_3,\varphi_3,z\right)\sin\varphi_3 + \xi_2^{III}\left(r_3,\varphi_3,z\right)\cos\varphi_3\right] a\,d\theta\,dz$$

$$\iint_{A_i}\xi_3^{II}\left(r_3,\varphi_3,z\right) a\,d\theta\,dz = \iint_{A_i}\xi_3^{III}\left(r_3,\varphi_3,z\right) a\,d\theta\,dz \qquad (26)$$

$$i = 1,2,3,\ldots m_2$$

which are the corresponding averages of the displacement components along the directions of x-, y-, and z-axes respectively, and in which A_i is an elemental area of the interfacial surface with m_2 being the number of elements.

From conditions (6d) through (6f), two averages of the corresponding components of the resultant force produced by normal and shearing stresses at an element of the interfacial surface between domains II and III are equal to each other.

$$\iint_{A_i} \Big\{ \Big[\sigma_{11}^{II}(r_3,\varphi_3,z) \cos(\varphi_3+\theta)\cos\varphi_3 + \sigma_{22}^{II}(r_3,\varphi_3,z) \sin(\varphi_3+\theta)\sin\varphi_3 - \sigma_{12}^{II}(r_3,\varphi_3,z) \sin(2\varphi_3+\theta)\Big] a\cos\theta \Big\} d\theta\, dz$$

$$= \iint_{A_i} \Big\{ \Big[\sigma_{11}^{III}(r_3,\varphi_3 z) \cos(\varphi_3+\theta)\cos\varphi_3 + \sigma_{22}^{III}(r_3,\varphi_3,z) \sin(\varphi_3+\theta)\sin\varphi_3 - \sigma_{12}^{III}(r_3,\varphi_3,z) \sin 2(\varphi_3+\theta)\Big] a\cos\theta \Big\} d\theta\, dz$$

$$\iint_{A_i} \Big\{ \Big[\sigma_{11}^{II}(r_3,\varphi_3,z) \cos(\varphi_3+\theta)\sin\varphi_3 + \sigma_{22}^{II}(r_3,\varphi_3,z) \sin(\varphi_3+\theta)\cos\varphi_3 + \sigma_{12}^{II}(r_3,\varphi_3,z) \cos(2\varphi_3+\theta)\Big] a\sin\theta \Big\} d\theta\, dz$$

$$= \iint_{A_i} \Big\{ \Big[\sigma_{11}^{III}(r_3,\varphi_3,z) \cos(\varphi_3+\theta)\sin\varphi_3 + \sigma_{22}^{III}(r_3,\varphi_3,\theta)\sin(\varphi_3+\theta)\cos\varphi_3 + \sigma_{12}^{III}(r_3,\varphi_3,z) \cos(2\varphi_3+\theta)\Big] a\sin\theta \Big\} d\theta\, dz$$

$$\iint_{A_i} \Big\{ \sigma_{13}^{II}(r_3,\varphi_3,z) \cos(\varphi_3+\theta) - \sigma_{23}^{II}(r_3,\varphi_3,z) \sin(\varphi_3+\theta) \Big\} ad\theta\, dz$$

$$= \iint_{A_i} \Big[\sigma_{13}^{III}(r_3,\varphi_3,z) \cos(\varphi_3+\theta) - \sigma_{23}^{III}(r_3,\varphi_3,z) \sin(\varphi_3+\theta) \Big] ad\theta\, dz \qquad (27)$$

$$i = 1,2,3,\ldots m_2$$

which are force components along x-, y-, and z-axes respectively.

According to condition (8), the average of the displacements normal to the hexagonal boundary must be equal to δ for any element of the boundary plane

$$\frac{1}{B_i}\iint_{B_i}\left[\xi_1^k(h\sec\psi,\varphi,z)\cos\psi + \xi_2^k(h\sec\psi,\varphi,z)\sin\psi\right]h\sec^2\psi\, d\psi\, dz = \delta \qquad (28)$$

where B_i is an elemental area of the boundary plane of the matrix or the unloaded fiber. The number m_3 of the elements of the matrix boundary is not necessarily equal to that of the fiber boundary.

Based on condition (10), the shearing forces acting at an elemental area of the hexagonal boundary must vanish.

$$\iint_{B_i}\left\{\left[\sigma_{11}^{III}(h\sec\psi,\varphi,z) - \sigma_{22}^{III}(h\sec\psi,\varphi,z)\right]\sin\psi\cos\psi - \sigma_{12}^{III}(h\sec\psi,\varphi,z)(\sin^2\psi - \cos^2\psi)\right\}h\sec^2\psi\, d\psi\, dz = 0 \qquad (29)$$

$$\iint_{B_i}\left[\sigma_{13}^{III}(h\sec\psi,\varphi,z)\cos\psi + \sigma_{23}^{III}(h\sec\psi,\varphi,z)\sin\psi\right]h\sec^2\psi\, d\psi\, dz = 0 \qquad (30)$$

$$i = 1,2,3,\ldots m_3$$

which are shearing forces along the boundary line C D (Figure 30) and the z-axis respectively.

Applying a similar approximation to condition (13), the vanishing of the shearing force which acts on a small element, R_i, of the end section area requires, in the directions of x- and y-axes,

$$\iint_{R_i}\left[\sigma_{31}^k(r,\varphi,\ell)\cos\varphi - \sigma_{32}^k(r,\varphi,\ell)\sin\varphi\right]rd\varphi\, dr = 0$$

$$\iint_{R_i}\left[\sigma_{31}^k(r,\varphi,\ell)\sin\varphi + \sigma_{32}^k(r,\varphi,\ell)\cos\varphi\right]rd\varphi\, dr = 0 \qquad (31)$$

$$k = I,II,III \qquad i = 1,2,3,\ldots m_4$$

It is seen that equations (25) through (31) can be reduced to conditions (3), (6), (8), (10), and (13) when the regions in which integrations in these equations are carried over become infinitesimally small. Therefore, these conditions are replaced by the corresponding equations.

If two functions are defined as

$$f(z) = \begin{cases} z & (0 < z < \ell) \\ 2\ell - z & (\ell < z < 2\ell) \end{cases}$$

$$g(z) = \begin{cases} z^2 & (0 < z < \ell) \\ -z^2 + 4\ell z - 2\ell^2 & (\ell < z < 2\ell) \end{cases} \tag{32}$$

then the variables z and z^2 contained in the P functions in displacements (16) and in the σ_{ij} of stresses (17) can be represented by

$$z = \frac{8\ell}{\pi^2} \sum_{k=1,3}^{\infty} (-1)^{k-1/2} \cdot \frac{1}{k^2} \sin\mu z$$

$$z^2 = \frac{32\ell^2}{\pi^3} \sum_{k=1,3}^{\infty} (-1)^{k+1/2} \cdot \frac{1}{k^3} \cos\mu z \tag{33}$$

The introduction of solutions (16) into (25), (26), (27), and (28), and (17) into (5d,e,f), (27), (24), and (31) leads to a system of linear algebraic equations in terms of arbitrary constants and the unknown δ. The infinite series in these equations are to be truncated in numerical computation. If the number of n values is denoted by $\bar{n}$, the number of k values in the solutions for domains I and II by $\bar{k}_{12}$, and the number of k values in the solution for domain III by k_3, then the total number of unknowns is

$$9 \times \bar{k}_{12} \times \bar{n} + 6 \times \bar{k}_{12} + 8 \times \bar{k}_3 + 8 \times \bar{n} + 12$$

The total number of equations to be satisfied is

$$8 \times \bar{k}_{12} \times \bar{n} + 5 \times \bar{k}_{12} + 7 \times \bar{n} + 3m_1 + 6m_2 + 4m_3 + 6m_4 + 6$$

Thus, infinite series existing in this work without any recurring relationship between their coefficients are to be truncated or the numbers m_1, m_2, m_3, and m_4 are to be chosen in such a way that the number of unknowns is equal to the number of equations. However, the order of the square matrix is extremely large. To reduce the order, the matrix is subdivided into a number of rectangular arrays, and each array in turn is a matrix. After some laborious computation, the maximum order of submatrices yields

$$\overline{k}_{12} \times \overline{n} + \overline{k}_{12} + \overline{n} + 2$$

or

$$4 \times \overline{k}_3 + 4$$

In this study, symmetry condition (1) of a hexagonal segment, periodic condition (2) of matrix and loaded fiber, continuity condition (5) at the interface between matrix and loaded fiber, and end conditions (11) and (12) have been exactly satisfied, while the other physical conditions are approximately fulfilled. It is expected that the vanishing of shearing stresses (10a) and (10b) at the hexagonal boundary of the matrix will be satisfied with sufficient accuracy and that the vanishing of shearing stresses (13a) through (13d) at the ends of matrix and loaded fiber and the constant displacement requirement (8a) at the hexagonal boundary of the matrix will be approximately fulfilled for a few values of $\overline{k}_{12}$ and $\overline{n}$. The price paid for increasing accuracy in the fulfillment of other conditions is that the order of the matrix must increase.

The variation in stresses of a long composite with every other fiber loaded is expected to be small in the middle portion of a hexagonal segment, and, hence, the corresponding elements chosen for computing efficiency should be larger than those close to the ends. The transfer of loads in the present case possibly is an end effect; that is, the transmission of the largest portion of loads from the externally stressed fiber in a hexagonal segment to six unloaded fibers through the matrix occurs in the neighborhood of the ends.

PART III — BUCKLING OF A FIBER IN A FINITE ELASTIC MATRIX UNDER AXIAL COMPRESSION

This study was concerned with the determination of the critical load of a fiber embedded in a soft elastic matrix subjected to axial compression.

The finite length composite cylinder is assumed to be free from initial stresses. When the load increases incrementally from zero, the fiber remains straight and the composite is under compression without bending. When the load continues to increase and reaches a certain value, the fiber deflects laterally. At this value, the compressive force is called the Euler critical load. Later on, the deflection increases rapidly with a small increase of the applied compression. Eventually the fiber buckles in a wavy shape and loses its natural function, the transmission of compressive forces. Therefore, the critical compressive load is very important in the design of such composite structures.

An analytical method has been developed by Sadowsky and Hussain (Reference 3) to determine the thermal critical load of an infinite fiber bonded to an infinite domain of matrix without mechanical loading. The matrix has been treated by the linear theory of elasticity as a three-dimensional body, and the fiber by one-dimensional elasticity. The method of approach is reasonable. In the present work, it additionally accounted for the moment produced by axial shear at the interface between fibers and matrix such that this shear influences the critical load. It should be pointed out that the total axial shearing force at the interface vanishes, but not the produced moments.

The method of approach to the present problem is similar to that developed by the above authors. Instead of using Boussinesque-Papkovitch potential functions, the equilibrium equations in cylindrical coordinates for the deformation of matrix are directly solved in this work. Equations of equilibrium for the critical load of the fiber are in a simple manner derived by the one-dimensional nonlinear theory of elastic stability, based on statics consideration different from that in the report by Sadowsky and Hussain. The contribution of axial shear at the interface to the equation of moment equilibrium is taken into account. The critical compressive load of the composite cylinder corresponding to the buckling of the fiber found in this study is a function of elastic constants, fiber radius, and outer radius of the composite.

General Description

Consider a composite cylinder of finite length L, fiber radius a, and outer radius b of the composite with two coordinate systems as shown in Figure 32.

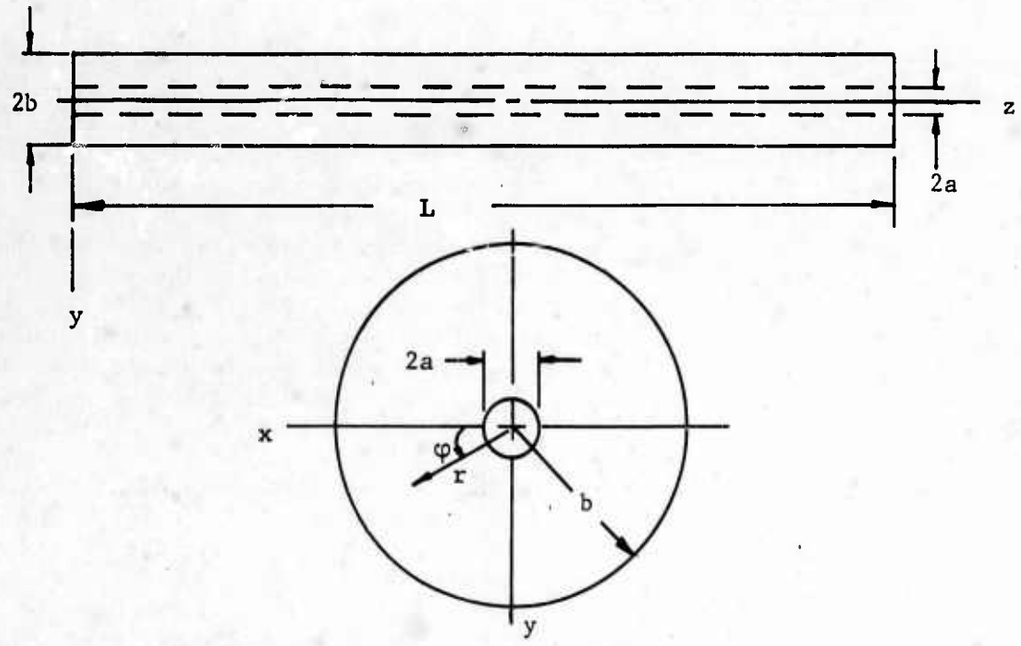

Figure 32. Geometry of a Composite Cylinder

Experiment shows that the buckling mode of a fiber in a low-modulus matrix subjected to axially compressive load is approximately a plane sine curve. If stresses of the matrix at the buckling of the fiber are within its elastic range, it will be appropriate to treat the matrix by the linear theory of elasticity as a three-dimensional body and the fiber by the non-linear theory of elastic stability as a slender bar subjected to compression and appropriate lateral loading. If the buckling wave is chosen in the yz-plane (Figure 33) and if the deflection of the fiber in the y-direction is denoted by v, then the buckling wave of the fiber can be written as

$$v = v_o \sin\alpha z \tag{34}$$

where v_o is the amplitude of the sine curve and where

$$\alpha = \frac{n\pi}{L} \tag{35}$$

with n being the number of half wavelength along the z-axis.

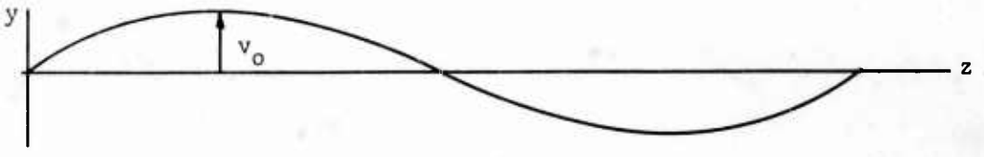

Figure 33. Fiber at the Buckling

Displacements and stresses given by (16) and (17) for load transfer through fibers in a matrix (Part II of this chapter: Three-Dimensional Load Transfer Among the Fibers in a Matrix) are suitable to the deformation of the matrix under consideration by appropriate choice of the Cartesian coordinate system. However, arbitrary constants in these expressions are difficult to determine in the present case. To simplify the problem, the approach described in Part I of this chapter (Parametric Studies) is applied.

Based on the three-dimensional theory of elasticity for a close-packed fiber composite under compression, stresses in the plane perpendicular to fiber axis were vanishingly small compared to the average axial stress for the epoxy-fiberglass composite.

It may be assumed in the present analysis, without introducing appreciable error in the results, that the stresses developed during buckling at the interface between the fiber and matrix are produced by bending only.

The displacements and stresses of the matrix are given in Appendix III to this report.

Equations of Equilibrium of the Fiber and Its Critical Compressive Load

Consider an element, AB , of the fiber with length dz before bending. It is suppositioned that this element has already been under compression. After bending, AB will displace to A'B' .

When some lateral deflection is produced in the compressed bar, there is some change in compression, but a more detailed investigation by S. Timoshenko (Reference 4) shows that this change is negligible. Since the compressive load is not changed, the fiber axis will be under the same axial force as that before bending, and there will be no change in the length along the neutral plane. During bending, axial forces N , transverse shearing forces Q , bending moments M at the ends of this element, lateral forces S per unit length, and axial shearing forces T per unit length are shown in Figure 34.

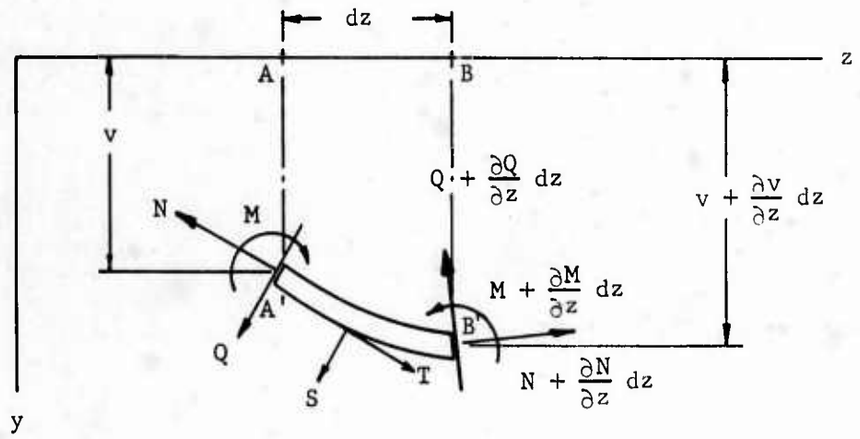

Figure 34. Geometry of the Fiber

The equation of equilibrium on the moment in the x-direction requires

$$\frac{dM}{dz} + Q + M_i = 0 \tag{36}$$

where the last term M_i is the contribution of moment per unit length produced by axial shear at the interface between fiber and matrix.

If the radius of curvature of the element dz is denoted by R, then the result of two transverse shearing forces is in the negative direction of the z-axis, with the magnitude being Qdz/R, and the result of two axial forces is Ndz/R in the negative direction of the y-axis. Therefore, the equilibrium equations on the force components along y- and z-axes are given by

$$\frac{dQ}{dz} - S + \frac{N}{R} = 0 \tag{37}$$

$$\frac{dN}{dz} + T - \frac{Q}{R} = 0 \tag{38}$$

where the nonlinearity has been introduced by considering the influence of the deflection v and where the angle of rotation of the element has been assumed to be small.

The moment M_s produced by axial shear $\sigma_{13}(a,\varphi,z)$ in the x-direction,*

$$M_s = 2a^2 \int_0^{\pi} \sigma_{13}\left(\rho_2,\varphi,z\right) \sin\varphi \, d\varphi$$

$$= \pi a^2 v_o \sigma_{13}^o \cos\alpha z \tag{39}$$

and the component of the moment produced by σ_{13} at the interface in the y direction automatically vanishes.

The lateral force S at the interface yields, by using (196),

$$S = \int_0^{2\pi} \left[\sigma_{11}\left(\rho_2,\varphi,z\right) \sin\varphi + \sigma_{12}\left(\rho_2,\varphi,z\right) \cos\varphi\right] a\,d\varphi$$

$$= \pi a v_o \left(\sigma_{11}^o + \sigma_{12}^o\right) \sin\alpha z \tag{40}$$

and the force component produced by stresses σ_{11} and σ_{12} at the interface in the x-direction automatically vanishes.

The axial shearing force T at the interface is from (196)

$$T = \int_0^{2\pi} \sigma_{13}\left(\rho_2,\varphi,z\right) a\,d\varphi = 0 \tag{41}$$

Using (34), (39), (40), and (41) and the relations

$$\frac{1}{R} \approx -\frac{d^2v}{dz^2} \tag{42}$$

$$M = \frac{E^I I}{R} \approx -\frac{\pi}{4} a^4 E^I \frac{d^2v}{dz^2} \tag{43}$$

---

* See equation (196).

Equilibrium equations (36), (37), and (38) are reduced to

$$\left.\begin{aligned} Q &= -\frac{\pi a^2}{4}\left[a^2 E^I \alpha^2 + \frac{4}{\alpha}\sigma_{13}^o\right]\beta \\ \frac{dQ}{d\beta} - N &= -\frac{\pi a}{\alpha^2}\left(\sigma_{11}^o + \sigma_{12}^o\right) \\ \frac{dN}{d\beta} + Q &= 0 \end{aligned}\right\} \qquad (44)$$

where β is the angle of rotation given by

$$\beta \approx \frac{dv}{dz} = v_o \alpha \cos\alpha z \qquad (45)$$

Elimination of Q from (44b and c) gives

$$\frac{d^2N}{d\beta^2} + N = \frac{\pi a}{\alpha^2}\left(\sigma_{11}^o + \sigma_{12}^o\right)$$

which has the solution

$$N = C_1 \cos\beta + C_2 \sin\beta + \frac{\pi a}{\alpha^2}\left(\sigma_{11}^o + \sigma_{12}^o\right) \qquad (46)$$

where C_1 and C_2 are arbitrary constants. Introduction of (46) into (44c) yields

$$Q = C_1 \sin\beta - C_2 \cos\beta \qquad (47)$$

In agreement with the assumption of small angle of rotation, functions $\sin\beta$ and $\cos\beta$ are replaced by β and 1 respectively. Thus, (46) and (47) are reduced to

$$\left.\begin{aligned} N &= C_1 + C_2 \beta + \frac{\pi a}{\alpha^2}\left(\sigma_{11}^o + \sigma_{12}^o\right) \\ Q &= C_1 \beta - C_2 \end{aligned}\right\} \qquad (48)$$

Comparing (48b) with (44a) leads to

$$C_2 = 0$$

$$C_1 = \frac{\pi a^2}{4}\left[a^2 E^I \alpha^2 + \frac{4}{\alpha}\sigma_{13}^o\right] \tag{49}$$

By substitution, the solution (48a) results in

$$N = \pi a^2\left[\frac{1}{4}E^I a^2 \alpha^2 + \frac{\sigma_{13}^o}{\alpha} - \frac{1}{a\alpha^2}\left(\sigma_{11}^o + \sigma_{12}^o\right)\right] \tag{50}$$

which is the internal axial force of the microfiber at any cross section.

If the applied compression of the microfiber is denoted by P^I, then we must have at its ends

$$N = -P^I \tag{51}$$

or

$$P^I = \pi a^2\left[\frac{1}{4}E^I a^2 \alpha^2 + \frac{\sigma_{13}^o}{\alpha} - \frac{1}{a\alpha^2}\left(\sigma_{11}^o + \sigma_{12}^o\right)\right] \tag{52}$$

in which σ_{1i} $(i=1,2,3)$ are functions of a, b, α and elastic constants of the matrix. Thus, (52) contains only the parameter α to be determined by the minimization of P^I

$$\frac{dP^I}{d\alpha} = 0 \tag{53}$$

from which α or the ratio of number of half wavelength to fiber length can be computed. The compressive force P^I corresponding to this value of α is the critical load of the fiber denoted by P_{cr}^I. The corresponding compressive force applied to the ends of the matrix is determined from the condition that the axial displacement of the matrix is the same as that of

the microfiber at the ends of the composite. If this load is denoted by P^{II}, we have from the above condition,

$$P^{II} = \frac{E^{II}}{E^{I}} \left[\left(\frac{b}{a} \right)^2 - 1 \right] P^{I}_{cr} \tag{54}$$

The total compressive load, P^* , applied at the ends of the composite is then given by

$$P^* = P^{I}_{cr} + P^{II} \tag{55}$$

which corresponds to the buckling of the fiber.

The constant axial displacement at the ends of the composite is not necessary to require the vanishing of the right-hand side of (193c). The axial displacement produced by bending is of influence with axial stresses, but not the axial force acting on a cross section because of geometrical symmetry of the fiber with respect to the neutral plane. Actually, the axial displacement produced by bending at the beginning of the fiber buckling can be neglected, since the length of the fiber axis does not change by bending and the angle of rotation is small. If this is done, the corresponding change in other equations is to set the right-hand side of (195) to zero.

It is seen from (52) that σ_{1i} (i=1,2,3) is the contribution, to the critical load, of interfacial pressure and circumferential and axial shearing stresses at the interface between fiber and matrix. The critical load P^I and, hence, P^{II} and P^* are simply functions of elastic constants of fiber and matrix, fiber radius, and outer radius of the matrix. Thermal buckling load of an infinite-length fiber bonded to an infinite domain of the matrix without mechanical loading and critical load of a finite-length fiber in lateral infinite matrix under axial compression can be treated as special cases of the present result by performing the integrals in (177), (181), and (185) analytically.

PART IV — ENERGY SOLUTIONS OF THE INSTABILITY PROBLEM

The problem of the buckling of microfiber embedded in a supporting matrix, under axial compression and under internal shrinkage load, was analytically investigated with energy methods in five different cases. The models include a single-fiber and multifiber reinforced composite of finite dimension, and a single fiber in an infinite matrix. The multifibers under internal shrinkage loads are treated with a simplified assumption, allowing the use of the Lagrange multiplier method of variation.

The Ritz-Galerkin method minimizing total potential energy was used in deriving the equation for obtaining the critical load of the fiber. In the present analysis, total potential energy contains the strain energy due to the bending and extension of the fiber, plus the energy of the interfacial pressure and longitudinal shear applied by the matrix to the fiber less the work done by external force. The stress field of the binder was determined by solving a plane elasticity problem. However, it was solved two-dimensionally as well as three-dimensionally for the case of the multifiber reinforced composite of finite size. The fiber and matrix elasticity are well matched at the interface by imposing boundary conditions requiring the continuity of stresses or displacements. Finally, the smallest buckling criterion was found by variation with respect to the wave parameter.

To formulate the problem, the following assumptions were made:

1. Both materials are linearly elastic, isotropic, and homogeneous.

2. Elongation, shear, and rotation of constituents are small in comparison with unity.

3. The deflection curve of the fiber and then the distribution of the interfacial force at the buckling state are sinusoidal in the axial direction.

4. Binder modulus is much smaller than fiber modulus.

5. The cross-sectional area of the fiber remains plane and circular after loading.

6. During buckling, there is no relative slip between fiber and matrix.

A. Buckling of Multifibers in a Finite Matrix

1. Buckling Load of the Fiber (Ritz Method)

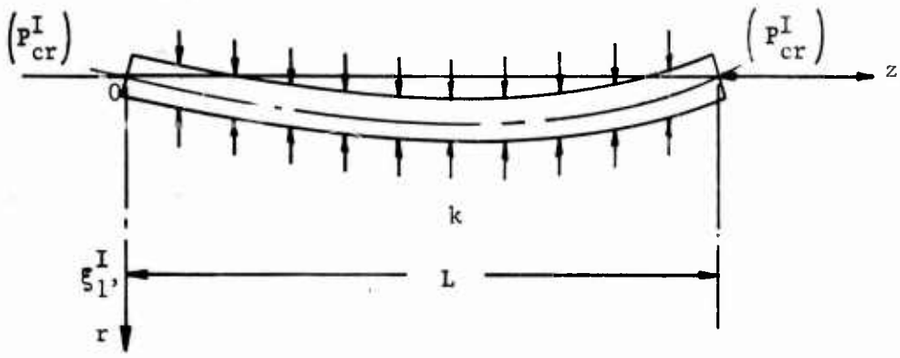

Figure 35. Half Critical Wavelength Shown on One Fiber

Geometric boundary conditions are, at

$$z = 0 \quad , \quad \xi^I_1 = 0 \tag{56}$$

and at

$$z = L \quad , \quad \xi^I_1 = 0 \tag{57}$$

Taking into consideration the geometrical boundary conditions of the fiber, we can assume its deflection curve,

$$\xi^I_1 = \sum_{n=1}^{\infty} \xi^I_{in} \sin \frac{n\pi z}{L} \tag{58}$$

In the present problem, the total potential energy includes strain energy due to the bending and extension of the fiber, plus the strain energy due to interfacial pressure and axial shear applied by matrix on the fiber, less the work done by external force.

The strain energy due to bending of the fiber is shown below (see Figure 36).

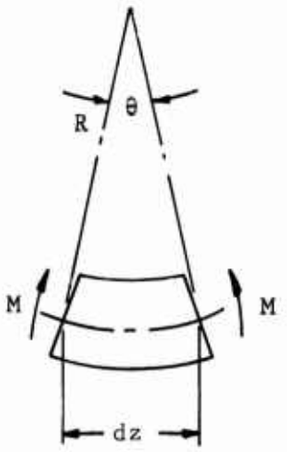

$$U_b = \frac{1}{2}\int_o^L E^I I^I \left(\frac{d^2 \xi_1^I}{dz^2}\right)^2 dz \qquad (59)$$

Figure 36. Bending of a Fiber Element

The strain energy due to the extension of the fiber is derived as follows (see Figure 37).

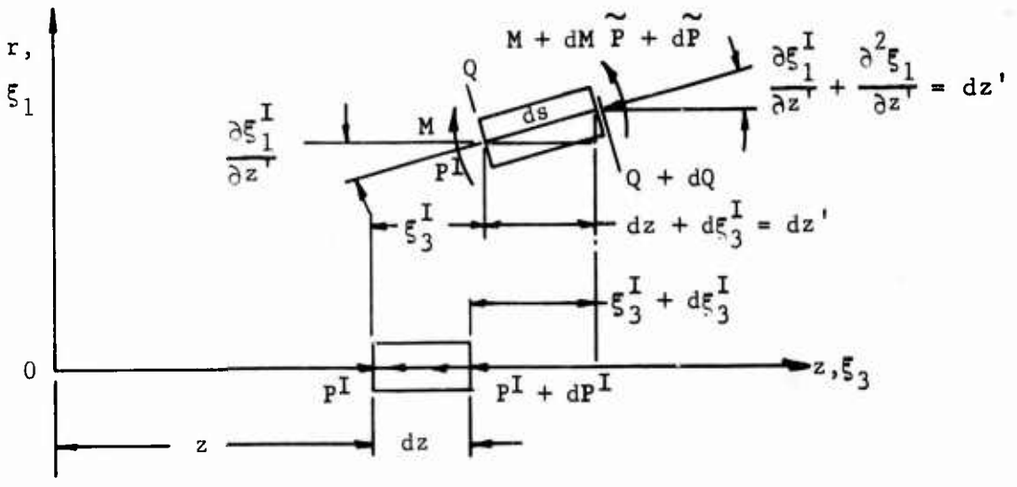

Figure 37. Schematic Diagram of a Fiber Element During Loading

The deformed length of an element of the fiber is

$$ds = \sqrt{\left(dz + d\,\xi_3^I\right)^2 + \left(d\,\xi_1^I\right)^2}$$

$$= dz\left[1 + \frac{d\,\xi_3^I}{dz} + \frac{1}{2}\left(\frac{d\,\xi_3^I}{dz}\right)^2 + \frac{1}{2}\left(\frac{d\,\xi_1^I}{dz}\right)^2 + \ldots\right]$$

Then the increase of strain energy due to the shortening of the fiber is

$$U_e = -\int_o^L P^I(ds - dz)$$

$$= -\int_o^L P^I\left[\frac{d\,\xi_3^I}{dz} + \frac{1}{2}\left(\frac{d\,\xi_1^I}{dz}\right)^2\right]dz \qquad (60)$$

The strain energy due to the interfacial pressure contributed by the matrix is

$$U_p = \int_o^L \frac{1}{2}\,p_{1n}\,\xi_1^I\,dz$$

$$= \frac{1}{2}\int_o^L k\left(\xi_1^I\right)^2 dz \qquad (61)$$

The strain energy due to axial shear contributed by matrix is depicted in Figure 38.

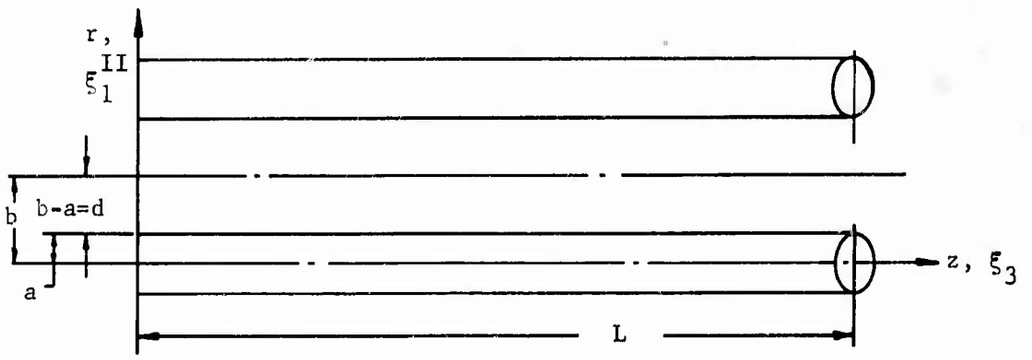

Figure 38. Geometry of Two Neighboring Fibers in a Multifiber Composite

In the matrix, shear strain is expressed by

$$\epsilon_{13}^{II} = \frac{\partial \xi_3^{II}}{\partial r} + \frac{\partial \xi_1^{II}}{\partial z} \tag{62}$$

Since shear strain should be continuous at the interface, then

$$\frac{\partial \xi_1^{II}(a)}{\partial z} = \frac{\partial \xi_1^{I}(a)}{\partial z}$$

Also

$$\frac{\partial \xi_3^{II}}{\partial r} = \frac{\xi_3^{II}(a) - \xi_3^{II}(b)}{d} \approx \frac{\xi_3^{II}(a)}{d}$$

But

$$\xi_3^{II} = a \frac{\partial \xi_1^{I}}{\partial z}$$

then

$$\epsilon_{13}^{II} = \left(1 + \frac{a}{d}\right) \frac{\partial \xi_1^{I}}{\partial z} \tag{63}$$

$$\sigma_{13}^{II} = G^{II} \epsilon_{13}^{II} = G^{II} \left(1 + \frac{a}{d}\right) \frac{\partial \xi_1^I}{\partial z} \tag{64}$$

Thus, the strain energy due to longitudinal shear of the matrix on the fiber is

$$U_s = \frac{\pi \left(b^2 - a^2\right) G^{II}}{2} \left(1 + \frac{a}{d}\right)^2 \int_o^L \left(\frac{\partial \xi_1^I}{\partial z}\right)^2 dz \tag{65}$$

The external work by prescribed loading during buckling is

$$W = P_L \xi_3^I(0) - P_R \xi_3^I(L) - \int_o^L \xi_3^I p_3 \, dz$$

$$= P_L \xi_3^I(0) - P_R \xi_3^I(L) + \int_o^L \xi_3^I \frac{dP^I}{dz} dz$$

$$= - P^I \xi_3^I \Big|_o^L + \int_o^L \xi_3^I \frac{dP^I}{dz} dz = - \int_o^L P^I \frac{d \xi_3^I}{dz} dz \tag{66}$$

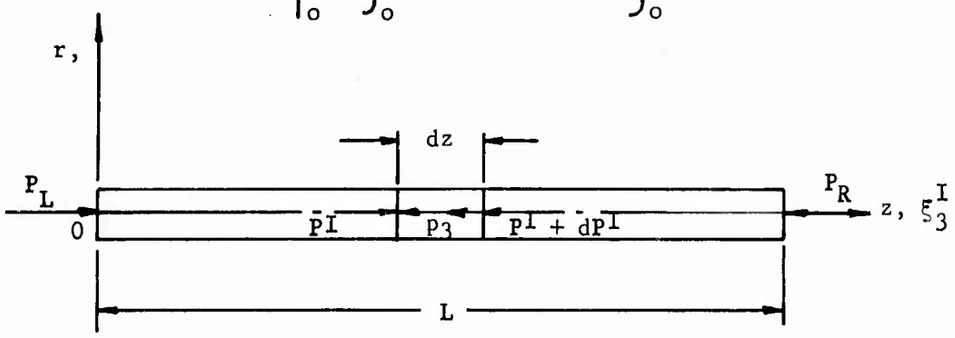

Figure 39. Schematic Diagram Showing One Fiber Under External Load

since

$$P^I - (P^I + dP^I) - p_3\, dz = 0$$

$$p_3 = \frac{dP^I}{dz} \tag{67}$$

Therefore, the total potential energy T_e is

$$T_e = U_b + U_e + U_p + U_s - W$$

$$= \frac{1}{2}\int_o^L E^I I^I \left(\frac{d^2\xi_1^I}{dz}\right)^2 dz - \int_o^L P^I \left[\frac{d\xi_3^I}{dz} + \frac{1}{2}\left(\frac{d\xi_1^I}{dz}\right)^2\right]dz +$$

$$\frac{1}{2}\int_o^L k\left(\xi_1^I\right)^2 dz + \frac{1}{2}\,\pi\left(b^2-a^2\right)G^{II}\left(1+\frac{a}{d}\right)^2 \int_o^L \left(\frac{\partial\xi_1^I}{dz}\right)^2 dz +$$

$$\int_o^L P^I \frac{d\xi_3^I}{dz}\, dz \tag{68}$$

Thus

$$T_e = \frac{E^I I^I}{2}\int_o^L \left(\frac{d^2\xi_1^I}{dz}\right)^2 dz - \frac{1}{2}P^I \int_o^L \left(\frac{d\xi_1^I}{dz}\right)^2 dz +$$

$$\frac{1}{2}\,k\int_o^L \left(\xi_1^I\right)^2 dz + \frac{1}{2}\,G^{II}\,\pi\left(b^2-a^2\right)\left(1+\frac{a}{d}\right)^2 \int_o^L \left(\frac{\partial\xi_1^I}{\partial z}\right)^2 dz \tag{69}$$

Substituting equation (58) into equation (69) and making use of integral identities, we get

$$T_e = \frac{1}{2} E^I I^I \frac{L}{2} \sum_{n=1}^{\infty} \left(\xi_{1n}^I\right)^2 \left(\frac{n\pi}{L}\right)^4 - \frac{1}{2} P^I \frac{L}{2} \sum_{n=1}^{\infty} \left(\xi_{1n}^I\right)^2 \left(\frac{n\pi}{L}\right)^2 +$$

$$\frac{1}{2} k \frac{L}{2} \sum_{n=1}^{\infty} \left(\xi_{1n}^I\right)^2 + \frac{1}{2} \pi G^{II} \left(b^2-a^2\right) \left(1 + \frac{a}{d}\right)^2 \frac{L}{2} \sum_{n=1}^{\infty} \left(\xi_{1n}^I\right)^2 \left(\frac{n\pi}{L}\right)^2 \quad (70)$$

Minimization of total potential energy with respect to the amplitude of the assumed curve gives the stationary condition; i.e.,

$$\frac{\partial T_e}{\partial \xi_{1j}^I} = 0 \qquad j = 1,2,3,\ldots$$

From equation (70)

$$\frac{\partial T_e}{\partial \xi_{1j}^I} = \frac{1}{2} E^I I^I L \xi_{1j}^I \left(\frac{j\pi}{L}\right)^4 + \frac{L}{2} k \xi_{1j}^I +$$

$$\frac{\pi^3}{2L} \left(b^2-a^2\right) G^{II} \left(1 + \frac{a}{d}\right)^2 \xi_{1j}^I j^2 - \frac{P^I L}{2} \xi_{1j}^I \left(\frac{j\pi}{L}\right)^2 = 0 \quad (71)$$

This equation either yields $\xi_{1j}^I = 0$, which gives the undesirable case of zero deflection, or the following results are obtained:

$$\frac{1}{2} E^I I^I \left(\frac{j\pi}{L}\right)^4 + \frac{1}{2} k + \frac{1}{2L^2} j^2 \pi^3 \left(b^2-a^2\right) \left(1 + \frac{a}{d}\right)^2 G^{II} -$$

$$\frac{1}{2} P_{cr}^I \left(\frac{j\pi}{L}\right)^2 = 0$$

which gives the critical load for the fiber; i.e.,

$$P_{cr}^{I} = \frac{n^2\pi^2}{L^2} E^{I} I^{I} + \frac{L^2}{n^2\pi^2} k + \pi\left(b^2-a^2\right)G^{II}\left(1+\frac{a}{d}\right)^2 \tag{72}$$

where k has the dimension of pound per square inch, and is equal to the ratio of interfacial force per unit length to unit lateral deflection.

Foundation constant k for the multifiber reinforced matrix is derived as shown in Figure 38.

We can imagine the matrix as a two-dimensional plate and under merely the normal interfacial force per unit length $p_1(z)$. The expression $p_1(z)$ must have similar distribution as

$$p_1(x) = \sum_{n=1}^{\infty} p_{1n} \sin\frac{n\pi z}{L} = \sum_{n=1}^{\infty} k\,\xi_{1n}^{II} \sin\frac{n\pi z}{L} \tag{73}$$

Therefore, the boundary conditions are, at $r = 0$,

$$\sigma_{11}^{II} = \frac{\sum_{n=1}^{\infty} k\,\xi_{1n}^{II} \sin\frac{n\pi z}{L}}{\pi a} \tag{74}$$

$$\sigma_{13}^{II} = 0 \tag{75}$$

and at $r = 2d$,

$$\sigma_{11}^{II} = \frac{\sum_{n=1}^{\infty} k\,\xi_{1n}^{II} \sin\frac{n\pi z}{L}}{\pi a} \tag{76}$$

$$\sigma_{13}^{II} = 0 \tag{77}$$

The stress field in the matrix can be represented by the following stress function

$$\Phi(r,z) = \sum_{n=1}^{\infty} \Phi_n(r) \sin \frac{n\pi z}{L} \tag{78}$$

By substituting this equation into the differential equation (from Reference 5)

$$\frac{\partial^4 \Phi}{\partial r^4} + 2 \frac{\partial^4 \Phi}{\partial r^2 \partial z^2} + \frac{\partial^4 \Phi}{\partial z^4} = 0 \tag{79}$$

we get

$$\left(\frac{n\pi}{L}\right)^4 \Phi_n(r) - 2 \left(\frac{n\pi}{L}\right)^2 \Phi_n''(r) + \Phi_n^{IV}(r) = 0 \tag{80}$$

The solution to the partial differential equation (79) is

$$\Phi(r,z) = \sum_{n=1}^{\infty} \left(\frac{L}{n\pi}\right)^2 \left[A_n \cosh\left(\frac{n\pi r}{L}\right) + B_n \left(\frac{n\pi r}{L}\right) \cosh\left(\frac{n\pi r}{L}\right) + C_n \sinh\left(\frac{n\pi r}{L}\right) + D_n \left(\frac{n\pi r}{L}\right) \sinh\left(\frac{n\pi r}{L}\right)\right] \cdot \sin\left(\frac{n\pi z}{L}\right) \tag{81}$$

The stress components are

$$\sigma_{33}^{II} = \frac{\partial^2 \Phi}{\partial r^2}$$

$$= \sum_{n=1,2,\ldots}^{\infty} \left[\left(A_n + 2\, D_n \right) \cosh \left(\frac{n\pi r}{L} \right) + B_n \left(\frac{n\pi r}{L} \right) \cosh \left(\frac{n\pi r}{L} \right) + \right.$$

$$\left. \left(2\, B_n + C_n \right) \sinh \left(\frac{n\pi r}{L} \right) + D_n \left(\frac{n\pi r}{L} \right) \sinh \left(\frac{n\pi r}{L} \right) \right] \cdot \sin \left(\frac{n\pi z}{L} \right) \qquad (82)$$

$$\sigma_{11}^{II} = \frac{\partial^2 \Phi}{\partial z^2}$$

$$- \sum_{n=1,2,\ldots}^{\infty} \left[A_n \cosh \left(\frac{n\pi r}{L} \right) + B_n \left(\frac{n\pi r}{L} \right) \cosh \left(\frac{n\pi r}{L} \right) + \right.$$

$$\left. C_n \sinh \left(\frac{n\pi r}{L} \right) + D_n \left(\frac{n\pi r}{L} \right) \sinh \left(\frac{n\pi r}{L} \right) \right] \cdot \sin \left(\frac{n\pi z}{L} \right) \qquad (83)$$

$$\sigma_{13}^{II} = \frac{\partial^2 \Phi}{\partial r \partial z}$$

$$= - \sum_{n=1,2,\ldots}^{\infty} \left[\left(A_n + D_n \right) \sinh \left(\frac{n\pi r}{L} \right) + B_n \left(\frac{n\pi r}{L} \right) \sinh \left(\frac{n\pi r}{L} \right) + \right.$$

$$\left. \left(B_n + C_n \right) \cosh \left(\frac{n\pi r}{L} \right) + D_n \left(\frac{n\pi r}{L} \right) \cosh \left(\frac{n\pi r}{L} \right) \right] \cdot \cos \left(\frac{n\pi z}{L} \right) \qquad (84)$$

Applying boundary conditions (74) to (77), we have

$$A_n = -\frac{k\,\xi_{1n}^{II}}{\pi a} \tag{85}$$

$$B_n + C_n = 0 \tag{86}$$

$$A_n \cosh\left(\frac{2n\pi d}{L}\right) + B_n\left(\frac{2n\pi d}{L}\right)\cosh\left(\frac{2n\pi d}{L}\right) + C_n \sinh\left(\frac{2n\pi d}{L}\right) + D_n\left(\frac{2n\pi d}{L}\right)\sinh\left(\frac{2n\pi d}{L}\right) = -\frac{k\,\xi_{1n}^{II}}{\pi a} \tag{87}$$

$$A_n \sinh\left(\frac{2n\pi d}{L}\right) + B_n\left[\left(\frac{2n\pi d}{L}\right)\sinh\left(\frac{2n\pi d}{L}\right) + \cosh\left(\frac{2n\pi d}{L}\right)\right] + C_n \cosh\left(\frac{2n\pi d}{L}\right) + D_n\left[\sinh\left(\frac{2n\pi d}{L}\right) + \left(\frac{2n\pi d}{L}\right)\cosh\left(\frac{2n\pi d}{L}\right)\right] = 0 \tag{88}$$

Substitution of (85) and (86) into (87) yields

$$-\frac{k\,\xi_{1n}^{II}}{\pi a}\cosh\left(\frac{2n\pi d}{L}\right) + B_n\left[\left(\frac{2n\pi d}{L}\right)\cosh\left(\frac{2n\pi d}{L}\right) - \sinh\left(\frac{2n\pi d}{L}\right)\right] + D_n\left[\left(\frac{2n\pi d}{L}\right)\sinh\left(\frac{2n\pi d}{L}\right)\right] = -\frac{k\,\xi_{1n}^{II}}{\pi a} \tag{89}$$

Substituting (85) and (86) into (88), we get

$$- \frac{k \xi_{1n}^{II}}{\pi a} \sinh\left(\frac{2 n\pi d}{L}\right) + B_n \left(\frac{2 n\pi d}{L}\right) \sinh\left(\frac{2 n\pi d}{L}\right) +$$

$$D_n \left[\sinh\left(\frac{2 n\pi d}{L}\right) + \left(\frac{2 n\pi d}{L}\right) \cosh\left(\frac{2 n\pi d}{L}\right)\right] = 0 \qquad (90)$$

The denominator of B_n and D_n, solved from equations (89) and (90), is

$$\left(\frac{2 n\pi d}{L}\right)^2 - \sinh^2\left(\frac{2 n\pi d}{L}\right) \qquad (91)$$

The numerator of coefficient B_n, solved from equations (89) and (90), is

$$\frac{k \xi_{1n}^{II}}{\pi a} \left[\left(\frac{2 n\pi d}{L}\right) - \frac{2 n\pi d}{L} \cosh\left(\frac{2 n\pi d}{L}\right) - \sinh\left(\frac{2 n\pi d}{L}\right) + \sinh\left(\frac{2 n\pi d}{L}\right) \cosh\left(\frac{2 n\pi d}{L}\right)\right] \qquad (92)$$

The numerator for coefficient D_n, found from (89) and (90), is

$$\frac{k \xi_{1n}^{II}}{\pi a} \sinh\left(\frac{2 n\pi d}{L}\right)\left[\frac{2 n\pi d}{L} - \sinh\left(\frac{2 n\pi d}{L}\right)\right] \qquad (93)$$

Then the results of coefficients are as follows:

$$A_n = - \frac{k \xi_{1n}^{II}}{\pi a} \qquad (94)$$

$$B_n = \left\{ \frac{k\,\xi_{1n}^{II}}{\pi a} \left[\left(\frac{2\,n\pi d}{L} \right) - \left(\frac{2\,n\pi d}{L} \right) \cosh \left(\frac{2\,n\pi d}{L} \right) - \sinh \left(\frac{2\,n\pi d}{L} \right) + \right. \right.$$

$$\left. \left. \sinh \left(\frac{2\,n\pi d}{L} \right) \cosh \left(\frac{2\,n\pi d}{L} \right) \right] \right\} \div \left\{ \left(\frac{2\,n\pi d}{L} \right)^2 - \sinh^2 \left(\frac{2\,n\pi d}{L} \right) \right\} \qquad (95)$$

$$C_n = - B_n \qquad (96)$$

$$D_n = \left\{ \frac{k\,\xi_{1n}^{II}}{\pi a} \sinh \left(\frac{2\,n\pi d}{L} \right) \left[\left(\frac{2\,n\pi d}{L} \right) - \sinh \left(\frac{2\,n\pi d}{L} \right) \right] \right\} \div$$

$$\left\{ \left(\frac{2\,n\pi d}{L} \right)^2 - \sinh^2 \left(\frac{2\,n\pi d}{L} \right) \right\} \qquad (97)$$

By law of two-dimensional elasticity for the plane stress problem, we have

$$\frac{\partial \xi_1^{II}}{\partial r} = \frac{\sigma_{11}^{II}}{E^{II}} - \frac{\nu^{II} \sigma_{33}^{II}}{E^{II}} \qquad (98)$$

$$\frac{\partial \xi_3^{II}}{\partial z} = \frac{\sigma_{33}^{II}}{E^{II}} - \frac{\nu^{II} \sigma_{11}^{II}}{E^{II}} \qquad (99)$$

Substituting expressions (94) through (97) into equations (83) and (84) and the results into (88), we obtain

$$\xi_1^{II} = \frac{1}{E^{II}} \int_o^{2d} \left(\sigma_{11}^{II} - \nu^{II} \sigma_{33}^{II} \right) dr \qquad (100)$$

By integrating equation (100), we get, after extensive analysis,

$$\xi_1^{II} = \frac{kL}{E^{II}\pi^2 a} \sum_{n=1}^{\infty} \frac{\xi_{1n}^{II}}{n} \left\{ \left[-8\, d_n + 8\, d_n \cosh\left(2\, d_n\right) - \right.\right.$$

$$2 \sinh^3\left(2\, d_n\right) - 4 \sinh\left(2\, d_n\right) \cosh\left(2\, d_n\right) +$$

$$\left. 2 \sinh\left(2\, d_n\right) + 2 \sinh\left(2\, d_n\right) \cosh^2\left(2\, d_n\right) \right] \div$$

$$\left. \left[\left(2\, d_n\right)^2 - \sinh^2\left(2\, d_n\right) \right] \right\} \sin\, \alpha_n z \qquad (101)$$

Thus

$$k = \frac{p_1}{\xi_1^{II}} = E^{II} \pi a \sum_{n=1}^{\infty} \alpha_n \left\{ \left[\left(2\, d_n\right)^2 - \sinh^2\left(2\, d_n\right) \right] \div \right.$$

$$\left[-8\, d_n + 8\, d_n \cosh\left(2\, d_n\right) - 2 \sinh^3\left(2\, d_n\right) + \right.$$

$$2 \sinh\left(2\, d_n\right) - 4 \sinh\left(2\, d_n\right) \cosh\left(2\, d_n\right) +$$

$$\left. \left. 2 \sinh\left(2\, d_n\right) \cosh^2\left(2\, d_n\right) \right] \right\} \qquad (102)$$

where

$$d_n = \frac{n\pi d}{L} = \frac{\pi d}{\ell} = \alpha_n d$$

2. Smallest Buckling Load and Buckling Wavelength of the Fiber

From equation (72), we have

$$P_{cr}^{I} = \frac{n^2\pi^2}{L^2} E^{I} I^{I} + \frac{L^2}{n^2\pi^2} k + \pi\left(b^2-a^2\right)G^{I}\left(1 + \frac{a}{d}\right)^2 \qquad (103)$$

Let $\frac{n\pi}{L} = \alpha_n$. Combination of equations (102) and (103) yields the expression for critical load

$$P_{cr}^{I} = \alpha_n^2 E^{I} I^{I} + \frac{\alpha_n}{\alpha_n^2} E^{II} \pi a \left\{\left(2\alpha_n d\right)^2 - \sinh^2\left(2\alpha_n d\right) \div \right.$$

$$\left[-2\sinh^3\left(2\alpha_n d\right) - 8\alpha_n d + 8\alpha_n d \cosh\left(2\alpha_n d\right) - \right.$$

$$4\sinh\left(2\alpha_n d\right)\cosh\left(2\alpha_n d\right) + 2\sinh\left(2\alpha_n d\right) +$$

$$\left.\left.2\sinh\left(2\alpha_n d\right)\cosh^2\left(2\alpha_n d\right)\right]\right\} + \pi\left(b^2-a^2\right)G^{II}\left(1 + \frac{a}{d}\right)^2 \qquad (104)$$

Since the buckling load (104) depends on the wavelength

$$\ell_{cr} = \frac{2\pi}{\alpha_j} \qquad (105)$$

(104) must be minimized with respect to α_n to obtain the critical wavelength corresponding to the smallest critical buckling load of the fiber

$$\frac{\partial P_{cr}^{I}}{\partial \alpha_n} = 0 \qquad (106)$$

The result of (106) is

$$2\alpha_n^3 E^I I^I \left[-2\sinh^3\left(2\alpha_n d\right) - 8\alpha_n d + 8\alpha_n d\cosh\left(2\alpha_n d\right) - \right.$$

$$4\sinh\left(2\alpha_n d\right)\cosh\left(2\alpha_n d\right) + 2\sinh\left(2\alpha_n d\right) +$$

$$\left.2\sinh\left(2\alpha_n d\right)\cosh^2\left(2\alpha_n d\right)\right]^2 + E^{II}\pi a\left\{\left[\left(2\alpha_n d\right)^2 - \right.\right.$$

$$4\alpha_n d\sinh\left(2\alpha_n d\right)\cosh\left(2\alpha_n d\right) + \sinh^2\left(2\alpha_n d\right)\Big] \cdot$$

$$\left[-2\sinh^3\left(2\alpha_n d\right) - 8\alpha_n d + 8\alpha_n d\cosh\left(2\alpha_n d\right) - \right.$$

$$4\sinh\left(2\alpha_n d\right)\cosh\left(2\alpha_n d\right) + 2\sinh\left(2\alpha_n d\right) +$$

$$\left.2\sinh\left(2\alpha_n d\right)\cosh^2\left(2\alpha_n d\right)\right] - \alpha_n\left[\left(2\alpha_n d\right)^2 - \sinh^2\left(2\alpha_n d\right)\right] \cdot$$

$$\left[-4d\sinh^2\left(2\alpha_n d\right)\cosh\left(2\alpha_n d\right) - 8d + 12d\cosh\left(2\alpha_n d\right) + \right.$$

$$16d^2\alpha_n\sinh\left(2\alpha_n d\right) - 8d\sinh^2\left(2\alpha_n d\right) - 8d\cosh^2\left(2\alpha_n d\right) +$$

$$\left.\left.4d\cosh^3\left(2\alpha_n d\right)\right]\right\} = 0 \qquad (107)$$

From equation (107), we can determine α_n as a function of $\frac{E^I}{E^{II}}$, a and b. In other words, we obtain the critical wavelength $\ell_{cr} = \frac{2\pi}{\alpha_j}$ as a function of the material constants, the diameter of the fibers, and the volume percentage of the fibers. Substituting this value of α_i into equation (104), we then get the minimized critical buckling load, $P^I_{cr\ min}$.

3. Alternative Way of Finding the Strain Energy Due to Longitudinal Shear

$$\frac{1}{2}\int_v \sigma_{13}^{II}\,\epsilon_{13}^{II}\,dv = \frac{1}{2\,G^{II}}\int_v \left(\sigma_{13}^{II}\right)^2 dv \qquad (108)$$

The expression σ_{13}^{II} from equation (84) has been introduced into (108). After performing the indicated operations, the results of strain energy due to longitudinal shear have been used to replace the last term of equation (103). In this manner, then, the smallest buckling load and corresponding wavelength were obtained.

$$P_{cr}^{I} = \alpha_n^2\,E^I\,I^I + \alpha_n^{-2}\,k + \frac{k^2 d\,\alpha_n^{-3}}{2\pi\,a^2\,G^{II}}\,Y \qquad (109)$$

Y is an analytical expression given in Appendix IV.A (198a). The equation for α_n is given in Appendix IV.A (200), while k (a kind of a foundation constant) is given in equation (102).

B. Buckling of a Single Fiber in a Finite Matrix

1. Constant k for Single Fiber in a Finite Matrix

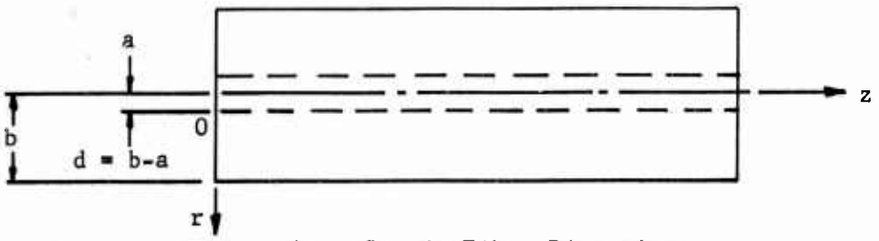

Figure 40. Single Fiber Dimensions

Assume load per unit length at the interface,

$$p_1(x) = \sum_{n=1,2,\ldots}^{\infty} p_{1n}\,\sin\frac{n\pi z}{L} \qquad (110)$$

The boundary conditions are:

$$\left.\begin{aligned} &\text{at } r = 0 , && \sigma_{11}^{II} = \frac{\sum_{n=1,2,\ldots}^{\infty} p_{1n} \sin \frac{n\pi z}{L}}{\pi a} , && \sigma_{13}^{II} = 0 \\ &\text{at } r = c = b-a , && \sigma_{11}^{II} = 0 , && \sigma_{13}^{II} = 0 \end{aligned}\right\} \quad (111)$$

By applying the solutions for stresses, equations (83) and (84) the integration constants are established [Appendix IV.B, equations (201) through (204)]. These constants are used in the displacements and stresses to express the strain energy during loading

$$\frac{1}{2}\int_V \sigma_{13}^{II}\, \epsilon_{13}^{V}\, dv = \frac{1}{2\, G^{II}}\int_V \left(\sigma_{13}^{II}\right)^2 dv \quad (112)$$

written out in Appendix IV.B, equation (214), which contains the strain energy due to shear at the interface. The critical load was then computed:

$$P_{cr}^{I} = \alpha_n^2 E^I I^I + \frac{E^{II}\pi a}{\alpha_n}\left[d_n^2 - \sinh^2 d_n\right] \div \left\{2\left(d_n - \sinh d_n\right)\left(\cosh d_n - 1\right)\right\} + E^{II}\pi d\left(1 + \nu^{II}\right)\frac{X}{\alpha_n}\left[d_n^2 - \sinh^2 d_n\right]^2 \div \left\{2\left(d_n - \sinh d_n\right)\left(\cosh d_n - 1\right)\right\}^2 \quad (113)$$

The expression α_n , X in equation (113) can be found in equation (220) and (215) respectively, while $d_n = \alpha_n d$.

C. Buckling of a Finite Single Fiber in an Infinite Matrix

If the matrix is infinite, then $b = \infty$. Thus, it is more convenient that the solution of the differential equation (79) takes the following form

$$\Phi = \sum_{n=1}^{\infty} \frac{1}{\alpha_n^2} \left[\bar{A}_n e^{\alpha_n r} + \bar{B}_n \left(\alpha_n r\right) e^{\alpha_n r} + \bar{C}_n e^{-\alpha_n r} + \right.$$

$$\left. \bar{D}_n \left(\alpha_n r\right) e^{-\alpha_n r} \sin\left(\alpha_n z\right) \right] \qquad (114)$$

By routine procedures, the stresses and strains are found from the potential Φ .*

$$k = \frac{p_1}{\xi_1^{II}} \qquad (115)$$

where p_1 is the lateral unit interfacial force and ξ_1^{II} is the lateral displacement. The minimum critical buckling load and the corresponding wavelength are derived in (236) through (237), and are restated here:

$$P_{cr}^{I} = 1.9 \left[\frac{E^{II} \pi a \left(3 + \nu^{II}\right)}{E^{I} I^{I} \left(1 - \nu^{II}\right)^2} \right]^{2/3} E^{I} I^{I} \qquad (116)$$

The wavelength corresponding to the critical load is

$$\ell_{cr} = \frac{2\pi}{\alpha_n} = \sqrt[3]{\frac{16\pi^2 E^{I} I^{I} \left(1 - \nu^{II}\right)^2}{a E^{II} \left(3 + \nu^{II}\right)}} \qquad (117)$$

The numerical results of the buckling wavelength for a single fiber coincide with test results obtained from experiment performed during this contract. In Figures 42 through 60, the critical wavelength and the buckling loads of a multifiber are plotted as a function of $\frac{E^{I}}{E^{II}}$, the fiber radius a , with volume percentage content of the fiber as a parameter. In Figures 61 and 62, the wavelength and buckling load of a single fiber are plotted versus the radius of the fiber.

* Equations (224) through (226) and (229).

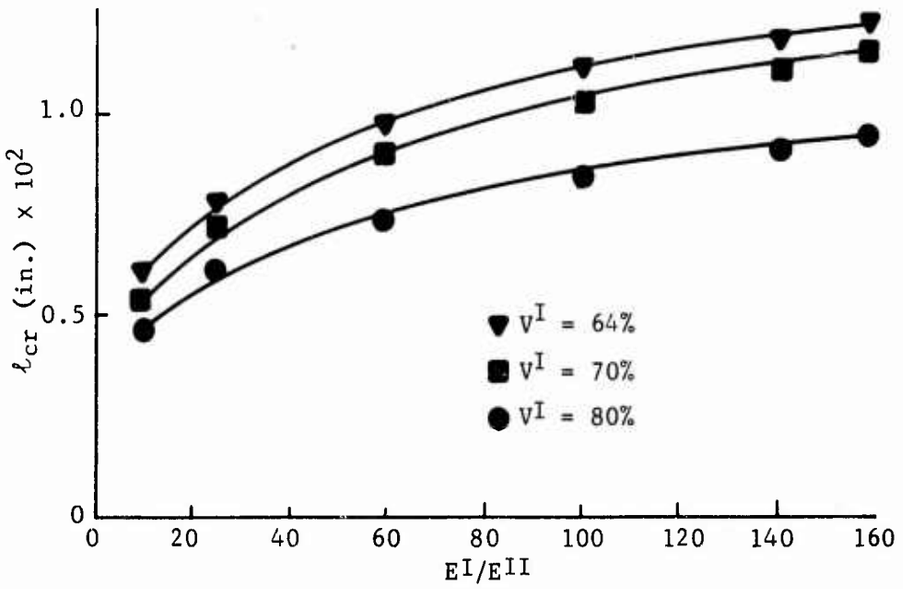

Figure 41. Critical Buckling Wavelength of the Fiber versus the Ratio of the Moduli ($a = 1 \times 10^{-3}$in.)

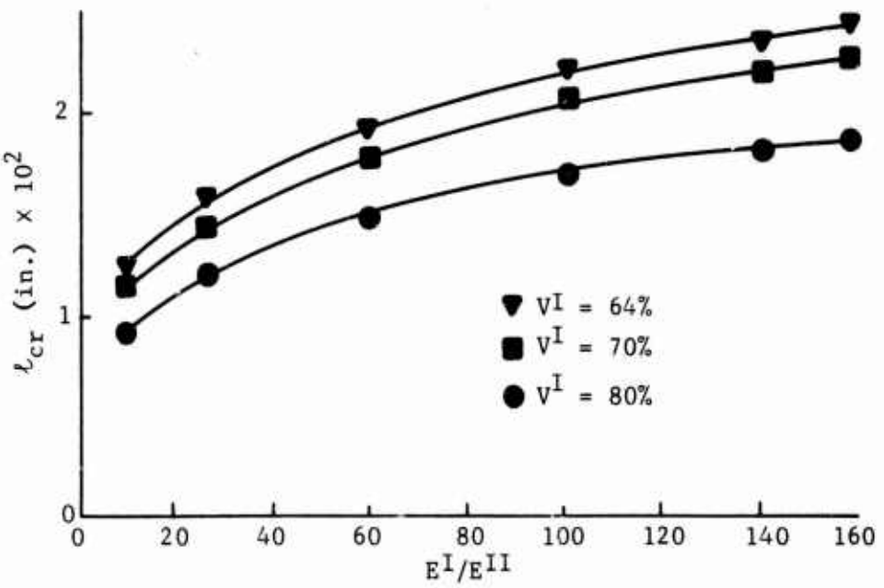

Figure 42. Critical Buckling Wavelength of the Fiber versus the Ratio of the Moduli ($a = 2.0 \times 10^{-3}$in.)

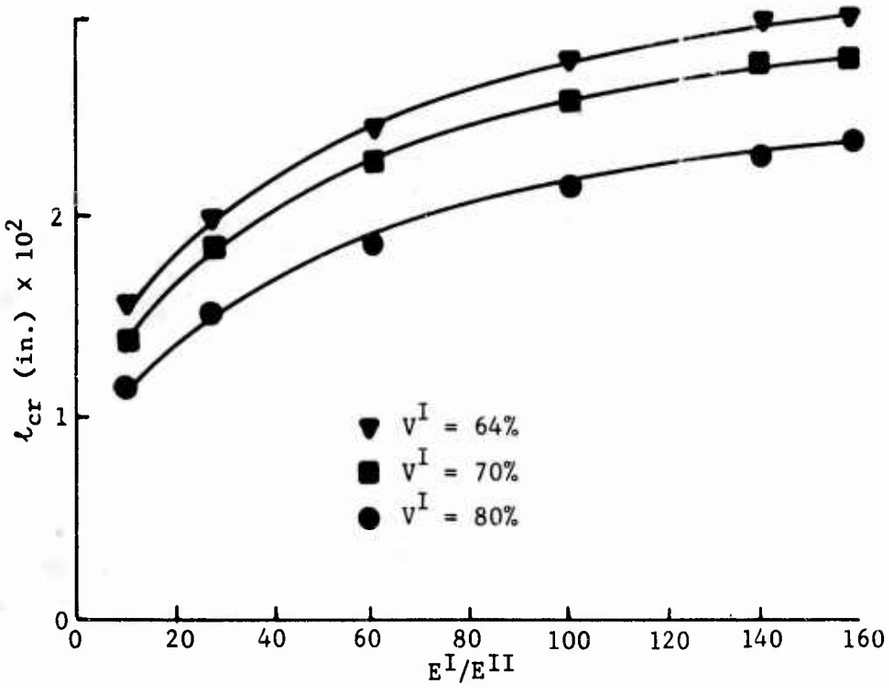

Figure 43. Critical Buckling Wavelength of the Fiber versus the Ratio of the Moduli ($a = 2.5 \times 10^{-3}$in.)

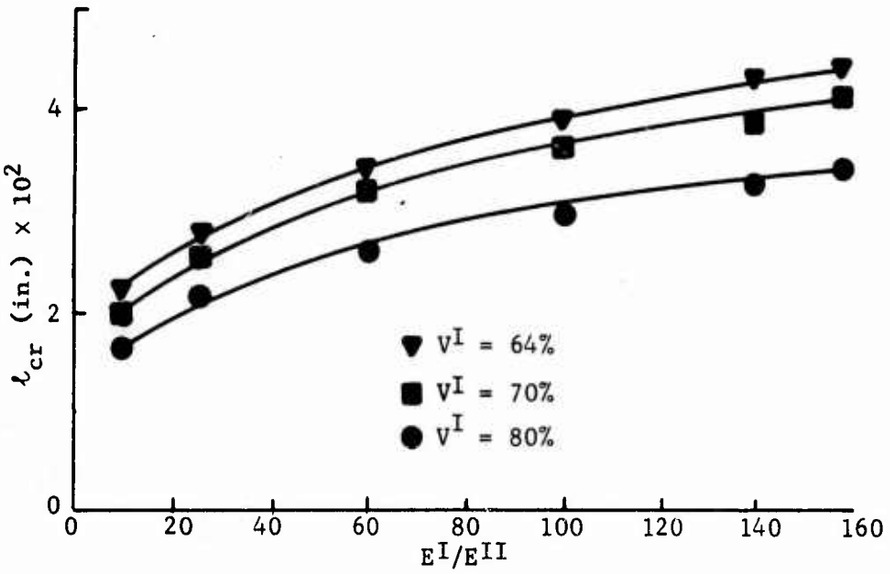

Figure 44. Critical Buckling Wavelength of the Fiber versus the Ratio of the Moduli ($a = 3.5 \times 10^{-3}$in.)

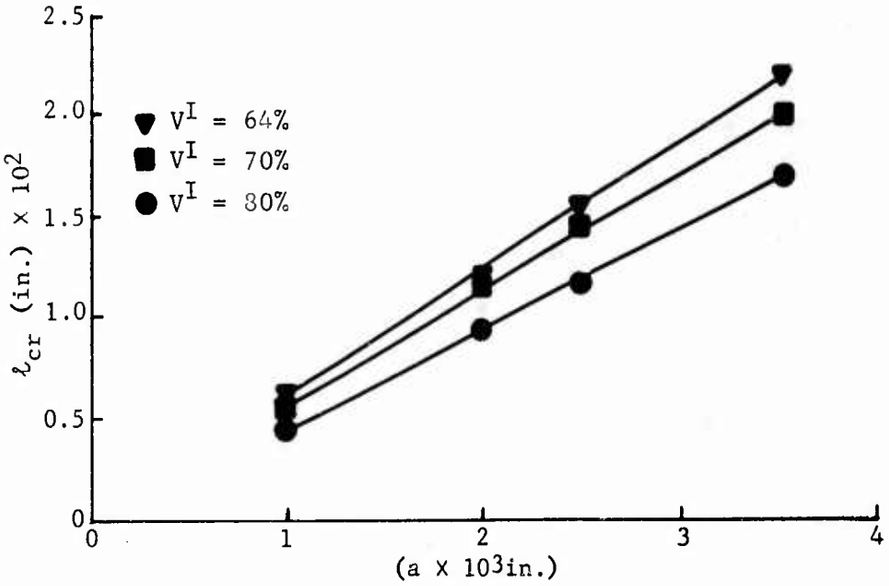

Figure 45. Critical Buckling Wavelength of the Fiber versus Radius of the Fiber (E^I = 3.8 x 10^6 psi, E^{II} = 3.8 x 10^5psi, or E^I/E^{II} = 10)

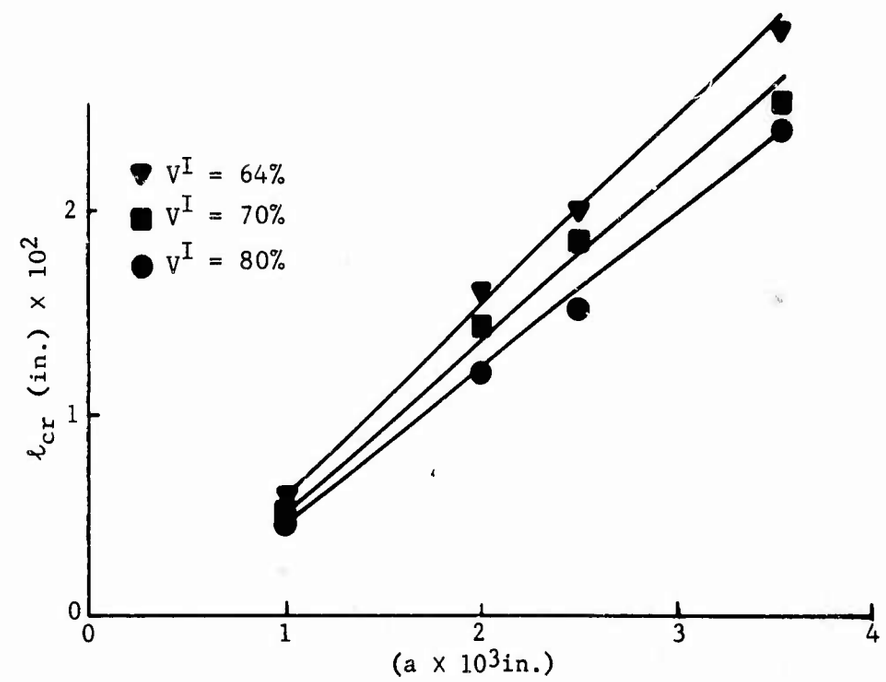

Figure 46. Critical Buckling Wavelength of the Fiber versus Radius of the Fiber (E^I = 1 x 10^7 psi, E^{II} = 3.8 x 10^5psi, or E^I/E^{II} = 26.4)

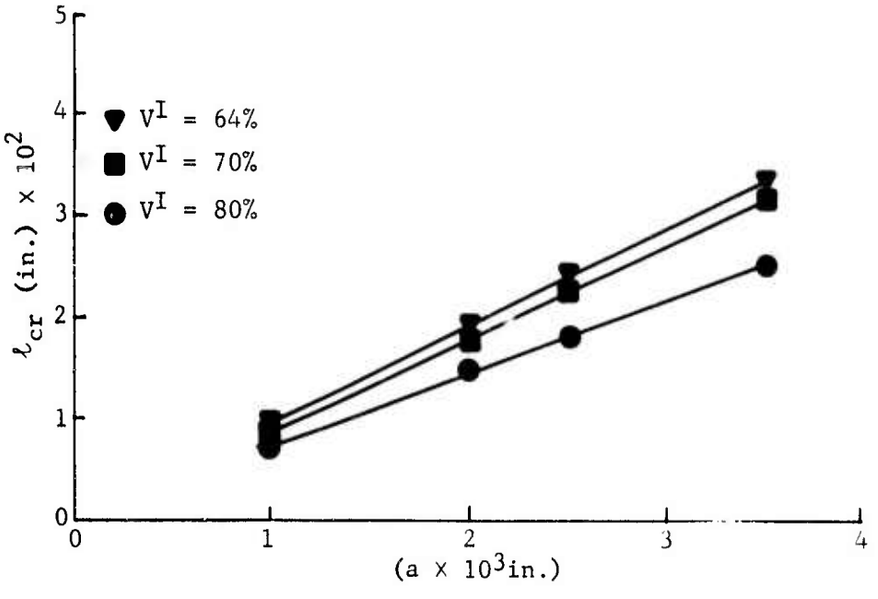

Figure 47. Critical Buckling Wavelength of the Fiber versus Radius of the Fiber (E^I = 2.28 x 10^6psi, E^{II} = 3.38 x 10^5psi, or E^I/E^{II} = 60)

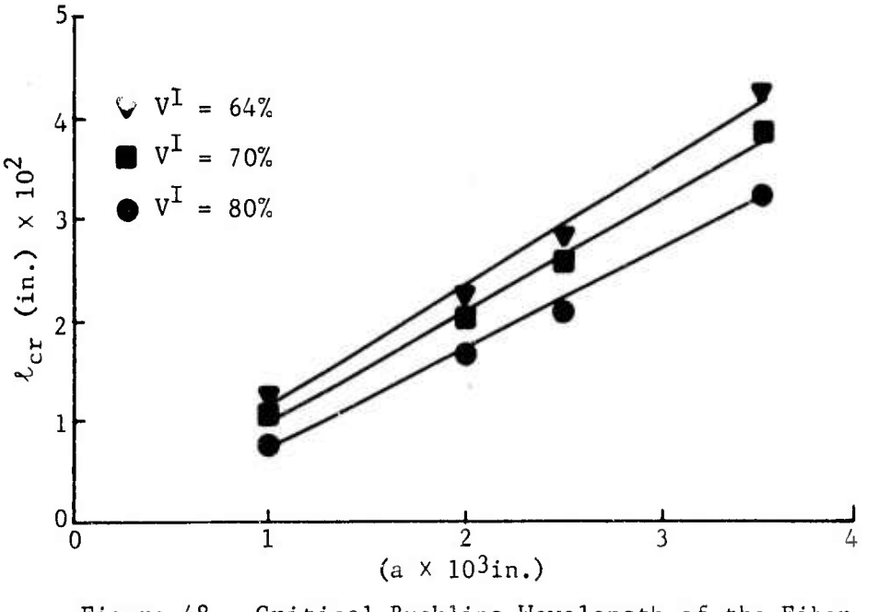

Figure 48. Critical Buckling Wavelength of the Fiber versus Radius of the Fiber (E^I = 3.8 x 10^7psi, E^{II} = 3.8 x 10^5psi, or E^I/E^{II} = 100)

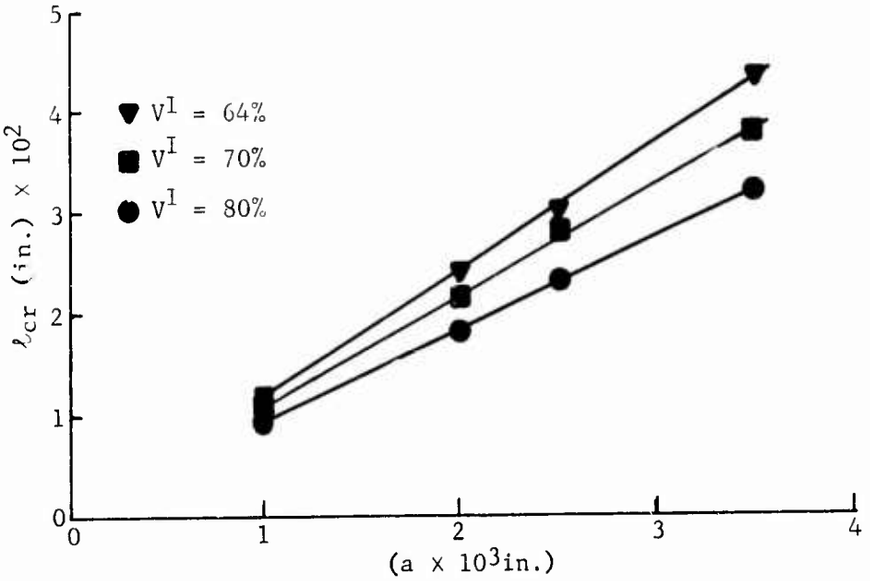

Figure 49. Critical Buckling Wavelength of the Fiber versus Radius of the Fiber (E^I = 5.32 × 10^7psi, E^{II} = 3.8 × 10^5psi, or E^I/E^{II} = 140)

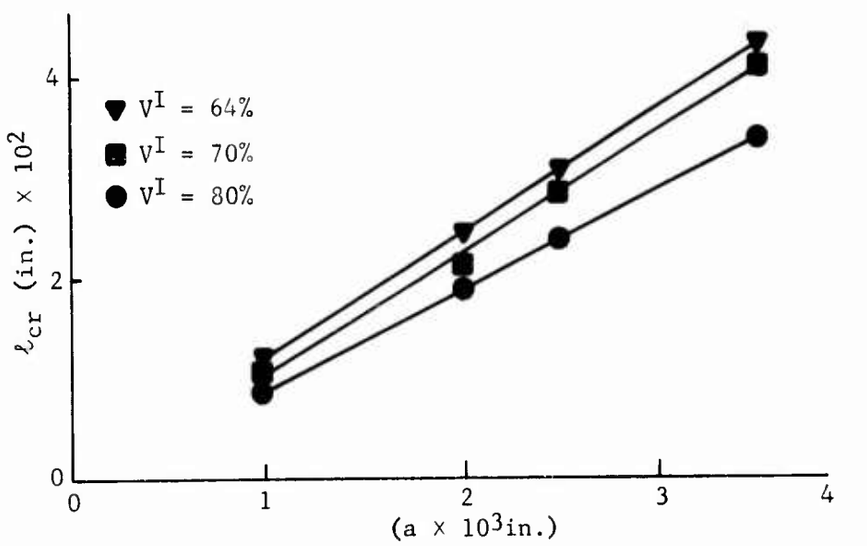

Figure 50. Critical Buckling Wavelength of the Fiber versus Radius of the Fiber (E^I = 6 × 10^7 psi, E^{II} = 3.8 × 10^5psi, or E^I/E^{II} = 158)

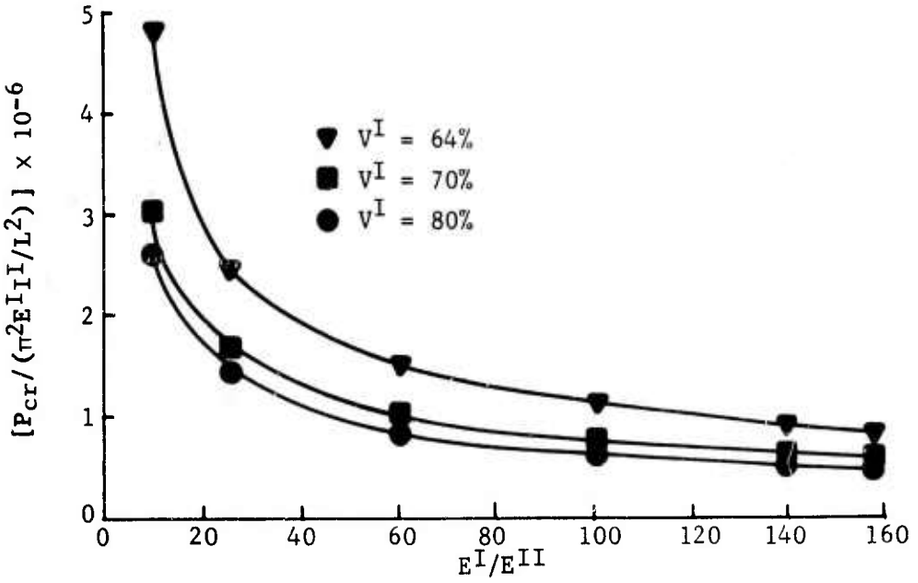

Figure 51. Critical Buckling Load of the Fiber versus the Ratio of Young's Moduli ($a = 1 \times 10^{-3}$in.)

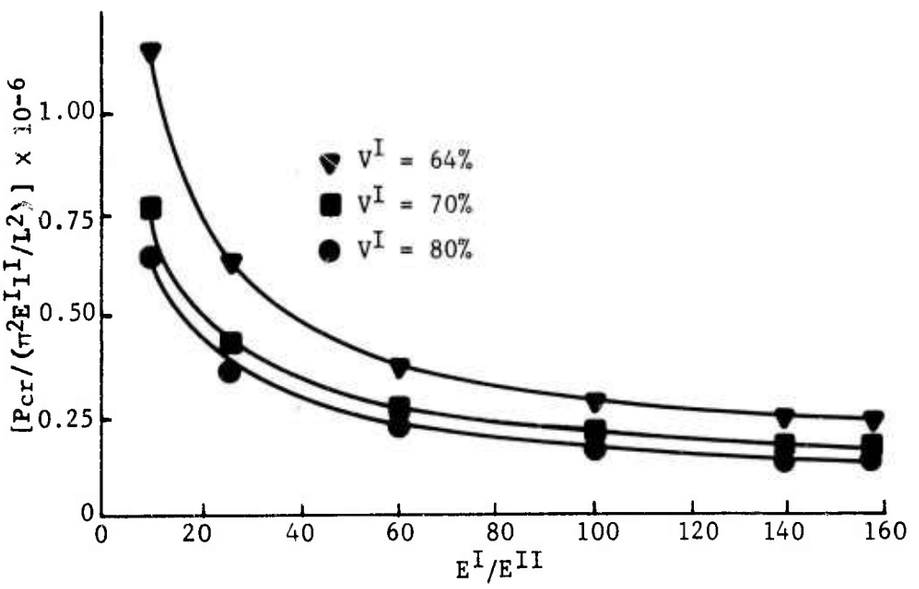

Figure 52. Critical Buckling Load of the Fiber versus the Ratio of Young's Moduli ($a = 2 \times 10^{-3}$in.)

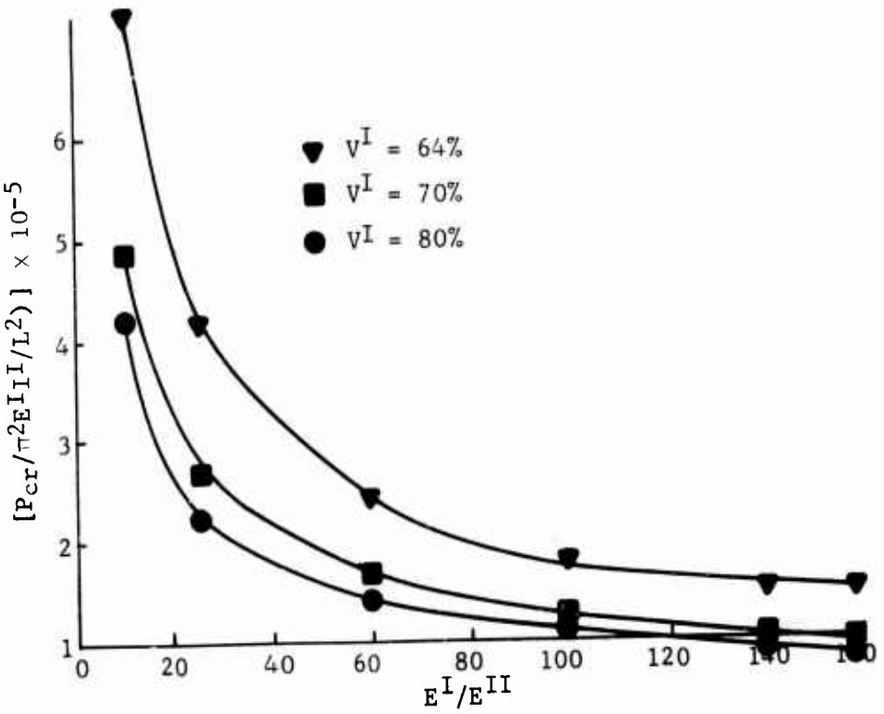

Figure 53. Critical Buckling Load of the Fiber versus the Ratio of Young's Moduli ($a = 2.5 \times 10^{-3}$in.)

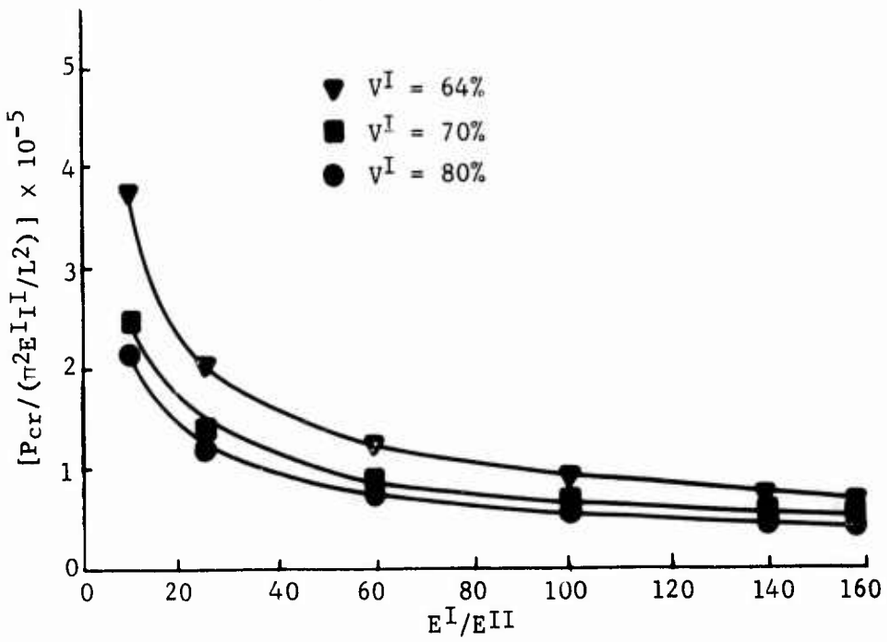

Figure 54. Critical Buckling Load of the Fiber versus the Ratio of Young's Moduli ($a = 3.5 \times 10^{-3}$in.)

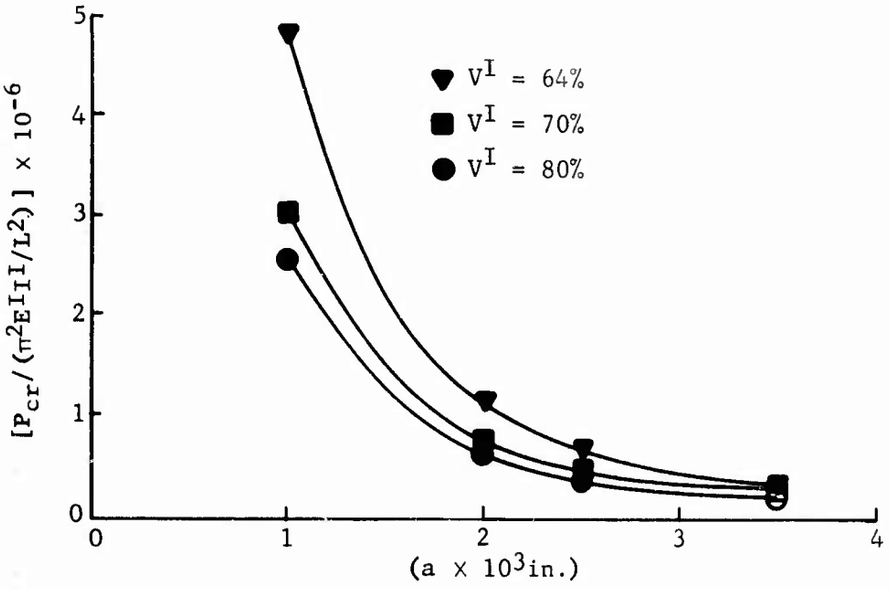

Figure 55. Critical Buckling Load of the Fiber versus Radius of the Fiber (E^I = 3.8 × 10^6psi, E^{II} = 3.8 × 10^5psi, or E^I/E^{II} = 10)

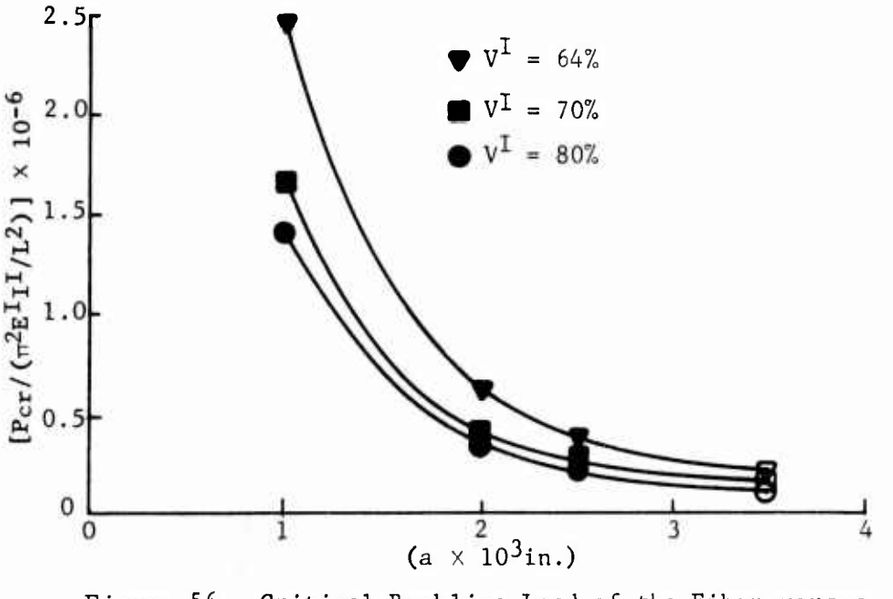

Figure 56. Critical Buckling Load of the Fiber versus Radius of the Fiber (E^I = 1 × 10^7psi, E^{II} = 3.8 × 10^5psi, or E^I/E^{II} = 26.4)

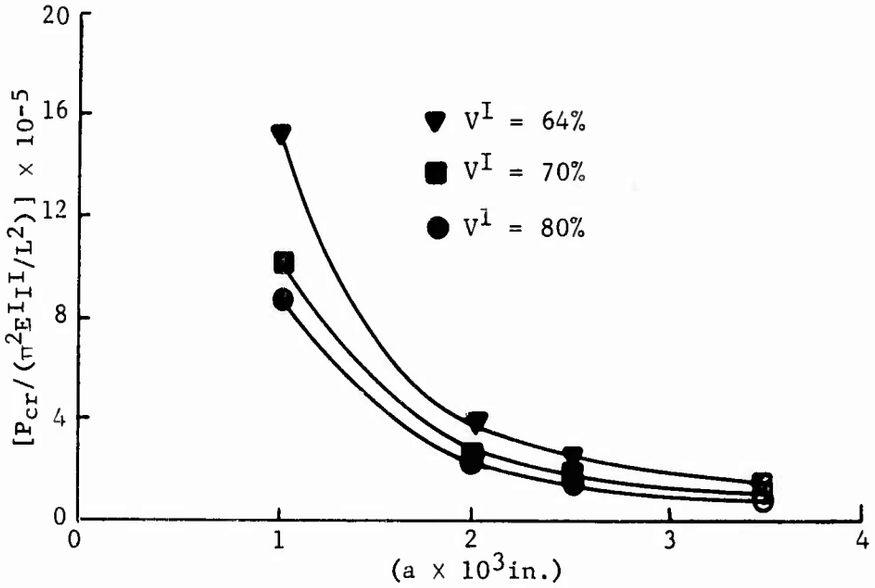

Figure 57. Critical Buckling Load of the Fiber versus Radius of the Fiber (E^I = 2.28 × 10^7psi, E^{II} = 3.8 × 10^5psi, or E^I/E^{II} = 60)

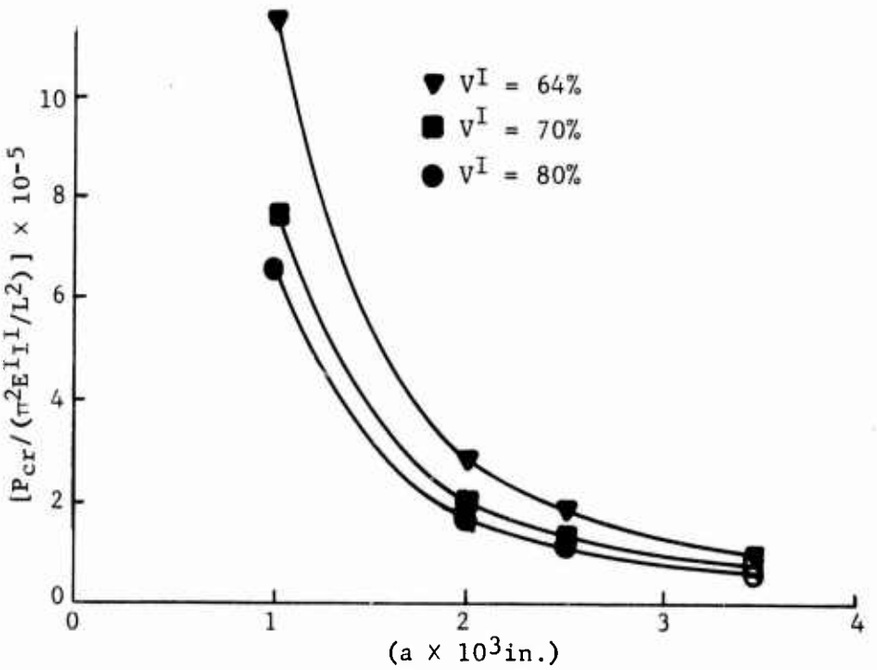

Figure 58. Critical Buckling Load of the Fiber versus Radius of the Fiber (E^I = 3.8 × 10^7psi, E^{II} = 3.8 × 10^5psi, or E^I/E^{II} = 100)

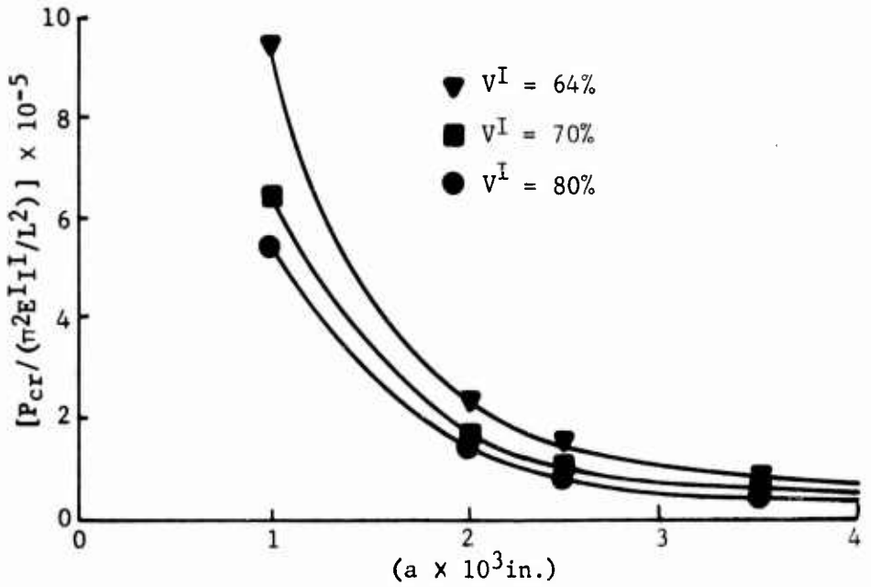

Figure 59. Critical Buckling Load of the Fiber versus Radius of the Fiber ($E^I = 5.32 \times 10^7$psi, $E^{II} = 3.8 \times 10^5$psi, or $E^I/E^{II} = 140$)

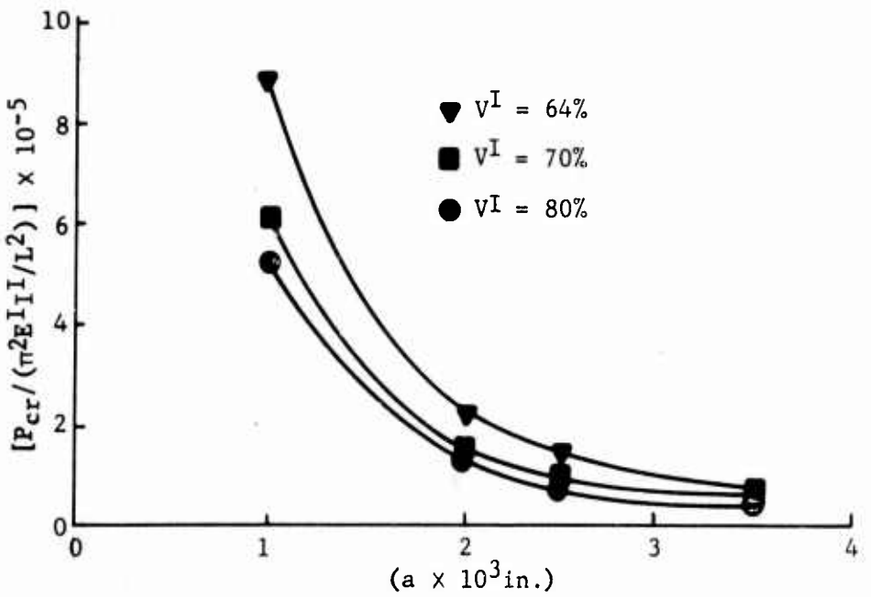

Figure 60. Critical Buckling Load of the Fiber versus Radius of the Fiber ($E^I = 6 \times 10^7$psi, $E^{II} = 3.8 \times 10^5$psi, or $E^I/E^{II} = 158$)

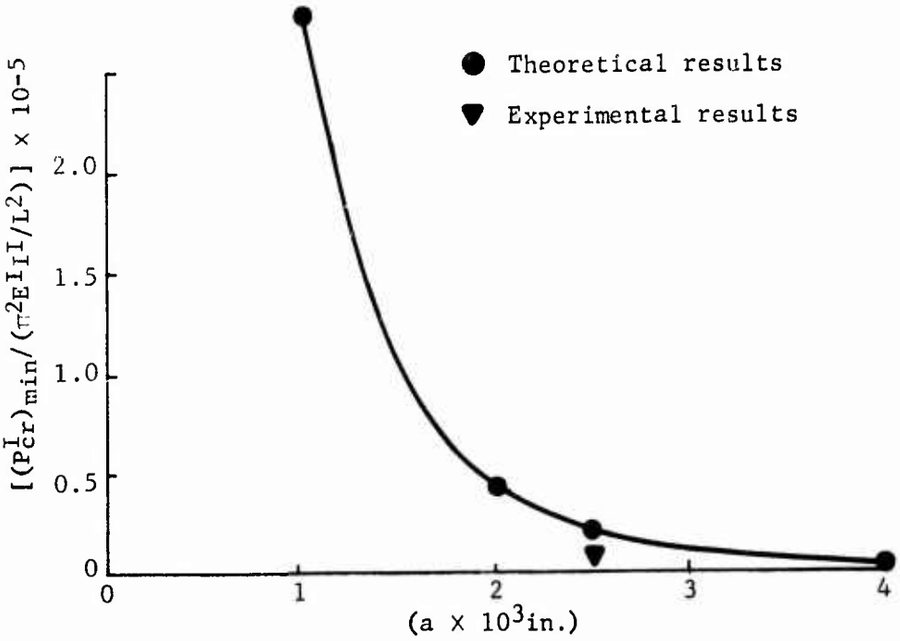

Figure 61. Critical Buckling Wavelength versus Radius of the Fiber

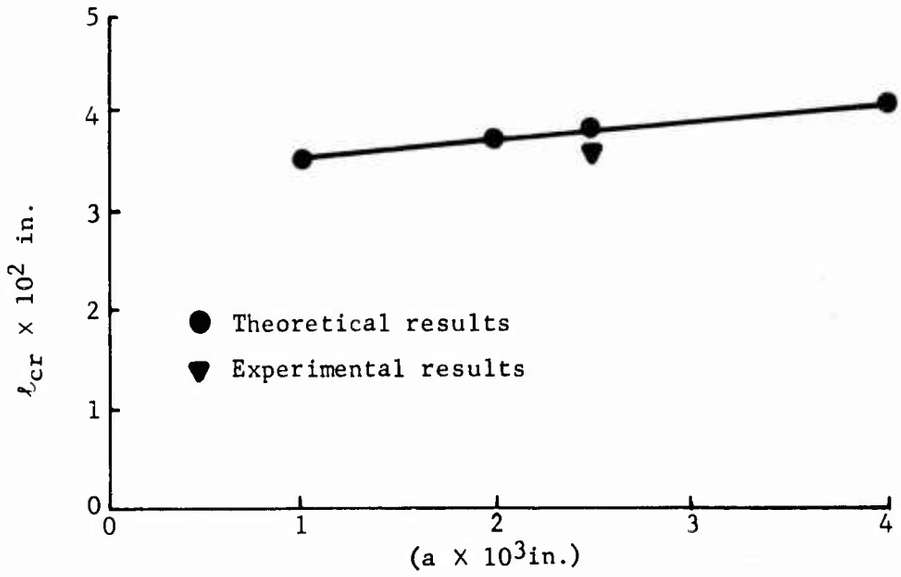

Figure 62. Smallest Critical Buckling Load of the Fiber versus Radius of the Fiber

D. Buckling of a Multifiber Composite Due to Resin Shrinkage

In this treatment, the energy was derived for a fiber resin cell. The equilibrium equation formulated as an energy variational problem derived in Appendix IV.D is

$$\delta \int_0^{\ell} \left\{ \frac{1}{2} \left[E^{I}A^{I} + E^{II}A^{II} \right] \varepsilon^2 + \frac{1}{2} \left[E^{I}I^{I} + E^{II}I^{II} \right] \varphi'^2 - E^{II}A^{II} \beta\varepsilon \right\} dz = \sum_{n=1}^{N} F_i^{(n)} \delta \ell_i^{(n)} \qquad (118)$$

with the restraining condition

$$\int_0^{\ell} \left\{ (1 + \varepsilon) \cos\varphi - (1 + \beta) \right\} dz = 0 \qquad (119)$$

In equation (118), the first brackets contain the compression energy in the axial direction; the second, the bending energy of the resin and the fiber. The third expression in (118) is the shrinkage energy of the resin. The right-hand expression in (118) is the energy introduced by the external force. The restraining condition (119) is derived from a simplifying assumption that the longitudinal change of the matrix is equal to that of the fiber. It must be emphasized that in this manner, the shear produced in longitudinal direction during buckling is neglected to simplify the resulting Lagrange equation.

The Lagrange equations corresponding to (118) are

$$\bar{P}\varepsilon + \bar{R} + \lambda \cos\varphi = 0 \qquad (120)$$

$$\bar{Q}\varphi'' + \lambda (1 + \varepsilon)\sin\varphi = 0 \qquad (121)$$

The factor λ is the Lagrange multiplier expressed in Appendix IV.D, equation (274). From equations (120) and (121), the following differential for φ is obtained:

$$\bar{Q}\varphi'' + \lambda\left(1 - \frac{\bar{R}}{\bar{P}} - \frac{\lambda}{\bar{P}}\cos\varphi\right)\sin\varphi = 0 \qquad (122)$$

The characteristic equation of (122) and the derivations necessary are given in Appendix IV.D* and are restated here:

$$\varphi^3 = -\frac{3}{k^2}\left\{E(\varphi;k) - F(\varphi;k)\frac{E(k)}{K(k)}\right\} \qquad (123)$$

To obtain the displacement of the fiber axis, φ has to be substituted into equation (351) of Appendix IV.D. The wavelength is obtained by equation (302), or by

$$z_w = \frac{2\pi\sqrt{2\bar{P}\bar{Q}}}{\sqrt{\lambda(\bar{P} - \bar{R} - \lambda)}} \qquad (124)$$

For small amplitudes of the maximum slope φ of the buckling curve, the Lagrange multiplier becomes, for the first approximation,**

$$\lambda = -(\bar{R} + \beta\bar{P}) \qquad (125)$$

This is a reasonably good solution for the eigenvalue λ. By calculating the second approximation, we must use equation (350) in Appendix IV.D. In this case, λ is the force exerted upon the fiber by the resin.

In spite of the fact that the interfacial shear was neglected, the results of this analysis coincide with the results obtained by Rosen (Reference 6). For $E^I = 10 \times 10^6$ psi and $E^{II} = 3.8 \times 10^5$ psi, where radius (a) = 2.5×10^{-3}, half distance of the fibers (b) = 2.976×10^{-3}, and the shrinkage $\beta = 1\%$.

---

* Equations (275) through (388).

** Reference equation (393).

The values in (124) and (125) are

$$\bar{P} = A^{I}E^{I} + A^{II}E^{II} = 199.56$$

$$\bar{R} = E^{II} A^{II} \beta^{II} = 4.56 \times 10^{-2}$$

$$\lambda = -(\bar{R} + \beta \bar{P}) = 1.95$$

$$\bar{Q} = E^{I}I^{I} + E^{II}I^{II} = 3.17 \times 10^{-4}$$

The computed wavelength is

$$z_w = 0.114 \text{ in.}$$

E. Buckling of Multifibers in a Matrix Under Axial Load With the Matrix Treated as a Three-Dimensional Cylinder

The critical buckling load of the fiber was found by minimizing total potential energy with respect to the amplitude of the assumed deflection curve of the fiber* and is rewritten as follows:

$$P_{cr}^{I} = \alpha_n^2 E^{I} I^{I} + \frac{k}{\alpha_n^2} + \pi\left(b^2 - a^2\right) G^{II} \left(1 + \frac{a}{d}\right)^2$$

where k is the unit interfacial force per unit lateral deflection; i.e.,

$$k = \frac{P_1}{\xi_1^{I}}$$

α_n is inversely proportional to the critical wavelength. Specifically,

$$\ell_{cr} = \frac{2\pi}{\alpha_j}$$

* Equations (70) through (72).

The displacement and stress fields in the matrix are determined by solving a three-dimensional elasticity problem (see Appendix IV.E). To obtain critical wavelength, we then take differentiation of P_{cr}^{I} with respect to α_n (equation 437) after substitution of k (equation 436) into equation (103). The expression for finding the value of α_j is given in equation (438). Therefore, the smallest critical buckling load can be found from equation (437) with the introduction of critical wavelength.

PART V – SHORT-FIBER STUDIES

During the contractual period, exploratory work was performed to establish any potential existing in the utilization of short fibers as reinforcing material in composites. Limited experiments were made to determine the elastic moduli and strength in compression, and the fatigue behavior of unidirectional composite in tension. The specimens were comprised of continuous glass fibers and short boron fibers oriented unidirectionally. The results of these exploratory experiments are reported in Appendix V.

The results of static tests in compression were compared with results available from tests made on pure glass fiber and pure boron fiber composite, and it has been concluded that the modulus of a composite can be adjusted to any level between that of the basic reinforcing constituents merely by varying their volumetric relationship at a constant resin content.

The primary purpose of the fatigue study was to determine whether the effect of the end of short boron fibers is one of destroying the matrix material and disintegrating the composite. According to the test results, it appears that this might indeed be the case. When comparing short fiber boron composite with continuous glass fiber composite and with 7075 aluminum, the very limited test results indicate that, although the short boron fiber is somewhat better in fatigue behavior than aluminum, it is inferior to continuous glass. However, an additional factor which must be considered is that due to the higher modulus, the deflections under load are smaller than those of a pure glass fiber composite.

An analysis of elasticity has not yet been applied to the short fiber composite. However, the experimental results appear to justify a strict analytical investigation of this type of material.

APPENDIX I

PARAMETRIC STUDIES

ANALYTICAL DISCUSSION

The following conditions and assumptions* pertain to the computer program which was developed to determine the three-dimensional stress, strain, and displacement fields in a composite. Also, a discussion and listing of the computer program are given at the end of this Appendix.

It was assumed that the composite consists of identical hexagonal elements. Each element has a centrally located fiber surrounded by resin as shown in Figure 62. Because of the symmetry involved, the following domains of the polar coordinates, r, φ, z, are sufficient to determine the displacement field in the hexagonal element.

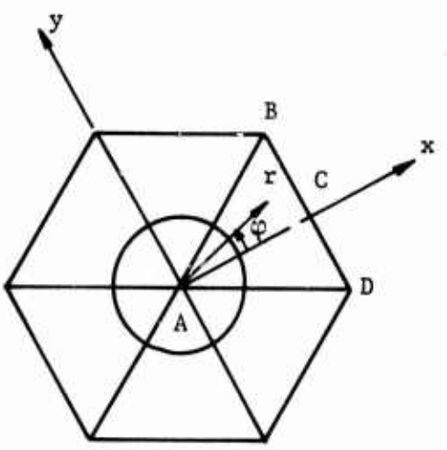

Figure 63. Typical Hexagonal Element of a Composite

*These conditions and assumptions are also presented in Reference 1.

For the fiber:

$$0 \leq r \leq a$$
$$0 \leq \varphi \leq 30^\circ$$
$$0 \leq z \leq \ell \qquad (126)$$

For the resin:

$$a \leq r \leq \frac{b}{\cos\varphi}$$
$$0 \leq \varphi \leq 30^\circ$$
$$0 \leq z \leq \ell \qquad (127)$$

The distance, b, is given in terms of the fiber volumetric content, V^I:

$$b = a\left[0.9069/V^I\right]^{1/2} \qquad (128)$$

At the interface, r = a, the displacements, ξ_i, and appropriate stresses, σ_{1i}, were assumed to be continuous:

$$\xi_i^I(a,\varphi,z) = \xi_i^{II}(a,\varphi,z)$$
$$\sigma_{1i}^I(a,\varphi,z) = \sigma_{1i}^{II}(a,\varphi,z) \qquad i = 1,2,3 \qquad (129)$$

At the hexagon boundary during shrinkage and axial loading, the plane forming the hexagon column containing $\bar{BD}$ and parallel to the z-axis or fiber axis remains a plane because it must be shared by the adjacent hexagonal element.

Relating the hexagonal elements in Figure 62 to a rectangular coordinate system x, y, and z, there is complete symmetry about the x = b plane. Therefore, the shear stresses must vanish in this plane so that

$$\sigma_{xy} = 0 \;, \quad \sigma_{xz} = 0$$

In addition to the vanishing shear, the normal displacement of $\bar{BD}$ relative to coordinates at point A must be

$$\xi_x = \epsilon_o$$

For the shrinkage case, ϵ_o/b would represent the total lateral composite shrinkage. For the loaded case, it would represent the total lateral expansion or contraction. Specifying the normal displacement and shear stresses at the hexagon boundary, however, has introduced another unknown: ϵ_o. An additional equation is obtained by considering that the total normal stress on the hexagon boundary plane $x = b$ in Figure 62 has to balance the external side loading. Because these side loads are zero for the present case, the normal stress must satisfy the equation

$$\int_0^{\ell} \int_0^{b \tan \pi/6} \sigma_{xx} \, dy \, dz = 0$$

The conditions for σ_{xy}, σ_{xz}, and ξ_x on the hexagon boundary must be satisfied for all values of y and z, such that

$$0 \leq y \leq b \tan \pi/6 \, , \quad 0 \leq z \leq \ell$$

The corresponding values in cylindrical coordinates become

$$r = b/\cos\phi \, , \quad 0 \leq \phi \leq \pi/6 \, , \quad 0 \leq z \leq \ell$$

The relation between the stresses, σ_{xx}, σ_{xy}, and σ_{xz}, and displacement, ξ_x, with reference to rectangular Cartesian coordinates and the stresses and displacements in polar coordinates are

$$\begin{aligned}
\sigma_{xx} &= \sigma_{11} \cos^2\phi - \sigma_{12} \sin 2\phi + \sigma_{22} \sin^2\phi \\
\sigma_{xy} &= \tfrac{1}{2} (\sigma_{11} - \sigma_{22}) \sin 2\phi + \sigma_{12} \cos 2\phi \\
\sigma_{xz} &= \sigma_{13} \cos\phi - \sigma_{23} \sin\phi \\
\xi_x &= \xi_1 \cos\phi - \xi_2 \sin\phi
\end{aligned} \tag{130}$$

The boundary conditions at the ends $z = \pm\ell$ of the composite are

$$\sigma_{33}^{I}(r, \varphi, \pm\ell) = \sigma_{\ell}^{I}$$
$$\sigma_{33}^{II}(r, \varphi, \pm\ell) = \sigma_{\ell}^{II}$$

Additionally, the following shear conditions at the composite ends are fulfilled.

$$\int\int \sigma_{3x}^{I}(r, \varphi, \pm\ell)\, r\, dr\, d\varphi = 0$$

$$\int\int \sigma_{3y}^{I}(r, \varphi, \pm\ell)\, r\, dr\, d\varphi = 0$$

$$\int\int \sigma_{3x}^{II}(r, \varphi, \pm\ell)\, r\, dr\, d\varphi = 0$$

$$\int\int \sigma_{3y}^{II}(r, \varphi, \pm\ell)\, r\, dr\, d\varphi = 0$$

For the shrinkage case, σ_{ℓ}^{I} and σ_{ℓ}^{II} are zero, and the shrinkage coefficients β^{I} and β^{II} are not zero. For the end loading case, β^{I} and β^{II} are zero and σ_{ℓ}^{I} and σ_{ℓ}^{II} have constant values. By superposition of the two cases, the total stress is obtained.

The materials were assumed to be individually isotropic linear material. The general assumptions for the classical theory of elasticity were used. From the many possibilities, the approach toward determining the solutions of the Navier equations by potentials connected with the names of Boussinesq, Papkovich, and Neuber has been selected. These general and complete solutions by potential functions for three-dimensional problems are given below in vector form to facilitate the resulting transformation to cylindrical coordinates.

$$\underset{\sim}{\xi} = \underset{\sim}{P} - \frac{1}{4(1-\nu)} \underset{\sim}{\nabla} \left(\underset{\sim}{R} \cdot \underset{\sim}{P} + P_0 \right)$$

$$\nabla^2 \underset{\sim}{P} = - \frac{2(1+\nu)}{E} \underset{\sim}{F}$$

$$\nabla^2 P_0 = \frac{2(1+\nu)}{E} \underset{\sim}{R} \cdot \underset{\sim}{F} \qquad (131)$$

In cylindrical coordinates, the vector quantities are expressed as

$$\underset{\sim}{\xi} = \xi_1 \underset{\sim}{e}_1 + \xi_2 \underset{\sim}{e}_2 + \xi_3 \underset{\sim}{e}_3$$

$$\underset{\sim}{P} = P_1 \underset{\sim}{e}_1 + P_2 \underset{\sim}{e}_2 + P_3 \underset{\sim}{e}_3 \qquad (132)$$

$$\underset{\sim}{R} = r \underset{\sim}{e}_1 + z \underset{\sim}{e}_3$$

and the operators become

$$\underset{\sim}{\nabla} = \frac{\partial}{\partial r} \underset{\sim}{e}_1 + \frac{1}{r} \frac{\partial}{\partial \phi} \underset{\sim}{e}_2 + \frac{\partial}{\partial z} \underset{\sim}{e}_3$$

$$\nabla^2 = \frac{\partial^2}{\partial r^2} + \frac{1}{r^2} \frac{\partial^2}{\partial \phi^2} + \frac{\partial^2}{\partial z^2}$$

When body forces are neglected, the solutions in terms of the vector components are

$$\begin{aligned} \xi_1 &= P_1 - \frac{1}{4(1-\nu)} \frac{\partial}{\partial r} S \\ \xi_2 &= P_2 - \frac{1}{4(1-\nu)} \frac{1}{r} \frac{\partial}{\partial \phi} S \\ \xi_3 &= P_3 - \frac{1}{4(1-\nu)} \frac{\partial}{\partial z} S \\ S &= r P_1 + z P_2 + P_0 \end{aligned} \qquad (133)$$

and

$$\nabla^2 [P_1 \underset{\sim}{e}_1 + P_2 \underset{\sim}{e}_2 + P_3 \underset{\sim}{e}_3] = \text{null vector}$$
$$\nabla^2 P_0 = 0 \tag{134}$$

Since $\underset{\sim}{e}_1$ and $\underset{\sim}{e}_2$ are functions of φ, it is more convenient to relate $\underset{\sim}{e}_1$ and $\underset{\sim}{e}_2$ to the unit vectors $\underset{\sim}{e}_x$ and $\underset{\sim}{e}_y$ associated with rectangular coordinates.

$$\underset{\sim}{e}_1 = \underset{\sim}{e}_x \cos\phi + \underset{\sim}{e}_y \sin\phi$$
$$\underset{\sim}{e}_2 = -\underset{\sim}{e}_x \sin\phi + \underset{\sim}{e}_y \cos\phi$$
$$\underset{\sim}{e}_3 = \underset{\sim}{e}_z \tag{135}$$

Then, by substituting (135) into the first equation of (134),

$$\nabla^2 [(P_1 \cos\phi - P_2 \sin\phi)\underset{\sim}{e}_x + (P_1 \sin\phi + P_2 \cos\phi)\underset{\sim}{e}_y + P_3 \underset{\sim}{e}_z] = \text{Null vector}$$

Since $\underset{\sim}{e}_x$, $\underset{\sim}{e}_y$, and $\underset{\sim}{e}_z$ are independent of position, then

$$\nabla^2 (P_1 \cos\phi - P_2 \sin\phi) = 0$$
$$\nabla^2 (P_1 \sin\phi + P_2 \cos\phi) = 0 \tag{136}$$

The solution of equations (136) and the last of (134) can be written in terms of the solution to Laplace's equation.

$$\nabla^2 L_i = 0 \qquad i = 0, 1, 2, 3 \tag{137}$$

where

$$L_0 = P_0$$
$$L_1 = P_1 \cos\phi - P_2 \sin\phi$$
$$L_2 = P_1 \sin\phi + P_2 \cos\phi$$
$$L_3 = P_3 \tag{138}$$

and the second and third equations of (138) can be solved for P_1 and P_2 so that P_i (i = 0, 1, 2, 3) can be written in terms of L_i (i = 0, 1, 2, 3).

$$
\begin{aligned}
P_0 &= L_0 \\
P_1 &= L_1 \cos\phi + L_2 \sin\phi \\
P_2 &= -L_1 \sin\phi + L_2 \cos\phi \\
P_3 &= L_3
\end{aligned}
\tag{139}
$$

The strains become

$$
\begin{aligned}
\epsilon_{11} &= \frac{\partial}{\partial r}\xi_1 \\
\epsilon_{22} &= \frac{1}{r}\frac{\partial}{\partial\phi}\xi_2 + \frac{1}{r}\xi_1 \\
\epsilon_{33} &= \frac{\partial}{\partial z}\xi_3 \\
\epsilon_{12} &= \frac{1}{2}\left(\frac{1}{r}\frac{\partial}{\partial\phi}\xi_1 + \frac{\partial}{\partial r}\xi_2 - \frac{1}{r}\xi_2\right) \\
\epsilon_{13} &= \frac{1}{2}\left(\frac{\partial}{\partial r}\xi_3 + \frac{\partial}{\partial z}\xi_1\right) \\
\epsilon_{23} &= \frac{1}{2}\left(\frac{\partial}{\partial z}\xi_2 + \frac{1}{r}\frac{\partial}{\partial\phi}\xi_3\right)
\end{aligned}
\tag{140}
$$

and the stresses are

$$
\sigma_{ij} = \frac{\nu E}{(1+\nu)(1-2\nu)}\delta_{ij}\, e + \frac{E}{1+\nu}\epsilon_{ij} \tag{141}
$$

Therefore, from the solution of (137), the Papkovitch functions can be determined by (139), then the general displacements by (133), and then the strains and stresses by (140) and (141) respectively.

DISPLACEMENT AND STRESS EQUATIONS

After deriving the general displacements and stresses, equations from (133) through (141), some of the symmetry and boundary conditions were used to reduce the equations to the following form.*

*The argument of all the Bessel functions is $\alpha_k r$.

The displacements for the fiber

$$\xi_1^I = \sum_{n=6,12,\cdots}^{\infty} \sum_{k=1,3,\cdots}^{\infty} \Big[A_{11nk}^I \Big(\frac{4-4\nu^I-n}{4(1-\nu^I)} I_{n-1} - \frac{\alpha_k r}{4(1-\nu^I)} I_n \Big) +$$

$$A_{21nk}^I \Big(\frac{4-4\nu^I+n}{4(1-\nu^I)} I_{n+1} - \frac{\alpha_k r}{4(1-\nu^I)} I_n \Big) +$$

$$\alpha_{nk}^I \Big(\frac{-\alpha_k}{4(1-\nu^I)} I_{n+1} - \frac{n}{4(1-\nu^I) r} I_n \Big) \Big] \cos \alpha_k z \sin n\varphi +$$

$$\sum_{k=1,3,\cdots}^{\infty} \Big[A_{210k}^I \Big(I_1 - \frac{\alpha_k r}{4(1-\nu^I)} I_0 \Big) + \alpha_{0k}^I \frac{-\alpha_k}{4(1-\nu^I)} I_1 \Big] \cos \alpha_k z +$$

$$\bar{A}_{210}^I \frac{1-2\nu^I}{2(1-\nu^I)} r$$

$$\xi_2^I = \sum_{n=6,12,\cdots}^{\infty} \sum_{k=1,3,\cdots}^{\infty} \Big[A_{11nk}^I \frac{-4+4\nu^I+n}{4(1-\nu^I)} I_{n-1} + A_{21nk}^I \frac{4-4\nu^I+n}{4(1-\nu^I)} I_{n+1} +$$

$$\alpha_{nk}^I \frac{n}{4(1-\nu^I) r} I_n \Big] \cos \alpha_k z \sin n\varphi$$

$$\xi_3^I = \sum_{n=6,12,\cdots}^{\infty} \sum_{k=1,3,\cdots}^{\infty} \Big[A_{11nk}^I \frac{\alpha_k r}{4(1-\nu^I)} I_{n-1} + A_{21nk}^I \frac{\alpha_k r}{4(1-\nu^I)} I_{n+1} +$$

$$+ \alpha_{nk}^I \frac{\alpha_k}{4(1-\nu^I)} I_n \Big] \sin \alpha_k z \cos n\varphi +$$

$$\sum_{k=1,3,\cdots}^{\infty} \Big[A_{210k}^I \frac{\alpha_k r}{4(1-\nu^I)} I_1 + \alpha_{0k}^I \frac{\alpha_k}{4(1-\nu^I)} I_0 \Big] \sin \alpha_k z + \frac{1-2\nu^I}{2(1-\nu^I)} \bar{C}_0^I z \tag{142}$$

The stresses for the fiber

$$\frac{1+\nu^I}{E^I}\sigma_{11}^I = \sum_{n=6,12\cdots}^{\infty}\sum_{k=1,3\cdots}^{\infty}\Big\{ f_{11nk}^I\Big[\Big(\frac{4-4\nu^I-n}{4(1-\nu^I)}\Big(\frac{n-1}{r}\Big)-\frac{\alpha_k^2 r}{4(1-\nu^I)}\Big)I_{n-1}+\frac{3\cdot 2\nu^I}{4(1-\nu^I)}\alpha_k I_n\Big]+$$

$$A_{21nk}^I\Big[\Big(-\frac{4-4\nu^I+n}{4(1-\nu^I)}\Big(\frac{n+1}{r}\Big)-\frac{\alpha_k^2 r}{4(1-\nu^I)}\Big)I_{n+1}+\frac{3\cdot 2\nu^I}{4(1-\nu^I)}\alpha_k I_n\Big]+$$

$$\alpha_{nk}^I\Big[\frac{\alpha_k}{4(1-\nu^I)r}I_{n+1}-\Big(\frac{(n-1)n}{4(1-\nu^I)r^2}+\frac{\alpha_k^2}{4(1-\nu^I)}\Big)I_n\Big]\Big\}\cos\alpha_k z\sin n\phi+$$

$$\sum_{k=1,3\cdots}^{\infty}\Big\{A_{210k}^I\Big[-\frac{1}{r}-\frac{\alpha_k^2 r}{4(1-\nu^I)}\Big)I_1+\frac{3\cdot 2\nu^I}{4(1-\nu^I)}\alpha_k I_0\Big]+$$

$$\alpha_{0k}^I\Big[\frac{\alpha_k}{4(1-\nu^I)r}I_1-\frac{\alpha_k^2}{4(1-\nu^I)}I_0\Big]\Big\}\cos\alpha_k z+$$

$$\frac{1}{2(1-\nu^I)}\bar{A}_{210}^I+\frac{1+\nu^I}{1-2\nu^I}\beta^I+\frac{\nu^I}{2(1-\nu^I)}\bar{C}_0^I$$

$$\frac{1+\nu^I}{E^I}\sigma_{12}^I = \sum_{n=6,12\cdots}^{\infty}\sum_{k=1,3,\cdots}^{\infty}\Big\{A_{11nk}^I\Big[\frac{-4+4\nu^I+n}{4(1-\nu^I)}\Big(\frac{n-1}{r}\Big)I_{n-1}+\frac{-2+2\nu^I+n}{4(1-\nu^I)}\alpha_k I_n\Big]+$$

$$A_{21nk}^I\Big[\frac{-4+4\nu^I-n}{4(1-\nu^I)}\Big(\frac{n+1}{r}\Big)I_{n+1}+\frac{2-2\nu^I+n}{4(1-\nu^I)}\alpha_k I_n\Big]+$$

$$\alpha_{nk}^I\Big[\frac{\alpha_k n}{4(1-\nu^I)r}I_{n+1}+\frac{n(n+1)}{4(1-\nu^I)r^2}I_n\Big]\Big\}\cos\alpha_k z\sin n\phi$$

$$\frac{1+\nu^I}{E^I}\sigma_{13}^I = \sum_{n=6,12\cdots}^{\infty}\sum_{k=1,3,\cdots}^{\infty}\Big\{A_{11nk}^I\Big[\frac{-2+2\nu^I+n}{4(1-\nu^I)}\alpha_k I_{n-1}+\frac{\alpha_k^2 r}{4(1-\nu^I)}I_n\Big]+$$

$$A_{21nk}^I\Big[\frac{-2+2\nu^I-n}{4(1-\nu^I)}\alpha_k I_{n+1}+\frac{\alpha_k^2 r}{4(1-\nu^I)}I_n\Big]+$$

$$\alpha_{nk}^I\Big[\frac{\alpha_k^2}{4(1-\nu^I)}I_{n+1}+\frac{n\alpha_k}{4(1-\nu^I)r}I_n\Big]\Big\}\sin\alpha_k\cos n\phi+$$

$$\sum_{k=1,3,\cdots}^{\infty}\left\{A_{210k}^{I}\left[-\frac{\alpha_k}{2}I_1+\frac{\alpha_k^2 r}{4(1-\nu^I)}I_0\right]+\alpha_{0k}^{I}\frac{\alpha_k^2}{4(1-\nu^I)}I_1\right\}\sin\alpha_k z$$

$$\frac{1+\nu^I}{E^I}\sigma_{22}^{I}=\sum_{n=6,12,\cdots}^{\infty}\sum_{k=1,3,\cdots}^{\infty}\left\{A_{11nk}^{I}\left[\frac{-4+4\nu^I+n}{4(1-\nu^I)}\left(\frac{n-1}{r}\right)I_{n-1}-\frac{1-2\nu^I}{4(1-\nu^I)}\alpha_k I_n\right]+\right.$$

$$A_{21nk}^{I}\left[\frac{4-4\nu^I+n}{4(1-\nu^I)}\left(\frac{n+1}{r}\right)I_{n+1}-\frac{1-2\nu^I}{4(1-\nu^I)}\alpha_k I_n\right]+$$

$$\left.\alpha_{nk}^{I}\left[-\frac{\alpha_k}{4(1-\nu^I)r}I_{n+1}+\frac{n(n-1)}{4(1-\nu^I)r^2}I_n\right]\right\}\cos\alpha_k z\cos n\phi+$$

$$\sum_{k=1,3,\cdots}^{\infty}\left[A_{210k}^{I}\left(\frac{1}{r}I_1-\frac{1-2\nu^I}{4(1-\nu^I)}I_0\right)+\alpha_{0k}^{I}\frac{-\alpha_k}{4(1-\nu^I)r}I_1\right]\cos\alpha_k z+$$

$$\frac{1}{2(1-\nu^I)}\bar{A}_{210}^{I}+\frac{\nu^I}{2(1-\nu^I)}\bar{C}_0^{I}+\frac{1+\nu^I}{1-2\nu^I}\beta^I$$

$$\frac{1+\nu^I}{E^I}\sigma_{23}^{I}=\sum_{n=6,12,\cdots}^{\infty}\sum_{k=1,3,\cdots}^{\infty}\left[A_{11nk}^{I}\frac{2-2\nu^I-n}{4(1-\nu^I)}\alpha_k I_{n-1}+A_{21nk}^{I}\frac{-2+2\nu^I-n}{4(1-\nu^I)}\alpha_k I_{n+1}+\right.$$

$$\left.\alpha_{nk}^{I}\frac{n\alpha_k}{4(1-\nu^I)r}I_n\right]\sin\alpha_k z\sin n\phi$$

$$\frac{1+\nu^I}{E^I}\sigma_{33}^{I}=\sum_{n=6,12,\cdots}^{\infty}\sum_{k=1,3,\cdots}^{\infty}\left\{A_{11nk}^{I}\left[\frac{\alpha_k^2 r}{4(1-\nu^I)}I_{n-1}+\frac{\alpha_k\nu^I}{2(1-\nu^I)}I_n\right]+\right.$$

$$A_{21nk}^{I}\left[\frac{\alpha_k^2 r}{4(1-\nu^I)}I_{n+1}+\frac{\alpha_k\nu^I}{2(1-\nu^I)}I_n\right]+$$

$$\left.\alpha_{nk}^{I}\frac{\alpha_k^2}{4(1-\nu^I)}I_n\right\}\cos\alpha_k z\cos n\phi+$$

$$\sum_{k=1,3,\cdots}^{\infty}\left\{A_{210k}^{I}\left[\frac{\alpha_k^2 r}{4(1-\nu^I)}I_1+\frac{\alpha_k\nu^I}{2(1-\nu^I)}I_0\right]+\alpha_{0k}^{I}\frac{\alpha_k^2}{4(1-\nu^I)}I_0\right\}\cos\alpha_k z+$$

$$\frac{\nu^I}{1-\nu^I}\bar{A}_{210}^{I}+\frac{1}{2}\bar{C}_0^{I}+\frac{1+\nu^I}{1-2\nu^I}\beta^I \qquad (143)$$

The displacements for the resin

$$\xi_1^{II} = \sum_{n=6,12\cdots}^{\infty} \sum_{k=1,3\cdots}^{\infty} \Big[A_{11nk}^{II} \Big(\frac{4-4\nu^{II}-n}{4(1-\nu^{II})} I_{n-1} - \frac{\alpha_k R}{4(1-\nu^{II})} I_n \Big) + A_{21nk}^{II} \Big(\frac{4-4\nu^{II}+n}{4(1-\nu^{II})} I_{n+1} - \frac{\alpha_k R}{4(1-\nu^{II})} I_n \Big) +$$

$$B_{11nk}^{II} \Big(\frac{4-4\nu^{II}-n}{4(1-\nu^{II})} K_{n-1} + \frac{\alpha_k R}{4(1-\nu^{II})} K_n \Big) + B_{21nk}^{II} \Big(\frac{4-4\nu^{II}+n}{4(1-\nu^{II})} K_{n+1} + \frac{\alpha_k R}{4(1-\nu^{II})} K_n \Big) +$$

$$\alpha_{nk}^{I} \Big(\frac{-\alpha_k}{4(1-\nu^{II})} I_{n+1} - \frac{n}{4(1-\nu^{II})R} I_n \Big) +$$

$$\beta_{nk}^{II} \Big(\frac{\alpha_k}{4(1-\nu^{II})} K_{n+1} - \frac{n}{4(1-\nu^{II})R} K_n \Big) \Big] \cos\alpha_k z \cos n\phi +$$

$$\sum_{k=1,3\cdots}^{\infty} \Big\{ A_{210k}^{II} \Big[I_1 - \frac{\alpha_k R}{4(1-\nu^{II})} I_0 \Big] + B_{210k}^{II} \Big[K_1 + \frac{\alpha_k R}{4(1-\nu^{II})} K_0 \Big] +$$

$$\alpha_{0k}^{II} \frac{-\alpha_k}{4(1-\nu^{II})} I_1 + \beta_{0k}^{II} \frac{\alpha_k}{4(1-\nu^{II})} K_1 \Big\} \cos\alpha_k z + A_{210}^{I} \frac{1-2\nu^{II}}{2(1-\nu^{II})} R + \bar{B}_{210}^{II} \frac{1}{R}$$

$$\xi_2^{II} = \sum_{n=6,12}^{\infty} \sum_{k=1,3\cdots}^{\infty} \Big[A_{11nk}^{II} \frac{-4+4\nu^{II}+n}{4(1-\nu^{II})} I_{n-1} + A_{21nk}^{II} \frac{4-4\nu^{II}+n}{4(1-\nu^{II})} I_{n+1} +$$

$$B_{11nk}^{II} \frac{-4+4\nu^{II}+n}{4(1-\nu^{II})} + B_{21nk}^{II} \frac{4-4\nu^{II}+n}{4(1-\nu^{II})} K_{n+1} +$$

$$\alpha_{nk}^{II} \frac{n}{4(1-\nu^{II})R} I_n + \beta_{nk}^{II} \frac{n}{4(1-\nu^{II})R} K_n \Big] \cos\alpha_k z \sin n\phi$$

$$\xi_3^{II} = \sum_{n=6,12}^{\infty} \sum_{k=1,3\cdots}^{\infty} \Big[A_{11nk}^{II} \frac{\alpha_k R}{4(1-\nu^{II})} I_{n-1} + A_{21nk}^{II} \frac{\alpha_k R}{4(1-\nu^{II})} I_{n+1} +$$

$$B_{11nk}^{II} \frac{\alpha_k R}{4(1-\nu^{II})} K_{n-1} + B_{21nk}^{II} \frac{\alpha_k R}{4(1-\nu^{II})} K_{n+1} +$$

$$\alpha_{nk}^{II}\frac{\alpha_k}{4(1-\nu^{II})}I_n+\beta_{nk}^{II}\frac{\alpha_k}{4(1-\nu^{II})}K_n\Big]\sin\alpha_k z\cos n\phi+$$

$$\sum_{k=1,3,\cdots}^{\infty}\Big[A_{210k}^{II}\frac{\alpha_k r}{4(1-\nu^{II})}I_1+B_{210k}^{II}\frac{\alpha_k r}{4(1-\nu^{II})}K_1+\alpha_{0k}^{II}\frac{\alpha_k}{4(1-\nu^{II})}I_0+$$

$$\beta_{0k}^{II}\frac{\alpha_k}{4(1-\nu^{II})}K_0\Big]\sin\alpha_k z+\frac{1-2\nu^{II}}{2(1-\nu^{II})}\bar{C}_0^{II}z \qquad (144)$$

The stresses for the resin

$$\frac{1+\nu^{II}}{E^{II}}\sigma_{11}^{II}=\sum_{n=6,12,\cdots}^{\infty}\sum_{k=1,3,\cdots}^{\infty}\Big\{A_{11nk}^{II}\Big[\Big(\frac{4-4\nu^{II}-n}{4(1-\nu^{II})}\Big(\frac{n-1}{r}\Big)-\frac{\alpha_k^2 r}{4(1-\nu^{II})}\Big)I_{n-1}+\frac{3-2\nu^{II}}{4(1-\nu^{II})}\alpha_k I_n\Big]+$$

$$A_{21nk}^{II}\Big[\Big(-\frac{4-4\nu^{II}+n}{4(1-\nu^{II})}\Big(\frac{n+1}{r}\Big)-\frac{\alpha_k^2 r}{4(1-\nu^{II})}\Big)I_{n+1}+\frac{3-2\nu^{II}}{4(1-\nu^{II})}\alpha_k I_n\Big]+$$

$$B_{11nk}^{II}\Big[\Big(\frac{4-4^{II}-n}{4(1-\nu^{II})}\Big(\frac{n-1}{r}\Big)-\frac{\alpha_k^2 r}{4(1-\nu^{II})}\Big)K_{n-1}-\frac{3-2\nu^{II}}{4(1-\nu^{II})}\alpha_k K_n\Big]+$$

$$B_{21nk}^{II}\Big[\Big(-\frac{4-4\nu^{II}+n}{4(1-\nu^{II})}\Big(\frac{n+1}{r}\Big)-\frac{\alpha_k^2 r}{4(1-\nu^{II})}\Big)K_{n+1}-\frac{3-2\nu^{II}}{4(1-\nu^{II})}\alpha_k K_n\Big]+$$

$$\alpha_{nk}^{II}\Big[\frac{\alpha_k}{4(1-\nu^{II})r}I_{n+1}-\Big(\frac{(n-1)n}{4(1-\nu^{II})r^2}+\frac{\alpha_k^2}{4(1-\nu^{II})}\Big)K_n\Big]\Big\}\times$$

$$\cos\alpha_k z\cos n\phi+$$

$$\sum_{k=1,3,\cdots}^{\infty}\Big\{A_{210k}^{II}\Big[-\Big(\frac{1}{r}+\frac{\alpha_k^2 r}{4(1-\nu^{II})}\Big)I_1+\frac{3-2\nu^{II}}{4(1-\nu^{II})}\alpha_k I_0\Big]+$$

$$B_{210k}^{II}\Big[-\Big(\frac{1}{r}+\frac{\alpha_k^2 r}{4(1-\nu^{II})}\Big)K_1-\frac{3-2\nu^{II}}{4(1-\nu^{II})}\alpha_k K_0\Big]+$$

$$\alpha_{0k}^{II}\Big(\frac{\alpha_k}{4(1-\nu^{II})r}I_1-\frac{\alpha_k^2}{4(1-\nu^{II})}I_0\Big]-\beta_{0k}^{II}\Big[\frac{\alpha_k}{4(1-\nu^{II})r}K_1+\frac{\alpha_k^2}{4(1-\nu^{II})}K_0\Big]\Big\}\times$$

$$\cos\alpha_k z+\frac{1}{2(1-\nu^{II})}\bar{A}_{210}+\frac{\nu^{II}}{2(1-\nu^{II})}\bar{C}_0^{II}-\bar{B}_{210}^{II}\frac{1}{r^2}+\frac{1+\nu^{II}}{1-2\nu^{II}}\beta^{II}$$

$$\frac{1+\nu^{II}}{E^{II}}\sigma_{12}^{II} = \sum_{n=6,12\cdots}^{\infty}\sum_{k=1,3}^{\infty}\Big\{A_{11nk}^{II}\Big[\frac{-4+4\nu^{II}+n}{4(1-\nu^{II})}\Big(\frac{n-1}{r}\Big)I_{n-1}+\frac{-2+2\nu^{II}+n}{4(1-\nu^{II})}\alpha_k I_n\Big]+$$

$$A_{21nk}^{II}\Big[\frac{-4+4\nu^{II}-n}{4(1-\nu^{II})}\Big(\frac{n+1}{r}\Big)I_{n+1}+\frac{2-2\nu^{II}+n}{4(1-\nu^{II})}\alpha_k I_n\Big]+$$

$$B_{11nk}^{II}\Big[\frac{-4+4\nu^{II}+n}{4(1-\nu^{II})}\Big(\frac{n-1}{r}\Big)K_{n-1}+\frac{2-2\nu^{II}-n}{4(1-\nu^{II})}\alpha_k K_n\Big]+$$

$$B_{21nk}^{II}\Big[\frac{-4+4\nu^{II}-n}{4(1-\nu^{II})}\Big(\frac{n+1}{r}\Big)K_{n+1}+\frac{-2+2\nu^{II}-n}{4(1-\nu^{II})}\alpha_k K_n\Big]+$$

$$\alpha_{nk}^{II}\Big[\frac{\alpha_k n}{4(1-\nu^{II})r}I_{n+1}+\frac{n(n-1)}{4(1-\nu^{II})r^2}I_n\Big]+$$

$$\beta_{nk}^{II}\Big[-\frac{\alpha_k n}{4(1-\nu^{II})r}K_{n+1}+\frac{n(n-1)}{4(1-\nu^{II})r^2}K_n\Big]\Big\}\cos\alpha_{kz}\sin n\phi$$

$$\frac{1+\nu^{I}}{E^{I}}\sigma_{13}^{II}=\sum_{n=6,12\cdots}^{\infty}\sum_{k=1,3,\cdots}^{\infty}\Big\{A_{11nk}^{II}\Big[\frac{-2+2\nu^{II}+n}{4(1-\nu^{II})}\alpha_k I_{n-1}+\frac{\alpha_k^2 r}{4(1-\nu^{II})}I_n\Big]+$$

$$A_{21nk}^{II}\Big[\frac{-2+2\nu^{II}-n}{4(1-\nu^{II})}\alpha_k I_{n+1}+\frac{\alpha_k^2 r}{4(1-\nu^{II})}I_n\Big]+$$

$$B_{11nk}^{II}\Big[\frac{-2+2\nu^{II}+n}{4(1-\nu^{II})}\alpha_k K_{n-1}-\frac{\alpha_k^2 r}{4(1-\nu^{II})}K_n\Big]+$$

$$B_{21nk}^{II}\Big[\frac{-2+2\nu^{II}-n}{4(1-\nu^{II})}\alpha_k K_{n+1}-\frac{\alpha_k^2 r}{4(1-\nu^{II})}K_n\Big]+$$

$$\alpha_{nk}^{II}\Big[\frac{\alpha_k^2}{4(1-\nu^{II})}I_{n+1}+\frac{n\alpha_k}{4(1-\nu^{II})r}I_n\Big]+$$

$$\beta_{nk}^{II}\Big[-\frac{\alpha_k^2}{4(1-\nu^{II})}K_{n+1}+\frac{n\alpha_k}{4(1-\nu^{II})r}K_n\Big]\Big\}\sin\alpha_k z\cos n\phi+$$

$$\sum_{k=1,3\cdots}^{\infty}\Big\{A_{210k}^{II}\Big[-\frac{\alpha_k}{2}I_1+\frac{\alpha_k^2 r}{4(1-\nu^{II})}I_0\Big]+B_{210k}^{II}\Big[-\frac{\alpha_k}{2}K_1-\frac{\alpha_k^2 r}{4(1-\nu^{II})}K_0\Big]+$$

$$\alpha_{0k}^{II}\frac{\alpha_k^2}{4(1-\nu^{II})}I_1-\beta_{0k}^{II}\frac{\alpha_k^2}{4(1-\nu^{II})}K_1\Big\}\sin\alpha_k z$$

$$\frac{1+\nu^{II}}{E^{II}}\sigma_{22}^{II} = \sum_{n=6,12,\cdots}^{\infty}\sum_{k=1,3,\cdots}^{\infty}\Big\{A_{11nk}^{II}\Big[\frac{-4+4\nu^{II}+n}{4(1-\nu^{II})}\Big(\frac{n-1}{r}\Big)I_{n-1} - \frac{1-2\nu^{II}}{4(1-\nu^{II})}\alpha_k I_n\Big] +$$

$$A_{21nk}^{II}\Big[\frac{4-4\nu^{II}+n}{4(1-\nu^{II})}\Big(\frac{n+1}{r}\Big)I_{n+1} - \frac{1-2\nu^{II}}{4(1-\nu^{II})}\alpha_k I_n\Big] +$$

$$B_{11nk}^{II}\Big[\frac{-4+4\nu^{II}+n}{4(1-\nu^{II})}\Big(\frac{n-1}{r}\Big)K_{n-1} + \frac{1-2\nu^{II}}{4(1-\nu^{II})}\alpha_k K_n\Big] +$$

$$B_{21nk}^{II}\Big[\frac{4-4\nu^{II}+n}{4(1-\nu^{II})}\Big(\frac{n+1}{r}\Big)K_{n+1} + \frac{1-2\nu^{II}}{4(1-\nu^{II})}\alpha_k K_n\Big] +$$

$$\alpha_{nk}^{II}\Big[-\frac{\alpha_k}{4(1-\nu^{II})r}I_{n+1} + \frac{n(n-1)}{4(1-\nu^{II})r^2}I_n\Big] +$$

$$\beta_{nk}^{II}\Big[\frac{\alpha_k}{4(1-\nu^{II})r}K_{n+1} + \frac{n(n-1)}{4(1-\nu^{II})r^2}K_n\Big]\Big\}\cos\alpha_k z\cos n\phi +$$

$$\sum_{k=1,3,\cdots}^{\infty}\Big\{A_{210k}^{II}\Big[\frac{1}{r}I_1 - \frac{1-2\nu^{II}}{4(1-\nu^{II})}\alpha_k I_0\Big] + B_{210k}^{II}\Big[\frac{1}{r}K_1 + \frac{1-2\nu^{II}}{4(1-\nu^{II})}\alpha_k K_0\Big] +$$

$$\alpha_{0k}^{II}\frac{-\alpha_k}{4(1-\nu^{II})r}I_1 + \beta_{0k}^{II}\frac{\alpha_k}{4(1-\nu^{II})r}K_1\Big\}\cos\alpha_k z +$$

$$\bar{B}_{210}^{II}\frac{1}{r^2} + \frac{i}{2(1-\nu^{II})}\bar{A}_{210}^{II} + \frac{\nu^{II}}{2(1-\nu^{II})}\bar{C}_0^{II} + \frac{1+\nu^{II}}{1-2\nu^{II}}\beta^{II}$$

$$\frac{1+\nu^{II}}{E^{II}}\sigma_{23}^{II} = \sum_{n=6,12,\cdots}^{\infty}\sum_{k=1,3,\cdots}^{\infty}\Big[A_{11nk}^{II}\frac{2-2\nu^{II}-n}{4(1-\nu^{II})}\alpha_k I_{n-1} + A_{21nk}^{II}\frac{-2+2\nu^{II}-n}{4(1-\nu^{II})}\alpha_k I_{n+1} +$$

$$B_{11nk}^{II}\frac{2-2\nu^{II}-n}{4(1-\nu^{II})}\alpha_k K_{n-1} + B_{21nk}^{II}\frac{-2+2\nu^{II}-n}{4(1-\nu^{II})}\alpha_k K_{n+1} +$$

$$\alpha_{nk}^{II}\frac{n\alpha_k}{4(1-\nu^{II})r}I_n + \beta_{nk}^{II}\frac{n\alpha_k}{4(1-\nu^{II})r}K_n\Big] \times$$

$$\sin\alpha_k z\sin n\phi$$

$$\frac{1+\nu^{II}}{E^{II}}\sigma_{33}^{II} = \sum_{n=6,12,\cdots}^{\infty}\sum_{k=1,3,\cdots}^{\infty}\Big\{A_{11nk}^{II}\Big[\frac{\alpha_k^2 r}{4(1-\nu^{II})}I_{n-1} + \frac{\alpha_k \nu^{II}}{2(1-\nu^{II})}I_n\Big] +$$

$$A_{21nk}^{II}\Big[\frac{\alpha_k^2 r}{4(1-\nu^{II})}I_{n+1} + \frac{2\alpha_k \nu^{II}}{2(1-\nu^{II})}I_n\Big] +$$

$$B_{11nk}^{II}\Big[\frac{\alpha_k^2 r}{4(1-\nu^{II})}K_{n-1} - \frac{\alpha_k \nu^{II}}{2(1-\nu^{II})}K_n\Big] +$$

$$B_{21nk}^{II}\Big[\frac{\alpha_k^2 r}{4(1-\nu^{II})}K_{n+1} - \frac{\alpha_k \nu^{II}}{2(1-\nu^{II})}K_n\Big] +$$

$$\alpha_{nk}^{II}\frac{\alpha_k^2}{4(1-\nu^{II})}I_n + \beta_{nk}^{II}\frac{\alpha_k^2}{4(1-\nu^{II})}K_n\Big] \times$$

$$\cos\alpha_k z\cos n\phi +$$

$$\sum_{k=1,3,\cdots}^{\infty}\Big\{A_{210k}^{II}\Big[\frac{\alpha_k^2 r}{4(1-\nu^{II})}I_1 + \frac{\alpha_k \nu^{II}}{2(1-\nu^{II})}I_0\Big] +$$

$$B_{210k}^{II}\Big[\frac{\alpha_k^2 r}{4(1-\nu^{II})}K_1 - \frac{\alpha_k \nu^{II}}{2(1-\nu^{II})}K_0\Big] + \alpha_{0k}^{II}\frac{\alpha_k^2}{4(1-\nu^{II})}I_0 +$$

$$\beta_{0k}^{II}\frac{\alpha_k^2}{4(1-\nu^{II})}K_0\Big\}\cos\alpha_k z + \frac{\nu^{II}}{1-\nu^{II}}\bar{A}_{210}^{II} +$$

$$\frac{1}{2}\bar{C}_0^{II} + \frac{1+\nu^{II}}{1-2\nu^{II}}\beta^{II} \qquad (145)$$

Equations (142) through (145) were then programmed in order to determine the remaining integration constants and then the displacement, strain, and stress fields.

APPENDIX II

THREE-DIMENSIONAL LOAD TRANSFER AMONG FIBERS IN A MATRIX

Displacements which satisfy symmetry conditions (1) can be written as:

$$
\begin{aligned}
4(1-\nu)\xi_1 = &\sum_{n=0}^{\infty}\sum_{k=0}^{\infty}\Big\{\Big\{A_{12nk}\left[(4-4\nu-n)I_{n-1}-\mu r I_n\right]+A_{21nk}\left[(4-4\nu+n)I_{n+1}-\mu r I_n\right]\\
&+B_{12nk}\left[(4-4\nu-n)K_{n-1}+\mu r K_n\right]+B_{21nk}\left[(4-4\nu+n)K_{n+1}+\mu r K_n\right]\\
&-A_{nk}\left[\mu I_{n+1}+\frac{n}{r}I_n\right]+B_{nk}\left[\mu K_{n+1}-\frac{n}{r}K_n\right]\Big\}\cos\mu z\\
&-\Big\{A_{3nk}\left[\mu I_{n+1}+\frac{n}{r}I_n\right]-B_{3nk}\left[\mu K_{n+1}-\frac{n}{r}K_n\right]\Big\}z\sin\mu z\Big\}\cos n\varphi\\
&+\sum_{k=0}^{\infty}\Big\{\Big\{A_{1k}\left[(3-4\nu)I_0-\mu r I_1\right]+B_{1k}\left[(3-4\nu)K_0+\mu r K_1\right]\Big\}\cos\varphi\cos\mu z\\
&+\Big\{A_{2k}\left[(3-4\nu)I_0-\mu r I_1\right]+B_{2k}\left[(3-4\nu)K_0+\mu r K_1\right]\Big\}\varphi\sin\varphi\cos\mu z\\
&+\Big\{A_{21k}\left[4(1-\nu)I_1-\mu r I_0\right]+B_{21k}\left[4(1-\nu)K_1+\mu r K_0\right]-A_k\mu I_1\\
&+B_k\mu K_1\Big\}\cos\mu z-\Big\{A_{3k}\mu I_1-B_{3k}\mu K_1\Big\}z\sin\mu z\Big\}\\
&+\sum_{n=0}^{\infty}\Big\{A_{4n}r^{n-1}+B_{4n}r^{-n-1}+A_{21n}(2-4\nu-n)r^{n+1}\\
&+B_{12n}(2-4\nu-n)r^{-n+1}-A_{3n}nr^{n-1}z^2+B_{3n}nr^{-n-1}z^2\Big\}\cos n\varphi\\
&+\Big\{A_1(3-4\nu)+B_1\left[(3-4\nu)\log r-1\right]\Big\}\cos\varphi\\
&+\Big\{A_2(3-4\nu)+B_2\left[(3-4\nu)\log r-1\right]\Big\}\varphi\sin\varphi\\
&+B_3z^2/r+A_{21}(2-4\nu)r+B_4/r
\end{aligned}
\qquad (146)
$$

$$
\begin{aligned}
4(1-\nu)\xi_2 = \sum_{n=0}^{\infty}\sum_{k=0}^{\infty}\Big[\Big\{ & A_{12nk}(n-4+4\nu)I_{n-1} + A_{21nk}(4-4\nu+n)I_{n+1} \\
& + B_{12nk}(n-4+4\nu)K_{n-1} + B_{21nk}(4-4\nu+n)K_{n+1} \\
& + \frac{n}{\mathfrak{r}}(A_{nk}I_n + B_{nk}K_n)\Big\}\cos\mu z \\
& + \frac{n}{\mathfrak{r}}\Big\{A_{3nk}I_n + B_{3nk}K_n\Big\} z\sin\mu z\Big]\sin n\varphi \\
- \sum_{k=0}^{\infty}\Big[\Big\{ & \big[A_{1k}(3-4\nu)+A_{2k}\big]I_0 + \big[B_{1k}(3-4\nu)+B_{2k}\big]K_0\Big\}\sin\varphi \\
& - (3-4\nu)\Big\{A_{2k}I_0 + B_{2k}K_0\Big\}\varphi\cos\varphi\Big]\cos\mu z \\
+ \sum_{n=0}^{\infty}\Big\{ & -A_{4n}\mathfrak{r}^{n-1} + B_{4n}\mathfrak{r}^{-n-1} + A_{21n}(4-4\nu+n)\mathfrak{r}^{n+1} \\
& + B_{12n}(n-4+4\nu)\mathfrak{r}^{-n+1} + A_{3n}n\mathfrak{r}^{n-1}z^2 \\
& + B_{3n}n\mathfrak{r}^{-n-1}z^2\Big\}\sin n\varphi \\
- \Big\{ & A_1(3-4\nu) + A_2 + \big[B_1(3-4\nu)+B_2\big]\log\mathfrak{r}\Big\}\sin\varphi \\
& + (3-4\nu)\big(A_2 + B_2\log\mathfrak{r}\big)\varphi\cos\varphi \qquad (147)
\end{aligned}
$$

$$
\begin{aligned}
4(1-\nu)\xi_3 = \sum_{n\geq 0}^{\infty}\sum_{k\geq 0}^{\infty}\Big\{\Big\{ & \mu r\left[A_{12nk}I_{n-1} + A_{21nk}I_{n+1} + B_{12nk}K_{n-1} + B_{21nk}K_{n+1}\right] \\
& + \mu\left(A_{nk}I_n + B_{nk}K_n\right) + (3-4\nu)\left(A_{3nk}I_n + B_{3nk}K_n\right)\Big\}\sin\mu z \\
& - \mu\left\{A_{3nk}I_n + B_{3nk}K_n\right\} z\cos\mu z\Big\}\cos n\varphi \\
+ \sum_{k\geq 0}^{\infty}\Big[\Big\{ & -\mu r\left[\left(A_{1k}I_0 + B_{1k}K_0\right)\cos\varphi + \left(A_{2k}I_0 + B_{2k}K_0\right)\varphi\sin\varphi\right] \\
& + \mu r\left(A_{21k}I_1 + B_{21k}K_1\right) + \mu\left(A_kI_0 + B_kK_0\right) \\
& + (3-4\nu)\left(A_{3k}I_0 + B_{3k}K_0\right)\Big\}\sin\mu z \\
& - \mu\left\{A_{3k}I_0 + B_{3k}K_0\right\} z\cos\mu z\Big] \\
+ \sum_{n\geq 0}^{\infty} & 2(1-2\nu)\left[A_{3n}r^n + B_{3n}r^{-n}\right] z\cos n\varphi \\
+ & 2(1-2\nu)\left[A_3 + B_3\log r\right] z
\end{aligned}
\tag{148}
$$

where $A_{4n} = A_{12n}(4-4\nu-n) - A_n n$

$B_{4n} = B_{21n}(4-4\nu+n) + B_n n$, $B_4 = 4(1-\nu)B_{21} - B$

and where I_n and K_n are modified Bessel functions of the first and second kinds and order n with argument μr being omitted.

The first numerical subscript of any coefficient in the above equations refers to the term contributed by the corresponding Pi (i=1,2,3) and the first two subscripts 12 or 21 by P1 and/or P2. The coefficient without numerical subscripts refers to the term contributed by Po. Therefore the four Papkovich-Neuber functions in cylindrical coordinates have to be considered in the present analysis.

$$\frac{4(1-\nu^2)}{E}\sigma_{11} = \sum_{n=0}^{\infty}\sum_{k=0}^{\infty}\Big[\Big\{A_{12nk}\Big[(4-4\nu-n)\frac{n-1}{r}I_{n-1} - \mu^2 r I_{n-1} + (3-2\nu)\mu I_n\Big]$$
$$+ B_{12nk}\Big[(4-4\nu-n)\frac{n-1}{r}K_{n-1} - \mu^2 r K_{n-1} - (3-2\nu)\mu K_n\Big]$$
$$- A_{21nk}\Big[(4-4\nu+n)\frac{n+1}{r}I_{n+1} + \mu^2 r I_{n+1} - (3-2\nu)\mu I_n\Big]$$
$$- B_{21nk}\Big[(4-4\nu+n)\frac{n+1}{r}K_{n+1} + \mu^2 r K_{n+1} + (3-2\nu)\mu K_n\Big]$$
$$+ A_{3nk}\Big[\frac{\mu}{r}I_{n+1} - \Big(\frac{n^2-n}{r^2}+\mu^2\Big)I_n\Big] - B_{3nk}\Big[\frac{\mu}{r}K_{n+1} + \Big(\frac{n^2-n}{r^2}+\mu^2\Big)K_n\Big]$$
$$+ 2\nu\mu\big[A_{3nk}I_n + B_{3nk}K_n\big]\Big\}\cos\mu z + \Big\{A_{3nk}\Big[\frac{\mu}{r}I_{n+1} - \Big(\frac{n^2-n}{r^2}+\mu^2\Big)I_n\Big]$$
$$- B_{3nk}\Big[\frac{\mu}{r}K_{n+1} - \Big(\frac{n^2-n}{r^2}+\mu^2\Big)K_n\Big]\Big\} z\sin\mu z\Big]\cos n\varphi$$
$$+ \sum_{k=0}^{\infty}\Big[\Big\{A_{1k}\mu\big[\mu r I_0 - 3(1-2\nu)I_1\big] - B_{1k}\mu\Big[\frac{\mu r}{1-2\nu}K_0 + (3-2\nu)K_1\Big]$$
$$+ A_{2k}\frac{2\nu}{r}I_0 + B_{2k}\frac{2\nu}{r}K_0\Big\}\cos\varphi\cos\mu z$$
$$+ \Big\{A_{2k}\mu\big[\mu r I_0 - 3(1-2\nu)I_1\big]$$
$$- B_{2k}\mu\Big[\frac{\mu r}{1-2\nu}K_0 + 3(1-2\nu)K_1\Big]\Big\}\varphi\sin\varphi\cos\mu z$$
$$- \Big\{A_{21k}\Big[\Big(\frac{4-4\nu}{r}+\mu^2 r\Big)I_1 - (3-2\nu)I_0\Big] + B_{21k}\Big[\Big(\frac{4-4\nu}{r}+\mu^2 r\Big)K_1 + (3-2\nu)K_0\Big]$$
$$- A_k\Big[\frac{\mu}{r}I_1 - \mu^2 I_0\Big] + B_k\Big[\frac{\mu}{r}K_1 + \mu^2 K_0\Big]$$
$$- 2\nu\mu\big[A_{3k}I_0 + B_{3k}K_0\big]\Big\}\cos\mu z$$
$$+ \Big\{A_{3k}\Big[\frac{\mu}{r}I_1 - \mu^2 I_0\Big] - B_{3k}\Big[\frac{\mu}{r}K_1 + \mu^2 K_0\Big]\Big\} z\sin\mu z\Big]$$
$$+ \sum_{n=0}^{\infty}\Big\{A_{4n}(n-1)r^{n-2} - B_{4n}(n+1)r^{-n-2} - A_{21n}(n+1)(n-2)r^n$$
$$- B_{12n}(n-1)(n+2)r^{-n} + A_{3n}\big[2\nu r^n - n(n-1)r^{n-2}z^2\big]$$
$$+ B_{3n}\big[2\nu r^{-n} - n(n+1)r^{-n-2}z^2\big]\Big\}\cos n\varphi$$
$$+ \frac{1}{r}\big[2\nu A_2 + B_1(3-2\nu) + 2\nu B_2\log r\big]\cos\varphi + \frac{B_2}{r}(3-2\nu)\varphi\sin\varphi$$
$$+ 2A_{21} - B_4 r^{-2} + 2\nu A_3 + B_3(z^2/r^2 + 2\nu\log r) \qquad (149)$$

$$\frac{4(1-\nu^2)}{E}\sigma_{12} = \sum_{n=0}^{\infty}\sum_{k=0}^{\infty}\Big[\Big\{A_{12nk}\Big[(n-4+4\nu)\frac{n-1}{r}I_{n-1}+(n-2+2\nu)\mu I_n\Big]$$
$$+B_{12nk}\Big[(n-4+4\nu)\frac{n-1}{r}K_{n-1}-(n-2+2\nu)\mu K_n\Big]$$
$$-A_{21nk}\Big[(n+4-4\nu)\frac{n+1}{r}I_{n+1}-(n+2-2\nu)\mu I_n\Big]$$
$$-B_{21nk}\Big[(n+4-4\nu)\frac{n+1}{r}K_{n+1}+(n+2-2\nu)\mu K_n\Big]$$
$$+A_{nk}\Big[\frac{n\mu}{r}I_{n+1}+\frac{n(n-1)}{r^2}I_n\Big]-B_{nk}\Big[\frac{n\mu}{r}K_{n+1}-\frac{n(n-1)}{r^2}K_n\Big]\Big\}$$
$$\cdot\cos\mu z+\Big\{A_{3nk}\Big[\frac{n\mu}{r}I_{n+1}+\frac{n(n-1)}{r^2}I_n\Big]$$
$$-B_{3nk}\Big[\frac{n\mu}{r}K_{n+1}+\frac{n(n-1)}{r^2}K_n\Big]\Big\}z\sin\mu z\Big]\sin n\varphi$$
$$+\sum_{k=0}^{\infty}\Big[\Big\{A_{2k}\Big[\frac{3-4\nu}{r}I_0+(1-2\nu)\mu I_1\Big]+B_{2k}\Big[\frac{3-4\nu}{r}K_0-(1-2\nu)\mu K_1\Big]\Big\}$$
$$\cdot\varphi\cos\varphi-\Big\{A_{1k}\Big[\frac{3-4\nu}{r}I_0+(1-2\nu)\mu I_1\Big]$$
$$+B_{1k}\Big[\frac{3-4\nu}{r}K_0-(1-2\nu)\mu K_1\Big]-A_{2k}\Big[\frac{1-2\nu}{r}I_0-\mu I_1\Big]$$
$$-B_{2k}\Big[\frac{1-2\nu}{r}K_0+\mu K_1\Big]\Big\}\sin\varphi\Big]\cos\mu z$$
$$+\sum_{n=0}^{\infty}\Big\{-A_{4n}(n-1)r^{n-2}-B_{4n}(n+1)r^{-n-2}$$
$$+A_{21n}n(n+1)r^n-B_{12n}n(n-1)r^{-n}$$
$$+A_{3n}n(n-1)r^{n-2}z^2+B_{3n}n(n+1)r^{-n-2}z^2\Big\}$$
$$\cdot\sin n\varphi$$
$$+\frac{1}{r}(1-2\nu)\Big[B_2\varphi\cos\varphi-(B_1-B_2\log r)\sin\varphi\Big] \qquad (150)$$

$$\frac{4(1-\nu^2)}{E}\sigma_{13} = \sum_{n>0}^{\infty}\sum_{k>0}^{\infty}\Big\{\Big\{A_{12nk}\big[(n-2+2\nu)\mu I_{n-1}+\mu^2 r I_n\big]+B_{12nk}\big[(n-2+2\nu)\mu K_{n-1}-\mu^2 r K_n\big]$$

$$-A_{21nk}\big[(n+2-2\nu)\mu I_{n+1}-\mu^2 r I_n\big]-B_{21nk}\big[(n+2-2\nu)\mu K_{n+1}+\mu^2 r K_n\big]$$

$$+A_{3nk}\Big[\mu^2 I_{n+1}+\frac{n\mu}{r}I_n\Big]-B_{3nk}\Big[\mu^2 K_{n+1}-\frac{n\mu}{r}K_n\Big]$$

$$+(1-2\nu)\Big[A_{3nk}\Big(\mu I_{n+1}+\frac{n}{r}I_n\Big)-B_{3nk}\Big(\mu K_{n+1}-\frac{n}{r}K_n\Big)\Big]\Big\}\sin\mu z$$

$$-\Big\{A_{3nk}\Big[\mu^2 I_{n+1}+\frac{n\mu}{r}I_n\Big]-B_{3nk}\Big[\mu^2 K_{n+1}-\frac{n\mu}{r}K_n\Big]\Big\}z\cos\mu z\Big\}\cos n\varphi$$

$$+\sum_{k>0}^{\infty}\Big[\Big\{A_{1k}\big[(1-2\nu)I_0-\mu r I_1\big]+B_{1k}\big[(1-2\nu)K_0+\mu r K_1\big]\Big\}$$

$$\cdot\mu\cos\varphi\sin\mu z$$

$$+\Big\{A_{2k}\big[(1-2\nu)I_0-\mu r I_1\big]+B_{2k}\big[(1-2\nu)K_0+\mu r K_1\big]\Big\}$$

$$\cdot\mu\varphi\sin\varphi\sin\mu z$$

$$+\Big\{A_{21k}\big[\mu^2 r I_0-2\mu(1-\nu)I_1\big]-B_{21k}\big[\mu^2 r K_0+2\mu(1-\nu)K_1\big]$$

$$+\mu^2(A_k I_1-B_k K_1)+(1-2\nu)\mu\big[A_{3k}I_1-B_{3k}K_1\big]\Big\}\sin\mu z$$

$$-\mu^2\big\{A_{3k}I_1-B_{3k}K_1\big\}z\cos\mu z\Big\}$$

$$-B_3\nu z/r \qquad (151)$$

$$\frac{4(1-\nu^2)}{E}\sigma_{22} = \sum_{n=0}^{\infty}\sum_{k=0}^{\infty}\Big[\Big\{A_{12nk}\Big[(n-4+4\nu)\frac{n-1}{r}I_{n-1}-(1-2\nu)\mu I_n\Big]$$
$$+B_{12nk}\Big[(n-4+4\nu)\frac{n-1}{r}K_{n-1}+(1-2\nu)\mu K_n\Big]$$
$$+A_{21nk}\Big[(n+4-4\nu)\frac{n+1}{r}I_{n+1}-(1-2\nu)\mu I_n\Big]$$
$$+B_{21nk}\Big[(n+4-4\nu)\frac{n+1}{r}K_{n+1}+(1-2\nu)\mu K_n\Big]$$
$$-A_{3nk}\Big[\frac{\mu}{r}I_{n+1}-\frac{n(n-1)}{r^2}I_n\Big]+B_{3nk}\Big[\frac{\mu}{r}K_{n+1}+\frac{n(n-1)}{r^2}K_n\Big]$$
$$+2\nu\mu\left[A_{3nk}I_n+B_{3nk}K_n\right]\Big\}\cos\mu z$$
$$-\Big\{A_{3nk}\Big[\frac{\mu}{r}I_{n+1}-\frac{n(n-1)}{r^2}I_n\Big]-B_{3nk}\Big[\frac{\mu}{r}K_{n+1}+\frac{n(n-1)}{r^2}K_n\Big]\Big\}$$
$$\cdot z\sin\mu z\Big]\cos n\varphi$$
$$+\sum_{k=0}^{\infty}\Big[\Big\{-A_{1k}(1-2\nu)\mu I_1+\frac{2}{r}(1-\nu)\left[A_{2k}I_0+B_{2k}K_0\right]$$
$$+B_{1k}\Big[\frac{2\nu}{1-2\nu}\mu^2 r K_0+(1-2\nu)\mu K_1\Big]\Big\}\cos\varphi\cos\mu z$$
$$-\Big\{A_{2k}(1-2\nu)\mu I_1+B_{2k}\Big[\frac{2\nu}{1-2\nu}\mu^2 r K_0-(1-2\nu)\mu K_1\Big]\Big\}$$
$$\cdot\varphi\sin\varphi\cos\mu z$$
$$+\Big\{A_{2k}\Big[\frac{4(1-\nu)}{r}I_1-(1-2\nu)\mu I_0\Big]+B_{2k}\Big[\frac{4(1-\nu)}{r}K_1+(1-2\nu)\mu K_0\Big]$$
$$-\frac{\mu}{r}(A_k I_1-B_k K_1)+2\nu\mu(A_{3k}I_0+B_{3k}K_0)\Big\}\cos\mu z$$
$$-\Big\{A_{3k}\frac{\mu}{r}I_1-B_{3k}\frac{\mu}{r}K_1\Big\}z\sin\mu z\Big]$$
$$+\sum_{n=0}^{\infty}\Big\{-A_{4n}(n-1)r^{n-2}+A_{21n}(n+1)(n+2)r^n$$
$$+B_{4n}(n+1)r^{-n-2}+B_{12n}(n-1)(n-2)r^{-n}$$
$$+A_{3n}n(n-1)r^{n-2}z^2+B_{3n}n(n+1)r^{-n-2}z^2\Big\}\cos n\varphi$$
$$+\frac{1}{r}\left[2(1-\nu)(A_2+B_2\log r)-(1-2\nu)B_1\right]\cos\varphi-\frac{B_2}{r}(1-2\nu)\varphi\sin\varphi$$
$$+2A_{21}+B_4r^{-2}+2\nu A_3-B_3\left(z^2/r-2\nu\log r\right) \quad (152)$$

$$\frac{4(1-\nu^2)}{E}\sigma_{23} = \sum_{n=0}^{\infty}\sum_{k=0}^{\infty}\Big[\Big\{A_{12nk}(2-2\nu-n)\mu I_{n-1} + B_{12nk}(2-2\nu-n)\mu K_{n-1}$$
$$+ A_{21nk}(2-2\nu+n)\mu I_{n+1} - B_{21nk}(2-2\nu+n)\mu K_{n+1}$$
$$+ \frac{n\mu}{r}(A_{nk}I_n + B_{nk}K_n) - \frac{n}{r}(1-2\nu)\left[A_{3nk}I_n + B_{3nk}K_n\right]\Big\}$$
$$\cdot \sin\mu z + \frac{n\mu}{r}\left\{A_{3nk}I_n + B_{3nk}K_n\right\} z\cos\mu z\Big\}\sin n\varphi$$
$$- \sum_{k=0}^{\infty}\Big\{\mu\left[(1-2\nu)(A_{1k}I_0 + B_{1k}K_0) + A_{2k}I_0 + B_{2k}K_0\right]$$
$$\cdot \sin\varphi - \mu(1-2\nu)\left[A_{2k}I_0 + B_{2k}K_0\right]\varphi\cos\varphi\Big\}\sin\mu z$$
$$+ \sum_{n=0}^{\infty} 2\nu n\left[A_{3n}r^{n-1} - B_{3n}r^{-n-1}\right] z\sin n\varphi$$

(153)

$$\frac{4(1-\nu^2)}{E}\sigma_{33} = \sum_{n=0}^{\infty}\sum_{k=0}^{\infty}\Big[\Big\{A_{12nk}\left[\mu^2 r I_{n-1} + 2\nu\mu I_n\right] + A_{21nk}\left[\mu^2 r I_{n+1} + 2\nu\mu I_n\right]$$
$$+ B_{12nk}\left[\mu^2 r K_{n-1} - 2\nu\mu K_n\right] + B_{21nk}\left[\mu^2 r K_{n+1} - 2\nu\mu K_n\right]$$
$$+ \mu^2\left[A_{nk}I_n + B_{nk}K_n\right] + \frac{\mu}{2}\left[A_{3nk}I_n + B_{3nk}K_n\right]\Big\}\cos\mu z$$
$$+ \mu^2\left\{A_{3nk}I_n + B_{3nk}K_n\right\} z\sin\mu z\Big\}\cos n\varphi$$
$$+ \sum_{k=0}^{\infty}\Big[\Big\{\Big[A_{1k}(2\nu\mu I_1 - \mu^2 r I_0) - B_{1k}\left(2\nu\mu K_1 + \frac{\mu^2 r}{1-2\nu}K_0\right)$$
$$+ \frac{2\nu}{r}(A_{2k}I_0 + B_{2k}K_0)\Big]\cos\varphi$$
$$+ \left[A_{2k}(2\nu\mu I_1 - \mu^2 r I_0) - B_{2k}\left(2\nu\mu K_1 + \frac{\mu^2 r}{1-2\nu}K_0\right)\right]\varphi\sin\varphi$$
$$+ A_{21k}(\mu^2 r I_1 + 2\nu\mu I_0) + B_{21k}(\mu^2 r K_1 - 2\nu\mu K_0)$$

$$+\mu^2(A_k I_0 + B_k K_0) + \frac{\mu}{2}(A_{3k} I_0 + B_{3k} K_0)\Big\}\cos\mu z$$
$$+\mu^2\{A_{3k} I_0 + B_{3k} K_0\}\, z \sin\mu z\Big]$$
$$+\sum_{n\neq 0}^{\infty}\Big\{[4\nu(n+1)A_{2n} + 2(1-\nu)A_{3n}]r^n - 4\nu(n-1)B_{1n} r^{-n}\Big\}\cos n\varphi$$
$$+\frac{2\nu}{r}\{[A_2 + B_1 + B_2 \log r]\cos\varphi + B_2\varphi\sin\varphi\}$$
$$+4\nu A_{21} + 2(1-\nu)(A_3 + B_3 \log r) \qquad (154)$$

Displacements and stresses as given above can be applied to any particular domain of the present problem by suitably specifying arbitrary constants.

To satisfy the periodic condition of matrix and loaded fiber, we take in (II-1), (II-2), and (II-3)

$$n = 6, 12, 18, 24, \ldots\ldots \qquad (155)$$

$$A_{ik}^{I,II} = B_{ik}^{I,II} = A_i^{I,II} = B_i^{I,II} = 0 \qquad i = 1,2 \qquad (156)$$

Satisfying the loading condition $\sigma_{33}^{I}(r, \varphi, \pm l) = \sigma_l^{I}$, we choose in the expression for σ_{33} (see equation II-9) the μ so that $\cos\mu l = 0$; therefore,

$$\mu^{I} = \frac{k\pi}{2l} \qquad k = 1, 3, 5, \text{ etc.}$$

$$A^{I}_{3nk} = A^{I}_{3k} = 0 \tag{157}$$

$$2\nu^{I}(n+1)A^{I}_{21n} + (1-\nu^{I})A^{I}_{3n} = 0$$

Hence,
$$(1-\nu^{I})A^{I}_{3} + 2\nu^{I}A^{I}_{21} = \frac{2[1-(\nu^{I})^{2}]\sigma^{I}_{l}}{E^{I}} \tag{158}$$

In addition, the unloaded condition, $\sigma^{II}_{33}(r, \varphi, \pm l) = 0$, of domain II leads to

$$\mu^{II} = \frac{k\pi}{2l} \qquad k = 1, 3, 5, \text{ etc.} \tag{159}$$

$$A^{II}_{3nk} = B^{II}_{3nk} = A^{II}_{3k} = B^{II}_{3k} = B^{II}_{12n} = B^{II}_{3} = 0$$

$$2\nu^{II}(n+1)A^{II}_{21n} + (1-\nu^{II})A^{II}_{3n} = 0 \tag{160}$$

$$(1-\nu^{II})A^{II}_{3} + 2\nu^{II}A^{II}_{21} = 0$$

The displacements in domain III do not have any periodic property* in the polar angle φ, and we discard the terms contained in the σ_{ij} and ξ_i functions in II-1 to II-9 characterized by the factor $\sin n\varphi$ or $\cos n\varphi$ for domain III.

$$A^{III}_{12nk} = B^{III}_{12nk} = A^{III}_{21nk} = B^{III}_{21nk} = 0$$

$$A^{III}_{3nk} = B^{III}_{3nk} = A^{III}_{nk} = B^{III}_{nk} = 0$$

$$A^{III}_{21n} = B^{III}_{12n} = A^{III}_{3n} = B^{III}_{3n} = 0 \qquad (161)$$

$$A^{III}_{4n} = B^{III}_{4n} = 0$$

The vanishing of the axial stress requires at the end of domain III in equation (II-9)

$$\mu^{III} = \frac{k\pi}{2\ell} \qquad k = 1, 3, 5, \text{ etc.} \qquad (162)$$

$$A^{III}_{3k} = B^{III}_{3k} = B^{III}_{2} = B^{III}_{3} = 0$$

$$A^{III}_{2} + B^{III}_{1} = (1-\nu^{III})A^{III}_{3} + 2\nu^{III}A^{III}_{21} = 0 \qquad (163)$$

*As far as a hexagonal element as shown in Fig.30 (a) is concerned, displacements of the six unloaded fibers possess sixfold symmetry. However, an elasticity solution is not valid for a discontinuous medium.

APPENDIX III

DISPLACEMENTS AND STRESSES OF THE MATRIX

Using equilibrium equations, Ref. 6, strain-displacement relations and generalized Hooke's law, the following is obtained:

$$\frac{1}{1-2\nu^{II}}\frac{\partial e}{\partial r}+\left(\nabla^2-\frac{1}{r^2}\right)\xi_1-\frac{2}{r^2}\frac{\partial \xi_2}{\partial \varphi}=0 \qquad (164)$$

$$\frac{1}{1-2\nu^{II}}\frac{\partial e}{r\partial \varphi}+\left(\nabla^2-\frac{1}{r^2}\right)\xi_2+\frac{2}{r^2}\frac{\partial \xi_2}{\partial \varphi}=0 \qquad (165)$$

$$\frac{1}{1-2\nu^{II}}\frac{\partial e}{\partial z}+\nabla^2\xi_3=0 \qquad (166)$$

where ∇^2 is the Laplacian operator defined by

$$\nabla^2=\frac{\partial^2}{\partial r^2}+\frac{1}{r}\frac{\partial}{\partial r}+\frac{1}{r^2}\frac{\partial^2}{\partial \varphi^2}+\frac{\partial^2}{\partial z^2} \qquad (167)$$

and where e is the dilatation satisfying Laplace's equation

$$\nabla^2 e=0 \qquad (168)$$

Since (168) has been derived from equilibrium equations (164) through (166), we may solve (164), (166), and (168) for radial, circumferential, and axial displacements, ξ_1, ξ_2, and ξ_3.

We seek the solution of (168) in the form

$$e = f_0(r) \sin\varphi \sin\alpha_n z \tag{169}$$

Substituting (169) into (168) yields

$$\frac{d^2 f_0}{d\rho^2} + \frac{1}{\rho}\frac{df_0}{d\rho} - \left(1 + \frac{1}{\rho^2}\right) f_0 = 0 \tag{170}$$

where $$\rho = \alpha_n r \tag{171}$$

The solution to (170) is given by

$$f_0(r) = A_1 I_1(\rho) + B_1 K_1(\rho) \tag{172}$$

where A_1 and B_1 are arbitrary constants.

Introduction of (169) into (166) gives

$$\frac{\partial^2 \xi_3}{\partial \rho^2} + \frac{1}{\rho}\frac{\partial \xi_3}{\partial \rho} + \frac{1}{\rho^2}\frac{\partial^2 \xi_3}{\partial \varphi^2} + \frac{1}{\alpha_n^2}\frac{\partial^2 \xi_3}{\partial z^2}$$
$$= C\left[A_1 I_1(\rho) + B_1 K_1(\rho)\right] \sin\varphi \cos\alpha_n z \tag{173}$$

where $$C = -\frac{1}{\alpha_n(1-2\nu^{II})} \tag{174}$$

The solution of (173) is written as

$$\xi_3 = \psi_3(\rho)\sin\varphi\cos\alpha_n z \tag{175}$$

From (173) and (175), we obtain an ordinary differential equation for ψ_3 with the solution

$$\psi_3(\rho) = A_1 f_1(\rho) + B_2 f_2(\rho) + A_2 I_1(\rho) + B_2 K_1(\rho) \tag{176}$$

where A_2 and B_2 are arbitrary constants and where

$$f_1(\rho) = C\left[I_1(\rho)\int_0^\rho \frac{I_1(\rho)K_1(\rho)}{g_0(\rho)}d\rho - K_1(\rho)\int_0^\rho \frac{I_1^2(\rho)}{g_0(\rho)}d\rho\right] \tag{177}$$

$$f_2(\rho) = C\left[I_1(\rho)\int_0^\rho \frac{K_1^2(\rho)}{g_0(\rho)}d\rho - K_1(\rho)\int_0^\rho \frac{I_1(\rho)K_1(\rho)}{g_0(\rho)}d\rho\right]$$

The function $g_0(\rho)$ in (177) is given by

$$g_0(\rho) = K_1(\rho)I_1'(\rho) - I_1(\rho)K_1'(\rho) \tag{178}$$

in which primes denote differentiation with respect to ρ.

By the definition of the dilatation e, we have

$$\frac{\partial \xi_2}{\partial \varphi} = r\left[e - \frac{1}{r}\frac{\partial}{\partial r}(r\xi_1) - \frac{\partial \xi_3}{\partial z}\right] \tag{179}$$

Substitution of (169), (175) and (179) into (164) leads to

$$\frac{\partial^2 \xi_1}{\partial \rho^2} + \frac{3}{\rho}\frac{\partial \xi_1}{\partial \rho} + \frac{1}{\rho^2}\left(\xi_1 + \frac{\partial^2 \xi_1}{\partial \varphi^2}\right) + \frac{1}{\alpha_n^2}\frac{\partial^2 \xi_1}{\partial z^2}$$
$$= \left[A_1 f_3(\rho) + B_1 f_4(\rho) + A_2 \frac{2I_1(\rho)}{\rho} + B_2 \frac{2K_1(\rho)}{\rho}\right] \sin\varphi \sin\alpha_n z \tag{180}$$

where
$$f_3(\rho) = cI_1'(\rho) + \frac{2}{\alpha_n \rho}\left[I_1(\rho) + \alpha_n f_1(\rho)\right]$$
$$f_4(\rho) = cK_1'(\rho) + \frac{2}{\alpha_n \rho}\left[K_1(\rho) + \alpha_n f_2(\rho)\right] \tag{181}$$

Assume the solution of (180) in the form

$$\xi_1 = \psi_1(\rho) \sin\varphi \sin\alpha_n z \tag{182}$$

Introducing (182) into (180) and changing the variable result in

$$(\rho\psi_1)'' + \frac{1}{\rho}(\rho\psi_1)' - \left(1 + \frac{1}{\rho^2}\right)(\rho\psi_1)$$
$$= A_1 f_3(\rho) + B_1 f_4(\rho) + A_2 \frac{2I_1(\rho)}{\rho} + B_2 \frac{2K_1(\rho)}{\rho} \tag{183}$$

whose solution is

$$\psi_1(\rho) = \frac{1}{\rho}\left[A_1 f_5(\rho) + B_1 f_6(\rho) + A_2 f_7(\rho) + B_2 f_8(\rho) + A_3 I_1(\rho) + B_3 K_1(\rho)\right] \tag{184}$$

where A_3 and B_3 are integration constants and where

$$f_5(\rho) = I_1(\rho)\int_0^\rho \frac{K_1(\rho) f_3(\rho)}{g_0(\rho)}\,d\rho - K_1(\rho)\int_0^\rho \frac{I_1(\rho) f_3(\rho)}{g_0(\rho)}\,d\rho$$

$$f_6(\rho) = I_1(\rho)\int_0^\rho \frac{K_1(\rho) f_4(\rho)}{g_0(\rho)}\,d\rho - K_1(\rho)\int_0^\rho \frac{I_1(\rho) f_4(\rho)}{g_0(\rho)}\,d\rho \tag{185}$$

$$f_7(\rho) = 2\left[I_1(\rho)\int_0^\rho \frac{I_1(\rho) K_1(\rho)}{\rho g_0(\rho)}\,d\rho - K_1(\rho)\int_0^\rho \frac{I_1^2(\rho)}{\rho g_0(\rho)}\,d\rho\right]$$

$$f_8(\rho) = 2\left[I_1(\rho)\int_0^\rho \frac{K_1^2(\rho)}{\rho g_0(\rho)}\,d\rho - K_1(\rho)\int_0^\rho \frac{I_1(\rho) K_1(\rho)}{\rho g_0(\rho)}\,d\rho\right]$$

Substituting (169), (175), and (182) into (179) and integrating the result with respect to φ lead to

$$\xi_2 = \psi_2(\rho)\cos\varphi \sin\alpha_n z + G_0(\rho, z) \tag{186}$$

where
$$\psi_2(\rho) = -\left[A_1\left\{\frac{\rho}{\alpha_n} I_1(\rho) - f_5'(\rho) + \rho f_1(\rho)\right\} + B_1\left\{\frac{\rho}{\alpha_n} K_1(\rho) - f_6' + \rho f_2\right\} + A_2\left\{\rho I_1(\rho) - f_7'\right\} + B_2\left\{\rho K_1(\rho) - f_8'\right\} - A_3 I_1'(\rho) - B_3 K_1'(\rho)\right] \tag{187}$$

The function G_0 in (186) is an arbitrary function to be determined. Now that the $yz-$ plane is the symmetrical plane, we have

$$\xi_2\left(\frac{\pi}{2}, \rho, z\right) = 0$$

which requires

$$G_0(\rho, z) = 0 \tag{188}$$

Stresses, σ_{ij}, of the matrix are related to strain ϵ_{ij} by generalized Hooke's law, as follows:

$$\sigma_{ij} = \frac{E^{II}}{2(1+\nu^{II})}\left[(1+\delta_{ij})\epsilon_{ij} + \delta_{ij}\frac{2\nu^{II}e}{1-2\nu^{II}}\right] \tag{189}$$

where δ_{ij} is the Kronecker delta.

By using displacements (175), (182), and (186) together with strain-displacement relations, stresses (189) can be written in the form

$$\begin{aligned}
\sigma_{ii} &= \tau_{ii}(\rho)\sin\varphi \sin\alpha_n z \qquad i=1,2,3 \\
\sigma_{12} &= \tau_{12}(\rho)\cos\varphi \sin\alpha_n z \\
\sigma_{13} &= \tau_{13}(\rho)\sin\varphi \cos\alpha_n z \\
\sigma_{23} &= \tau_{23}(\rho)\cos\varphi \cos\alpha_n z
\end{aligned} \tag{190}$$

where τ_{ij} are functions of ρ only.

It is seen from (175), (182), (186) and (190) that displacement components ξ_1 and ξ_3 and stresses σ_{11}, σ_{22}, σ_{33}, and σ_{13} characterized by a factor $\sin\varphi$ vanish at the $xz-$plane (or the neutral plane), are symmetrical with respect to the $y-z$ plane (or the symmetrical plane), and have maximum values at the $yz-$plane for constant x and z. The displacement component ξ_2 and shearing stresses σ_{12} and σ_{23} characterized by a factor $\cos\varphi$ are symmetrical with respect to the $xz-$plane, vanish at the $yz-$plane, and reach their maxima at the $xz-$plane for constant x and z. Obviously, these properties satisfy the physical requirements of the bending of the matrix in the present analysis.

The arbitrary constants A_i and B_i (i=1,2,3) in the expressions for displacements and stresses are to be determined by boundary conditions. The outer surface of the matrix is assumed to be free from stresses, and hence we have

$$\sigma_{1i}(\rho_1, \varphi, z) = 0 \qquad i=1,2,3 \tag{191}$$

where $$\rho_1 = \alpha_n b \tag{192}$$

The continuity condition of the interface on the components of displacement in the directions of Cartesian coordinates x, y, and z requires

$$\xi_1(\rho_2, \varphi, z)\cos\varphi - \xi_2(\rho_2, \varphi, z)\sin\varphi = 0$$

$$\xi_1(\rho_2, \varphi, z)\sin\varphi + \xi_2(\rho_2, \varphi, z)\cos\varphi = v_0 \sin\alpha_n z \tag{193}$$

$$\xi_3(\rho_2, \varphi, z) = -a v_0 \alpha_n \cos\alpha_n z \sin\varphi$$

where $$\rho_2 = \alpha_n a \tag{194}$$

The condition (193c) has been obtained by assuming that the angle of rotation of a fiber element is small compared to the unity and that a normal cross section of the fiber remains normal during bending.

Substituting (175), (182), (186), and (190 a, d, e) into conditions (191) and (193) yields

$$\tau_{1i}(\rho_1) = 0 \qquad i = 1,2,3$$

$$\psi_i(\rho_2) = v_0 \qquad i = 1,2 \tag{195}$$

$$\psi_3(\rho_2) = -a v_0 \alpha_n$$

The constants A_i and B_i (i=1,2,3) in displacements (175), (182), (186), and stresses (190) can be determined by solving equations (195) simultaneously. Each of these constants is then characterized by the presence of the amplitude v_0 as a factor. Therefore, stresses at the interface can be written as

$$\sigma_{11}(\rho_2, \varphi, z) = v_0 \sigma_{11}^{\circ} \sin\varphi \sin\alpha_n z$$

$$\sigma_{12}(\rho_2, \varphi, z) = v_0 \sigma_{12}^{\circ} \cos\varphi \sin\alpha_n z \tag{196}$$

$$\sigma_{13}(\rho_2, \varphi, z) = v_0 \sigma_{13}^{\circ} \sin\varphi \cos\alpha_n z$$

where σ_{11}°, σ_{12}°, and σ_{13}° are functions of ν^{II}, E^{II}, a, b, and α_n.

APPENDIX IV

ENERGY SOLUTIONS

A. ALTERNATIVE WAY TO FIND SMALLEST BUCKLING LOAD AND BUCKLING WAVELENGTH OF FIBER FOR MULTIFIBER CASE

The strain energy due to longitudinal shear along the fiber surface can be also found as follows:

$$\frac{1}{2}\int_V \sigma_{13}^{II}\,\epsilon_{13}^{II}\,dV = \frac{1}{2G^{II}}\int_V (\sigma_{13}^{II})^2\,dV$$

$$= \frac{\pi d}{2G^{II}}\int_0^L\int_a^b \left\{ \frac{k\xi_{in}^{x}}{\pi a}\left(1 - \frac{\sinh(2\alpha_n d)}{2\alpha_n d + \sinh(2\alpha_n d)}\right)\sinh(\alpha_n r) \right.$$

$$- \frac{(k\xi_{in}^{II}/\pi a)\,(1-\cosh(2\alpha_n d))}{(2\alpha_n d)+\sinh(2\alpha_n d)}(\alpha_n r)\sinh(\alpha_n r)$$

$$\left. - \frac{(k\xi_{in}^{II}/\pi a)\sinh(2\alpha_n d)}{(2\alpha_n d)+\sinh(2\alpha_n d)}(\alpha_n r)\cosh(\alpha_n r)\right\}^2 \cdot$$

$$\cdot \cos^2(\alpha_n z)\,dz\,dr$$

$$= \frac{k^2(\xi_{in}^{x})^2 d}{2G^{x}\pi a^2\alpha_n}\left(\frac{L}{2}\right)\left\{\left(\frac{2\alpha_n d}{2\alpha_n d+\sinh(2\alpha_n d)}\right)^2\left(\frac{\sinh(2\alpha_n b)-\sinh(2\alpha_n a)}{4}\right.\right.$$

$$\left. - \frac{\alpha_n b - \alpha_n a}{2}\right)$$

$$+ \frac{1}{2}\left[\frac{1-\cosh(2\alpha_n d)}{(2\alpha_n d)+\sinh(2\alpha_n d)}\right]^2 \cdot \left[\frac{1}{8}((2\alpha_n b)^2+2)\sinh(2\alpha_n b)\right.$$

$$- \frac{(\alpha_n b)^3}{3} + \frac{(\alpha_n a)^3}{3} - \frac{1}{8}((2\alpha_n a)^2+2)\sinh(2\alpha_n a)$$

$$\left. - \frac{1}{2}(\alpha_n b)\cosh(2\alpha_n b) + \frac{1}{2}(\alpha_n a)\cosh(2\alpha_n a)\right]$$

$$+\frac{1}{2}\left(\frac{\sinh(2\alpha_n d)}{2\alpha_n d+\sinh(2\alpha_n d)}\right)^2\cdot\left[\frac{1}{8}((2\alpha_n b)^2+2)\sinh(2\alpha_n b)\right.$$

$$-\frac{1}{8}((2\alpha_n a)^2+2)\sinh(2\alpha_n a)-\frac{1}{2}(\alpha_n b)\cosh(2\alpha_n b)$$

$$\left.+\frac{1}{2}(\alpha_n a)\cosh(2\alpha_n a)-\frac{(\alpha_n b)^3}{3}+\frac{(\alpha_n a)^3}{3}\right]$$

$$-\frac{2\alpha_n d(1-\cosh(2\alpha_n d))}{(2\alpha_n d+\sinh(2\alpha_n d))^2}\cdot\left[\frac{1}{2}(\alpha_n b)\sinh(2\alpha_n b)\right.$$

$$-\frac{1}{2}(\alpha_n a)\sinh(2\alpha_n a)-\frac{1}{4}\cosh(2\alpha_n b)$$

$$\left.+\frac{1}{4}\cosh(2\alpha_n a)-2(\alpha_n b)^2+2(\alpha_n a)^2\right]$$

$$-\frac{2\alpha_n d\sinh(2\alpha_n d)}{(2\alpha_n d+\sinh(2\alpha_n d))^2}\cdot\left[\frac{1}{2}(\alpha_n b)\cosh(2\alpha_n b)\right.$$

$$-\frac{1}{2}(\alpha_n a)\cosh(2\alpha_n a)-\frac{1}{4}\sinh(2\alpha_n b)$$

$$\left.+\frac{1}{4}\sin(2\alpha_n a)\right]$$

$$+\frac{1}{8}\frac{(1-\cosh(2\alpha_n d))\sinh(2\alpha_n d)}{(2\alpha_n d+\sinh(2\alpha_n d))^2}\cdot\left\{\left[((2\alpha_n b)^2+2)\cosh(2\alpha_n b)\right.\right.$$

$$-((2\alpha_n a)^2+2)\cosh(2\alpha_n a)$$

$$\left.\left.-4(\alpha_n b)\sinh(2\alpha_n b)+4(\alpha_n a)\sinh(2\alpha_n a)\right]\right\}$$

(197)

Then the expression for buckling load of the fiber is

$$P_{cr}^{I} = \alpha_n^2 E^I I^I + \alpha_n^{-2} k + \frac{k^2 d\, \alpha_n^{-3}}{2 G^{II} \pi a^2} \cdot Y \qquad (198)$$

where

$Y = \{\quad\}$ of equation (197)

Combinations of equations (197) and (198) yields

$$\begin{aligned} P_{cr}^{I} = {} & \alpha_n^2 E^I I^I + \frac{E^{II}\pi a}{\alpha_n}\left\{\left[(2\alpha_n d)^2 - \sinh^2(2\alpha_n d)\right]\right. \\ & \div\left[-2\sinh^3(2\alpha_n d) - 8\alpha_n d + 8\alpha_n d\cosh(2\alpha_n d)\right. \\ & \quad -4\sinh(2\alpha_n d)\cosh(2\alpha_n d) + 2\sinh(2\alpha_n d) \\ & \quad \left.\left. + 2\sinh(2\alpha_n d)\cosh^2(2\alpha_n d)\right]\right\} \\ & + E^I \pi d (1+\nu^{II}) \frac{Y}{\alpha_n}\left\{\left[(2\alpha_n d)^2 - \sinh^2(2\alpha_n d)\right]\right. \\ & \div\left[-2\sinh^3(2\alpha_n d) - 8\alpha_n d + 8\alpha_n d\cosh(2\alpha_n d)\right. \\ & \quad -4\sinh(2\alpha_n d)\cosh(2\alpha_n d) + 2\sinh(2\alpha_n d) \\ & \quad \left.\left. + 2\sinh(2\alpha_n d)\cosh^2(2\alpha_n d)\right]^2\right\} \end{aligned} \qquad (199)$$

SMALLEST BUCKLING LOAD AND BUCKLING WAVELENGTH OF THE FIBER

The smallest buckling load of the fiber can be obtained by minimizing P_{cr}^{I} of equation (198) with respect to α_n. $\partial P_{cr}^{I}/\partial \alpha_n = 0$ goes.

$$2\alpha_n E^{I} I^{I} + E^{II}\pi a\Big\{\Big[(2d)^2 - \frac{4d}{\alpha_n}\sinh(2\alpha_n d)\cosh(2\alpha_n d) + \alpha_n^{-2}\sinh^2(2\alpha_n d)\Big]\cdot$$

$$\cdot\Big[-2\sinh^3(2\alpha_n d) - 8\alpha_n d + 8\alpha_n d\cosh(2\alpha_n d) - 4\sinh(2\alpha_n d)\cosh(2\alpha_n d) + 2\sinh(2\alpha_n d) + 2\sinh(2\alpha_n d)\cosh^2(2\alpha_n d)\Big]^{-1}\Big\}$$

$$-E^{II}\pi a\Big\{\Big[(2d)^2\alpha_n - \alpha_n^{-1}\sinh^2(2\alpha_n d)\Big]\cdot$$

$$\cdot\Big[-2\sinh^3(2\alpha_n d) - 8\alpha_n d + 8\alpha_n d\cosh(2\alpha_n d) - 4\sinh(2\alpha_n d)\cosh(2\alpha_n d) + 2\sinh(2\alpha_n d) + 2\sinh(2\alpha_n d)\cosh^2(2\alpha_n d)\Big]^{-2}\cdot$$

$$\cdot\Big[-12d\sinh^2(2\alpha_n d)\cosh(2\alpha_n d) - 8d + 8d\cosh(2\alpha_n d) + 16d^2\alpha_n\sinh(2\alpha_n d) - 8d\sinh^2(2\alpha_n d) - 8d\cosh^2(2\alpha_n d) + 4d\cosh(2\alpha_n d) + 4d\cosh^3(2\alpha_n d) + 8d\sinh^2(2\alpha_n d)\cosh(2\alpha_n d)\Big]\Big\}$$

$$+E^{II}\pi d(1+\nu^{I})\alpha_n^{-1}\Big\{\Big[(2\alpha_n d) - \sinh(2\alpha_n d)\Big]^2\cdot$$

$$\cdot\Big[-2\sinh^3(2\alpha_n d) - 8\alpha_n d + 8\alpha_n d\cosh(2\alpha_n d) - 4\sinh(2\alpha_n d)\cosh(2\alpha_n d) + 2\sinh(2\alpha_n d) + 2\sinh(2\alpha_n d)\cosh^2(2\alpha_n d)\Big]^{-2}\Big\}\cdot$$

$$\cdot\left\{ 8\alpha_n d^2\left(\frac{\sinh(2\alpha_n b)-\sinh(2\alpha_n a)}{4} - \frac{\alpha_n b-\alpha_n a}{2}\right)\right.$$

$$+(2\alpha_n d)^2\left[\frac{b\cosh(2\alpha_n b)-a\cosh(2\alpha_n a)-b+a}{2}\right]$$

$$-\left[1-\cosh(2\alpha_n d)\right]\cdot\left[2\sinh(2\alpha_n d)\right]\cdot$$

$$\cdot\left[\frac{1}{8}((2\alpha_n b)^2+2)\sinh(2\alpha_n b)\right.$$

$$-\frac{1}{8}((2\alpha_n a)^2+2)\sinh(2\alpha_n a)-\frac{1}{2}\alpha_n b\cosh(2\alpha_n b)$$

$$\left.+\frac{1}{2}\alpha_n a\cosh(2\alpha_n a)-\frac{(\alpha_n b)^3}{3}+\frac{(\alpha_n a)^3}{3}\right]$$

$$+\frac{1}{2}\left[1-\cosh(2\alpha_n d)\right]^2\cdot$$

$$\cdot\left[\frac{1}{8}(4\alpha_n b^2)\sinh(2\alpha_n b)+\frac{b}{4}((\alpha_n b)^2+2)\cosh(2\alpha_n b)\right.$$

$$-\frac{1}{8}(4\alpha_n a^2)\sinh(2\alpha_n a)-\frac{a}{4}((\alpha_n a)^2+2)\cosh(2\alpha_n a)$$

$$-\frac{b}{2}\cosh(2\alpha_n b)-\alpha_n b^2\sinh(2\alpha_n b)$$

$$+\frac{a}{2}\cosh(2\alpha_n a)+\alpha_n a^2\sinh(2\alpha_n a)$$

$$\left.-\alpha_n^2 b^3+\alpha_n^2 a^3\right]$$

$$+\left[2d\sinh(\alpha_n d)\cosh(\alpha_n d)\right]\cdot$$

$$\cdot\left[\frac{1}{8}((2\alpha_n b)^2+2)\sinh(2\alpha_n b)-\frac{1}{8}((2\alpha_n a)^2+2)\sinh(2\alpha_n a)\right.$$

$$\left.-\frac{1}{2}\alpha_n b\cosh(2\alpha_n b)+\frac{1}{2}(\alpha_n a)\cosh(2\alpha_n a)\right.$$

$$+\frac{(\alpha_n b)^3}{3}-\frac{(\alpha_n a)^3}{3}\Big]$$

$$+\frac{1}{2}\sinh^2(2\alpha_n d)\Big[\frac{1}{8}(4\alpha_n b^2)\sinh(2\alpha_n b)$$

$$+\frac{b}{4}((2\alpha_n b)^2+2)\cosh(2\alpha_n b)-$$

$$-\frac{1}{8}(4\alpha_n a^2)\sinh(2\alpha_n a)-\frac{a}{4}((2\alpha_n a)^2+2)\cosh(2\alpha_n a)$$

$$-\frac{b}{2}\cosh(2\alpha_n b)-\alpha_n b^2\sinh(2\alpha_n b)$$

$$+\frac{a}{2}\cosh(2\alpha_n a)+\alpha_n a^2\sinh(2\alpha_n a)$$

$$+\alpha_n^2 b^3-\alpha_n^2 a^3\Big]$$

$$-\Big[2d(1-\cos(2\alpha_n d))-4\alpha_n d^2\sinh(2\alpha_n d)\Big]\cdot$$

$$\cdot\Big[\frac{1}{2}(\alpha_n b)\sinh(2\alpha_n b)-\frac{1}{2}(\alpha_n a)\sinh(2\alpha_n a)$$

$$-\frac{1}{4}\cosh(2\alpha_n b)+\frac{1}{4}\cosh(2\alpha_n a)-2(\alpha_n b)^2+2(\alpha_n a)^2\Big]$$

$$-\Big[2\alpha_n d(1-\cosh(2\alpha_n d))\Big]\cdot$$

$$\cdot\Big[\alpha_n b^2\cosh(2\alpha_n b)-\alpha_n a^2\cosh(2\alpha_n a)$$

$$-4\alpha_n b^2+4\alpha_n a^2\Big]$$

$$-\Big[2d\sinh(2\alpha_n d)+4\alpha_n d^2\cosh(2\alpha_n d)\Big]\cdot$$

$$\cdot\left[\frac{1}{2}\alpha_n b\cosh(2\alpha_n b)-\frac{1}{2}\alpha_n a\cosh(2\alpha_n a)\right.$$
$$\left.-\frac{1}{4}\sinh(2\alpha_n b)+\frac{1}{4}\sinh(2\alpha_n a)\right]$$
$$-\left[(2\alpha_n d)\sinh(2\alpha_n d)\right]\cdot\left[\alpha_n b^2\sinh(2\alpha_n b)\right.$$
$$\left.-\alpha_n a^2\sinh(2\alpha_n a)\right]$$
$$+\frac{1}{8}\left[2d\cosh(2\alpha_n d)(1-\cosh(2\alpha_n d))\right.$$
$$\left.-2d\sinh^2(2\alpha_n d)\right]\cdot$$
$$\cdot\left[((2\alpha_n b)^2+2)\cosh(2\alpha_n b)\right.$$
$$-((2\alpha_n a)^2+2)\cosh(2\alpha_n a)-4\alpha_n b\sinh(2\alpha_n b)$$
$$\left.+4\alpha_n a\sinh(2\alpha_n a)\right]$$
$$+\frac{1}{8}\left[(1-\cosh(2\alpha_n d))\sinh(2\alpha_n d)\right]\cdot$$
$$\cdot\left[4\alpha_n b^2\cosh(2\alpha_n b)+2b((2\alpha_n b)^2+2)\sinh(2\alpha_n b)\right.$$
$$-4\alpha_n a^2\cosh(2\alpha_n a)-2a((2\alpha_n a)^2+2)\sinh(2\alpha_n a)$$
$$-4b\sinh(2\alpha_n b)-8\alpha_n b^2\cosh(2\alpha_n b)$$
$$\left.+4a\sinh(2\alpha_n a)+8\alpha_n a^2\cosh(2\alpha_n a)\right]\Big\}$$
$$+E^{II}\pi d(1+\nu^{II})\left\{2\left[(2\alpha_n d)-\sinh(2\alpha_n d)\right]\cdot\left[2d-2d\cosh(2\alpha_n d)\right]\cdot\alpha_n^{-1}\cdot\right.$$

$$\cdot\Big[-2\sinh^3(2\alpha_n d)-8\alpha_n d+8\alpha_n d\cosh(2\alpha_n d)$$
$$-4\sinh(2\alpha_n d)\cosh(2\alpha_n d)+2\sinh(2\alpha_n d)$$
$$+2\sinh(2\alpha_n d)\cosh^2(2\alpha_n d)\Big]^{-2}$$
$$-\Big[(2\alpha_n d)-\sinh(2\alpha_n d)\Big]^2\cdot\alpha_n^{-2}\cdot$$
$$\cdot\Big[-2\sinh^3(2\alpha_n d)-8\alpha_n d+8\alpha_n d\cosh(2\alpha_n d)$$
$$-4\sinh(2\alpha_n d)\cosh(2\alpha_n d)+2\sinh(2\alpha_n d)$$
$$+2\sinh(2\alpha_n d)\cosh^2(2\alpha_n d)\Big]^{-2}$$
$$-2\Big[(2\alpha_n d)-\sinh(2\alpha_n d)\Big]^2\cdot\alpha_n^{-1}\cdot$$
$$\cdot\Big[-2\sinh^3(2\alpha_n d)-8\alpha_n d+8\alpha_n d\cosh(2\alpha_n d)$$
$$-4\sinh(2\alpha_n d)\cosh(2\alpha_n d)+2\sinh(2\alpha_n d)$$
$$+2\sinh(2\alpha_n d)\cosh^2(2\alpha_n d)\Big]^{-3}\cdot$$
$$\cdot\Big[-12d\sinh^2(2\alpha_n d)\cosh(2\alpha_n d)-8d$$
$$+8d\cosh(2\alpha_n d)+16\alpha_n d^2\sinh(2\alpha_n d)$$
$$-8d\sinh^2(2\alpha_n d)-8d\cosh^2(2\alpha_n d)$$
$$+4d\cosh(2\alpha_n d)+4d\cosh^3(2\alpha_n d)$$
$$+8d\sinh^2(2\alpha_n d)\cosh(2\alpha_n d)\Big]\Big\}\cdot$$

$$\cdot\left\{(2\alpha_n d)^2\left[\frac{\sinh(2\alpha_n b)-\sinh(2\alpha_n a)}{4}-\frac{\alpha_n b-\alpha_n a}{2}\right]\right.$$

$$+\frac{1}{2}\left[1-\cosh(2\alpha_n d)\right]^2\cdot$$

$$\cdot\left[\frac{1}{8}((2\alpha_n b)^2+2)\sinh(2\alpha_n b)-\frac{1}{8}((2\alpha_n a)^2+2)\sinh(2\alpha_n a)\right.$$

$$-\frac{1}{2}(\alpha_n b)\cosh(2\alpha_n b)+\frac{1}{2}(\alpha_n a)\cosh(2\alpha_n a)$$

$$\left.-\frac{(\alpha_n b)^3-(\alpha_n a)^3}{3}\right]$$

$$+\frac{1}{2}\sinh^2(2\alpha_n d)\left[\frac{1}{8}((2\alpha_n b)^2+2)\sinh(2\alpha_n b)\right.$$

$$-\frac{1}{8}((2\alpha_n a)^2+2)\sinh(2\alpha_n a)-\frac{1}{2}(\alpha_n b)\cosh(2\alpha_n b)$$

$$\left.+\frac{1}{2}(\alpha_n a)\cosh(2\alpha_n a)+\frac{(\alpha_n b)^3-(\alpha_n a)^3}{3}\right]$$

$$-2\alpha_n d\left[1-\cosh(2\alpha_n d)\right]\cdot$$

$$\cdot\left[\frac{1}{2}(\alpha_n b)\sinh(2\alpha_n b)-\frac{1}{2}(\alpha_n a)\sinh(2\alpha_n a)\right.$$

$$\left.-\frac{1}{4}\cosh(2\alpha_n b)+\frac{1}{4}\cosh(2\alpha_n a)-2(\alpha_n b)^2+2(\alpha_n a)^2\right]$$

$$-\left[(2\alpha_n d)\sinh(2\alpha_n d)\right]\cdot$$

$$\cdot\left[\frac{1}{2}\alpha_n b\cosh(2\alpha_n b)-\frac{1}{2}\alpha_n a\cosh(2\alpha_n a)\right.$$

$$\left.-\frac{1}{4}\sinh(2\alpha_n b)+\frac{1}{4}\sinh(2\alpha_n a)\right]$$

$$+\frac{1}{8}\left[(1-\cosh(2\alpha_n d))\sinh(2\alpha_n d)\right]\cdot$$

$$\cdot\left[((2\alpha_n b)^2+2)\cosh(2\alpha_n b)-((2\alpha_n a)^2+2)\cosh(2\alpha_n a)\right.$$

$$\left.-4\alpha_n b\sinh(2\alpha_n b)+4\alpha_n a\sinh(2\alpha_n a)\right]\Big\}$$

$$=0 \qquad (200)$$

From equation (200), we find the buckling wavelength $\ell_{cr} = 2\pi/\alpha_j$. Therefore, the smallest buckling load of the fiber, $(P^I_{cr})_{min}$, can be obtained by substituting ℓ_{cr} into equation (199).

B. BUCKLING OF A SINGLE FIBER IN A FINITE MATRIX UNDER AXIAL COMPRESSION

INTEGRATION CONSTANTS AND LATERAL DEFLECTION

By applying boundary conditions (111) to equations (83) and (84), and solving them, we obtain the results of integration constants as follows:

$$A_n = -\frac{\phi_{1n}}{\pi a} \tag{201}$$

$$B_n = \left(\frac{\phi_{1n}}{\pi a}\right)\left[\frac{\alpha_n d + \sinh d_n \cosh d_n}{d_n^2 - \sinh^2 d_n}\right] \tag{202}$$

$$C_n = -\left(\frac{\phi_{1n}}{\pi a}\right)\left[\frac{\alpha_n d + \sinh d_n \cosh d_n}{d_n^2 - \sinh^2 d_n}\right] \tag{203}$$

$$D_n = -\left(\frac{\phi_{1n}}{\pi a}\right)\left[\frac{\sinh^2 d_n}{d_n^2 - \sinh^2 d_n}\right] \tag{204}$$

where

$$d_n = \alpha_n d = \frac{n\pi}{L}(b-a) \tag{205}$$

The relationships between displacements and stresses of two-dimensional elasticity problems are quoted as

$$\frac{\partial \xi_1^{II}}{\partial x} = \frac{\sigma_{11}^{II}}{E^{II}} - \frac{\nu^{II}\sigma_{33}^{II}}{E^{II}} \tag{206}$$

$$\frac{\partial \xi_3^{II}}{\partial z} = \frac{\sigma_{33}^{II}}{E^{II}} - \frac{\nu^{II}\sigma_{11}^{II}}{E^{II}} \tag{207}$$

Therefore, the deflection in re-direction is

$$\xi_1^{II} = \int_0^d \left(\frac{\sigma_{11}^{II}}{E^{II}} - \frac{\nu^{II}\sigma_{33}^{II}}{E^{II}} \right) dz$$

$$= \frac{1}{E^{II}\pi a} \sum_{n=1}^{\infty} \left\{ \frac{p_{in}}{\alpha_n} \left[\sinh d_n - \frac{d_n + \sinh d_n \cosh d_n}{d_n^2 - \sinh^2 d_n} \cdot \right.\right.$$

$$\cdot \left(d_n \sinh d_n - \cosh d_n + 1 \right)$$

$$+ \frac{d_n + \sinh d_n \cosh d_n}{d_n^2 - \sinh^2 d_n} \left(\cosh d_n - 1 \right)$$

$$\left.\left. + \frac{\sinh^2 d_n}{d_n^2 - \sinh^2 d_n} \left(d_n \cosh d_n - \sinh d_n \right) \right] \right\} \cdot$$

$$\cdot \sin(\alpha_n z)$$

$$+ \frac{\nu^{II}}{E^{II}\pi a} \sum_{n=1}^{\infty} \left\{ \frac{p_{in}}{\alpha_n} \left[\left(1 + \frac{2\sinh^2 d_n}{d_n^2 - \sinh^2 d_n} \right) \sinh d_n \right.\right.$$

$$- \frac{d_n + \sinh d_n \cosh d_n}{d_n^2 - \sinh^2 d_n} \cdot d_n \sinh d_n$$

$$\left.\left. + \frac{\sinh^2 d_n}{d_n^2 - \sinh^2 d_n} \left(d_n \cosh d_n - \sinh d_n \right) \right] \right\} \cdot$$

$$\cdot \sin(\alpha_n z) \qquad (208)$$

and the interfacial force per unit length of fiber per unit deflection is

$$k = \frac{p_{in}}{\xi_{in}^{II}} \qquad (209)$$

STRAIN ENERGY DUE TO LONGITUDINAL SHEAR AT THE INTERFACE

The strain energy due to longitudinal shear at the fiber surface is defined as

$$U_S = \int_V \frac{1}{2}\sigma_{13}^{II}\epsilon_{13}^{II}\,dV = \frac{1}{2G^{II}}\int_V (\sigma_{13}^{II})^2\,dV \qquad (210)$$

or

$$U_S = \frac{\pi c}{2G^{II}}\int_0^L\int_a^b \left\{ \frac{k_1\xi_{1n}^{II}}{\pi a}\left(1+\frac{\sinh^2 d_n}{d_n^2-\sinh^2 d_n}\right)\sinh(\alpha_n r) \right.$$
$$- \frac{k_1\xi_{1n}^{II}}{\pi a}\left(\frac{d_n+\sinh d_n\cosh d_n}{d_n^2-\sinh^2 d_n}\right)(\alpha_n r)\sinh(\alpha_n r)$$
$$\left. + \frac{k_1\xi_{1n}^{II}}{\pi a}\left(\frac{\sinh^2 d_n}{d_n^2-\sinh^2 d_n}\right)(\alpha_n r)\cosh(\alpha_n r)\right\}^2 \cdot$$
$$\cdot \cos^2(\alpha_n z)\,dz\,dr \qquad (211)$$

Integration of equation (211) gives

$$U_S = \frac{k^2(\xi_{1n}^{II})^2 d}{2G^{II}\pi a^2\alpha_n}\left(\frac{L}{2}\right)\left\{\left(\frac{d_n^2}{d_n^2-\sinh^2 d_n}\right)^2\cdot\left[\left(\sinh(2\alpha_n b)-\right.\right.\right.$$
$$\left.\left.\left. -\sinh(2\alpha_n a)\right)/4 - (\alpha_n b-\alpha_n a)/2\right]\right.$$
$$+\frac{1}{2}\left(\frac{d_n+\sinh d_n\cosh d_n}{d_n^2-\sinh^2 d_n}\right)\cdot$$
$$\cdot\left\{\frac{1}{8}\left((2\alpha_n b)^2+2\right)\sinh(2\alpha_n b) - \right.$$
$$\left. -\frac{1}{8}\left((2\alpha_n a)^2+2\right)\sinh(2\alpha_n a)\right.$$

$$
\begin{aligned}
&- \frac{\alpha_n b}{2}\cosh(2\alpha_n b) + \frac{\alpha_n a}{2}\cosh(2\alpha_n a) \\
&- \frac{(\alpha_n b)^3}{3} + \frac{(\alpha_n a)^3}{3} \Big] \\
&+ \frac{1}{2}\left(\frac{\sinh^2 d_n}{d_n^2 - \sinh^2 d_n}\right)^2 \cdot \Big[\frac{1}{8}((2\alpha_n b)^2 + 2)\sinh(2\alpha_n b) \\
&- \frac{1}{8}((2\alpha_n a)^2 + 2)\sinh(2\alpha_n a) \\
&- \frac{1}{2}\alpha_n b\cosh(2\alpha_n b) + \frac{1}{2}\alpha_n a\cosh(2\alpha_n a) \\
&+ \frac{(\alpha_n b)^3}{3} - \frac{(\alpha_n a)^3}{3} \Big] \\
&- \left(\frac{d_n^2}{d_n^2 - \sinh^2 d_n}\right)\cdot\left(\frac{d_n + \sinh d_n \cosh d_n}{d_n^2 - \sinh^2 d_n}\right)\cdot \\
&\cdot \Big[\frac{\alpha_n b}{2}\sinh(2\alpha_n b) - \frac{\alpha_n a}{2}\sinh(2\alpha_n a) \\
&- \frac{1}{4}\cosh(2\alpha_n b) + \frac{1}{4}\cosh(2\alpha_n a) \\
&- 2(\alpha_n b)^2 + 2(\alpha_n a)^2 \Big] \\
&+ \left(\frac{d_n^2}{d_n^2 - \sinh^2 d_n}\right)\cdot\left(\frac{\sinh^2 d_n}{d_n^2 - \sinh^2 d_n}\right)\cdot \\
&\cdot \Big[\frac{\alpha_n b}{2}\cosh(2\alpha_n b) - \frac{\alpha_n a}{2}\cosh(2\alpha_n a) \\
&- \frac{1}{4}\sinh(2\alpha_n b) + \frac{1}{4}\sinh(2\alpha_n a)\Big] \\
&- \frac{1}{8}\left(\frac{d_n + \sinh d_n \cosh d_n}{d_n^2 - \sinh^2 d_n}\right)\cdot\left(\frac{\sinh^2 d_n}{d_n^2 - \sinh^2 d_n}\right)\cdot
\end{aligned}
$$

$$\cdot\Big[\big((2\alpha_n b)^2+2\big)\cosh(2\alpha_n b)-4\alpha_n b\sinh(2\alpha_n b)$$
$$-\big((2\alpha_n a)^2+2\big)\cosh(2\alpha_n a)+4\alpha_n a\sinh(2\alpha_n a)\Big]\Big\} \tag{212}$$

BUCKLING LOAD OF THE FIBER

Total potential energy of the fiber during loading is defined as

$$T_e = U_b + U_e + U_p + U_s - W \tag{213}$$

Combination of equations (70), (208), (209), and (212) yields

$$T_e = \frac{1}{2} E^I I^I \left(\frac{L}{2}\right) \sum_{n=1}^{\infty} \left(\xi_{1n}^I\right)^2 \alpha_n^4 + \frac{1}{2} k \left(\frac{L}{2}\right) \sum_{n=1}^{\infty} \left(\xi_{1n}^I\right)^2$$
$$+ \frac{k^2 d}{2 G^{II} \pi a^2} \left(\frac{L}{2}\right) \sum_{n=1}^{\infty} \left(\xi_{1n}^I\right)^2 \frac{1}{\alpha_n} X$$
$$- \frac{1}{2} P^I \left(\frac{L}{2}\right) \sum_{n=1}^{\infty} \left(\xi_{1n}^I\right)^2 \alpha_n^2 \tag{214}$$

where

$$X = \{\ \} \quad \text{of equation (212)} \tag{215}$$

Minimization of total potential energy with respect to ξ_{in}^I gives critical buckling load of the fiber.

$$P_{cr}^{I} = \alpha_n^2 E^I I^I + \frac{k}{\alpha_n^2} + \frac{k^2 d}{2G^{II}\pi a^2}\left(\frac{1}{\alpha_n}\right)^3 X \tag{216}$$

where

$$\alpha_n = \frac{n\pi}{L} \tag{217}$$

Substitution of equations (208), (209), and (212) into (216) results.

$$P_{cr}^{I} = \alpha_n^2 E^I I^I + \frac{E^{II}\pi a}{\alpha_n}(d_n^2 - \sinh^2 d_n)\cdot$$
$$\cdot\left[2(d_n - \sinh d_n)(\cosh d_n - 1)\right]^{-1}$$
$$+ E^{II}\pi d(1+\nu^I)\alpha_n^{-1} X (d_n^2 - \sinh^2 d_n)^2\cdot$$
$$\cdot\left[2(d_n - \sinh d_n)(\cosh d_n - 1)\right]^{-2} \tag{218}$$

SMALLEST BUCKLING LOAD AND BUCKLING WAVELENGTH OF THE FIBER

The buckling wavelength of the fiber is determined by minimizing P_{cr}^{I} with respect to α_n ; i.e., $\frac{\partial P_{cr}^{I}}{\partial \alpha_n} = 0.$ (219)

From equations (212), (215), and (219), we have

$$2\alpha_n E^{I} I^{I} + E^{II}\pi a\left\{ d^2 + \alpha_n^{-2}\sinh^2(\alpha_n d) - 2d\alpha_n^{-1}\sinh(\alpha_n d)\cosh(\alpha_n d)\right\}\cdot$$
$$\cdot\left\{2(\alpha_n d - \sinh(\alpha_n d))(\cosh(\alpha_n d)-1)\right\}^{-1}$$
$$-E^{II}\pi a\left\{\alpha_n d^2 - \alpha_n^{-1}\sinh^2(\alpha_n d)\right\}\cdot$$
$$\cdot\left\{2(\alpha_n d - \sinh(\alpha_n d))(\cosh(\alpha_n d)-1)\right\}^{-2}\cdot$$
$$\cdot\left\{2\left[-d(1-\cosh(\alpha_n d))^2 + d\sinh(\alpha_n d)(\alpha_n d - \sinh(\alpha_n d))\right]\right.$$
$$+E^{II}\pi d(1+\nu^{II})\alpha_n^{-1}\left\{2(\alpha_n d - \sinh(\alpha_n d))(\cosh(\alpha_n d)-1)\right\}^{-2}\cdot$$
$$\cdot\left\{\alpha_n^3 d^4\left[\sinh(2\alpha_n b) - \sinh(2\alpha_n a) - 2(\alpha_n b - \alpha_n a)\right]\right.$$
$$+(\alpha_n d)^4\left[b\cosh(2\alpha_n b) - a\cosh(2\alpha_n a) - b + a\right]/2$$
$$+(\alpha_n d + \sinh(\alpha_n d)\cosh(\alpha_n d))\cdot(d + d\cosh^2(\alpha_n d)$$
$$+d\sinh^2(\alpha_n d))\cdot\left[\frac{1}{8}((2\alpha_n b)^2+2)\sinh(2\alpha_n b)\right.$$
$$-\frac{1}{8}((2\alpha_n a)^2+2)\sinh(2\alpha_n a)$$
$$-\frac{\alpha_n b}{2}\cosh(2\alpha_n b) + \frac{\alpha_n a}{2}\cosh(2\alpha_n a)$$
$$\left.-\frac{(\alpha_n b)^3}{3} + \frac{(\alpha_n a)^3}{3}\right]$$

$$+\frac{1}{2}(\alpha_n d+\sinh(\alpha_n d)\cosh(\alpha_n d))^2\cdot$$
$$\cdot\Big[\frac{\alpha_n b^2}{2}\sinh(2\alpha_n b)+\frac{b}{4}((\alpha_n b)^2+2)\cosh(2\alpha_n b)$$
$$-\frac{\alpha_n a^2}{2}\sinh(2\alpha_n a)-\frac{a}{4}((\alpha_n a)^2+2)\cosh(2\alpha_n a)$$
$$-\frac{b}{2}\cosh(2\alpha_n b)-\alpha_n b^2\sinh(2\alpha_n b)$$
$$+\frac{a}{2}\cosh(2\alpha_n a)+\alpha_n a^2\sinh(2\alpha_n a)$$
$$-\alpha_n^2 b^3+\alpha_n^2 a^3\Big]$$
$$+\Big[2d\sinh^3(\alpha_n d)\cosh(\alpha_n d)\Big]\cdot\Big[\frac{((2\alpha_n b)^2+2)}{8}\sinh(2\alpha_n b)$$
$$-\frac{((2\alpha_n a)^2+2)}{8}\sinh(2\alpha_n a)-\frac{\alpha_n b}{2}\cosh(2\alpha_n b)$$
$$+\frac{\alpha_n a}{2}\cosh(2\alpha_n a)+\frac{(\alpha_n b)^3}{3}-\frac{(\alpha_n a)^3}{3}\Big]$$
$$+\frac{1}{2}\sinh^4(\alpha_n d)\cdot\Big[\frac{\alpha_n b^2}{2}\sinh(2\alpha_n b)-\frac{\alpha_n a^2}{2}\sinh(2\alpha_n a)$$
$$+\frac{b}{4}((2\alpha_n b)^2+2)\cosh(2\alpha_n b)-\frac{b}{2}\cosh(2\alpha_n b)$$
$$-\frac{a}{4}((2\alpha_n a)^2+2)\cosh(2\alpha_n a)+\frac{a}{2}\cosh(2\alpha_n a)$$
$$-\alpha_n b^2\sinh(2\alpha_n b)+\alpha_n a^2\sinh(2\alpha_n a)$$
$$+\alpha_n^2 b^3-\alpha_n^2 a^3\Big]$$
$$-\Big[3\alpha_n^2 d^3+2\alpha_n d^2\sinh(\alpha_n d)\cosh(\alpha_n d)$$

$$+\alpha_n^2 d^3 \sinh^2(\alpha_n d) + \alpha_n^2 d^3 \cosh^2(\alpha_n d)\Big] \cdot$$

$$\cdot\Big[\frac{\alpha_n b}{2}\sinh(2\alpha_n b) - \frac{\alpha_n a}{2}\sinh(2\alpha_n a)$$

$$-\frac{1}{4}\cosh(2\alpha_n b) + \frac{1}{4}\cosh(2\alpha_n a) - 2(\alpha_n b)^2 + 2(\alpha_n a)^2\Big]$$

$$-\Big[(\alpha_n d)^3 + (\alpha_n d)^2 \sinh(\alpha_n d)\cosh(\alpha_n d)\Big] \cdot$$

$$\cdot\Big[\alpha_n b^2 \cosh(2\alpha_n b) - \alpha_n a^2 \cosh(2\alpha_n a)$$

$$-4\alpha_n b^2 + 4\alpha_n a^2\Big]$$

$$+\alpha_n d^2\Big[\sinh^2(\alpha_n d) + (\alpha_n d)\sinh(\alpha_n d)\cosh(\alpha_n d)\Big] \cdot$$

$$\cdot\Big[\alpha_n b \cosh(2\alpha_n b) - \alpha_n a \cosh(2\alpha_n a)$$

$$-\frac{1}{2}\sinh(2\alpha_n b) + \frac{1}{2}\sinh(2\alpha_n a)\Big]$$

$$+\Big[(\alpha_n d)^2 \sinh^2(\alpha_n d)\Big] \cdot$$

$$\cdot\Big[\alpha_n b^2 \sinh(2\alpha_n b) - \alpha_n a^2 \sinh(2\alpha_n a)\Big]$$

$$-\frac{d}{8}\Big[\sinh^2(\alpha_n d) + 2\alpha_n d \sinh(\alpha_n d)\cosh(\alpha_n d)$$

$$+3\sinh^2(\alpha_n d)\cosh^2(\alpha_n d) + \sinh^4(\alpha_n d)\Big] \cdot$$

$$\cdot\Big[((2\alpha_n b)^2 + 2)\cosh(2\alpha_n b) - 4\alpha_n b \sinh(2\alpha_n b)$$

$$-((2\alpha_n a)^2 + 2)\cosh(2\alpha_n a) + 4\alpha_n a \sinh(2\alpha_n a)\Big]$$

$$-\frac{1}{2}\left[\alpha_n d \sinh^2(\alpha_n d) + \sinh^3(\alpha_n d)\cosh(\alpha_n d)\right]\cdot$$

$$\cdot\left[\alpha_n b^2 \cosh(2\alpha_n b) + b(2(\alpha_n b)^2+1)\sinh(2\alpha_n b)\right.$$

$$-\alpha_n a^2\cosh(2\alpha_n a) - a(2(\alpha_n a)^2+1)\sinh(2\alpha_n a)$$

$$-b\sinh(2\alpha_n b) + a\sinh(2\alpha_n a)$$

$$\left.-2\alpha_n b^2\cosh(2\alpha_n b) + 2\alpha_n a^2\cosh(2\alpha_n a)\right]\Big\}$$

$$-E^{II}\pi d(1+\nu^{II})\Big\{\left[2\alpha_n(\alpha_n d - \sinh(\alpha_n d))(\cosh(\alpha_n d)-1)\right]^{-2}$$

$$+2\alpha_n^{-1}\left[2\alpha_n(\alpha_n d - \sin(\alpha_n d)(\cosh(\alpha_n d)-1)\right]^{-3}\cdot$$

$$\cdot\left[2d(-(\cosh\alpha_n d - 1)^2\right.$$

$$\left.+(\alpha_n d - \sinh\alpha_n d)\sinh(\alpha_n d))\right]\Big\}\cdot$$

$$\cdot\Big\{(\alpha_n d)^4\left[\frac{\sinh(2\alpha_n b)-\sinh(2\alpha_n a)}{4} - \frac{\alpha_n b - \alpha_n a}{2}\right]$$

$$+\frac{1}{2}\left[\alpha_n d + \sinh(\alpha_n d)\cosh(\alpha_n d)\right]^2\cdot$$

$$\cdot\left[\frac{1}{8}((2\alpha_n b)^2+2)\sinh(2\alpha_n b) - \frac{\alpha_n b}{2}\cosh(2\alpha_n b)\right.$$

$$-\frac{1}{8}((2\alpha_n a)^2+2)\sinh(2\alpha_n a) + \frac{\alpha_n a}{2}\cosh(2\alpha_n a)$$

$$\left.-((\alpha_n b)^3 - (\alpha_n a)^3)/3\right]$$

$$+\frac{1}{2}\sinh^4(\alpha_n d)\left[\frac{1}{8}((2\alpha_n b)^2+2)\sinh(2\alpha_n b)\right.$$

$$-\frac{1}{8}((2\alpha_n a)^2+2)\sinh(2\alpha_n a)$$

$$-\frac{\alpha_n b}{2}\cosh(2\alpha_n b)+\frac{\alpha_n a}{2}\cosh(2\alpha_n a)$$

$$\left.-\frac{(\alpha_n b)^3-(\alpha_n a)^3}{3}\right]$$

$$-(\alpha_n d)^2\left[\alpha_n d+\sinh(\alpha_n d)\cosh(\alpha_n d)\right]\cdot$$

$$\cdot\left[\frac{\alpha_n b}{2}\sinh(2\alpha_n b)-\frac{\alpha_n a}{2}\sinh(2\alpha_n a)\right.$$

$$-\frac{1}{4}\cosh(2\alpha_n b)+\frac{1}{4}\cosh(2\alpha_n a)$$

$$\left.-2(\alpha_n b)^2+2(\alpha_n a)^2\right]$$

$$+(\alpha_n d)^2\sinh^2(\alpha_n d)\cdot\left[\frac{\alpha_n b}{2}\cosh(2\alpha_n b)\right.$$

$$\left.-\frac{\alpha_n a}{2}\cosh(2\alpha_n a)-\frac{1}{4}\sinh(2\alpha_n b)+\frac{1}{4}\sinh(2\alpha_n a)\right]$$

$$-\frac{1}{8}\left[(\alpha_n d)+\sinh(\alpha_n d)\cosh(\alpha_n d)\right]\cdot$$

$$\cdot\sinh^2(\alpha_n d)\cdot\left[((2\alpha_n b)^2+2)\cosh(2\alpha_n b)\right.$$

$$-((2\alpha_n a)^2+2)\cosh(2\alpha_n a)$$

$$\left.\left.-4\alpha_n b\sinh(2\alpha_n b)+4(\alpha_n a)\sinh(2\alpha_n a)\right]\right\}$$

$$= 0 \qquad (220)$$

C. BUCKLING OF A SINGLE FIBER IN AN INFINITE MATRIX UNDER AXIAL COMPRESSION

INTERFACIAL FORCE PER UNIT LENGTH PER UNIT LATERAL DEFLECTION, k

Now let us take $b \longrightarrow \infty$, or the matrix is infinite in size. Thus, it is more convenient that the solution of differential equation (79) takes the following form:

$$\Phi = \sum_{n=1}^{\infty} \alpha_n^{-2} \left[A_{1n} e^{\alpha_n r} + B_{1n}(\alpha_n r) e^{\alpha_n r} + C_{1n} e^{-\alpha_n r} + D_{1n}(\alpha_n r) e^{-\alpha_n r} \right] \sin(\alpha_n z) \quad (221)$$

The stresses are

$$\sigma_{33}^{II} = \sum_{n=1}^{\infty} \left[(A_{1n} + 2B_{1n}) e^{\alpha_n r} + B_{1n}(\alpha_n r) e^{\alpha_n r} + (C_{1n} - 2D_{1n}) e^{-\alpha_n r} + D_{1n}(\alpha_n r) e^{-\alpha_n r} \right] \cdot \sin(\alpha_n z) \quad (222)$$

$$\sigma_{11}^{II} = -\sum_{n=1}^{\infty} \left[A_{1n} e^{\alpha_n r} + B_{1n}(\alpha_n r) e^{\alpha_n r} + C_{1n} e^{-\alpha_n r} + D_{1n}(\alpha_n r) e^{-\alpha_n r} \right] \sin(\alpha_n z) \quad (223)$$

$$\sigma_{13}^{II} = -\sum_{n=1}^{\infty} \left[(A_{1n} + B_{1n}) e^{\alpha_n z} + B_{1n} (\alpha_n z) e^{\alpha_n z} - (C_{1n} - D_{1n}) e^{-\alpha_n z} - D_{1n} (\alpha_n z) e^{-\alpha_n z} \right] \cdot \cos(\alpha_n z) \tag{224}$$

Since when $r \to \infty$, all stresses have to be finite, then

$$A_{1n} = 0 \tag{225}$$

$$B_{1n} = 0 \tag{226}$$

and

$$C_{1n} = \phi_{1n} / \pi a \tag{227}$$

$$D_{1n} = 0 \tag{228}$$

Therefore, the displacement in lateral direction is found as follows:

$$\xi_1^{II} = \frac{1}{E^{II}} \sum_{n=1}^{\infty} \left\{ \int_0^{\infty} \frac{\phi_{1n}}{\pi a} e^{-\alpha_n z} \sin(\alpha_n z)\, dz - \nu^{II} \int_0^{\infty} \frac{\phi_{1n}}{\pi a} e^{-\alpha_n z} \sin(\alpha_n z)\, dz \right\}$$

$$= \frac{1 - \nu^{II}}{E^{II}} \sum_{n=1}^{\infty} \frac{\phi_{1n}}{\alpha_n \pi a} \sin(\alpha_n z) \tag{229}$$

$$k = \frac{p_1}{S_1^{II}} = \frac{\sum_{n=1}^{\infty} p_{1n} \sin(\alpha_n z)}{\sum_{n=1}^{\infty} \left(\frac{1-\nu^{II}}{E^{II}}\right) \frac{p_{1n}}{\alpha_n \pi a} \sin(\alpha_n z)} \tag{230}$$

or

$$k = \frac{\pi a E^{II}}{1-\nu^{II}} \sum_{n=1}^{\infty} \alpha_n \tag{231}$$

SMALLEST BUCKLING LOAD AND BUCKLING WAVELENGTH OF THE FIBER

The expression for buckling load of the fiber is derived as follows:

$$P_{cr}^{I} = \alpha_n^{\,2} E^{I} I^{I} + \alpha_n^{-1} \frac{\pi a E^{II}(3+\nu^{II})}{(1-\nu^{II})^2} \tag{232}$$

In deriving this equation, the value of k in equation (231) has been introduced.

Again, α_n α_n^* is determined by minimization of P_{cr}^{I} with respect to of (232); i.e.,

$$\frac{\partial P_{cr}^{I}}{\partial \alpha_n} = 0 \tag{233}$$

which yields

$$\alpha_n = \sqrt[3]{\frac{E^{II}\pi a(3+\nu^{II})}{2E^{I}I^{I}(1-\nu^{II})^2}} \tag{234}$$

Substitution of (234) into (232) gives the smallest buckling load of the fiber.

$$\left(P_{cr}^{I}\right)_{min} = \left[\frac{E^{II}\pi a(3+\nu^{II})}{2E^{I}I^{I}(1-\nu^{II})^{2}}\right]^{2/3} E^{I}I^{I} + \left[\frac{E^{II}\pi a(3+\nu^{II})}{2E^{I}I^{I}(1-\nu^{II})^{2}}\right]^{-1/3} \cdot \left[\frac{\pi a E^{II}(3+\nu^{II})}{(1-\nu^{II})^{2}}\right] \quad (235)$$

or

$$\left(P_{cr}^{I}\right)_{min} = 3 \cdot 2^{-2/3} \left[\frac{E^{II}\pi a(3+\nu^{II})}{E^{I}I^{I}(1-\nu^{II})^{2}}\right]^{2/3} E^{I}I^{I} \quad (236)$$

The corresponding critical wavelength is

$$\ell_{cr} = \frac{2\pi}{\alpha_n} = 2\pi \left[\frac{E^{II}\pi a(3+\nu^{II})}{2E^{I}I^{I}(1-\nu^{II})^{2}}\right]^{1/3} \quad (237)$$

D. BUCKLING OF A MULTIFIBER COMPOSITE DUE TO RESIN SHRINKAGE

Because of the smallness of the cell diameter compared to the length of the fiber, we can make some simplifying assumptions such as:

1. Fiber cross section deformations due to stresses perpendicular to the axis of symmetry are neglected.

2. Cross sections remain plane after deformation.

3. The shape of a cross section is maintained after deformation.

4. Cross sections orthogonal to the axis of symmetry remain orthogonal to the deformed axis of symmetry (no deformation due to shear).

Figure 64 shows the deflected axis of symmetry of a fiber and its associated hexagonal cell in the z-direction. An arbitrary point P at the nondeflected axis has the distance z from the origin. After deformation, Point P rests at $\bar{P}$ with the coordinates ξ_3 and ξ_1. Similar is $\bar{Q}$, the end position of Q after deflection. The point X is an off-axis point of the elastic medium. It will be at $\bar{X}$ after deflection. Because of assumption 4, the line $\bar{X}\bar{P}$ must be orthogonal to the tangenial line of the deflected line of symmetry at $\bar{P}$.

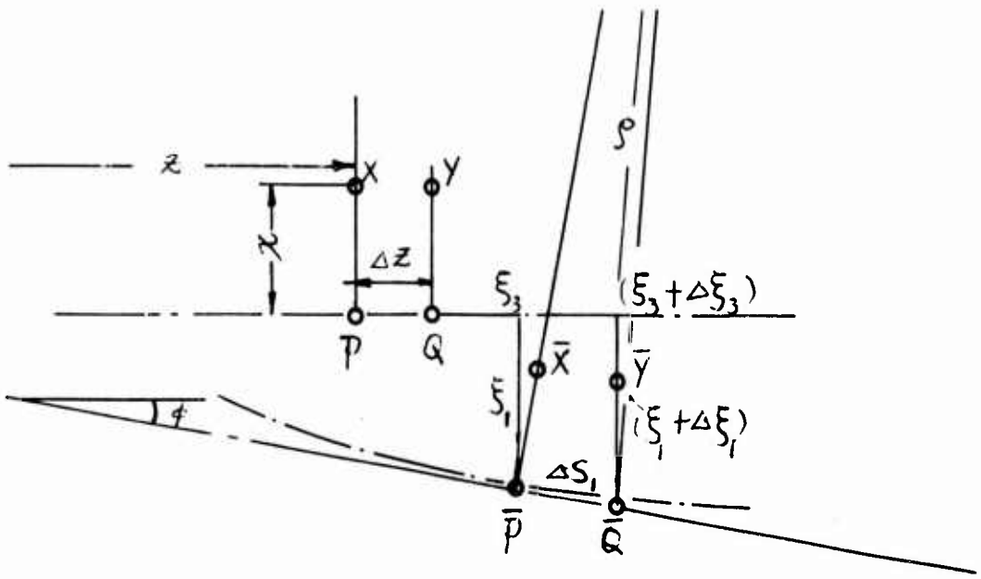

Figure 64. Deflection Geometry of a Fiber

The strain of the element $\overline{XY}$ is

$$\varepsilon_3(x) = \frac{\overline{XY} - XY}{XY} = \frac{\frac{\Delta s_1}{\rho}(\rho - x) - \Delta z}{\Delta z} = \frac{\Delta s}{\Delta z}\left(1 - \frac{x}{\rho}\right) - 1$$

or for the limit $\Delta z \to 0$,

$$\varepsilon_3(x) = \frac{ds}{dz}\left(1 - \frac{x}{\rho}\right) - 1 \tag{238}$$

For $x = 0$, we get the strain of the line element along the axis of symmetry

$$\varepsilon_3(0) = \frac{ds}{dz} - 1 \tag{239}$$

and therefore (238),

$$\varepsilon_3(x) = \varepsilon_3(0) - x \frac{ds}{dz} \frac{1}{\rho}$$

ρ is the radius of curvature of the deflected axis at P. Because $d\varphi = \frac{ds}{\rho}$, it follows further that

$$\varepsilon_3(x) = \varepsilon_3(0) - x \frac{d\varphi}{dz} \tag{240}$$

$\varepsilon_3(x)$ is only a function of x. Therefore, all fiber elements with the distance x from the plane normal to the plane of symmetry (in Figure 64 the plane through line PQ normal to the paper plane) experience the same strain. The strain in the x- and y-direction is caused by transversal contraction. Quantity ν is the Poisson's ratio of transversal contraction of the material.

We get

$$\varepsilon_1(x) = -\nu^I \varepsilon_3(x) \tag{241}$$

$$\varepsilon_2(x) = -\nu^I \varepsilon_3(x) \tag{242}$$

Considering infinitesimal distortion, we can write the strain as follows (putting $\epsilon_3(0) = \epsilon$):

$$D_{11} = \varepsilon_1(x) = -\nu^I \varepsilon_3(x) = -\nu^I\left(\varepsilon - x\,\frac{d\varphi}{dx}\right) \tag{243}$$

$$D_{22} = \varepsilon_2(x) = -\nu^I \varepsilon_3(x) = -\nu^I\left(\varepsilon - x\,\frac{d\varphi}{dx}\right) \tag{244}$$

$$D_{33} = \varepsilon_3(x) = \varepsilon - x\,\frac{d\varphi}{dx} \tag{245}$$

By neglecting the shear, we obtain

$$D_{12} = D_{23} = D_{13} = 0 \tag{246}$$

The variation of energy is

$$\delta A^{(1)} = \frac{E^I}{2(1+\nu^I)} \delta \int \left\{ D_{ij}^{(1)} D_{ij}^{(1)} + \frac{\nu^I}{1-2\nu^I} \left[D_{kk}^{(1)}\right]^2 \right\} dv \tag{247}$$

Putting $dv = dz \cdot dx\,dy$,

$$\delta A^{(1)} = \frac{E^I}{2} \delta \int_0^{\ell} \int_{A_1} \varepsilon_3^2(x)\, dx\, dy\, dz \tag{248}$$

and

$$\delta A^{(2)} = \frac{E^{II}}{2} \delta \int_0^{\ell} \int_{A_2} \left[\varepsilon_3^2(x) - 2\beta \varepsilon_3(x) \right] dx\, dy\, dz \tag{249}$$

Introducing (245) gives

$$\delta A^{(1)} = \delta \frac{E^{I}}{2} \int_0^{\ell} dz \int_{A_1} \left(\varepsilon^2 - 2x\varepsilon \frac{d\varphi}{dz} + x^2 \left(\frac{d\varphi}{dz} \right)^2 \right) dx\, dy \tag{250}$$

$$\delta A^{(2)} = \delta \frac{E^{II}}{2} \int_0^{\ell} dz \int_{A_2} \left(\varepsilon^2 - 2x\varepsilon \frac{d\varphi}{dz} + x^2 \left(\frac{d\varphi}{dz} \right)^2 - 2\beta\varepsilon + 2\beta x \frac{d\varphi}{dz} \right) dx\, dy \tag{251}$$

Performing the integration over x and y, we get

$$\int_{A_1} dx\, dy = A^{I} \tag{252}$$

$$\int_{A_2} dx\, dy = A^{II} \tag{253}$$

where A_1 and A_2 are the cross-sectional area of the fiber and resin in the cell.

Furthermore,

$$\int_{A_1} x^2 dx\, dy = I^I \tag{254}$$

$$\int_{A_2} x^2 dx\, dy = I^{II} \tag{255}$$

the areal moments of inertia with respect to the neutral (non-strained) plane.

Because of symmetry

$$\int_{A_1} x\, dx\, dy = 0 \tag{256}$$

$$\int_{A_2} x\, dx\, dy = 0 \tag{257}$$

then (250) and (251) become:

$$\delta A^{(1)} = \delta \frac{E^I}{2} \int_0^{\ell} \left[\varepsilon^2 A^I + I^I (\varphi')^2 \right] dz \tag{258}$$

$$\delta A^{(2)} = \delta \frac{E^{II}}{2} \int_0^{\ell} \left[\varepsilon^2 A^{II} + I^{II} (\varphi')^2 - 2 \beta^{II} \varepsilon A^{II} \right] dz \tag{259}$$

The equilibrium equation in energy form for a fiber resin cell will be written, after introducing (258) and (259), as follows:

$$\delta \int_0^{\ell} \left\{ \frac{1}{2} \left[E^I A^I + E^{II} A^{II} \right] \varepsilon^2 + \frac{1}{2} \left[E^I I^I + E^{II} I^{II} \right] (\varphi')^2 - E^{II} A^{II} \beta^{II} \varepsilon \right\} dz = \sum_{n=1}^{N} F_i^{(n)} \delta \ell_i^{(n)} \tag{260}$$

Due to deflection of the axis of symmetry, the projection of $\bar{PQ}$ on the undeflected axis of symmetry, the length $\Delta\xi$, will be different from Δz, the original projection of PQ. The difference $\Delta\xi - \Delta z$ means the longitudinal change of length, Δw, of the axis element Δz.

$$\Delta w = \Delta \xi_3 - \Delta z = \left(\frac{\Delta \xi_3}{\Delta z} - 1 \right) \Delta z$$

Taking the limit $\Delta z \to 0$, then

$$dw = \left(\frac{d\xi_3}{dz} - 1 \right) dz \tag{261}$$

Because of (239),

$$\frac{d\xi_3}{dz} = \frac{d\xi_3}{ds}\,\frac{ds}{dz} = \frac{ds}{dz}\cos\varphi = (1+\varepsilon)\cos\varphi$$

and combining the foregoing equation with equation (261) gives

$$dw = \left[(1+\varepsilon)\cos\varphi - 1\right] dz \tag{262}$$

The total change of length will therefore be

$$w(\ell) = \int_0^{\ell} \left\{(1+\varepsilon)\cos\varphi - 1\right\} dz \tag{263}$$

We assume that the fiber is restrained to the matrix such that the longitudinal change of the fiber is equal to the longitudinal change of the matrix. Therefore it will be

$$w(\ell) = \overset{\text{II}}{\beta}(\ell) \tag{264}$$

and

$$\int_0^{\ell} \left\{(1+\varepsilon)\cos\varphi - \left(1+\overset{\text{II}}{\beta}\right)\right\} dz = 0 \tag{265}$$

The solutions

$$\varepsilon = \varepsilon(z) \tag{266}$$

$$\varphi = \varphi(z) \tag{267}$$

of (260) have to satisfy equation (265).

We consider the case $F_i^{(n)} = 0$ and get the following equations:

$$\delta \int_0^{\ell} \left\{ \frac{1}{2}\left[E^I A^I + E^{II} A^{II}\right] \varepsilon^2 + \frac{1}{2}\left[E^I I^I + E^{II} I^{II}\right] \varphi'^2 - E^{II} A^{II} \beta^{II} \varepsilon \right\} dz = 0 \tag{268}$$

with the restraining conditions (265),

$$\int_0^{\ell} \left\{ (1+\varepsilon)\cos\varphi - (1+\beta^{II}) \right\} dz = 0$$

The Euler-Lagrange equations of this variational problem with two independent variables are

$$P\varepsilon + R + \lambda \cos\varphi = 0 \tag{269}$$

$$Q\varphi'' + \lambda(1+\varepsilon)\sin\varphi = 0 \tag{270}$$

where we use the abbreviations

$$P = E^I A^I + E^{II} A^{II} \tag{271}$$

$$Q = E^I I^I + E^{II} I^{II} \tag{272}$$

$$R = -E^{II} A^{II} \beta^{II} > 0 \tag{273}$$

and the parameter λ being the Lagrangian multiplier. Solutions of the set of equations (269) and (270) must satisfy (265).

From (265), we can determine λ by substitution of ε from (269) in (265)

$$\int_0^\ell \left\{ \left(1 - \frac{R}{P} - \lambda \frac{\cos\varphi}{P}\right) \cos\varphi \, dz = \left(1 + \beta^{II}\right) \ell \right.$$

or

$$\lambda = \frac{(P-R) \int_0^\ell \cos\varphi \, dz - \left(1+\beta^{II}\right) P\ell}{\int_0^\ell \cos^2\varphi \, dz} \tag{274}$$

In order to give a physical interpretation of λ, we consider the resin around the fiber not shrunk ($\beta^{II} = 0$). Instead, we apply an axial force $F_i^{(1)} = F$ acting at $z = \ell$. Then we have to apply (260) with $\beta^{II} = 0$ and

$$-\sum_{n=1}^{N} F_i^{(n)} \delta \ell_i^{(n)} = \delta \left(F \int_0^\ell \left[(1+\varepsilon) \cos\varphi - 1 \right] dz \right)$$

The variational problem for this case will be

$$\delta \int_0^\ell \left\{ \frac{1}{2} P \varepsilon^2 + \frac{1}{2} Q \varphi'^2 + R\varepsilon + F(1+\varepsilon)\cos\varphi - F \right\} dz = 0$$

from which we get the Euler-Lagrange equation of the form (269), (270) but $\lambda = +F$. <u>The parameter λ therefore represents the axial load of the fiber which is generated by the resin due to shrinkage</u>. We can assume λ to be known and substitute ε in (270) by ε from (269).

The following differential equation in φ is obtained:

$$Q\varphi'' + \lambda\left(1 \mp \frac{R}{P} - \frac{\lambda}{P}\cos\varphi\right)\sin\varphi = 0 \tag{275}$$

After multiplication by $d\varphi$, we can integrate (275) at once, and obtain

$$\frac{1}{2}Q\varphi'^2 - \lambda\left(1 - \frac{R}{P}\right)\cos\varphi + \frac{\lambda^2}{4P}\cos 2\varphi = \bar{C} \tag{276}$$

We assume $\varphi^1 = 0$ at $\varphi = \varphi_{max}{}^1$; therefore,

$$C = -\lambda\left(1 - \frac{R}{P}\right)\cos\varphi_{max} + \frac{\lambda^2}{4P}\cos 2\varphi_{max} \tag{277}$$

and (276):

$$\varphi' = \sqrt{\frac{2\lambda}{Q}\left(1 - \frac{R}{P}\right)\left(\cos\varphi - \cos\varphi_{max}\right) - \frac{\lambda^2}{4P}\left(\cos 2\varphi - \cos 2\varphi_{max}\right)} \tag{278}$$

(278) can be integrated by quadrature:

$$z = \int \frac{d\varphi}{\sqrt{\frac{2\lambda}{Q}\left(1 - \frac{R}{P}\right)\left(\cos\varphi - \cos\varphi_{max}\right) - \frac{\lambda^2}{2P}\left(\cos^2\varphi - \cos^2\varphi_{max}\right)}} + \bar{C}_1 \tag{279}$$

The integral in (279) cannot be expressed by elementary functions. Using the abbreviation

$$\bar{a} = \frac{2\lambda}{Q}\left(1 - \frac{R}{r}\right) > 0 \tag{280}$$

$$\bar{b} = \frac{\lambda^2}{2PQ} > 0 \tag{281}$$

the integral to be determined is as follows:

$$z = \int \frac{d\varphi}{\sqrt{\bar{a}(\cos\varphi - \cos\varphi_{max}) - \bar{b}(\cos^2\varphi - \cos^2\varphi_{max})}} + \bar{C}_1$$

$$= \int \frac{d\varphi}{\sqrt{(\cos\varphi - \cos\varphi_{max})(\bar{a} - \bar{b}(\cos\varphi_{max} - \cos\varphi))}} + \bar{C}_1 \tag{282}$$

with $\cos\varphi = 1 - 2\sin^2\frac{\varphi}{2}$ follows:

$$z = \frac{1}{2\sqrt{\frac{\bar{a}}{2} - \bar{b}}} \int \frac{d\varphi}{\sqrt{\left(\sin^2\frac{\varphi_{max}}{2} - \sin^2\frac{\varphi}{2}\right) + \frac{2\bar{b}}{\bar{a} - 2\bar{b}}\left(\sin^2\frac{\varphi}{2} + \sin^2\frac{\varphi_{max}}{2}\right)}}$$

$$+ \bar{C}_1 \tag{283}$$

We use the abbreviation

$$p = \sin^2 \frac{\varphi_{max}}{2} \tag{284}$$

and

$$q = \frac{\bar{b}}{\frac{\bar{a}}{2} - \bar{b}} \sin^2 \frac{\varphi_{max}}{2} \tag{285}$$

Furthermore, we substitute

$$\sin \frac{\varphi}{2} = \sqrt{\xi} \qquad \sin \frac{\varphi_{max}}{2} = \sqrt{\xi p}$$

$$d\varphi = \frac{d\xi \sqrt{p}}{\sqrt{\xi(1-\xi p)}} \tag{286}$$

and get

$$z = \frac{1}{2\sqrt{\frac{\bar{a}}{2} - \bar{b}}} \int \frac{d\xi}{\sqrt{(1-\xi)\xi(1-p\xi)(1+q+q\xi)}} + \bar{C}_1 \tag{287}$$

Now we use the substitution

$$\xi = \frac{w(1+q)}{1+2q-qw} \tag{288}$$

and get

$$z = \frac{1}{2\sqrt{\frac{a}{2} - b}} \int \frac{dw}{\sqrt{(1-w)w\left(1+2q-w\left[q+p(1+q)\right]\right)}} + \bar{C}_1 \qquad (289)$$

Finally, we substitute

$$w = \sin^2\vartheta$$
$$dw = 2\sqrt{w(1-w)}\, d\vartheta \qquad (290)$$

and get

$$z = \frac{1}{\sqrt{\left(\frac{a}{2} - b\right)(1+2q)}} \int \frac{d\vartheta}{\sqrt{1 - \frac{q+p(1+q)}{1+2q}\sin^2\vartheta}} + C_1 \qquad (291)$$

The integral in (291) is an elliptic integral of the first kind. Its inverse functions are Jacobi's elliptic functions. From (291) we get

$$(z - c_1)\sqrt{\left(\frac{a}{2} - b\right)(1+2q)} = \int \frac{d\vartheta}{\sqrt{1 - k^2\sin^2\vartheta}}$$

with

$$k = \sqrt{\frac{q+(1+q)p}{1+2q}} \qquad (292)$$

$$\sin\vartheta = \operatorname{sn}\left[(z-\bar{c}_1)\sqrt{\left(\frac{\bar{a}}{2}-\bar{b}\right)(1+2q)}\;\right] \tag{293}$$

Re-substitution gives

$$w = \sin^2\vartheta = \frac{\xi(1+2q)}{1+q+\xi q} = \frac{(1+2q)\sin^2\frac{\varphi}{2}}{p\left(1+q+\frac{q}{p}\sin^2\frac{\varphi}{2}\right)} \tag{294}$$

Solving for $\sin^2\frac{\varphi}{2}$ gives

$$\sin^2\frac{\varphi}{2} = \frac{\sin^2\vartheta\,(1+q)}{\frac{1+2q}{p}-\frac{q}{p}\sin^2\vartheta}$$

or

$$\sin\frac{\varphi}{2} = \pm\operatorname{sn}\left[(z-\bar{c}_1)K\right]\sqrt{\frac{1+q}{\frac{1+2q}{p}-\frac{q}{p}\operatorname{sn}^2\left[(z-\bar{c}_1)K\right]}} \tag{295}$$

with

$$K = \sqrt{\left(\frac{\bar{a}}{2}-\bar{b}\right)(1+2q)} = \sqrt{\frac{\bar{a}}{2}-\bar{b}\cos\varphi_{max}} \tag{296}$$

Because of

$$1+q = \frac{\bar{a}/2-\bar{b}\cos^2\frac{\varphi_{max}}{2}}{\bar{a}/2-\bar{b}}$$

follows (295)

$$\sin\frac{\varphi}{2} = \pm\sin\frac{\varphi_{max}}{2}\operatorname{sn}\left[(z-\bar{c}_1)K\sqrt{\frac{\frac{\bar{a}}{2}-\frac{\bar{b}}{2}(1+\cos\varphi_{max})}{\frac{\bar{a}}{2}-\bar{b}\cos\varphi_{max}-\bar{b}\sin^2\frac{\varphi_{max}}{2}\operatorname{sn}^2\left[(z-\bar{c}_1)K\right]}}\right] \tag{297}$$

Parameter k is from (292):

$$\bar{k} = \sin\frac{\varphi_{max}}{2}\sqrt{\frac{1+\frac{\bar{b}}{\bar{a}}(1-\cos\varphi_{max})}{1-\frac{2\bar{b}}{\bar{a}}\cos\varphi_{max}}} \tag{298}$$

We need the inverse function of (297), which we get from (294):

$$sn=\left[(z-\bar{c}_1)\bar{K}\right]=\pm\frac{\sin\frac{\varphi}{2}}{\sin\frac{\varphi_{max}}{2}}\sqrt{\frac{\frac{\bar{a}}{2}-\bar{b}\cos\varphi_{max}}{\frac{\bar{a}}{2}-\frac{\bar{b}}{2}(\cos\varphi+\cos\varphi_{max})}} \tag{299}$$

At $z = 0$, $\varphi = +\varphi_{max}$ gives $sn[-\bar{c}_1\bar{K}] = +1$.

Therefore,

$$\bar{c}_1 = -\frac{1}{\bar{K}}\int_0^{\pi/2}\frac{d\vartheta}{\sqrt{1-\bar{k}^2\sin^2\vartheta}} = -\frac{\bar{K}}{\bar{K}} \tag{300}$$

K (k) is the complete elliptic integral of the first kind.
Therefore (297),

$$\sin\frac{\varphi}{2} = sn\left[z\bar{K}+\bar{K}\right]\sqrt{\frac{\frac{\bar{a}}{\bar{b}}-1-\cos\varphi_{max}}{\frac{\bar{a}}{\bar{b}}-2\cos\varphi_{max}-sn^2\left[z\bar{K}+\bar{K}\right]}} \tag{301}$$

φ is a periodic function in z, with the periodicity z_w

$$z_w\bar{K} = 4\,\bar{K}$$

or

$$z_w = \frac{4}{\varkappa} K(k) \tag{302}$$

z_w is the wavelength of the waving fiber under internal stress. From (296), one can see that the wavelength depends on φ_{max} and λ.

In order to find the deviation η of the deflected axis of symmetry from the nondeflected axis, we have to get the differential equation for η first.

It is

$$\frac{d\xi_1}{dz} = \frac{d\xi_1}{ds} \frac{ds}{dz}$$

Since $\frac{d\xi_1}{ds} = \sin\varphi$ and using (239), it follows:

$$\frac{d\xi_1}{dz} = (1+\varepsilon)\sin\varphi \tag{303}$$

Substituting ϵ from (269) yields

$$\frac{d\xi_1}{dz} = \left(1 - \frac{R}{\rho} - \frac{\lambda}{\rho}\cos\varphi\right)\sin\varphi \tag{304}$$

which is the desired differential equation for η.

We obtain function $\xi_1(z)$ by quadrature:

$$\xi_1 = \int_0^z \left[1 - \frac{R}{P} - \frac{\lambda}{P}\cos\varphi\right] \sin\varphi \, dz \tag{305}$$

$\sin\varphi$ and $\cos\varphi$ are known functions of z according to (301).

We are now also able to calculate λ according to (274). The calculation of ξ_1 and λ depends on the calculation of the following four definite integrals:

$$J_1 = \int_0^l \cos\varphi \, dz = l - 2\int_0^l \sin^2\frac{\varphi}{2} \, dz \tag{306}$$

$$J_2 = \int_0^l \sin\varphi \, dz = 2\int_0^l \sin\frac{\varphi}{2}\cos\frac{\varphi}{2} \, dz \tag{307}$$

$$J_3 = \int_0^l \cos 2\varphi \, dz = l - 8\int_0^l \sin^2\frac{\varphi}{2} \, dz - 8\int_0^l \sin^4\frac{\varphi}{2} \, dz \tag{308}$$

$$J_4 = \int_0^l \sin 2\varphi \, dz = 4\int_0^l \sin\frac{\varphi}{2}\cos\frac{\varphi}{2} \, dz - 8\int_0^l \sin^3\frac{\varphi}{2}\cos\frac{\varphi}{2} \, dz \tag{309}$$

We have to solve the following four basic integrals:

$$\underset{I}{I} = \int_0^{\ell} \sin^2\frac{\varphi}{2}\, dz \tag{310}$$

$$\underset{II}{J} = \int_0^{\ell} \sin\frac{\varphi}{2}\cos\frac{\varphi}{2}\, dz \tag{311}$$

$$\underset{III}{J} = \int_0^{\ell} \sin^4\frac{\varphi}{2}\, dz \tag{312}$$

and

$$\underset{IV}{J} = \int_0^{\ell} \sin^3\frac{\varphi}{2}\cos\frac{\varphi}{2}\, dz \tag{313}$$

For that purpose, we have to evaluate $\cos\frac{\varphi}{2}$ from (295). It is

$$\cos^2\frac{\varphi}{2} = \frac{1+2q-q\,sn^2[2x+k]-(1+q)p\,sn^2[2x+k]}{1+2q-q\,sn^2[2x+k]}$$

$$= \frac{1+2q\left[1-\frac{(1+q)p+q}{1+2q}\,sn^2[2x+k]\right]}{1+2q-q\,sn^2[2x+k]}$$

Because of (292) and

$$dn^2[zx+K] = 1 - k^2 sn^2[zx+K]$$

follows

$$\cos\frac{\varphi}{2} = dn[zx+K]\sqrt{\frac{\frac{\bar{a}}{2b} - \cos\varphi_{max}}{\frac{4(\frac{\bar{a}}{2b} - \cos\varphi_{max})}{1-\cos\varphi_{max}} - sn^2[zx+K]}} \tag{314}$$

All integrals J_I, J_{II}, J_{III}, J_{IV} can be found in a closed form.

It is

$$J_I = \frac{(1+q)p}{q}\int_0^{\ell} \frac{sn^2(zx+K)\,dz}{\frac{1+2q}{q} - sn^2(xz+K)} \tag{315}$$

$$J_{II} = \frac{\sqrt{(1+q)(1+2q)p}}{q}\int_0^{\ell} \frac{dn(zx+K)\,sn(zx+K)\,dz}{\frac{1+2q}{q} - sn^2(xz+K)} \tag{316}$$

$$J_{III} = \left[\frac{(1+q)p}{q}\right]^2 \int_0^{\ell} \frac{sn^4(xz+K)\,dz}{\left[\frac{1+2q}{q} - sn^2(xz+K)\right]^2} \tag{317}$$

$$J_{\underline{IV}} = \frac{[(1+q)p]^{3/2}\sqrt{1+2q}}{q^2} \int_0^{\ell} \frac{sn^3(\kappa z+K)\, dn(\kappa z+K)\, dz}{\left[\frac{1+2q}{q} - sn^2(\kappa z+K)\right]^2} \tag{318}$$

We solve (315) first:

$$J_{\underline{I}} = \frac{(1+q)p}{q} \left[\int_0^{\ell} \frac{dz}{1-\frac{q}{1+2q} sn^2(\kappa z+K)} - \int_0^{\ell} dz \right]$$

$$= \frac{p}{q}(1+q)\left[\frac{1}{\kappa}\int_K^{K+\ell\kappa} \frac{d\zeta}{1-\frac{q}{1+2q} sn^2\zeta} - \ell\right] \tag{319}$$

For the first integral, we substitute

$$sn\zeta = t, \quad dt = \sqrt{(1-t^2)(1-k^2t^2)}\, d\zeta$$

and get

$$\int_K^{K+\ell\kappa} \frac{d\zeta}{1-\frac{q}{1+2q} sn^2\zeta} = \int_1^{sn(K+\ell\kappa)} \frac{dt}{(1-\frac{q}{1+2q}t^2)\sqrt{(1-t^2)(1-k^2t^2)}}$$

$$= \Pi\left(sn(K+\alpha\ell)\,;\,k,\,-\frac{q}{1+2q}\right)$$

$$-\Pi\left(1\,;\,k,\,-\frac{q}{1+2q}\right) \qquad (320)$$

$$\Pi(t;k,n) = \int_0^t \frac{1}{(1+nt^2)\sqrt{(1-t^2)(1-k^2t^2)}}$$

is the elliptic integral of the third kind.

The integral (319) therefore is

$$J_I = \frac{p}{q}(1+q)\left[\frac{1}{\pi}\Pi\left(sn(K+\alpha\ell);k,-\frac{q}{1+2q}\right)\right.$$

$$\left.-\frac{1}{\pi}\Pi\left(1;k,-\frac{q}{1+2q}\right)-\ell\right] \qquad (321)$$

Next, we treat the integral J_{II}.

Here we substitute $\mathrm{cn}(\kappa z + K) = t$

with

$$dt = -\kappa\, sn(\kappa z+K)\, dn(\kappa z+K)\, dz$$

$$sn^2(\kappa z+K) = 1 - cn^2(\kappa z+K) = 1-t^2$$

We get

$$J_{II} = -\frac{1}{\kappa q}\sqrt{p(1+q)(1+2q)} \int_0^{cn(\kappa\ell+K)} \frac{dt}{\frac{1+q}{q} + t^2}$$

$$J_{II} = -\frac{1}{\kappa}\sqrt{\frac{p}{q}(1+2q)}\ \arctan\left(t\sqrt{\frac{q}{1+q}}\right)\Bigg|_0^{cn(K+\kappa\ell)}$$

$$= -\frac{1}{\kappa}\sqrt{\frac{p}{q}(1+2q)}\ \arctan\left(cn(K+\kappa\ell)\sqrt{\frac{q}{1+q}}\right)$$

(322)

The third integral will be solved by using the transformation

$$sn(\varkappa z + K) = t$$

$$dt = \varkappa \sqrt{(1-t^2)(1-k^2t^2)}\, dz$$

$$J_{III} = \frac{1}{\varkappa}\left[p\,\frac{1+q}{q}\right]^2 \int_{snK}^{sn(\varkappa\ell+K)} \frac{t^4\, dt}{\left[\frac{1+2q}{q} - t^2\right]^2 \sqrt{(1-t^2)(1-t^2k^2)}} \tag{323}$$

Since the rational factor of the elliptic radical is of even power in t, we can rewrite (323) to bring into a more common form. But first we have to expand (323) into partial fractions. Setting for abbreviation

$$\frac{q}{1+2q} = n^2 \tag{324}$$

we get

$$J_{III} = \frac{n^4}{\varkappa}\left(p\,\frac{1+q}{q}\right)^2 \int_{snK}^{sn(K+\varkappa\ell)} \frac{t^4\, dt}{(1-n^2t^2)^2\sqrt{(1-t^2)(1-k^2t^2)}} \tag{325}$$

Because of

$$\left[\frac{t^2}{1-n^2t^2}\right]^2 = \frac{1}{n^4}\left[\frac{1}{1-n^2t^2} - 1\right]^2 = \frac{1}{n^4}\left[1 - \frac{2}{1-n^2t^2} + \frac{1}{(1-n^2t^2)^2}\right]$$

follows (325)

$$J_{III} = \frac{1}{\pi}\left(p\frac{1+q}{q}\right)^2 \left\{ \int_{sn\,K}^{sn(K+\pi\ell)} \frac{dt}{\sqrt{(1-t^2)(1-k^2t^2)}} \right.$$

$$- 2\int_{sn\,K}^{sn(K+\pi\ell)} \frac{dt}{(1-n^2t^2)\sqrt{(1-t^2)(1-k^2t^2)}}$$

$$\left. + \int_{sn\,K}^{sn(K+\pi\ell)} \frac{dt}{(1-n^2t^2)^2\sqrt{(1-t^2)(1-k^2t^2)}} \right\} = \left(p\frac{1+q}{q}\right)^2 \left\{ \ell - \right.$$

$$- \frac{2}{\pi}\left[\Pi\left(sn(K+\pi\ell); -n^2, k\right) - \Pi\left(1; -n^2, k\right)\right]$$

$$\left. + \frac{1}{\pi}\int_{sn\,K}^{sn(K+\pi\ell)} \frac{dt}{(1-n^2t^2)^2\sqrt{(1-t^2)(1-k^2t^2)}} \right\}$$

(326)

In order to evaluate the last integral, we shall derive a recursion formula for this kind of elliptic integral, since all elliptic integrals can be reduced to the three basic kinds of elliptic integrals and rational, logarithmic, and inverse trigonometric functions in t and the elliptic radical $\sqrt{(1-t^2)(1-k^2t^2)}$.

First we expand the polynomial

$$y^2 = (1-t^2)(1-k^2t^2) = 1-(1+k^2)t^2+k^2t^4 \qquad (327)$$

$$(1-n^2t^2)$$

in the power of $(1-n^2t^2)$

Setting $t^2 = \xi$, then

$$y^2 = \sum_{v=0}^{2} \frac{(-1)^v}{v!} \frac{d^v y^2}{d\xi^v}\left(\frac{1}{n}\right)\left(\frac{1}{n^2} - t^2\right)^v$$

$$= \sum_{v=0}^{2} \frac{(-1)^v}{v!\,n^{2v}} \frac{d^v y^2}{d\xi^v}\left(\frac{1}{n^2}\right)\left(1-n^2t^2\right)^v$$

$$y^2\left(\frac{1}{n^2}\right) = 1-(1+k^2)\frac{1}{n^2} + \frac{k^2}{n^4} = \frac{k^2(1-n^2)-n^2+n^4}{n^4}$$

$$\frac{d\,y^2}{d\xi}\left(\frac{1}{n^2}\right) = -(1+k^2) + 2k^2\frac{1}{n^2} = \frac{2k^2-n^2(1+k^2)}{n^2}$$

$$\frac{d^2y^2}{d\xi^2}\left(\frac{1}{n^2}\right) = 2k^2$$

$$y^2 = \frac{n^4+k^2-n^2(1+k^2)}{n^4}$$

$$+\frac{-2k^2+n^2(1+k^2)}{n^4}\left(1-n^2t^2\right) + \frac{k^2}{n^4}\left(1-n^2t^2\right)^2 \qquad (328)$$

We use the abbreviation

$$A_0 = \frac{n^4 + k^2 - n^2(1+k^2)}{n^4} \tag{329}$$

$$A_1 = \frac{n^2(1+k^2) - 2k^2}{n^4} \tag{330}$$

$$A_2 = \frac{k^2}{n^4} \tag{331}$$

to simplify (328)

$$y^2 = A_0 + A_1(1-n^2t^2) + A_2(1-n^2t^2)^2 \tag{332}$$

Dividing (332) by $y\,(1 - n^2t^2)^{\nu}$ we get

$$\frac{y}{(1-n^2t^2)^{\nu}} = \frac{A_0}{(1-n^2t^2)^{\nu} y} + \frac{A_1}{(1-n^2t^2)^{\nu-1} y} + \frac{A_2}{(1-n^2t^2)^{\nu-2} y} \tag{333}$$

We define the integral

$$J_\nu = \int \frac{dt}{(1-n^2t^2)^{\nu} y} = \int \frac{dt}{(1-n^2t^2)^{\nu}\sqrt{(1-t^2)(1-k^2t^2)}} \tag{334}$$

and integration of (333) is therefore

$$\int \frac{y\,dt}{(1-n^2t^2)^\nu} = A_0 J_\nu + A_1 J_{\nu-1} + A_2 J_{\nu-2} \tag{335}$$

The left-hand side integral we integrate by part

$$\int \frac{y\,dt}{(1-n^2t^2)^\nu} = \frac{yt}{(1-n^2t^2)^\nu} - \int t\left\{\frac{(-\nu)(-2n^2t)}{(1-n^2t^2)^{\nu+1}}\,y + \frac{\frac{d(y^2)}{dt}}{(1-n^2t^2)^\nu\ 2y}\right\} dt \tag{336}$$

Evaluating

$$\frac{d(y^2)}{dt} = \frac{d(y^2)}{d(1-n^2t^2)}\ \frac{d(1-n^2t^2)}{dt}$$

$$= \left(A_1 + 2A_2(1-n^2t^2)\right)(-2n^2t)$$

and then (336) becomes

$$\int \frac{y\,dt}{(1-n^2t^2)^\nu} = \frac{yt}{(1-n^2t^2)^\nu} - \int \frac{n^2t^2}{(1-n^2t^2)^{\nu+1}\,y}\Big\{2\nu\left[A_0 + A_1(1-n^2t^2) + A_2(1-n^2t^2)^2\right] - A_1(1-n^2t^2) - 2A_2(1-n^2t^2)^2\Big\}\,dt$$

or

$$\int \frac{y\,dt}{(1-n^2t^2)^\nu} = \frac{yt}{(1-n^2t^2)^\nu} - \int \frac{dt}{(1-n^2t^2)^{\nu+1}y}\left\{2\nu A_0 + A_1(2\nu-1)(1-n^2t^2) + 2(\nu-1)A_2(1-n^2t^2)^2\right\}$$

$$+ \int \frac{dt}{(1-n^2t^2)^\nu y}\left\{2\nu A_0 + A_1(2\nu-1)(1-n^2t^2) + 2(\nu-1)A_2(1-n^2t^2)^2\right\}$$

$$= \frac{yt}{(1-n^2t^2)^\nu} - 2\nu A_0 J_{\nu+1} + (2\nu A_0 - A_1(2\nu-1))J_\nu + (A_1(2\nu-1) - 2(\nu-1)A_2)J_{\nu-1} + (2\nu-2)A_2 J_{\nu-2} \quad (337)$$

Replacing the left-hand side of (335) by (337), we get the following recursion formula:

$$2\nu A_0 J_{\nu+1} + [(1-2\nu)A_0 + A_1(2\nu-1)]J_\nu + [-2(\nu-1)A_1 + 2(\nu-1)A_2]J_{\nu-1} - (2\nu-3)A_2 J_{\nu-2} = \frac{yt}{(1-n^2t^2)^\nu} \quad (338)$$

Because of (329), (330) and (331) are

$$2\nu A_0 = \frac{2\nu}{n^4}\left(n^4 + k^2 - n^2(1+k^2)\right) \tag{339}$$

$$(2\nu-1)(A_1 - A_0) = -\frac{2\nu-1}{n^4}\left(n^4 - 2n^2(1+k^2) + 3k^2\right) \tag{340}$$

$$2(\nu-1)(A_2 - A_1) = \frac{2(\nu-1)}{n^4}\left(3k^2 - n^2(1+k^2)\right) \tag{341}$$

$$-(2\nu-3)A_2 = -\frac{2\nu-3}{n^4}k^2 \tag{342}$$

From (338), we get our integral in (326) immediately by setting $\nu = 1$:

$$2A_0 J_2 = \frac{yt}{1-n^2t^2} + (A_0 - A_1)J_1 - A_2 J_{-1}$$

or

$$J_2 = \frac{yt}{2(1-n^2t^2)A_0} + \frac{A_0 - A_1}{2A_0}J_1 - \frac{A_2}{2A_0}J_{-1} \tag{343}$$

We have to modify

$$J_{-1} = \int \frac{1-n^2t^2}{y}\,dt$$

into the canonical form. We get

$$J_{-1} = \int \frac{1-n^2t^2}{y}\,dt = \frac{n^2}{k^2}\int \frac{1-k^2t^2}{y}\,dt + \left(1 - \frac{n^2}{k^2}\right)\int \frac{dt}{y}$$

$$= \frac{n^2}{k^2}E(t;k) + \left(1 - \frac{n^2}{k^2}\right)F(t;k) \tag{344}$$

E (t, K) is the elliptic integral of the second kind. Now we know that the elliptic integral of the third kind is

$$J_1 = \Pi(t; -n^2, k)$$

therefore,

$$J_2 = \int \frac{dt}{(1-n^2t^2)^2\sqrt{(1-t^2)(1-k^2t^2)}}$$

$$= \frac{y\,t}{2A_0(1-n^2t^2)} + \frac{A_0 - A_1}{2A_0}\Pi(t; -n^2, k)$$

$$- \frac{A_2}{2A_0}\left[\frac{n^2}{k^2}E(t;k) + \left(1 - \frac{n^2}{k^2}\right)F(t;k)\right] \tag{345}$$

From (329), (330), and (331)

$$\frac{A_0 - A_1}{A_0} = \frac{n^4 - 3k^2 - 2n^2(1+k^2)}{n^4 + k^2 - n^2(1+k^2)}$$

$$\frac{A_2}{A_0} = \frac{k^2}{n^4 + k^2 - n^2(1+k^2)}$$

and (345), finally

$$\int \frac{dt}{(1-n^2t^2)^2\sqrt{(1-t^2)(1-k^2t^2)}} = \frac{n^4 t\sqrt{(1-t^2)(1-k^2t^2)}}{2(1-n^2t^2)(n^4+k^2-n^2(1+k^2))}$$

$$+ \frac{n^4-3k^2-2n^2(1+k^2)}{2(n^4+k^2-n^2(1+k^2))}\Pi(t;-n^2;k)$$

$$- \frac{n^2}{2(n^4+k^2-n^2(1+k^2))}E(t;k)$$

$$- \frac{k^2-n^2}{2(n^4+k^2-n^2(1+k^2))}F(t;k) \qquad (346)$$

Finally, we are able to write the solution for J_{III} from (326) with (396) as follows:

$$J_{III} = \left(p\frac{1+q}{q}\right)^2\left\{\ell + \frac{n^4\,sn'(K+x\ell)\,cn(K+x\ell)\,dn(K+x\ell)}{2x(1-n^2sn^2(K+x\ell))(n^4+k^2-n^2(1+k^2))}\right.$$

$$- \frac{3n^4+7k^2-2n^2(1+k^2)}{2x(n^4+k^2-n^2(1+k^2))}\left[\Pi(sn(K+x\ell);-n^2;k)\right.$$

$$\left.- \Pi(1;-n^2;k)\right]$$

$$- \frac{n^2}{2x(n^4+k^2-n^2(1+k^2))}\left[E(sn(K+x\ell);k)\right.$$

$$\left.\left.- E(1;k)\right]\right.$$

$$- \frac{(k^2-n^2)}{2\pi(n^4+k^2-n^2(1+k^2))}\left[\pi\ell + K - K\right]\Bigg\} =$$

$$J_{\underline{III}} = \frac{\left(p\,\frac{1+q}{q}\right)^2}{2\left[n^4+k^2-n^2(1+k^2)\right]}\Bigg\{\ell\left(2n^4-n^2-2n^2k^2\right)$$

$$+ \frac{n^4}{\pi}\,\frac{sn(K+\pi\ell)\,cn(K+\pi\ell)\,dn(K+\pi\ell)}{(1-n^2sn^2(K+\pi\ell))}$$

$$-\frac{1}{\pi}\left(3n^4+7k^2-2n^2(1+k^2)\right)\Big[\Pi\left(sn(K+\pi\ell);-n^2;k\right)$$

$$-\Pi(1;-n^2;k)\Big] - \frac{n^2}{\pi}\Big[E\left(sn(K+\pi\ell);k\right) - E(1;k)\Big]\Bigg\} \tag{347}$$

We must now evaluate (318), which is simple to do.

We substitute

$$cn(\pi z+K) = t$$

with
$$dt = -\,sn(\pi z+K)\,dn(\pi z+K)\,\pi\,dz$$

and
$$sn^2(\pi z+K) = 1-t^2$$

so we get

$$-J_{\underline{IV}} = \frac{\left[(1+q)p\right]^{3/2}}{\pi q^2}\sqrt{1+2q}\int_0^{cn(K+\pi\ell)}\frac{(t^2-1)\,dt}{\left[\frac{1}{n^2}-1+t^2\right]^2}$$

$$= \frac{[(1+q)p]^{3/2}[1+2q]^{1/2}}{\pi q^2}\left\{\int_0^{cn(K+\pi\ell)} \frac{dt}{t^2+\frac{1}{n^2}-1}\right.$$

$$\left. -\frac{1}{n^2}\int_0^{cn(K+\pi\ell)} \frac{dt}{\left[\frac{1}{n^2}-1+t^2\right]^2}\right\}. \tag{348}$$

After some transformation, we get for (348)

$$J_{IV} = \frac{[(1+q)p]^{3/2}[1+2q]^{1/2}n^2}{\pi q^2(1-n^2)}\left\{\frac{n}{\sqrt{1-n^2}}\left[1-\frac{1}{2n^2}\right]\right.$$

$$\left. \arctan\left(\frac{n\,cn(K+\pi\ell)}{\sqrt{1-n^2}}\right) - \frac{1}{2}\,\frac{cn(K+\pi\ell)}{1-n^2+cn^2(K+\pi\ell)}\right\}$$

or with (324),

$$J_{IV} = -\frac{1}{2\pi}\,\frac{p}{q}\sqrt{\frac{p}{q}(1+2q)}\,\arctan\left(\sqrt{\frac{q}{1+q}}\,cn(K+\pi\ell)\right)$$

$$-\frac{1}{2\pi}\,\frac{p}{q}\sqrt{p(1+q)(1+2q)}\,\frac{cn(K+\pi\ell)}{1-n^2+cn^2(K+\pi\ell)} \tag{349}$$

After this rather extensive evaluation of the four integrals, we are now able to give the analytical expression of the deflection coordinate η of the deflected line of symmetry. According to (305), (307), (309), (311), (313),

$$\xi_1(z) = 2\left(1 - \frac{R}{P}\right) J_{II}(z) - \frac{\lambda}{P}\left[2\, J_{II}(z) - 4\, J_{IV}(z)\right]$$
$$= 2\left(1 - \frac{R+\lambda}{P}\right) J_{II}(z) + \frac{4\lambda}{P}\, J_{IV}(z) \qquad (350)$$

We can now express J_{II} and J_{IV} explicitly by (322) and (349) and get

$$\xi_1(z) = \frac{1}{\pi}\left\{2\left(1 + \frac{R+\lambda}{P}\right)\frac{\sqrt{pq(1+2q)}}{q} - \frac{2\lambda}{P}\,\frac{(1+2q)^{1/2}\, q^{1/2}}{q^2}\right\} \times \arctan\left(\sqrt{\frac{q}{1+q}}\, cn(K+\pi z)\right)$$
$$- \frac{2\lambda}{P\pi}\,\frac{p}{q}\sqrt{(1+q)(1+2q)p}\;\;\frac{cn(K+\pi z)}{1-n^2+cn^2(K+\pi z)}$$

or

$$\xi_1(z) = \frac{2}{\pi}\sqrt{\frac{p}{q}(1+2q)}\left[\frac{R+\lambda\left(1-\frac{p}{q}\right)}{P} - 1\right] \cdot$$
$$\arctan\left(\sqrt{\frac{q}{1+q}}\, cn\,(K+\pi z)\right)$$

$$-2\frac{\lambda}{P}\frac{1}{\kappa}\frac{p}{q}\sqrt{p(1+q)(1+2q)}\;\frac{cn(K+\kappa z)}{1-n^2+cn^2(K+\kappa z)} \tag{351}$$

(351) represents the deflection curve. The periodicity of this curve is the same as the periodicity, z_w (as found for $\varphi(z)$), in equation (302).

We shall introduce the original physical parameters

$$1-n^2=\frac{\bar{a}-\bar{b}\cos\varphi_{max}}{\bar{a}-2\bar{b}\cos\varphi_{max}} \tag{352}$$

$$\frac{p}{q}=\frac{\bar{a}}{2\bar{b}}-1=\frac{P-R}{\lambda}-1=\frac{P-R-\lambda}{\lambda} \tag{353}$$

$$\frac{R+\lambda\left(1-\frac{p}{q}\right)}{P}-1=2\left(\frac{R+\lambda}{P}-1\right) \tag{354}$$

$$1+q=\frac{\frac{\bar{a}}{2\bar{b}}-\frac{1}{2}(1+\cos\varphi_{max})}{\frac{\bar{a}}{2\bar{b}}-1}=\frac{P-R-\lambda(1+\cos\varphi_{max})}{2(P-R-\lambda)} \tag{355}$$

$$1+2q=\frac{P-R-\lambda(2-\cos\varphi_{max})}{P-R-\lambda} \tag{356}$$

$$\kappa=\sqrt{\lambda}\,\frac{1}{\sqrt{2PQ}}\sqrt{P-R-\lambda\cos\varphi_{max}} \tag{357}$$

We have to determine φ_{max} and λ. φ_{max} can be determined from (304) and (262):

$$\frac{d\xi_1}{d\xi_3}(0) = \frac{1}{\frac{d\xi_3}{dz}(z=0)} \quad \frac{d\xi_1}{dz}(z=0) = \tan\varphi_{max} \frac{1}{\frac{d\xi_3}{dz}(z=0)}$$

and because of the assumption $\epsilon \simeq \beta^{II}$,

$$\frac{\tan\varphi_{max}}{(1+\beta^{II})\cos\varphi_{max}} = \left[\left(1-\frac{R}{P}\right) - \frac{\lambda}{P}\cos\varphi_{max}\right]\sin\varphi_{max}$$

or

$$\frac{1}{1+\beta^{II}}\frac{P}{\lambda} = \cos^2\varphi_{max}\left(\frac{P-R}{\lambda} - \cos\varphi_{max}\right) \tag{358}$$

or

$$\cos^3\varphi_{max} - \cos^2\varphi_{max}\frac{P-R}{\lambda} + \frac{P}{\lambda}\frac{1}{1+\beta^{II}} = 0 \tag{359}$$

Then, λ is determined by means of (274), (306), (308), (308), (321), and (347).

It is

$$\lambda = \frac{(P-R)\left[1 - \frac{2}{\ell}J_I(\ell)\right] - (1+\beta)P}{1 - \frac{4}{\ell}J_I(\ell) - \frac{4}{\ell}J_{III}(\ell)} \tag{360}$$

In (360), the expressions (321) and (347) apply. (360) is a transcendental equation in λ, since $J_I(\ell)$ and $J_{III}(\ell)$ are functions of λ. In order to evaluate λ numerically, an iterative method should be applied. In order to do this, we have to approximate the functions $J_I(\ell)$ and $J_{III}(\ell)$, so that the first value of λ becomes reasonably accurate. But this means that (321) and (347) must be specially investigated.

First of all, we consider that ℓ is large, such that

$$\frac{\pi \ell}{K} = 4N - 1$$

or

$$\ell = (4N-1)\frac{K(k)}{\pi} = (N-\tfrac{1}{4})\,2\omega \tag{361}$$

where N is a large integer number (number of waves!).

Therefore,

$$E(sn(K+\pi\ell);k) = 4NE \tag{362}$$

where E is the complete elliptic integral of the second kind

$$E = \int_0^{\pi/2} \sqrt{1-k^2\sin^2\varphi}\, d\varphi \tag{363}$$

Similarly,

$$\Pi(sn(K+\pi\ell);-n^2,k) = 4N \int_0^{\pi/2} \frac{d\varphi}{(1-n^2\sin^2\varphi)\sqrt{1-k^2\sin^2\varphi}} \tag{364}$$

The complete integral of the third kind $\pi(-n^2, k)$ can be expressed by $K(x_1 k)$ and $E(x_1 k)$ as follows:

$$\Pi(-n^2, k) = K(k) + \frac{n}{\sqrt{(1-n^2)(k^2-n^2)}} \left[E\left(\frac{n}{k}; k\right) K(k) - F\left(\frac{n}{k}; k\right) E(k) \right] \tag{365}$$

for $/ n / < / k /$, which is the case in this problem. For $N \gg 1$, J_I is

$$J_I = \frac{p}{q}(1+q) \frac{(4N-1)}{\pi} \frac{n}{\sqrt{(1-n^2)(k^2-n^2)}} \left[E\left(\frac{n}{k}; k\right) K(k) - F\left(\frac{n}{k}; k\right) E(k) \right] \tag{366}$$

The integral (347) is

$$J_{III} = \frac{\left(p \frac{1+q}{q}\right)^2}{2(n^4 + k^2 - n^2(1+k^2))\pi} \left\{ (4N-1) K(k) (-n^4 + n^2 - 7k^2) - (3n^4 + 7k^2 - 2n^2(1+k^2)) \frac{(4N-1)n}{\sqrt{(1-n^2)(k^2-n^2)}} \left[E\left(\frac{n}{k}; k\right) K(k) - F\left(\frac{n}{k}; k\right) E(k) \right] - (4N-1) n^2 E(k) \right\} \tag{367}$$

Therefore, (360)

$$\lambda = \frac{U(\lambda, \varphi_{max})}{V(\lambda, \varphi_{max})} \tag{368}$$

with

$$U(\lambda,\varphi_{max}) = -(R+\beta P) - (P-R)\frac{p}{q}(1+q)\frac{2n}{\sqrt{(1-n^2)(k^2-n^2)}}\left[E\left(\frac{n}{k};k\right) - F\left(\frac{n}{k};k\right)\frac{E(k)}{K(k)}\right]$$

(369)

$$V(\lambda,\varphi_{max}) = 1 - \frac{2\left(p\frac{1+q}{q}\right)^2}{n^4+k^2-n^2(1+k^2)}\left\{+n^4+7k^2-n^2\left(1-\frac{E(k)}{K(k)}\right)\right\} + 2\left(p\frac{1+q}{q}\right)\left[\frac{3n^4+7k^2-2n^2(1+k^2)}{n^4+k^2-n^2(1+k^2)}\frac{p}{q}(1+q)-2\right]\frac{n}{\sqrt{(1-n^2)(k^2-n^2)}}\left[E\left(\frac{n}{k};k\right)-F\left(\frac{n}{k};k\right)\frac{E(k)}{K(t)}\right]$$

From (324) and (292) follows (370)

$$\frac{n}{\sqrt{(1-n^2)(k^2-n^2)}} = \frac{1+q}{1+2q}\sqrt{p} \tag{371}$$

$$\frac{k^2}{n^2} = 1+p+\frac{p}{q} \tag{372}$$

$$1+k^2 = \frac{1+3q+(1+q)p}{1+2q} \tag{373}$$

$$n^2 = \frac{q}{1+2q} = \frac{1}{2+\frac{1}{q}} \tag{374}$$

$$\frac{n^4+7k^2-n^2\left(1-\frac{E(k)}{K(k)}\right)}{n^4+k^2-n^2(1-k^2)} = \frac{-\left(1-\frac{E(k)}{K(k)}\right)+n^2+7\frac{k^2}{n^2}}{-(1+k^2)+n^2+\frac{k^2}{n^2}} \tag{375}$$

g is with (280) and (281)

$$q = \frac{\sin^2\frac{\varphi_{max}}{2}}{\frac{2(p-R)}{\lambda}-1} \tag{376}$$

It is $p-R>\lambda$; therefore, $q<1$

and

$$n^2 \approx q \tag{377}$$

$$k^2 \approx p \tag{378}$$

$$\frac{n^2}{k^2} \approx \frac{q}{p} \; ; \; \frac{k^2}{n^2} \approx \frac{p}{q} = \frac{2(p-R)}{\lambda}-1 \approx \frac{2(p-R)}{\lambda} \tag{379}$$

Therefore,

$$\frac{n^4+7k^2-n^2\left(1-\frac{E(k)}{K(k)}\right)}{n^4+k^2-n^2(1+k^2)} \approx 7 \tag{380}$$

$$\frac{3n^4+7k^2-2n^2(1+k^2)}{n^4+k^2-n^2(1+k^2)} = \frac{3n^2+7\frac{k^2}{n^2}-2(1+k^2)}{n^2+\frac{k^2}{n^2}-(1+k^2)} \approx 7 \tag{381}$$

$$V(\lambda,\varphi_{max}) = 1-4\frac{p}{q}\sqrt{p}\left[E\left(\sqrt{\frac{q}{p}};\sqrt{p}\right)-F\left(\sqrt{\frac{q}{p}},\sqrt{p}\right)\frac{E(\sqrt{p})}{K(\sqrt{p})}\right] \tag{382}$$

$$U(\lambda, \varphi_{max}) = -(R + \beta P) - (P - R)\frac{p}{q}\sqrt{p}\left[E\left(\sqrt{\frac{q}{p}}; \sqrt{p}\right) - F\left(\sqrt{\frac{q}{p}}, \sqrt{p}\right)\frac{E(\sqrt{p})}{K(\sqrt{p})}\right] \tag{383}$$

It is

$$F(\varphi, k) = \sum_{\nu=0}^{\infty} \binom{-\frac{1}{2}}{\nu} (-k^2)^{\nu} j_{2\nu}(\varphi) \tag{384}$$

$$E(\varphi, k) = \sum \binom{\frac{1}{2}}{\nu} (-k^2)^{\nu} j_{2\nu}(\varphi) \tag{385}$$

with the recursion formula

$$j_{2\nu}(\varphi) = \frac{2\nu - 1}{2\nu} j_{2\nu-2}(\varphi) - \frac{1}{2\nu} \sin^{2\nu-1}\varphi \cos\varphi \tag{386}$$

$$j_0(\varphi) = \varphi \tag{387}$$

$\nu = 1$

$$j_2(\varphi) = \frac{1}{2}\varphi - \frac{1}{2}\sin\varphi\cos\varphi$$

$\nu = 2$

$$j_4(\varphi) = \frac{3}{4} j_2(\varphi) - \frac{1}{4}\sin^3\varphi\cos\varphi$$

$$= \frac{3}{4}\cdot\frac{1}{2}\varphi - \frac{3}{4}\frac{1}{2}\sin\varphi\cos\varphi - \frac{1}{4}\sin^3\varphi\cos\varphi$$

$\nu = 3$

$$j_6(\varphi) = \frac{5}{6}\frac{3}{4}\frac{1}{2}\varphi - \frac{5}{6}\frac{3}{4}\frac{1}{2}\sin\varphi\cos\varphi - \frac{5}{6}\cdot\frac{1}{4}\sin^3\cos\varphi - \frac{1}{6}\sin^5\varphi\cos\varphi$$

For $k = \sqrt{p}$ small is $E(k) \approx K(k) \approx \frac{\pi}{2}$

and

$$E(\varphi ; p) - F(\varphi ; k) \frac{E(\sqrt{p})}{K(\sqrt{p})} =$$

$$\sum_{\nu=0}^{\infty} (-k^2)^{\nu} j_{2\nu}(\varphi) \left[\binom{\frac{1}{2}}{\nu} - \binom{-\frac{1}{2}}{\nu} \right]$$

$$\binom{\frac{1}{2}}{\nu} = \frac{(\frac{1}{2})!}{\nu!\,(\nu - \frac{1}{2})!} \quad ; \quad \binom{-\frac{1}{2}}{\nu} = \frac{(-\frac{1}{2})!}{\nu!\,(\nu + \frac{1}{2})!}$$

$$(\tfrac{1}{2})! = \tfrac{1}{2}(-\tfrac{1}{2})!$$

$$(\nu + \tfrac{1}{2})! = (\nu + \tfrac{1}{2})(\nu - \tfrac{1}{2})!$$

$$\binom{\frac{1}{2}}{\nu} - \binom{-\frac{1}{2}}{\nu} = \frac{1}{\nu!}(-\tfrac{1}{2})! \frac{1}{(\nu + \frac{1}{2})!} \left[(\nu + \tfrac{1}{2})\tfrac{1}{2} - 1 \right]$$

$$(-\tfrac{1}{2})! = \sqrt{\pi}$$

Therefore,

$$E(\varphi ; k) - F(\varphi ; k) \frac{E(k)}{K(k)}$$

$$\frac{2}{\pi}\left(\varphi - \frac{\sin 2\varphi}{2}\right)(E(k) - K(k))$$

$$= -\frac{2}{3}\left[\frac{2}{\pi}(E(k) - K(k)) + \frac{k^2}{2}\right] \sin^3\varphi \cos\varphi$$

and for small φ and small k

$$E(\varphi;k) - F(\varphi;k)\frac{E(k)}{K(k)} = -\frac{1}{3}k^2\varphi^3 \tag{388}$$

Therefore, with $\varphi = \frac{n}{K} \approx \frac{q}{p}$, $K = \sqrt{p}$

$$U(\lambda, \varphi_{max}) \approx -(R+\lambda P) + (P-R)\frac{p}{q}\sqrt{p}\left(-\frac{1}{3}q\sqrt{\frac{q}{p}}\right)$$
$$= -(R+\lambda P) - p\frac{\sqrt{q}(P-R)}{3} \tag{389}$$

$$V = 1 + \frac{4}{3}p\sqrt{q} \tag{390}$$

g can be approximated by

$$q \approx \frac{\lambda}{2(P-R)}\sin^2\frac{\varphi_{max}}{2}$$

therefore, (368) with (389) and (390)

$$\lambda = \frac{-(R+\beta P) - \frac{1}{3\sqrt{2}}(P-R)^{1/2}\lambda^{1/2}\sin^3\frac{\varphi_{max}}{2}}{1 + \frac{4}{3\sqrt{2}}\frac{\lambda^{1/2}}{(P-R)^{1/2}}\sin^3\frac{\varphi_{max}}{2}} \tag{391}$$

Setting $\lambda^{\frac{1}{2}} = x$, we get the following third-order equation:

$$x^3 + x^2\frac{3\sqrt{2}}{4}\frac{(P-R)^{1/2}}{\sin^3\frac{\varphi_{max}}{2}} + x\frac{P-R}{4}$$
$$+ \frac{3\sqrt{2}}{4}\frac{(R+\beta P)(P-R)^{1/2}}{\sin^3\frac{\varphi_{max}}{2}} = 0 \tag{392}$$

For small φ_{max}, the first and third terms can be ignored, and we get

$$\chi^2 = \lambda = -(\mathcal{R} + \beta \mathcal{P}) \tag{393}$$

as a reasonably good solution for the eigenvalue λ. The eigenvalue λ does not depend (or does not strongly depend) on φ_{max}.

E. BUCKLING OF FINITE MULTIFIBERS IN A MATRIX UNDER AXIAL LOAD, THREE-DIMENSIONAL

k FOR THE MULTIFIBER REINFORCED COMPOSITE WITH THE FINITE MATRIX TREATED AS A THREE-DIMENSIONAL CYLINDER

The displacement components of the matrix, in terms of Papkovich functions, in cylindrical coordinates, are as follows:

$$\xi_1^{II} = P_1\cos\phi + P_2\sin\phi - \frac{1}{4(1-\nu^{II})}\frac{\partial}{\partial r}\left[r(P_1\cos\phi + P_2\sin\phi) + P_0\right] \tag{394}$$

$$\xi_2^{II} = -P_1\sin\phi + P_2\cos\phi - \frac{1}{4(1-\nu^{II})}\frac{\partial}{r\partial\phi}\left[r(P_1\cos\phi + P_2\sin\phi) + P_0\right] \tag{395}$$

$$\xi_3^{II} = -\frac{1}{4(1-\nu^{II})}\frac{\partial}{\partial z}\left[r(P_1\cos\phi + P_2\sin\phi) + P_0\right] \tag{396}$$

where P_0, P_1, and P_2 are harmonic functions such that

$$\nabla^2 P_0 = \nabla^2 P_1 = \nabla^2 P_2 = 0 \tag{397}$$

∇^2 is a Laplacian operator in cylindrical coordinates; i.e.,

$$\nabla^2 = \frac{\partial^2}{\partial r^2} + \frac{1}{r}\frac{\partial}{\partial r} + \frac{1}{r^2}\frac{\partial^2}{\partial\phi^2} + \frac{\partial^2}{\partial z^2} \tag{398}$$

The six stress components in cylindrical coordinates are:

$$\sigma_{11}^{II} = 2G^{II}\left(\frac{\partial P_1}{\partial r}\cos\phi + \frac{\partial P_2}{\partial r}\sin\phi\right) + \frac{G^{II}}{2(1-\nu^{II})}\left(\nu^{II}\nabla^2 - \frac{\partial^2}{\partial r^2}\right)\left[r(P_1\cos\phi + P_2\sin\phi) + P_0\right] \quad (399)$$

$$\sigma_{22}^{II} = -\frac{G^{II}}{2(1-\nu^{II})}\left(\frac{1}{r}\frac{\partial}{\partial r} + \frac{1}{r^2}\frac{\partial^2}{\partial\phi^2}\right)\left[r(P_1\cos\phi + P_2\sin\phi) + P_0\right] \quad (400)$$

$$\sigma_{33}^{II} = \frac{G^{II}}{2(1-\nu^{II})}\left(\nu^{II}\nabla^2 - \frac{\partial^2}{\partial z^2}\right)\left[r(P_1\cos\phi + P_2\sin\phi) + P_0\right] \quad (401)$$

$$\sigma_{12}^{II} = G^{II}\left[\left(\cos\phi\frac{\partial}{r\partial\phi} - \sin\phi\frac{\partial}{\partial r}\right)P_1 + \left(\sin\phi\frac{\partial}{r\partial\phi} + \cos\phi\frac{\partial}{\partial r}\right)P_2\right] + \frac{G^{II}}{2(1-\nu^{II})}\left(\frac{1}{r^2}\frac{\partial}{\partial\phi} - \frac{1}{r}\frac{\partial^2}{\partial r\partial\phi}\right)\left[r(P_1\cos\phi + P_2\sin\phi) + P_0\right] \quad (402)$$

$$\sigma_{13}^{II} = G^{II}\left(\cos\phi\frac{\partial P_1}{\partial z} + \sin\phi\frac{\partial P_2}{\partial z}\right) - \frac{G^{II}}{2(1-\nu^{II})}\frac{\partial^2}{\partial r\partial z}\left[r(P_1\cos\phi + P_2\sin\phi) + P_0\right] \quad (403)$$

$$\sigma_{23}^{II} = G^{II}\left(\cos\phi\frac{\partial P_2}{\partial z} - \sin\phi\frac{\partial P_1}{\partial z}\right) - \frac{G^{II}}{2(1-\nu^{II})}\frac{\partial^2}{r\partial\phi\partial z}\left[r(P_1\cos\phi + P_2\sin\phi) + P_0\right] \quad (404)$$

The product solution form of a harmonic function in cylindrical coordinates is

$$\left[I_m(\alpha_n r) + K_m(\alpha_n r) \right] \cdot \left[\sin(m\phi) + \cos(m\phi) \right] \cdot \left[\sin(\alpha_n z) + \cos(\alpha_n z) \right] \tag{405}$$

In considering the boundary conditions of the present problem, we choose the solutions of Papkovich functions as follows:

$$P_0 = \left[A_1 I_1(\alpha_n r) + B_1 K_1(\alpha_n r) \right] \cos\phi \sin(\alpha_n z) \tag{406}$$

$$P_1 = \left[C_1 I_2(\alpha_n r) + D_1 K_2(\alpha_n r) \right] \cos(2\phi) \sin(\alpha_n z) + \left[E_2 I_0(\alpha_n r) + F_2 K_0(\alpha_n r) \right] \sin(\alpha_n z) \tag{407}$$

$$P_2 = \left[C_1 I_2(\alpha_n r) + D K_2(\alpha_n r) \right] \sin(2\phi) \sin(\alpha_n z) \tag{408}$$

Then

$$P_1 \cos\phi + P_2 \sin\phi = \left[C_1 I_2(\alpha_n r) + D_1 K_2(\alpha_n r) + E_1 I_0(\alpha_n r) + F_1 K_0(\alpha_n r) \right] \cos\phi \sin(\alpha_n z) \tag{409}$$

$$-P_1 \sin\phi + P_2 \cos\phi = \left[C_1 I_2(\alpha_n r) + D_1 K_2(\alpha_n r) - E_1 I_0(\alpha_n r) - F_1 K_0(\alpha_n r) \right] \sin\phi \sin(\alpha_n z) \tag{410}$$

Substitution of the foregoing equations (406) through (410) into equations (394) through (396) yields the following solutions for displacements:

$$\xi_1^{II} = \frac{1}{4(1-\nu^{II})}\Big\{(3-4\nu^{II})\Big[C_1 I_2(\alpha_n r) + D_1 K_2(\alpha_n r) + E_1 I_0(\alpha_n r) + F_1 K_0(\alpha_n r)\Big] - \Big[A_1 I_1'(\alpha_n r) + B_1 K_1'(\alpha_n r)\Big] - r\Big[C_1 I_2'(\alpha_n r) + D_1 K_2'(\alpha_n r) + E_1 I_0'(\alpha_n r) + F_1 K_0'(\alpha_n r)\Big]\Big\} \cos\phi \sin(\alpha_n z) \quad (411)$$

$$\xi_2^{II} = \frac{1}{4(1-\nu^{II})}\Big\{\frac{1}{r}\Big[A_1 I_1(\alpha_n r) + B_1 K_1(\alpha_n r)\Big] + (5-4\nu^{II})\Big[C_1 I_2(\alpha_n r) + D_1 K_2(\alpha_n r)\Big] - (3-4\nu^{II})\Big[E_1 I_0(\alpha_n r) + F_1 K_0(\alpha_n r)\Big]\Big\} \cdot \sin\phi \sin(\alpha_n z) \quad (412)$$

$$\xi_3^{II} = -\frac{\alpha_n}{4(1-\nu^{II})}\Big\{A_1 I_1(\alpha_n r) + B_1 K_1(\alpha_n r) + r\Big[C_1 I_2(\alpha_n r) + D_1 K_2(\alpha_n r) + E_1 I_0(\alpha_n r) + F_1 K_0(\alpha_n r)\Big]\Big\} \cdot \cos\phi \cos(\alpha_n z) \quad (413)$$

The displacement components in Cartesian coordinates are

$$\begin{aligned}
\xi_x^{II} &= \xi_1^{II}\cos\phi - \xi_2^{II}\sin\phi \\
&= -\frac{1}{8(1-\nu^{II})}\Big\{\frac{1}{r}\Big[A_1 I_1(\alpha_n r)+B_1 K_1(\alpha_n r)\Big] \\
&\qquad +2\Big[C_1 I_2(\alpha_n r)+D_1 K_2(\alpha_n r)\Big] \\
&\qquad -2(3-4\nu^{II})\Big[E_1 I_0(\alpha_n r)+F_1 K_0(\alpha_n r)\Big] \\
&\qquad +\Big[A_1 I_1'(\alpha_n r)+B_1 K_1'(\alpha_n r)\Big] \\
&\qquad +r\Big[C_1 I_2'(\alpha_n r)+D_1 K_2'(\alpha_n r)+E_1 I_0'(\alpha_n r) \\
&\qquad\quad +F_1 K_0'(\alpha_n r)\Big]\Big\}\sin(\alpha_n z) \\
&\quad +\frac{1}{8(1-\nu^{II})}\Big\{\frac{1}{r}\Big[A_1 I_1(\alpha_n r)+B_1 K_1(\alpha_n r)\Big] \\
&\qquad +8(1-\nu^{II})\Big[C_1 I_2(\alpha_n r)+D_1 K_2(\alpha_n r)\Big] \\
&\qquad -\Big[A_1 I_1'(\alpha_n r)+B_1 K_1'(\alpha_n r)\Big] \\
&\qquad -r\Big[C_1 I_2'(\alpha_n r)+D_1 K_2'(\alpha_n r)+E_1 I_0'(\alpha_n r) \\
&\qquad\quad +F_1 K_0'(\alpha_n r)\Big]\Big\}\cos(2\phi)\sin(\alpha_n z)
\end{aligned} \tag{414}$$

where $$I_0'(\alpha_n r) = \frac{d\,I_0(\alpha_n r)}{dr}, \text{ etc.} \tag{415}$$

$$\xi_y^{II} = \xi_1^{II}\sin\phi + \xi_2^{II}\cos\phi$$

$$= \frac{1}{8(1-\nu^{II})}\Big\{\frac{1}{r}\big[A_1 I_1(\alpha_n r) + B_1 K_1(\alpha_n r)$$

$$+ 8(1-\nu^{II})\big[C_1 I_2(\alpha_n r) + D_1 K_2(\alpha_n r)\big]$$

$$- \big[A_1 I_1'(\alpha_n r) + B_1 K_1'(\alpha_n r)\big]$$

$$- r\big[C_1 I_2'(\alpha_n r) + D_1 K_2'(\alpha_n r) + E_1 I_0'(\alpha_n r)$$

$$+ F_1 K_0'(\alpha_n r)\big]\Big\}\sin(2\phi)\sin(\alpha_n z) \tag{416}$$

$$\xi_z^{II} = \xi_3^{II} \tag{417}$$

The radial stress σ_{11}^{II} and shear stress σ_{12}^{II} are found from equations (399), (402), (406), to 407, ~

$$\sigma_{11}^{II} = \Big\{2G^{II}\big[C_1 I_2'(\alpha_n r) + D_1 K_2'(\alpha_n r) + E_1 I_0'(\alpha_n r)$$

$$+ F_1 K_0'(\alpha_n r)\big]$$

$$+ \frac{G^{II}}{2(1-\nu^{II})}\Big[-\alpha_n^2\big(A_1 I_1(\alpha_n r) + B_1 K_1(\alpha_n r) + r\,II\big)$$

$$- \frac{1}{r^2}\big(A_1 I_1(\alpha_n r) + B_1 K_1(\alpha_n r)\big)$$

$$+ r\big(C_1 I_2(\alpha_n r) + D_1 K_2(\alpha_n r)$$

$$+ E_1 I_0(\alpha_n r) + F_0 K_0(\alpha_n r)\big)$$

$$+\frac{1}{r}\left(A_1 I_1'(\alpha_n r)+B_1 K_1'(\alpha_n r)+\Pi+r\Pi'\right)\Big]$$

$$-\frac{G^{II}}{2}\left(A_1 I_1''(\alpha_n r)+B_1 K_1''(\alpha_n r)+2\Pi'+r\Pi''\right)\Big\}\cdot$$

$$\cdot\cos\phi\sin(\alpha_n z) \qquad (418)$$

or

$$\sigma_{11}^{II}=\frac{G^{II}}{2(1-\nu^{II})}\Big\{A_1\Big[-(\alpha_n^2+\frac{1}{r^2})I_1(\alpha_n r)+\frac{1}{r}I_1'(\alpha_n r)+(\nu^{II}-1)I_1''(\alpha_n r)\Big]$$

$$+B_1\Big[-(\alpha_n^2+\frac{1}{r^2})K_1(\alpha_n r)+\frac{1}{r}K_1'(\alpha_n r)+(\nu^{II}-1)K_1''(\alpha_n r)\Big]$$

$$+\alpha_n^2 r\Pi+(2\nu^{II}-1)\Pi'+(\nu^{II}-1)r\Pi''\Big\}\cdot$$

$$\cdot\cos\phi\sin(\alpha_n z) \qquad (419)$$

where

$$\Pi=C_1 I_2(\alpha_n r)+D_1 K_2(\alpha_n r)+E_1 I_0(\alpha_n r)+F_1 K_0(\alpha_n r)$$

$$\Pi'=C_1 I_2'(\alpha_n r)+D_1 K_2'(\alpha_n r)+E_1 I_0'(\alpha_n r)+F_1 K_0'(\alpha_n r)$$

and

$$\Pi''=C_1 I_2''(\alpha_n r)+D_1 K_2''(\alpha_n r)+E_1 I_0''(\alpha_n r)+F_1 K_0''(\alpha_n r) \qquad (420)$$

$$\sigma_{12}^{II} = -\frac{G^{II}}{2(1-\nu^{II})}\Big\{ \frac{A_1}{r}\Big[\frac{1}{r}I_1(\alpha_n r) - I_1'(\alpha_n r)\Big]$$
$$+ \frac{B_1}{r}\Big[\frac{1}{r}K_1(\alpha_n r) - K_1'(\alpha_n r)\Big]$$
$$+ C_1\Big[\frac{4(1-\nu^{II})}{r}I_2(\alpha_n r) - (3-2\nu^{II})I_2'(\alpha_n r)\Big]$$
$$+ D_1\Big[\frac{4(1-\nu^{II})}{r}K_2(\alpha_n r) - (3-2\nu^{II})K_2'(\alpha_n r)\Big]$$
$$+ E_1(1-2\nu^{II})I_0'(\alpha_n r) + F_1(1-2\nu^{II})K_0'(\alpha_n r)\Big\}\cdot$$
$$\cdot \sin\phi \sin(\alpha_n z) \qquad (421)$$

$$\sigma_{13}^{II} = -\frac{G^{II}\alpha_n}{2(1-\nu^{II})}\Big\{A_1 I_1'(\alpha_n r) + B_1 K_1'(\alpha_n r)$$
$$- C_1\Big[(1-2\nu^{II})I_2(\alpha_n r) - r I_2'(\alpha_n r)\Big]$$
$$- D_1\Big[(1-2\nu^{II})K_2(\alpha_n r) - r K_2'(\alpha_n r)\Big]$$
$$- E_1\Big[(1-2\nu^{II})I_0(\alpha_n r) - r I_0'(\alpha_n r)\Big]$$
$$- F_1\Big[(1-2\nu^{II})K_0(\alpha_n r) - r K_0'(\alpha_n r)\Big]\Big\}\cdot$$
$$\cdot \cos\phi \cos(\alpha_n z) \qquad (422)$$

Equations (414) through (422) contain six constants (A_1, B_1, C_1, D_1, E_1, and F_1) which must be determined by boundary conditions. These conditions include the continuity of displacements and stresses at the interface and will yield six simultaneous equations with six unknowns which are hardly amenable. For simplicity, it is then assumed that the radius of the fiber is much smaller than that of the composite; the three coefficients for modified Bessel functions of the second kind will be automatically dropped because of the finiteness of stress and displacements at the neighborhood of the origin.

The boundary conditions at interface r = a to be used are

$$\xi_x^{II} = \xi_x^{I} = \xi_{1n}^{I} \sin(\alpha_n z)$$
$$\xi_y^{II} = \xi_y^{I} = 0$$
$$\xi_z^{II} = \xi_z^{I} = 0 \qquad (423)$$

Substitution of equation (423) into equations (414), (416), and (417) yields

$$-\frac{1}{8(1-\nu^{II})}\left\{\left[\frac{1}{a} I_1(\alpha_n a) + I_1'(\alpha_n a)\right] A_1 + \left[2 I_2(\alpha_n a) + a I_2'(\alpha_n a)\right] C_1 + \left[-2(3-4\nu^{II}) I_0(\alpha_n a) + a I_0'(\alpha_n a)\right] E_1\right\} = \xi_{1n}^{I} \qquad (424)$$

$$\left[\frac{1}{a} I_1(\alpha_n a) - I_1'(\alpha_n a)\right] A_1 + \left[\delta(1-\nu^{II}) I_2(\alpha_n a) - a I_2'(\alpha_n a)\right] C_1$$
$$- \left[a I_0'(\alpha_n a)\right] E_1 = 0 \qquad (425)$$

and

$$A_1 I_1(\alpha_n a) + C_1 a I_2(\alpha_n a) + E_1 a I_0(\alpha_n a) = 0 \qquad (426)$$

Solving these equations, we can obtain the solutions of A_1, C_1, and E_1 in terms of ξ_{in}^{I}.

The denominator of coefficients A_1, C_1, and E_1 is designated as Δ, and is written out as below.

$$\Delta = -2\left\{(1-4\nu^{II}) I_0^2(\alpha_n a) I_1(\alpha_n a)\right.$$
$$-\left[\frac{2(3-4\nu^{II})}{\alpha_n a} + \alpha_n a\right] I_0(\alpha_n a) I_1^2(\alpha_n a)$$
$$\left. + (\alpha_n a) I_0^3(\alpha_n a) + I_1^3(\alpha_n a)\right\} \qquad (427)$$

The results of the coefficients are

$$A_1 = \frac{\xi_{in}^{I} a}{\Delta}\left\{2(5-4\nu^{II}) I_0^2(\alpha_n a) - 4(5-4\nu^{II}) \frac{I_0(\alpha_n a) I_1(\alpha_n a)}{\alpha_n a}\right.$$
$$\left. - 2 I_1^2(\alpha_n a)\right\} \qquad (428)$$

$$C_1 = \frac{\xi_{1n}^{I}}{\Delta}\left\{(\alpha_n a)I_0^2(\alpha_n a) - 2I_0(\alpha_n a)I_1(\alpha_n a) - (\alpha_n a)I_1^2(\alpha_n a)\right\}$$

and (429)

$$E_1 = \frac{\xi_{1n}^{I}}{\Delta}\left\{-(\alpha_n a)I_0^2(\alpha_n a) - 2(3-4\nu^{II})I_0(\alpha_n a)I_1(\alpha_n a) + \left[\frac{16(1-\nu^{II})}{\alpha_n a} + \alpha_n a\right]I_1^2(\alpha_n a)\right\} \quad (430)$$

The force per unit length applied by the matrix to the fiber due to the normal pressure and circumferential shear at the interface is

$$p_1 = \int_0^{2\pi}(\sigma_{11}^{II}\cos\phi - \sigma_{12}^{II}\sin\phi)\,r\,d\phi\Big|_{r=a} \quad (431)$$

By substitution of equations (419) and (421) into (431), and the identities of definite integrals

$$\int \sin^2\phi\,d\phi = \frac{\phi}{2} - \frac{\sin(2\phi)}{4} \quad (432)$$

and

$$\int \cos^2\phi\,d\phi = \frac{\phi}{2} + \frac{\sin(2\phi)}{4},$$ we then have

$$p_1 = \frac{\pi a G^{II}}{2(1-\nu^{II})}\left\{A_1\left[-\alpha_n^2 I_1(\alpha_n a) + (\nu^{II}-1)I_1''(\alpha_n a)\right] + C_1\left[\frac{1}{a}\left((\alpha_n a)^2 + 4(1-\nu^{II})\right)I_2^{-}(\alpha_n a) + 4(\nu^{II}-1)I_2'(\alpha_n a) + (\nu^{II}-1)aI_2''(\alpha_n a)\right]\right.$$

$$+E_1\left[\frac{1}{a}(\alpha_n a)^2 I_0(\alpha_n a)+(\nu^{II}-1)\,a\,I_0''(\alpha_n a)\right]\Big\}\cdot$$

$$\cdot \sin(\alpha_n z) \qquad (433)$$

Since it was assumed that the fiber buckles on x-z plane, then

$$k = \frac{p_1}{\xi_x^{I}} = \frac{p_1}{\xi_x^{II}} \qquad (434)$$

Combination of equations (433), (434), (414) and (425) through (427) gives the unit interfacial force per unit lateral deflection, k, due to surface normal force and circumferential shear, and is resulted as below:

$$k = \frac{\pi G^{II}}{2(1-\nu^{II})\Delta}\Big\{8(1-\nu^{I})(2-\nu^{II})(\alpha_n a)\,I_0^3(\alpha_n a)$$

$$+\left[16(2-\nu^{II})(1-\nu^{II})-3\nu^{II}(\alpha_n a)^2\right]I_1^3(\alpha_n a)$$

$$-4\left[8(2-\nu^{II})(1-\nu^{II})+(6-5\nu^{II})(\alpha_n a)^2\right]\cdot$$

$$\cdot I_0^2(\alpha_n a)\,I_1(\alpha_n a)$$

$$+4\Big[2(4-2\nu^{II}-\nu^{II2})(\alpha_n a)$$

$$+8(2-\nu^{II})(1-\nu^{II})(\alpha_n a)^{-1}+(\alpha_n a)^3\Big]\cdot$$

$$\cdot I_0(\alpha_n a)\,I_1^2(\alpha_n a)\Big\} \qquad (435)$$

BUCKLING LOAD OF THE FIBER

Combination of equations (72) and (435) yields

$$
\begin{aligned}
P_{cr}^{I} = {} & \alpha_n^2 E^{I} I^{I} \\
& - \frac{\pi E^{II}}{4\alpha_n^2 (1-\nu^{II2})\Delta} \Big\{ 8(1-\nu^{II})(2-\nu^{II})(\alpha_n a) I_0^3(\alpha_n a) \\
& + \Big[16(2-\nu^{II})(1-\nu^{II}) - 3\nu^{II}(\alpha_n a)^2 \Big] \cdot \\
& \cdot I_1^3(\alpha_n a) \\
& - \Big[4(6-5\nu^{II})(\alpha_n a)^2 + 32(1-\nu^{II})(2-\nu^{II}) \Big] \cdot \\
& \cdot I_0^2(\alpha_n a) I_1(\alpha_n a) \\
& + 4 \Big\{ 2(4-2\nu^{II}-\nu^{II2})(\alpha_n a) \\
& + 8(2-\nu^{II})(1-\nu^{II})(\alpha_n a)^{-1} \\
& + (\alpha_n a)^3 \Big] I_0(\alpha_n a) I_1^2(\alpha_n a) \Big\} \\
& + \frac{\pi(b^2-a^2) E^{II}}{2(1+\nu^{II})} \left(1+\frac{a}{d}\right)^2
\end{aligned}
\tag{436}
$$

where Δ is defined in equation (427).

SMALLEST BUCKLING LOAD AND BUCKLING WAVELENGTH OF THE FIBER

Minimization of P_{cr} with respect to α_n, i.e., $\frac{\partial P_{cr}}{\partial \alpha_n} = 0$ (437), gives

$$
\begin{aligned}
&8\alpha_n E^{I} I^{I}\Big\{ \alpha_n^3 a\, I_0^3(\alpha_n a) + \alpha_n^2 I_1(\alpha_n a) + (1-4\nu^{II})\alpha_n^2 \cdot \\
&\qquad \cdot I_0^2(\alpha_n a)\, I_1(\alpha_n a) \\
&\qquad -\left[2(3-4\nu^{II})\alpha_n a^{-1} + \alpha_n^3 a\right] I_0(\alpha_n a) I_1^2(\alpha_n a)\Big\}^2 \\
&+ \frac{\pi E^{II}}{2(1-\nu^{II2})}\Big\{ (1-4\nu^{II})\alpha_n^2 I_0(\alpha_n a) I_1(\alpha_n a) \\
&\qquad -\left[2(3-4\nu^{II})\alpha_n a^{-1} + \alpha_n^3 a\right] I_0(\alpha_n a) I_1^2(\alpha_n a) \\
&\qquad + (\alpha_n^3 a) I_0^3(\alpha_n a) + \alpha_n^2 I_1^3(\alpha_n a)\Big\} \cdot \\
&\qquad \cdot\Big\{ 8(1-\nu^{II})(2-\nu^{II})\left[a I_0^3(\alpha_n a) + 3\alpha_n a^2 I_0^2(\alpha_n a) \cdot \right. \\
&\qquad\qquad \left. \cdot I_1(\alpha_n a)\right] \\
&\qquad -6\nu^{II}(\alpha_n a^2) I_1^3(\alpha_n a) \\
&\qquad -3a\left[3\nu^{II}(\alpha_n a)^2 - 16(2-\nu^{II})(1-\nu^{II})\right] I_1^2(\alpha_n a) \cdot \\
&\qquad\qquad \cdot\left[I_0(\alpha_n a) - (\alpha_n a)^{-1} I_1(\alpha_n a)\right] \\
&\qquad -8\left[(6-5\nu^{II})\alpha_n a^2\right] I_0^2(\alpha_n a) I_1(\alpha_n a)
\end{aligned}
$$

$$
\begin{aligned}
&-4\left[(6-5\nu^{II})(\alpha_n a)^2+8(1-\nu^{II})(2-\nu^{II})\right]\cdot \\
&\quad\cdot\left[2a I_0(\alpha_n a)\, I_1^2(\alpha_n a)-\alpha_n^{-1} I_0^2(\alpha_n a) I_1(\alpha_n a)\right. \\
&\qquad \left.+a I_0^3(\alpha_n a)\right] \\
&+4\left[2(4-2\nu^{II}-\nu^{II2})a+3\alpha_n^2 a^3\right. \\
&\qquad \left.-8(2-\nu^{II})(1-\nu^{II})\alpha_n^{-2}a^{-1}\right] I_0(\alpha_n a) I_1^2(\alpha_n a) \\
&+4\left[2(4-2\nu^{II}-\nu^{II2})(\alpha_n a)+(\alpha_n a)^3\right. \\
&\qquad \left.+8(2-\nu^{II})(1-\nu^{II})(\alpha_n a)^{-1}\right]\cdot \\
&\quad\cdot\left[a I_1^3(\alpha_n a)+2a I_0^2(\alpha_n a) I_1(\alpha_n a)\right. \\
&\qquad \left.-2\alpha_n^{-1} I_0(\alpha_n a) I_1^2(\alpha_n a)\right]\Big\} \\
&-\frac{\pi E^{II}}{2(1-\nu^{II2})}\Big\{8(1-\nu^{II})(2-\nu^{II})(\alpha_n a) I_0^3(\alpha_n a) \\
&\quad -\left[3\nu^{II}(\alpha_n a)^2-16(2-\nu^{II})(1-\nu^{II})\right] I_1^3(\alpha_n a) \\
&\quad -4\left[(6-5\nu^{II})(\alpha_n a)^2+8(2-\nu^{II})(1-\nu^{II})\right]\cdot \\
&\qquad \cdot I_0^2(\alpha_n a) I_1(\alpha_n a) \\
&\quad +4\left[2(4-2\nu^{II}-\nu^{II2})(\alpha_n a)+(\alpha_n a)^3\right.
\end{aligned}
$$

$$+8(2-\nu^{II})(1-\nu^{II})(\alpha_n a)^{-1}\Big]\cdot$$
$$\cdot I_0(\alpha_n a) I_1^2(\alpha_n a)\Big\}\cdot$$
$$\cdot\Big\{(1-4\nu^{II})\Big[\alpha_n I_0^2(\alpha_n a) I_1(\alpha_n a)+2\alpha_n^2 a I_0(\alpha_n a) I_1^2(\alpha_n a)$$
$$+\alpha_n^2 a I_0^3(\alpha_n a)\Big]$$
$$-\Big[2(3-4\nu^{II})a^{-1}+3\alpha_n^2 a\Big] I_0(\alpha_n a) I_1^2(\alpha_n a)$$
$$-\Big[2(3-4\nu^{II})\alpha_n+\alpha_n^3 a^2\Big]\cdot\Big[I_1^3(\alpha_n a)$$
$$+2 I_0^2(\alpha_n a) I_1(\alpha_n a)-2(\alpha_n a)^{-1}\cdot$$
$$\cdot I_0(\alpha_n a) I_1^2(\alpha_n a)\Big]$$
$$+3\alpha_n^2 a I_0^3(\alpha_n a)+3\alpha_n^3 a^2 I_0^2(\alpha_n a) I_1(\alpha_n a)$$
$$-\alpha_n I_1^3(\alpha_n a)+3\alpha_n^2 a I_1^2(\alpha_n a) I_0(\alpha_n a)\Big\} \qquad (438)$$

$$= 0$$

This equation determines the critical buckling wavelength of the fiber, $\ell_{cr} = 2\pi/\alpha_j$. After substituting the obtained value of α_j into equation (436), we then get the smallest critical buckling load of the fiber, $(P^I_{cr})_{min}$.

APPENDIX V

EXPERIMENTAL INVESTIGATION OF SHORT BORON FIBER COMPOSITES

1. MODULUS TESTS

The specimens consisted of a laminate comprised of 8-ply S-glass Scotchply tape (50% by weight), seven interspersed layers of approximately 2-inch-long boron fibers (23%) by weight), and epoxy Epon 828/1031 resin (27% by weight).

The specimens were tested in compression and resulted in values summarized in Table IIL For comparison, reported values of pure S-glass tape and pure unidirectional boron composite are listed in the same table.

TABLE III

COMPARISON OF SHORT BORON FIBER COMPOSITES*

IN AXIAL COMPRESSION

Load Application	Short-Fiber Composite	S-Glass**	Boron***
Max strength, psi	133,000	120,000	220,000
Max modulus, 10^6 psi	13.7	8.9	38.0

* Unidirectional
** Minnesota Mining & Manufacturing information
*** From Air Force sponsored boron work at Narmco

In comparing the short-fiber specimen with pure glass and pure boron composites, it can be said that the values follow a generally logical pattern,which is obvious in the graphical presentation, Figure 65.

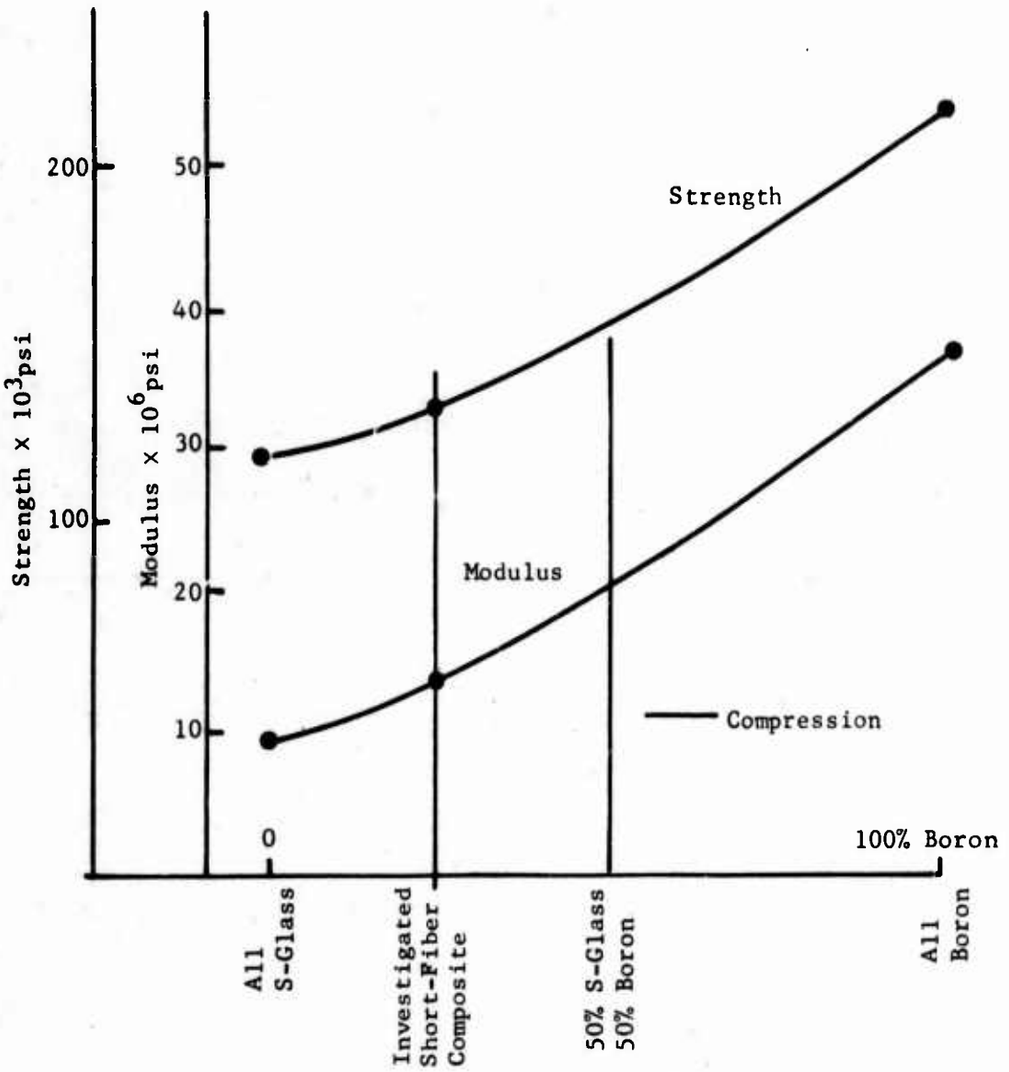

Figure 65. Effect of Boron Additions on Properties (Test Data)

Based on this diagram, it appears that approximately 50% short boron fibers and 50% glass fibers will provide the desired 20 x 10^6 psi modulus combined with a high compressive and flexural strength. In comparing these projected values with high-strength aluminum, there appears to be noticeable improvement of material properties as summarized in Table IV.

TABLE IV

MATERIAL EFFICIENCIES

Material	Density lb/in.^{3}	Compressive Yield Strength, 10^3 psi	Compressive Modulus, 10^6 psi	Specific Strength, 10^6 psi	Specific Modulus, 10^6 psi
Al 7075-T6	0.101	65	10.5	0.64	104
Short Boron* Composite	0.074	160	20.0	2.16	270
Improvement	27%	146%	90%	238%	160%
* Estimated, based on Figure 65.					

The relative improvement expressed in percent is exceptional and would justify additional research, even if it resulted in somewhat lower structural improvement than indicated by the preliminary test results.

2. FATIGUE TESTS

The fatigue test data of a short boron fiber composite were compared with fatigue data of 7075-T6 aluminum (MIL-HDBK 5) and a composite which was fabricated with a Scotchply 1002 resin and unidirectional S-glass (FPL Tech. Rep. AFML 7R-64-403 October 1964).

The properties utilized for these materials are presented in the following table.

TABLE V

MATERIAL PROPERTIES

Material	Density #/cu.in.	Ultimate Tensile Strength, psi	Modulus 10^6 psi
Aluminum 7075-T6	0.101	80,000	10.3
S-glass & Scotchply	0.069	160,000	6.1
S-glass & short boron	0.079	180,000	17.2

Two panels were fabricated with unidirectional short boron fibers and unidirectional S-glass (single-end roving). The physical and mechanical properties are given in the following table.

TABLE VI

PROPERTIES OF TESTED PANELS

Panel No.	Specific Gravity	Boron Content Vol.%	Ultimate Tensile Strength, psi	Tensile Modulus, psi
935	2.11	11.4	180,000	-
936	2.26	17.1	180,000	17.2×10^6

The fatigue data for each of the above panels is shown in the following table.

TABLE VII

FATIGUE TEST DATA

Panel No.	Mean Stress % of Ultimate	Alternating Stress % of Ultimate	Cycles to Failure
935	30	±23	5.2×10^3
935	30	±15	1.53×10^5
935	30	±10	$8.65 \times 10^{6*}$
936	50	±10	1.03×10^5
936	50	±8	2.63×10^5
936	50	±5	$6.1 \times 10^{6*}$

The fatigue data are also presented in Figures 66 through 69. Figure 66 is a modified Goodman diagram for the fatigue life of the short boron fiber panels, No. 935 and No. 936. The curves are estimates based on the data of Table IV and previous experience with other boron glass composites. Figure 67 presents S-N curves for the aluminum 7075-T6, S-glass and Scotchply, and the short boron and S-glass. The curves are plotted as a function of the alternating stress (% of ultimate) and cycles to failure for various mean stresses. Figure 68 is a comparison of the aluminum, S-glass and Scotchply, and short boron and S-glass at 0 mean stress plotted as a function of actual alternating stress and number of cycles to failure. Figure 69 is a comparison of the aluminum, S-glass and Scotchply, and short boron and S-glass at 0 mean stress plotted as a function of number of cycles to failure and the specific alternating stress. The specific alternating stress is obtained by the ratio of the alternating stress to the density of the material.

* Specimen did not fail.

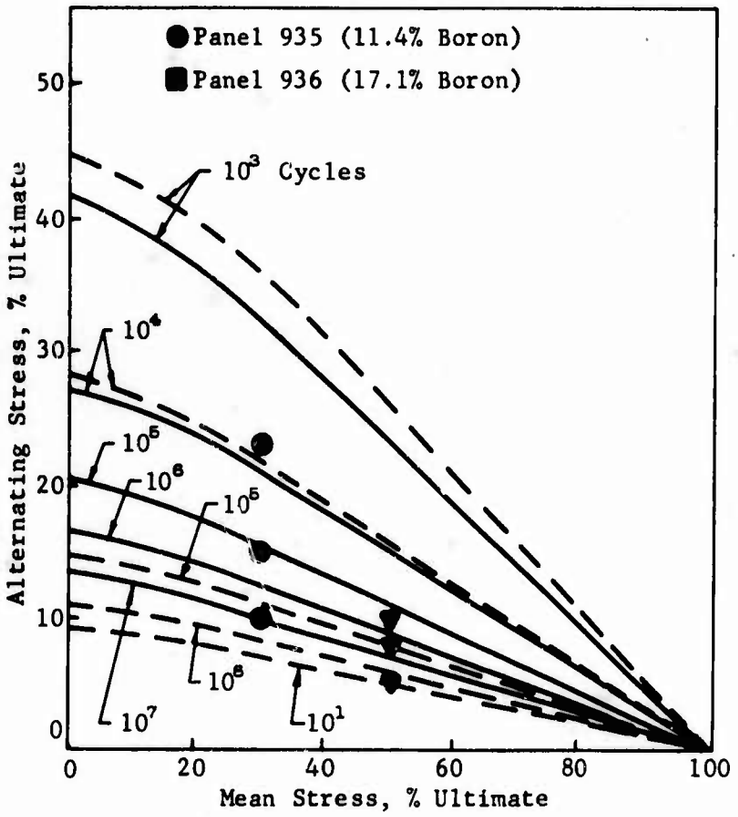

Figure 66. Modified Goodman Diagram for the Fatigue Life of Unidirectional Short Boron Fibers and Unidirectional S-Glass Composite

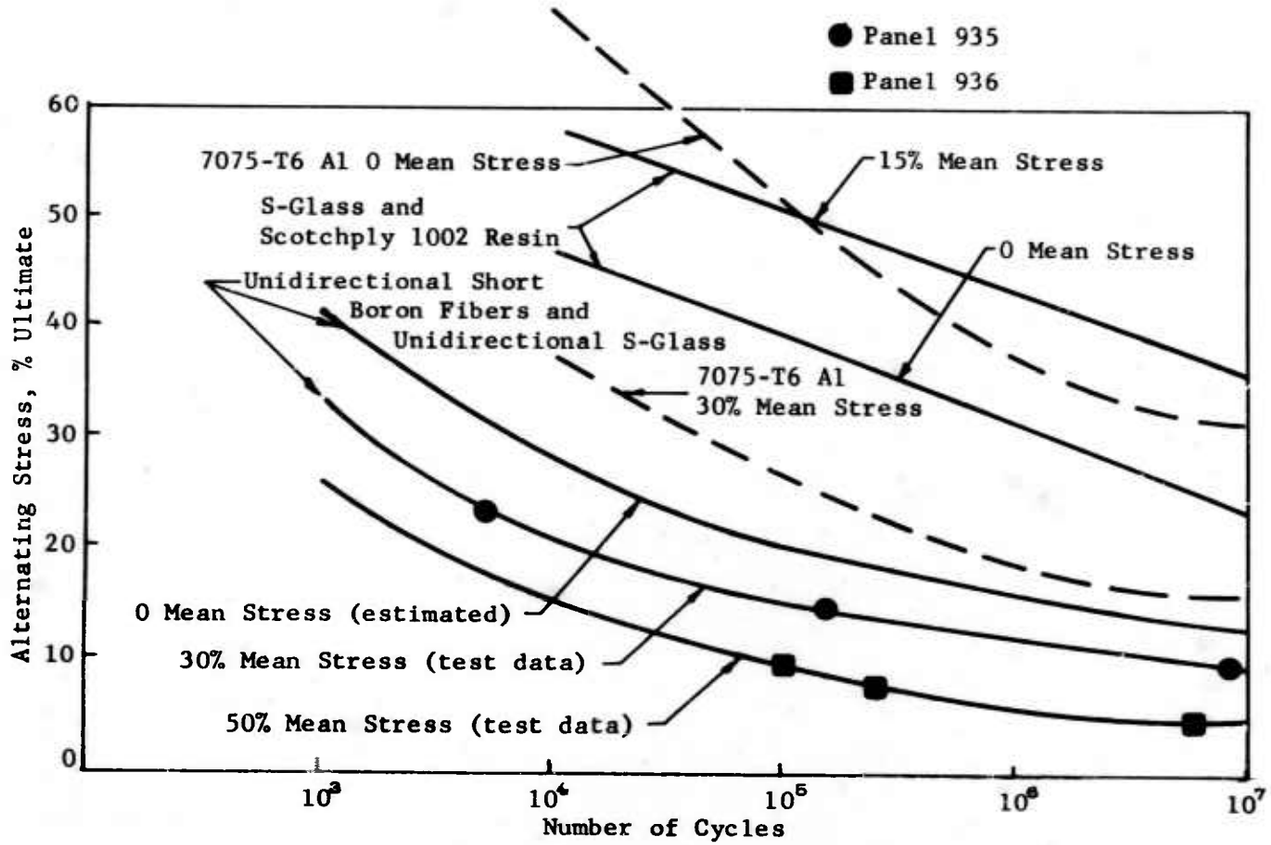

Figure 67. S-N Curves for Various Composites and Aluminum

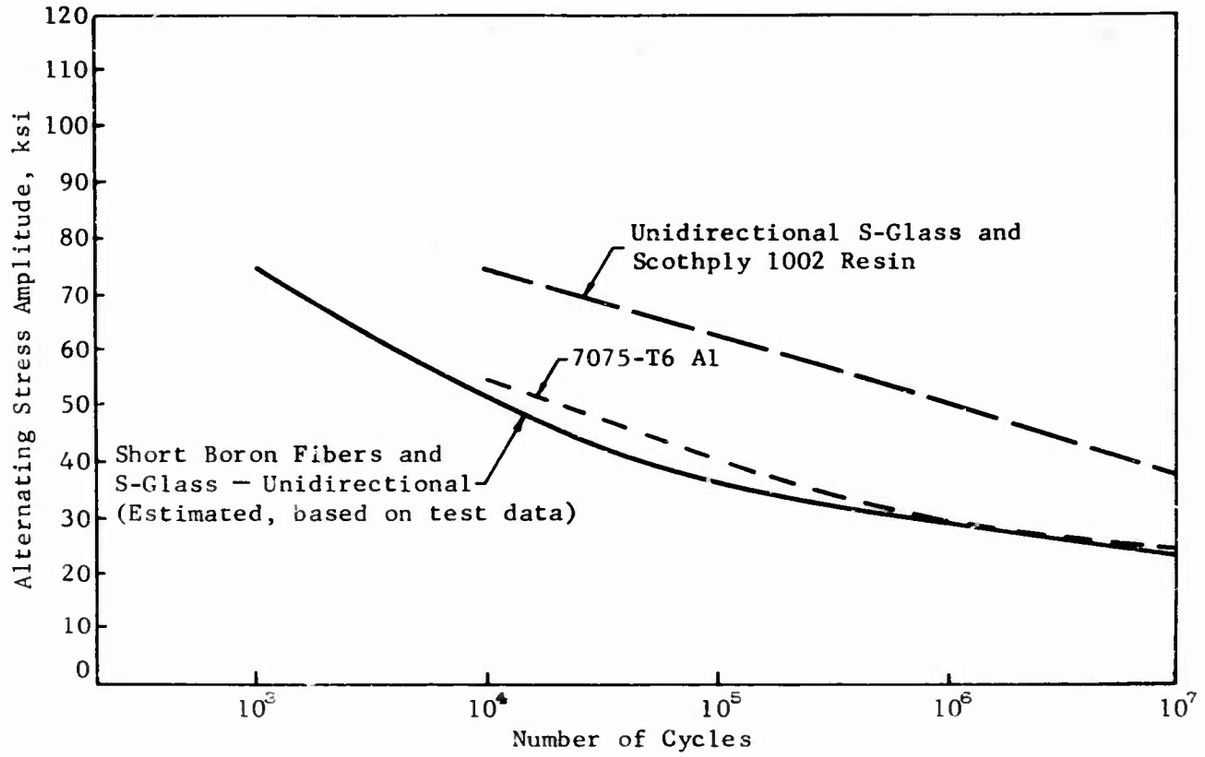

Figure 68. S-N Curves for Various Composites and Aluminum for 0 Mean Stress

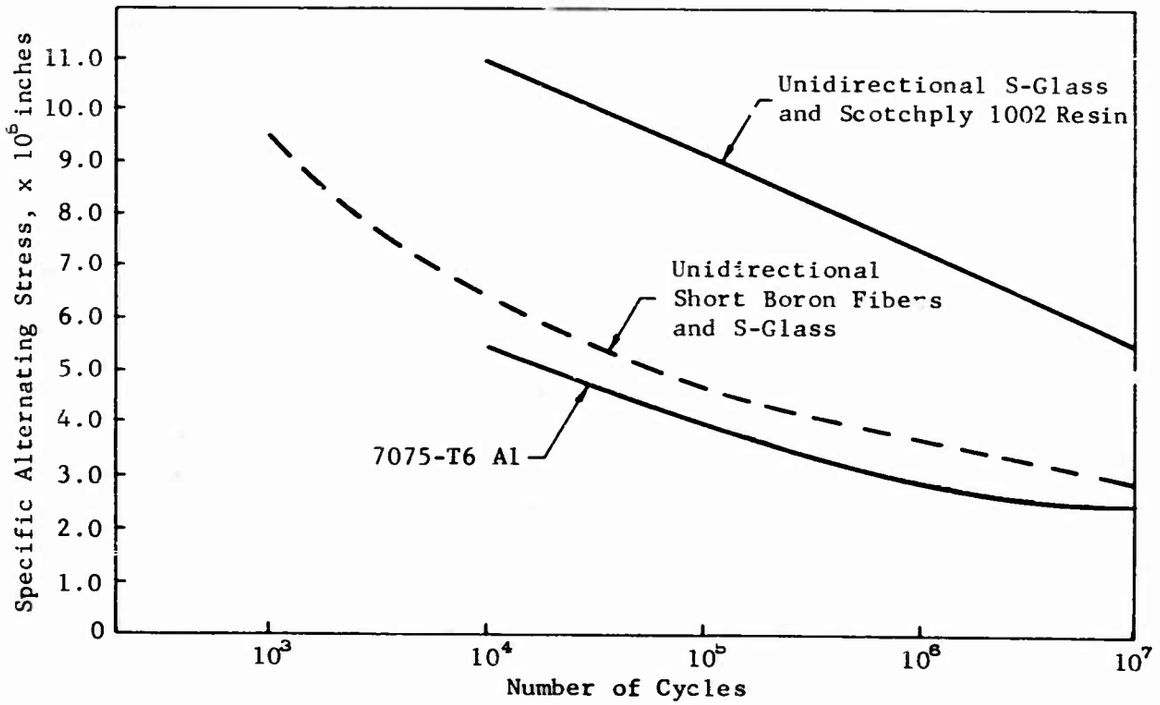

Figure 69. S-N Curves for Various Composites and Aluminum for 0 Mean Stress Plotted as a Function of Specific Alternating Stress

REFERENCES

1. Juan Haener, "Micromechanical Behavior of Fiber Reinforced Plastics," Contract DA 44-177-AMC-320(T), USAAVLABS Technical Report 66-62, US Army Aviation Materiel Laboratories, September 1966

2. Juan Haener and Noel Ashbaugh, "Three-Dimensional Stress Distribution in a Unidirectional Composite," Journal of Composite Materials, Vol. 1, No. 1, January 1967

3. M. A. Sadowski and M. A. Hussain, Buckling of Microfibers, Part I: Classical Microfibers without Couple Stresses, Technical Report WVT 6607, Benet Laboratories, Watervliet Arsenal, New York, March 1966

4. S. Timoshenko, Mathematik and Physik, Vol. 58, 1910, p. 337

5. C. T. Wang, Applied Elasticity, McGraw-Hill Book Company, Inc., New York, 1953

6. B. W. Rosen, Mechanics of Composite Strengthening, Report R 64SD80, Reprint No. 289, General Electric Company, Missile and Space Division, Valley Forge, Pa.

7. Wang, Ibid., pp. 30, 102, and 103

UNCLASSIFIED
Security Classification

DOCUMENT CONTROL DATA - R&D
(Security classification of title, body of abstract and indexing annotation must be entered when the overall report is classified)

1. ORIGINATING ACTIVITY (Corporate author)
Whittaker Corporation
Narmco Research & Development Division
San Diego, California

2a. REPORT SECURITY CLASSIFICATION
Unclassified

2b. GROUP
N/A

3. REPORT TITLE
INVESTIGATION OF MICROMECHANICAL BEHAVIOR OF FIBER REINFORCED PLASTICS

4. DESCRIPTIVE NOTES (Type of report and inclusive dates)
Final Report (14 June 1966 through 14 March 1967)

5. AUTHOR(S) (Last name, first name, initial)
Haener, Juan
Ashbaugh, Noel
Chia, Chuen-Yuan
Feng, Ming-Yuan

6. REPORT DATE	7a. TOTAL NO. OF PAGES	7b. NO. OF REFS
February 1968	234	7

8a. CONTRACT OR GRANT NO.
DA 44-177-AMC-441(T)

b. PROJECT NO.
1F125901A17002

c.

d.

9a. ORIGINATOR'S REPORT NUMBER(S)
USAAVLABS Technical Report 67-66

9b. OTHER REPORT NO(S) (Any other numbers that may be assigned this report)

10. AVAILABILITY/LIMITATION NOTICES

11. SUPPLEMENTARY NOTES

12. SPONSORING MILITARY ACTIVITY
U. S. Army Aviation Materiel Laboratories
Fort Eustis, Virginia

13. ABSTRACT
The stress fields in the components of a unidirectional composite due to shrinkage and external loads are computed for 20 matrix/reinforcement combinations having various volumetric contents. Further, the load transmissions between loaded and unloaded fibers are formulated as three-dimensional elasticity solutions. The instability problem of a composite is treated by both the static and the energy method, resulting in critical loads and buckling wavelengths which depend on material constants and geometries. The theoretical results are in good agreement with experiments. The work reported herein encompasses the following principal areas: (1) parametric studies (internal stresses and displacements computed for unidirectional composites comprised of different matrices and reinforcements combinations and different volumetric contents); (2) three-dimensional load transfer among loaded and unloaded fibers in a matrix; (3) buckling of fibers in a matrix under axial load as an elasticity solution; (4) the buckling of fibers in a matrix under axial load, solved with the Ritz-Galerkin method; and (5) buckling of fibers in a matrix due to matrix shrinkage.

DD FORM 1 JAN 64 1473

UNCLASSIFIED
Security Classification

UNCLASSIFIED

Security Classification

14. KEY WORDS	LINK A		LINK B		LINK C	
	ROLE	WT	ROLE	WT	ROLE	WT
Micromechanics						
Fiber-Reinformed Plastics						
Instability						

INSTRUCTIONS

1. ORIGINATING ACTIVITY: Enter the name and address of the contractor, subcontractor, grantee, Department of Defense activity or other organization *(corporate author)* issuing the report.

2a. REPORT SECURITY CLASSIFICATION: Enter the overall security classification of the report. Indicate whether "Restricted Data" is included. Marking is to be in accordance with appropriate security regulations.

2b. GROUP: Automatic downgrading is specified in DoD Directive 5200.10 and Armed Forces Industrial Manual. Enter the group number. Also, when applicable, show that optional markings have been used for Group 3 and Group 4 as authorized.

3. REPORT TITLE: Enter the complete report title in all capital letters. Titles in all cases should be unclassified. If a meaningful title cannot be selected without classification, show title classification in all capitals in parenthesis immediately following the title.

4. DESCRIPTIVE NOTES: If appropriate, enter the type of report, e.g., interim, progress, summary, annual, or final. Give the inclusive dates when a specific reporting period is covered.

5. AUTHOR(S): Enter the name(s) of author(s) as shown on or in the report. Enter last name, first name, middle initial. If military, show rank and branch of service. The name of the principal author is an absolute minimum requirement.

6. REPORT DATE: Enter the date of the report as day, month, year; or month, year. If more than one date appears on the report, use date of publication.

7a. TOTAL NUMBER OF PAGES: The total page count should follow normal pagination procedures, i.e., enter the number of pages containing information.

7b. NUMBER OF REFERENCES: Enter the total number of references cited in the report.

8a. CONTRACT OR GRANT NUMBER: If appropriate, enter the applicable number of the contract or grant under which the report was written.

8b, 8c, & 8d. PROJECT NUMBER: Enter the appropriate military department identification, such as project number, subproject number, system numbers, task number, etc.

9a. ORIGINATOR'S REPORT NUMBER(S): Enter the official report number by which the document will be identified and controlled by the originating activity. This number must be unique to this report.

9b. OTHER REPORT NUMBER(S): If the report has been assigned any other report numbers *(either by the originator or by the sponsor)*, also enter this number(s).

10. AVAILABILITY/LIMITATION NOTICES: Enter any limitations on further dissemination of the report, other than those imposed by security classification, using standard statements such as:

(1) "Qualified requesters may obtain copies of this report from DDC."

(2) "Foreign announcement and dissemination of this report by DDC is not authorized."

(3) "U. S. Government agencies may obtain copies of this report directly from DDC. Other qualified DDC users shall request through _____."

(4) "U. S. military agencies may obtain copies of this report directly from DDC. Other qualified users shall request through _____."

(5) "All distribution of this report is controlled. Qualified DDC users shall request through _____."

If the report has been furnished to the Office of Technical Services, Department of Commerce, for sale to the public, indicate this fact and enter the price, if known.

11. SUPPLEMENTARY NOTES: Use for additional explanatory notes.

12. SPONSORING MILITARY ACTIVITY: Enter the name of the departmental project office or laboratory sponsoring *(paying for)* the research and development. Include address.

13. ABSTRACT: Enter an abstract giving a brief and factual summary of the document indicative of the report, even though it may also appear elsewhere in the body of the technical report. If additional space is required, a continuation sheet shall be attached.

It is highly desirable that the abstract of classified reports be unclassified. Each paragraph of the abstract shall end with an indication of the military security classification of the information in the paragraph, represented as *(TS)*, *(S)*, *(C)*, or *(U)*.

There is no limitation on the length of the abstract. However, the suggested length is from 150 to 225 words.

14. KEY WORDS: Key words are technically meaningful terms or short phrases that characterize a report and may be used as index entries for cataloging the report. Key words must be selected so that no security classification is required. Identifiers, such as equipment model designation, trade name, military project code name, geographic location, may be used as key words but will be followed by an indication of technical context. The assignment of links, rules, and weights is optional.

UNCLASSIFIED

Security Classification